Development of patient-derived PcrV-antibodies targeting multidrug-resistant *Pseudomonas aeruginosa*

Inaugural Dissertation

zur

Erlangung des Doktorgrades

Dr. nat. med.

der Medizinischen Fakultät

und

der Mathematisch-Naturwissenschaftlichen Fakultät

der Universität zu Köln

vorgelegt von

Dr. med. Alexander Simonis

aus Engelskirchen

Köln, 2026

Betreuer*in: Prof. Dr. Dr. Jan Lars Rybniker

Referenten: Prof. Dr. Florian Klein

Prof. Dr. Berenike Maier

Prof. Dr. Hedda Wardemann

Datum der mündlichen Prüfung: 28.04.2026

Table of content

1. Abbreviations

AMR	Antimicrobial resistance
CDC	Centers for Disease Control and Prevention
CF	Cystic fibrosis
CFTR	Cystic fibrosis transmembrane conductance regulator
Cryo-EM	Cryogenic electron microscopy
DMSO	Dimethyl sulfoxide
EC_{50}	Half-maximal effective concentration
ELISA	Enzyme-linked immunosorbent assay
Fab	Fragment antigen-binding
HEK	Human embryonic kidney
IC_{50}	Half maximal inhibitory concentration
IgG	Immunoglobulin G
IVIG	Intravenous immunoglobulin
mAbs	Monoclonal antibodies
MDR	Multidrug-resistant
MOI	Multiplicity of infection
NCFB	Non-cystic fibrosis bronchiectasis
NLRP3	NACHT, LRR and PYD domains-containing protein 3
PA	*Pseudomonas aeruginosa*
PBMCs	Peripheral blood mononuclear cells
PBS	Phosphate-buffered saline
PCR	Polymerase chain reaction
PEI	Polyethylenimine
RBC	Red blood cells
RNA	Ribonucleic acid
SDS-PAGE	Sodium dodecyl sulfate polyacrylamide gel electrophoresis
ST	Salmonella Typhimurium
T3SS	Type III secretion system
WHO	World Health Organization

2. Summary (English)

The global rise of antimicrobial resistance represents a major public health crisis, highlighting the urgent need for novel therapies. As the pace of antibiotic discovery has declined, research has shifted toward antivirulence strategies, which disarm pathogens by neutralizing virulence factors rather than directly inhibiting bacterial growth. Such approaches are especially promising for severe, drug-resistant infections.

In this context, *Pseudomonas aeruginosa* (PA) stands out as an opportunistic Gram-negative pathogen exhibiting extensive resistance to numerous antibiotic classes. PA is responsible for approximately 10% of all hospital-acquired infections and is an important cause of chronic pulmonary infections, particularly in individuals with underlying lung diseases such as cystic fibrosis (CF). A key virulence determinant of PA is the Type III Secretion System (T3SS), a needle-like protein complex that injects effector toxins into host cells, leading to cell death and extensive tissue damage. The needle-tip protein PcrV plays a central role in this process by facilitating effector translocation, and it has emerged as a promising target for antivirulence therapy.

To identify potential T3SS inhibitors, we developed a robust, scalable screening platform based on quantifying T3SS-induced cytotoxicity in host cells. Screening over 10,000 small molecules yielded several candidates capable of reducing PA pathogenicity *in vitro*. Although small molecules with antivirulence activity could be identified in our study, the overall low hit rate and the need for subsequent chemical optimization to achieve favorable pharmacokinetics and safety remain major challenges. As an alternative, monoclonal antibodies (mAbs) offer several advantages, including high specificity, long half-lives, and well-established safety profiles. While the effectiveness of mAbs against viral infections is well established, the potential of the human humoral immune response to generate highly neutralizing antibacterial antibodies remains poorly understood.

Following our screening for novel T3SS inhibitors, we investigated the feasibility of leveraging the natural B cell response to PA in individuals with CF, a population characterized by prolonged exposure to PA antigens due to chronic or intermittent colonization. In this study, we screened sera from 51 individuals with CF, most of whom had chronic PA infections, using a T3SS-dependent hemolysis assay. Several individuals exhibited high levels of T3SS-neutralizing IgG antibodies targeting the PcrV protein. From these individuals, we isolated and characterized PcrV-specific B cells, leading to the generation of human anti-PcrV mAbs. A subset of these mAbs demonstrated potent neutralizing activity against a range of clinical PA isolates including multidrug-resistant strains. Structural analysis by cryogenic electron microscopy showed that anti-PcrV mAbs recognized a conserved, surface-exposed C-terminal epitope of PcrV. The most effective mAbs were more potent than currently available murine-derived antibodies and led to a

marked reduction in bacterial load in a mouse pneumonia model, with efficacy comparable to that of standard antibiotic treatments.

In conclusion, our findings highlight the therapeutic potential of human-derived mAbs targeting the T3SS of PA. Based on our study, we developed an efficient and comprehensive approach for generating human-derived antibodies targeting the T3SS of PA. These findings support the continued preclinical and clinical development of anti-PcrV mAbs as novel prophylactic and therapeutic agents for the treatment of PA infections, including those caused by multidrug-resistant strains. Moreover, they highlight the broader potential of antivirulence strategies as a complementary approach in the fight against antibiotic resistance.

3. Summary (German)

Die weltweite Zunahme von antimikrobiellen Resistenzen stellt eine erhebliche Bedrohung für die öffentliche Gesundheit dar und unterstreicht die dringende Notwendigkeit innovativer therapeutischer Ansätze jenseits konventioneller Antibiotika. Zunehmend richtet sich die Forschung auf Antivirulenz-Strategien. Diese verfolgen das Ziel, Krankheitserreger durch die gezielte Neutralisierung einzelner Virulenzfaktoren funktionsunfähig zu machen und dadurch die bakterielle Pathogenese zu beeinträchtigen, ohne das Wachstum der Mikroorganismen direkt zu hemmen oder sie abzutöten. Solche Ansätze könnten insbesondere bei der Therapie schwerer Infektionen mit antibiotikaresistenten Erregern von großem Nutzen sein.

Ein in diesem Zusammenhang besonders relevanter Erreger ist *Pseudomonas aeruginosa* (PA), ein opportunistisches, gramnegatives Bakterium, das sich durch eine ausgeprägte intrinsische sowie erworbene Resistenz gegenüber zahlreichen Antibiotikaklassen auszeichnet. PA ist für etwa 10 Prozent aller nosokomialen Infektionen verantwortlich und stellt zudem eine bedeutende Ursache chronischer pulmonaler Infektionen dar, insbesondere bei Patientinnen und Patienten mit chronischen Lungenerkrankungen wie der Mukoviszidose. Ein zentraler Virulenzfaktor von PA ist das Typ-III-Sekretionssystem (T3SS), ein nadelartiger Proteinkomplex, der Toxine direkt in Wirtszellen injiziert und dort Zelltod sowie ausgeprägte Gewebeschäden verursacht. Eine Schlüsselkomponente dieses Systems ist das Nadelspitzenprotein PcrV, das eine entscheidende Rolle bei der Translokation der Toxine spielt und sich daher als vielversprechendes Ziel für antivirulente Therapieansätze etabliert hat.

Zur Identifizierung potenzieller T3SS-Inhibitoren entwickelten wir eine robuste und skalierbare Screening-Plattform, basierend auf der Quantifizierung T3SS-induzierter Zytotoxizität in Wirtszellen. Das Screening von über 10.000 niedermolekularen Verbindungen ergab mehrere Kandidaten, die die Pathogenität von PA *in vitro* reduzieren konnten. Trotz der Identifizierung aktiver Substanzen stellt die insgesamt geringe Trefferquote sowie der nachfolgende Bedarf an chemischer Optimierung zur Sicherstellung günstiger pharmakokinetischer Eigenschaften und Sicherheitsprofile eine wesentliche Herausforderung dar. Als alternative Strategie bieten monoklonale Antikörper (mAbs) mehrere Vorteile, darunter eine hohe Spezifität, lange Halbwertszeiten und gut dokumentierte Sicherheitsprofile. Während ihre Wirksamkeit gegen virale Infektionen gut belegt ist, bleibt das Potenzial der humanen humoralen Immunantwort zur Generierung hochneutralisierender antibakterieller Antikörper bislang unzureichend verstanden.

Aufbauend auf unserem Screening nach T3SS-Inhibitoren untersuchten wir daher die Möglichkeit, die natürliche B-Zell-Antwort gegen PA bei der Mukoviszidose zu nutzen, da bei dieser häufig eine langjährige Exposition gegenüber PA-Antigenen aufgrund einer chronischen oder intermittierenden Kolonisation besteht. Im Rahmen dieser Studie analysierten wir Seren von 51 Personen mit Mukoviszidose, von denen die Mehrheit eine chronische PA-Infektion aufwies, mittels eines T3SS-abhängigen Hämolyse-Assays. Mehrere Proben zeigten hohe Spiegel T3SS-neutralisierender IgG-Antikörper gegen das PcrV-Protein. Von diesen Personen isolierten und charakterisierten wir PcrV-spezifische B-Zellen, was zur Generierung humaner anti-PcrV-mAbs führte. Ein Teil dieser Antikörper wies eine ausgeprägte neutralisierende Aktivität gegenüber einer Vielzahl klinischer PA-Isolate auf, einschließlich multiresistenter Stämme. Strukturanalysen mittels Kryo-Elektronenmikroskopie zeigten, dass diese Antikörper ein konserviertes, oberflächenexponiertes C-terminales Epitop von PcrV erkennen. Die wirksamsten mAbs zeigten eine höhere Potenz als bisherige murine Antikörper und reduzierten die bakterielle Last in einem murinen Pneumonie-Modell signifikant und vergleichbar mit konventionellen Antibiotika vergleichbar war.

Zusammenfassend belegen unsere Ergebnisse das therapeutische Potenzial humaner monoklonaler Antikörper, die gegen das T3SS von PA gerichtet sind. Auf Grundlage dieser Arbeit konnten wir einen effizienten und umfassenden Ansatz zur Entwicklung humaner anti-PcrV-Antikörper etablieren. Diese Erkenntnisse unterstützen die weiterführende präklinische und klinische Entwicklung solcher mAbs als neuartige prophylaktische und therapeutische Optionen zur Behandlung von PA-Infektionen, einschließlich solcher, die durch multiresistente Stämme verursacht werden. Darüber hinaus unterstreichen sie die Relevanz antivirulenter Strategien als ergänzenden Ansatz im Kampf gegen die zunehmende Antibiotikaresistenz.

4. List of publications and contribution to the present investigation

First publication:

von Ambüren J, Schreiber F, Fischer J, Winter S, van Gumpel E, **Simonis A**, Rybniker J. Comprehensive Host Cell-Based Screening Assays for Identification of Anti-Virulence Drugs Targeting *Pseudomonas aeruginosa* and *Salmonella* Typhimurium. Microorganisms. 2020 Jul 22;8(8):1096. doi: 10.3390/microorganisms8081096

Contribution: In this study, a cell-based high-throughput screening assay was established for the identification of T3SS inhibitors. While Julia von Ambüren and Fynn Schreiber were responsible for the technical development and optimization of the screening assays as part of their medical dissertation, I was primarily involved in data analysis, interpretation of results, and manuscript preparation. Due to my significant scientific contributions, I was awarded shared last authorship and also served as a corresponding author alongside the senior author Prof. Dr. Dr. Jan Rybniker.

Second publication:

Simonis A, Kreer C, Albus A, Rox K, Yuan B, Holzmann D, Wilms JA, Zuber S, Kottege L, Winter S, Meyer M, Schmitt K, Gruell H, Theobald SJ, Hellmann AM, Meyer C, Ercanoglu MS, Cramer N, Munder A, Hallek M, Fätkenheuer G, Koch M, Seifert H, Rietschel E, Marlovits TC, van Koningsbruggen-Rietschel S, Klein F, Rybniker J. Discovery of highly neutralizing human antibodies targeting *Pseudomonas aeruginosa*. Cell. 2023 Nov 9;186(23):5098-5113.e19. doi: 10.1016/j.cell.2023.10.002.

Contribution: This study explored the therapeutic potential of human antibodies targeting the T3SS protein PcrV in individuals with cystic fibrosis, a group commonly affected by chronic PA infections. I wrote the study protocol and initiated the ethical approval process. In addition to overseeing study initiation, I was responsible for coordinating sample collection and preparation. The analysis of clinical characteristics was carried out in close collaboration with the cystic fibrosis outpatient clinic. I developed and optimized a range of functional assays to assess antibody binding to PcrV and their inhibitory effects on the T3SS. I also performed the recombinant expression of PcrV for B-cell isolation and initiated the isolation process. Antibody production was carried out in collaboration with Professor Florian Klein's laboratory. The in-depth analysis of the B-cell repertoire was conducted by Dr. Christoph Kreer, who integrated this work into his habilitation on infection-related B-cell responses. Following recombinant antibody expression, I performed the functional characterization. *In vivo* testing was conducted by our collaborator Dr. Katharina Rox, while I carried out subsequent analyses, including cytokine measurements and

histological evaluations. Furthermore, I prepared Fab fragments for cryogenic electron microscopy (Cryo-EM) in collaboration with Dr. Biao Yuan and Professor Thomas Marlovits. The experimental planning, execution, data interpretation, and initial manuscript draft writing were primarily under my responsibility. I am co–first author of this publication, together with Dr. Christoph Kreer, and also act as corresponding author alongside the senior author Prof. Dr. Dr. Jan Rybniker.

Third publication:

Albus A, Kreer C, Klein F, Rybniker J, **Simonis A**. Protocol for developing *Pseudomonas aeruginosa* type III secretion system-neutralizing monoclonal antibodies from human B cells. STAR Protoc. 2024 Dec 20;5(4):103440. doi: 10.1016/j.xpro.2024.103440.

Contribution: Building on the results of previous studies, this comprehensive methodological article describes a detailed workflow for the generation of T3SS-neutralizing antibodies. I successfully introduced and established techniques for the isolation of fully human antibodies from single B cells, an approach that was not previously available in our department. This work represents a foundational contribution, enabling the future generation of additional antibacterial antibodies within our department. The workflow outlined is already being applied to various bacterial targets. I played a central role in conceptualizing the study, designing the experimental framework, and preparing the manuscript. I am the last and corresponding author of this publication.

5. Introduction

The rise of antimicrobial resistance (AMR) represents one of the most significant and rapidly escalating global health threats of the 21st century.[1] The widespread and often inappropriate use of antimicrobial agents across human and veterinary medicine, agriculture, and aquaculture has accelerated the evolution of resistant strains, leading to infections that are increasingly difficult, and in some cases, impossible, to treat with existing antibiotics.[2] In Europe, infections caused by multidrug-resistant (MDR) organisms are estimated to result in around 130,000 deaths each year and account for nearly three million disability-adjusted life-years lost.[3] These data underscore the burden that resistant pathogens place on public health systems and patient outcomes. Gram-negative bacteria are especially challenging in clinical settings due to their intrinsic and acquired resistance mechanisms.[4] A defining characteristic of Gram-negative bacteria is their complex cell envelope, which contains an outer membrane that serves as an effective physical barrier and limits the penetration of antibiotics.[5] Beyond this structural barrier, Gram-negative bacteria employ a wide range of resistance mechanisms, including the use of multidrug efflux pumps, enzymatic degradation or modification of antimicrobial agents, and the acquisition of resistance determinants through horizontal gene transfer.[5]

In this context, *Pseudomonas aeruginosa* (PA) represents a major concern and has been designated a high-priority pathogen by the World Health Organization, underscoring its clinical relevance.[6,7] It commonly causes healthcare-associated infections, including ventilator-associated pneumonia, bloodstream infections, urinary tract infections, and wound infections.[8] Data from national surveillance programs show that PA accounts for roughly 8% of all healthcare-associated infections in the United States, ranking it among the most prevalent nosocomial pathogens.[8] The economic burden is considerable, as infections caused by multidrug-resistant strains are linked to higher treatment costs, prolonged hospital stays, and increased mortality rates.[9-11]

In addition to its involvement in acute infections, PA is particularly notable for its role in chronic pulmonary infections, especially in individuals with underlying respiratory conditions such as cystic fibrosis (CF) and non-cystic fibrosis bronchiectasis (NCFB).[12,13] In CF, mutations in the cystic fibrosis transmembrane conductance regulator (CFTR) gene impair mucociliary clearance, resulting in the accumulation of thick, viscous mucus within the airways.[14] In contrast, NCFB is characterized by impaired mucociliary clearance secondary to various insults, including post-infectious damage (e.g., severe pneumonia), recurrent aspiration, primary ciliary dyskinesia, or structural airway abnormalities.[15] In both CF and NCFB, the impairment of mucociliary function facilitates bacterial colonization and chronic infection, which in turn drive persistent inflammation and progressive structural lung damage.[14,15] This self-perpetuating cycle of

infection, inflammation, and tissue injury leads to frequent exacerbations and a gradual decline in pulmonary function, a critical determinant of quality of life, morbidity, and mortality in affected individuals.[13,16] Given the favorable airway environment and its remarkable capacity for adaptation and antibiotic resistance, PA is particularly well-suited for persistent colonization in both CF and NCFB.[12,17] As a result, eradication or long-term suppression of this pathogen remains a clinical challenge. Frequent administration of antibiotics is often necessary to reduce bacterial load and attenuate inflammation-driven tissue injury; however, the therapeutic benefits are often limited and may be further compromised by the development of multidrug resistance.[13,18,19]

PA causes disease through a wide range of virulence factors, molecules and structural elements it produces to help it colonize the host, evade immune defenses, invade tissues, and damage cells.[20,21] Although these components are not required for the bacterium to survive outside the host, they are essential for initiating infection and shaping its severity and course. In the early phase of infection, PA attaches to epithelial cells or extracellular-matrix components through structures such as flagella, type IV pili, and specific outer-membrane proteins.[22-24] Biofilm formation, a key determinant in the persistence of chronic and device-associated infections, is mediated by the production of exopolysaccharides including alginate, Psl, and Pel.[25] These extracellular polymers constitute a protective matrix that enhances resistance to antimicrobial agents and impedes host immune clearance mechanisms.[26,27] To thrive in iron-limited host environments, PA secretes high-affinity siderophores, such as pyoverdine and pyochelin, which efficiently scavenge iron from host sources.[28] Proteolytic enzymes such as elastase and alkaline protease further contribute to immune evasion by degrading essential host defense proteins, including components of the complement system.[29,30] Lipopolysaccharide, a major constituent of the outer membrane, exerts additional immunomodulatory effects, promoting inflammation while simultaneously impairing effective immune responses.[31] Moreover, the bacterium produces cytotoxic virulence factors that directly damage host cells. Exotoxin A, a potent ADP-ribosylating enzyme, inhibits eukaryotic protein synthesis, culminating in cell death.[32-34] Pyocyanin, a redox-active phenazine pigment, generates reactive oxygen species that induce oxidative stress, epithelial injury, and further compromise host defense mechanisms.[35-37]

Among these virulence determinants, the type III secretion system (T3SS) represents another particularly critical mechanism of pathogenesis.[38] This highly specialized protein translocation apparatus enables the direct injection of bacterial effector proteins into the cytosol of host cells.[39] Functioning as a molecular syringe, the T3SS facilitates bacterial invasion and immune evasion by manipulating host cell signaling pathways, disrupting cytoskeletal integrity, and inducing cell death.[40-45] The system comprises over 30 structural and regulatory proteins encoded by five principal operons, which together govern the assembly, regulation, and functional deployment of

the secretion machinery.[46] T3SS gene expression is tightly regulated and highly responsive to environmental changes and host-derived signals.[47] This regulation involves a network of transcriptional activators and modulators, most notably ExsA, a member of the AraC/XylS family of transcriptional regulators.[48-50]

The structural core of the T3SS includes the needle complex, which traverses both the inner and outer bacterial membranes and is capped by a translocon that integrates into the host plasma membrane (**Figure 1**).[39] Analogous to injectisomes of other Gram-negative pathogens such as *Yersinia spp., Salmonella enterica*, and *Shigella flexneri*, the PA needle complex includes key components such as PscF (needle filament), PscN (ATPase), and PscC and PscW (outer membrane proteins).[51-54] The translocon consists primarily of PopB, PopD, and PcrV; while PopB and PopD form the translocation pore, PcrV is essential for translocon assembly and stability, although it is not directly incorporated into the pore structure.[55,56]

The major effector proteins delivered by the T3SS in PA include ExoS, ExoT, ExoU, and ExoY, each exerting distinct pathogenic effects: ExoS and ExoT share both GTPase-activating and ADP-ribosyltransferase domains, enabling them to disrupt cytoskeletal organization, inhibit phagocytosis, and impair tissue repair.[42,45,57-63] ExoU, a potent phospholipase A2, induces rapid host cell lysis and is strongly associated with acute cytotoxicity and severe tissue damage.[64,65] ExoY, an adenylate cyclase, increases intracellular cAMP levels, disrupting endothelial barrier function and contributing to vascular leakage.[66,67]

Clinical observations indicate a strong correlation between T3SS expression and increased disease severity and mortality, particularly in acute PA infections.[46,68-70] This association is further supported by experimental studies, which have consistently highlighted the critical role of the T3SS in driving disease.[71,72] While, these studies and models reveal that T3SS-mediated effector translocation significantly enhances bacterial virulence, impairs host immune responses, and promotes systemic dissemination in acute infections, PA undergoes a phenotypic adaptation characterized by reduced T3SS expression and a shift toward a biofilm-dominant lifestyle during chronic infections.[73-75] This transition involves increased production of exopolysaccharides such as alginate, which contribute to immune evasion, antimicrobial resistance, and long-term persistence.[76-78] The repression of T3SS under these conditions likely confers a selective advantage, as excessive cytotoxicity may be detrimental to sustained colonization and coexistence with host tissues. With the rising threat of drug-resistant PA and the slowdown in new antibiotic development, interest in non-traditional treatment options has grown.[79,80] These include bacteriophage therapy, small molecule inhibitors, antimicrobial peptides, host-directed therapies, and antivirulence approaches.[80-82]

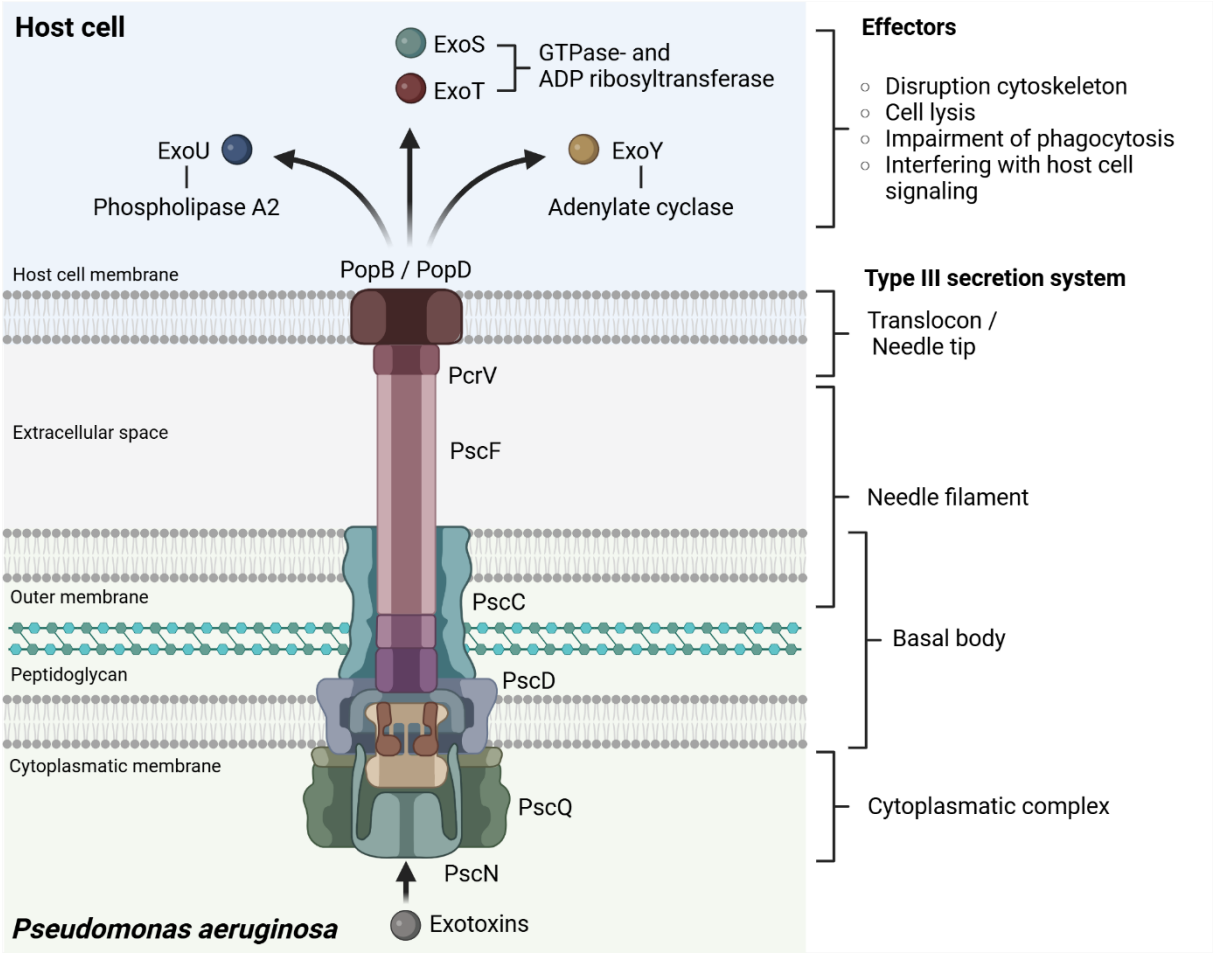

Figure 1: Schematic representation of the type III secretion system (T3SS) in *PA*

The T3SS consists of a needle complex that spans the bacterial inner and outer membranes, comprising proteins such as PscF (needle filament), PscC (outer membrane ring proteins), PscD (inner membrane ring protein anchoring the basal body), PscQ (sorting platform protein), and PscN (cytoplasmic ATPase). The translocon, composed of PopB, PopD, and PcrV, inserts into the host plasma membrane to enable effector translocation. PopB and PopD form the translocation pore, while PcrV is essential for translocon assembly and stability. The system delivers effector proteins (ExoS, ExoT, ExoU, and ExoY) into host cells, each contributing to pathogenesis through distinct mechanisms, ranging from cytoskeletal disruption and inhibition of immune responses to direct cytotoxicity and vascular permeability.

Created in BioRender. Simonis, A. (2025) https://BioRender.com/uqfig8n

Because virulence factors play a key role in the pathogenesis of PA infections, therapeutic approaches that interfere with these mechanisms rather than directly targeting bacterial viability have emerged as a promising alternative to conventional antibiotics.[79] By reducing selective pressure, such strategies may limit the development of resistance while preserving the host's commensal microbiota.[83] In this context, the Type III secretion system (T3SS), a key contributor to disease severity and poor clinical outcomes, has drawn particular attention as a promising target for antivirulence therapy development.[84]

The cytotoxic effects mediated by the PA T3SS can be inhibited through three main strategies: i.) suppression of T3SS gene transcription, ii.) direct interference with T3SS apparatus functionality,

and iii.) inhibition of T3SS effector protein activity. Transcriptional downregulation of T3SS components or effector protein expression has been achieved using various small molecules, including salicylidene acylhydrazides (e.g., INP0341), N-hydroxy-benzimidazoles, and plant-derived phenolic compounds such as TS027 and TS103.[85-87] Functional inhibition of the secretion machinery itself has been reported for several structurally distinct compound classes. For example, hydroxyquinolines, thiazolidinones, and phenoxy-acetamides have been shown to interfere with essential T3SS components, such as PscN, PscC, and PscF, respectively.[88-90] Furthermore, inhibition of effector protein activity has been demonstrated using small molecules that target the enzymatic functions of T3SS effectors, including the ADP-ribosyltransferase activity of ExoS and the phospholipase A2 activity of ExoU.[91,92]

In addition to small molecule inhibitors, T3SS function can also be disrupted through antibody-based approaches. Among the various components of the secretion system, PcrV has emerged as a particularly promising target due to its surface exposure and critical role in translocon complex formation.[93] One of the most thoroughly investigated mAb candidates is KB001-A, a PEGylated, recombinant, humanized monoclonal Fab fragment directed against PcrV.[94] KB001-A advanced to phase 1 and 2 clinical trials in both mechanically ventilated patients and individuals with CF.[95,96] In ventilated patients, KB001-A demonstrated a favorable safety and pharmacokinetic profile, along with preliminary evidence suggesting a potential reduction in the incidence of PA pneumonia in colonized ICU patients.[95] In CF patients, treatment with KB001-A led to modest improvements in lung function and reductions in selected inflammatory markers in sputum.[96] However, the intervention did not extend the time to the need for antibiotic therapy. The limited clinical benefit observed in this population may be partially attributed to the reduced expression of T3SS proteins typically found in chronically infected CF airways.[73,97]

A further antibody-based approach that progressed to clinical evaluation is MEDI3902, a bispecific antibody targeting both PcrV and Psl, an exopolysaccharide critical for bacterial adhesion and biofilm formation.[98] This dual-targeting strategy was designed to simultaneously inhibit T3SS function and impair biofilm integrity, thereby enhancing protective efficacy. MEDI3902 advanced to a phase 2 clinical trial focused on the prevention of PA pneumonia in mechanically ventilated patients at high risk.[99] Although the study failed to achieve its primary endpoint, analyses of specific subgroups indicated possible clinical benefit in selected patient populations. Despite the translational hurdles observed during clinical development, the T3SS remains an attractive therapeutic target given its key role in PA virulence and pathogenesis. In line with this, the objective of this thesis was to further explore and define the therapeutic potential of T3SS inhibition.

6. Present investigation – "Development of patient-derived PcrV-antibodies targeting multidrug-resistant *Pseudomonas aeruginosa*"

6.1. Comprehensive Host Cell-Based Screening Assays for Identification of Anti-Virulence Drugs Targeting *Pseudomonas aeruginosa* and *Salmonella Typhimurium*

In this study, we developed and validated a high-throughput, host cell-based assay to identify small molecules that interfere with bacterial virulence mechanisms or promote host cell survival during infection. By targeting T3SS-mediated cytotoxicity and employing host cell viability as a functional readout, this platform enables the discovery of both antivirulence agents and host-directed therapeutics aimed at preventing T3SS-induced cell death.

Development and Optimization of a High-Throughput Host Cell-Based Assay for PA

To establish a reliable and scalable platform for the evaluation of anti-T3SS agents, we developed a high-throughput, cell-based infection assay utilizing the human lung epithelial cell line A549. This cell line was selected due to its widespread use in pulmonary infection models, including those involving PA.[100] The primary aim was to design an assay that eliminates washing steps and enables direct quantification of host cell viability following bacterial infection.

Using the optimized protocol, A549 cells were seeded in 96-well plates with the test compounds and incubated for 3 h to allow attachment before infection with the wild-type PA strain PAO1. Infections were carried out at a multiplicity of infection (MOI) of 0.5. After a 4-hour incubation period, antibiotics (gentamicin and moxifloxacin) were added to inhibit further bacterial replication. The assay was incubated overnight, and cell viability was subsequently assessed using a resazurin-based fluorometric readout (excitation/emission: 560/590 nm).

Assay parameters, including cell density, MOI, incubation time, and temperature, were systematically optimized. The optimal conditions identified were 2×10^4 cells per well, 3-hour preincubation, MOI 0.5, and a 4-hour infection period. To assess assay robustness and dynamic range, we calculated the Z'-factor as a statistical measure of assay quality. A MOI of 0.5 yielded a Z' value of 0.84, indicative of excellent assay performance. In contrast, reducing the MOI to 0.3 decreased the assay's discriminatory power, as reflected by a Z' value of 0.38. Biological validation of the assay was performed using a T3SS-deficient mutant strain (PAO1Δ*pscD*), lacking a key inner membrane ring component essential for functional T3SS assembly. Infections with the Δ*pscD* mutant resulted in a fivefold increase in host cell viability compared to the wild-type strain, confirming the assay's sensitivity to T3SS-dependent cytotoxicity and its suitability for screening antivirulence compounds.

High-throughput screening for antivirulence compounds targeting PA

To discover novel anti-virulence agents against PA, we conducted a high-throughput screen of 10,000 small molecules from the Specs "World Diversity Set 3" library using our optimized cell-based T3SS inhibition assay.[101] Compounds were tested at a final concentration of 20 μM, and host cell viability was assessed post-infection as a readout of antivirulence activity. Among the screened compounds, one molecule (G5 193) produced a pronounced increase in fluorescence intensity, indicative of enhanced host cell survival. In total, six compounds yielded greater than 150% relative viability compared to untreated, infected controls. These primary hits were re-sourced and subjected to confirmatory dose-response testing at 20 μM and 50 μM. All six compounds demonstrated reproducible, concentration-dependent protective effects on host cells.

Importantly, none of the active compounds exhibited antibacterial activity in standard *in vitro* growth assays, suggesting a selective anti-virulence mechanism rather than direct bactericidal or bacteriostatic effects. Structural characterization revealed that all six active compounds shared a common indoline-2-one scaffold, a chemical motif previously implicated in quorum sensing interference and virulence attenuation in PA.[102] To further investigate the underlying mode of action, we conducted RNA sequencing on PAO1 cultures exposed to G5 193. Transcriptomic analysis identified over 900 differentially expressed genes, including significant downregulation of virulence-associated genes involved in the biosynthesis of key secondary metabolites such as phenazine, pyochelin, and pyoverdine (e.g., phzA1, phzB1, phzS, pchD, pvdM, pvdS). These findings are consistent with previous reports on indoline derivatives and support the hypothesis that G5 193 and related compounds act through interference with quorum sensing pathways and downstream virulence regulation in PA.[102]

Notably, no compounds with measurable anti-T3SS activity were identified in the PA screening. In parallel, we evaluated the protective efficacy of the same 10,000-compound library against *Salmonella enterica* serovar Typhimurium (ST) using an infection model in J774.2 macrophage-like cells. This screen identified 69 compounds that significantly enhanced host cell viability post-infection. Importantly, only one of these 69 compounds exhibited direct antibacterial activity in broth microdilution assays, reinforcing the likelihood that the majority act through anti-virulence or host-directed mechanisms rather than through growth inhibition. Among the active hits, several shared the previously noted indoline-2-one scaffold. However, one compound (E9 423) lacked this structural motif yet demonstrated potent cytoprotective effects, increasing host cell viability to 159% relative to infected controls, without affecting bacterial growth. Based on its protective phenotype and lack of bactericidal activity, we hypothesized that E9 423 might interfere with T3SS function. To test this, we performed a protein secretion assay under T3SS-inducing

conditions. Bacterial cultures were treated with E9 423, and supernatants were analyzed by SDS-PAGE. Treatment with E9 423 resulted in a pronounced reduction in secreted T3SS proteins, confirming its ability to disrupt T3SS-dependent secretion. These findings support E9 423 as a candidate virulence-specific inhibitor with a novel chemical scaffold, distinct from previously characterized indoline derivatives.

Concluding remarks

This study presents the establishment of a robust, scalable platform for medium- to high-throughput screening of antivirulence compounds targeting Gram-negative pathogens, specifically PA and ST. The simplified batch assay format, which eliminates washing steps, enables reliable, reproducible screening with strong performance metrics, as evidenced by high Z'-factor values and the assay's sensitivity in detecting known virulence-deficient mutants.

The successful identification of several indoline-2-one derivatives with cytoprotective activity, as well as a structurally distinct compound (E9 423) that inhibits T3SS-dependent secretion in ST, highlights the potential of host cell-based phenotypic assays to discover anti-virulence agents beyond conventional bactericidal approaches. Notably, the majority of hits identified in both screens did not impair bacterial growth in broth culture, underscoring their specificity for virulence-associated pathways rather than essential metabolic functions. This is particularly relevant in the context of rising global antimicrobial resistance, where discovery of new antibiotics is increasingly hindered by the conserved nature of essential bacterial targets and intrinsic resistance mechanisms.[103-105] As such, interest has shifted toward antivirulence and host-targeted strategies, which aim to disarm pathogens or enhance host resilience without exerting direct selective pressure.[79] Our findings reflect this shift: out of 10,000 compounds screened, only one demonstrated traditional antibacterial activity, whereas multiple others enhanced host cell viability through mechanisms consistent with virulence inhibition or host response modulation. Indole derivatives have emerged as particularly promising scaffolds for broad-spectrum antivirulence therapy. Prior studies have linked this class of compounds to quorum sensing inhibition, disruption of flagellar assembly, and interference with secondary metabolite production.[102,106,107]

Our transcriptomic analysis of PA exposed to G5 193 revealed significant downregulation of genes involved in phenazine, pyochelin, and pyoverdine biosynthesis, corroborating previous reports and supporting a mechanism involving suppression of key virulence regulons.[102] Additionally, interspecies variability in compound efficacy suggests species-specific differences in regulatory circuits governing virulence gene expression, which may be exploited for selective targeting. In contrast, E9 423 represents a particularly compelling candidate for ST-specific T3SS

inhibition. Although it lacks the characteristic indoline core, it demonstrated potent cytoprotective effects and markedly reduced T3SS-dependent protein secretion under inducing conditions. While its precise molecular target remains unknown, preliminary evidence suggests interference with the secretion apparatus itself. The novelty of its chemical structure offers a unique opportunity for further mechanistic dissection and potential lead optimization.

Interestingly, several additional compounds improved host cell viability without directly affecting bacterial secretion systems. Structural analysis suggests that some may act via modulation of host cell death pathways, such as pyroptosis, which is activated during *Salmonella*-induced inflammasome signaling.[108-110] Structural similarities to known NLRP3 inflammasome inhibitors support this hypothesis and point to the utility of host-directed therapeutics as complementary tools in infectious disease management.

In summary, we demonstrate the feasibility and effectiveness of a streamlined, cost-efficient screening platform for the discovery of antivirulence and host-protective agents. Screening a chemically diverse 10,000-compound library, we identified multiple indoline-2-one-based virulence inhibitors, a novel T3SS inhibitor specific to ST, and several putative host-directed agents with potential relevance to inflammasome modulation. These findings underscore the utility of virulence-targeted and host-oriented screening strategies in the face of growing antimicrobial resistance.

Future work should focus on mechanistic elucidation of lead compounds through target identification, chemical proteomics, and *in vivo* validation. Larger-scale screening and structure-activity relationship studies may yield additional candidates with species-specific or broad-spectrum activity. Ultimately, integrating antivirulence and host-targeted approaches may offer a promising path forward in the development of novel therapeutics against multidrug-resistant bacterial pathogens.

6.2. Discovery of highly neutralizing human antibodies targeting *Pseudomonas aeruginosa*

Given the low success rate observed in the high-throughput screen of 10,000 small molecules and the lack of newly identified T3SS inhibitors active against PA, we redirected our efforts toward an immunotherapeutic approach aimed at inhibiting T3SS function in PA. In particular, our objective was to generate neutralizing mAbs directed against PcrV, a structural component of the T3SS needle tip that has previously been identified as a promising target for antibody-based therapies.[93]

Whereas earlier attempts to generate anti-PcrV mAbs have largely depended on animal models, recent advances in antibody discovery, especially in viral diseases, have highlighted the advantages of isolating potent and broadly neutralizing antibodies directly from human donors.[111] In viral infection research, highly effective antibodies have been obtained from convalescent, infected, or vaccinated individuals through approaches by functional screening followed and single-B cell sequencing.[112-114] Building on this paradigm, we hypothesized that individuals chronically colonized with PA, such as people with cystic fibrosis (pwCF), may similarly develop highly matured and specific B cell responses due to prolonged and repeated antigen exposure.

This hypothesis is supported by the frequent detection of antibody titers against structural components of the T3SS in pwCF, despite the fact that T3SS expression is generally downregulated during chronic infection.[73,115] The persistence of these antibody responses likely reflects earlier immune activation during acute phases of infection or colonization, when T3SS expression is known to be elevated.[116] These early immune events may sufficient to induce a strong adaptive response, and the resulting antibodies may persist over time, maintained by long-lived plasma cells and memory B cells, even in the absence of continuous antigen expression. Moreover, the PA populations within the CF lung are highly heterogeneous, with subpopulations that may transiently re-express T3SS under specific microenvironmental conditions, such as during biofilm disruption or in hypoxic niches.[12,78] These episodic reactivation events may contribute to ongoing immune stimulation. In addition, recurrent infections or co-infections with genetically distinct strains may provide repeated antigen exposure, further sustaining the humoral response.

Together, these observations suggest that chronically infected individuals, particularly pwCF, represent a valuable source for the identification of naturally occurring, high-affinity antibodies targeting conserved virulence factors such as PcrV. By leveraging this human-derived immune repertoire, we aim to generate mAbs with superior specificity, reduced immunogenicity, and enhanced clinical efficacy, offering a promising alternative to traditional anti-infective strategies and a novel therapeutic avenue for combating multidrug-resistant PA infections.

Detection of T3SS-neutralizing antibodies from chronically infected pwCF

To elucidate whether chronic colonization by PA in pwCF promotes the generation of functional anti-T3SS humoral immunity, particularly against the protein PcrV, we conducted a comparative investigation between pwCF with chronic PA infection (n = 51) and healthy, PA-naive controls (n = 51) (**Figure 2A**). Phenotypic screening was performed using a cytotoxicity assay based T3SS-mediated lysis of red blood cells (RBCs), wherein optical density served as a surrogate for hemolytic activity (**Figure 2B**). RBCs incubated with wild-type PA strain PA14 exhibited marked hemolysis, significantly mitigated by gentamicin co-treatment, validating T3SS dependency of the assay. Serum samples from both cohorts were heat-inactivated and tested at serial dilutions. Across all concentrations, pwCF-derived sera demonstrated significantly greater neutralizing capacity, as evidenced by reduced RBC lysis, compared to healthy controls.

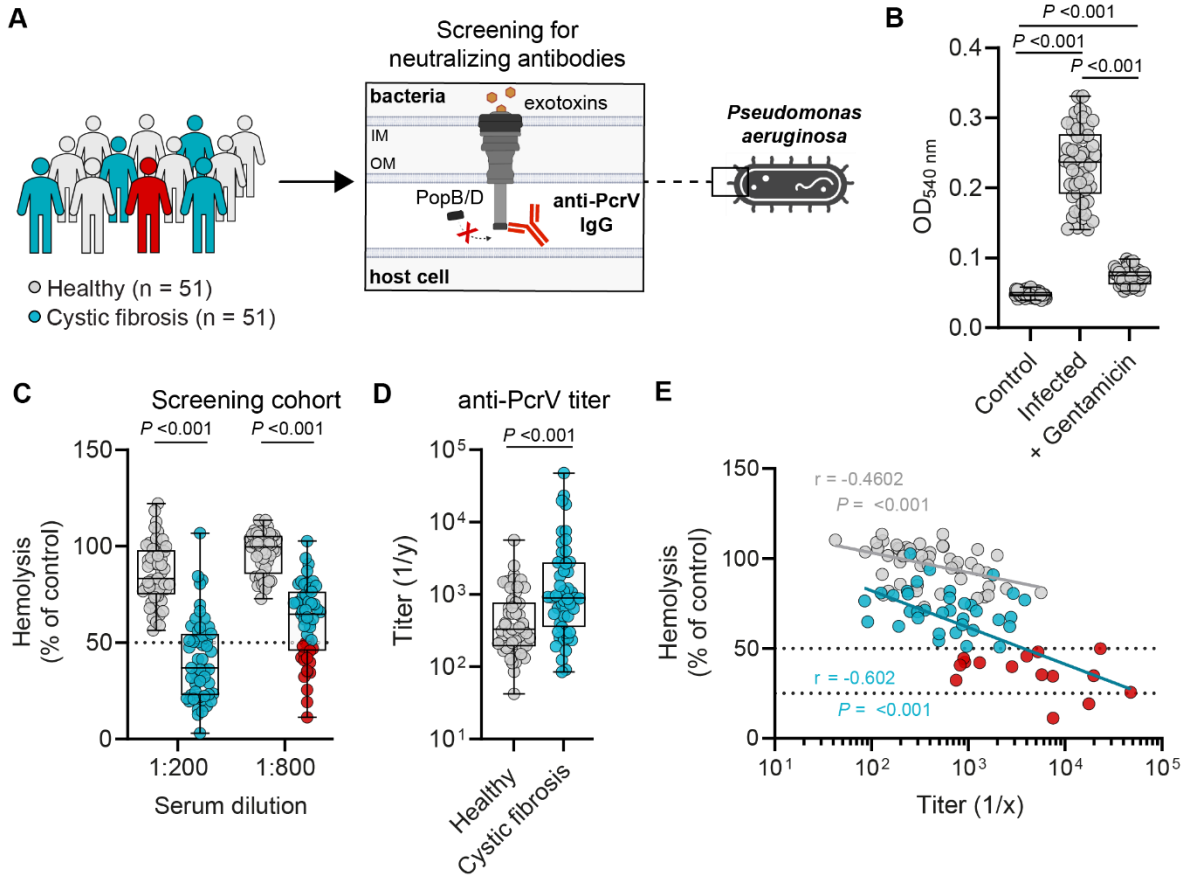

Figure 2: Identification of T3SS-neutralizing antibodies in chronically infected individuals with cystic fibrosis

(**A**) Study design: Serum samples from 51 individuals with cystic fibrosis (pwCF) with persistent PA in sputum and 51 healthy controls were screened for antibodies neutralizing the type III secretion system (T3SS). (**B**) Human red blood cells (RBCs) were exposed to the PA14 wild-type strain (MOI = 1) with or without gentamicin (20 µg/mL) or left untreated (control). Hemolysis was quantified by OD at 540 nm. Statistical analysis was performed using one-way ANOVA with Tukey's post-test. (**C**) Heat-inactivated sera from pwCF (n = 51, cyan) and controls (n = 51, grey) were added at 1:200 or 1:800 dilutions during RBC infection with PA14 (as in B). Hemolysis was calculated relative to untreated infected RBCs. Individuals with strong neutralizing activity (hemolysis < 50% at 1:800) are marked in red. Significance was determined by two-way ANOVA with Sidak's multiple comparisons within each dilution. (**D**) PcrV-binding ELISAs were performed

using diluted serum from pwCF (n = 51) and controls (n = 51). EC_{50} values from binding curves were used as PcrV titers. Group differences were tested with the Mann–Whitney U test. (**E**) Anti-PcrV titers (D) were plotted against hemolysis at 1:800 dilution (C) for pwCF (cyan) and controls (grey). Spearman's correlation was used to assess significance. Highly neutralizing individuals (hemolysis < 50% at 1:800) are shown in red. Box plots display medians, interquartile ranges, and minimum/maximum values. Data points represent the technical mean of independent experiments/biological replicates.

Notably, sera from 15/51 pwCF maintained hemolysis inhibition >50% even at a 1:800 dilution, a feature absent in controls (**Figure 2C**). This variability in the pwCF group suggested interindividual differences in antibody titers and affinities. To exclude non-IgG or off-target IgG effects, purified immunoglobulin preparations and pooled IgG from healthy donors (IVIG) were assessed, showing no intrinsic anti-T3SS activity or impact on PA growth. The observed hemolytic neutralization was further linked to elevated anti-PcrV IgG titers, determined via ELISA. Median half-maximal effective concentration (EC_{50}) for PcrV binding was substantially higher in pwCF compared to controls (1:892 vs. 1:330) (**Figure 2D**). Despite variability, a consistent correlation emerged between high anti-PcrV titers and strong hemolytic inhibition, confirming the specificity and functional relevance of the humoral response (**Figure 2E**). Interestingly, while no correlation was found between antibody activity and clinical parameters such as lung function or hospitalization rate, a trend emerged linking colonization duration to neutralization efficacy.

Evidence of a Clonal and Polyclonal B Cell Response Against PcrV in pwCF

To dissect the cellular origins of the observed antibody responses, we employed fluorescently labeled PcrV probes for B cell enrichment and flow cytometric identification. Initial validation involved transfected HEK293T cells expressing a mouse-derived PcrV-specific antibody (1F3), which successfully bound labeled PcrV. PBMCs from selected pwCF with high serum neutralizing capacity were then processed for PcrV-specific B cell sorting. In these individuals, PcrV-reactive B cells constituted a small but discernible subpopulation (0.024 – 0.047%) within the $CD20^+$ IgG^+ compartment. From 186 sorted cells, 151 productive heavy and 138 light chain sequences were retrieved, revealing donor-specific clonotypes with no public clonotype overlap. CDRH3 length and variable gene usage were broadly distributed, aligning with known IgG repertoires. IgG1 was the predominant isotype, although IgG2 enrichment was noted in two donors, suggesting class-switch recombination possibly influenced by bacterial polysaccharide exposure. These findings imply an antigen-driven, polyclonal expansion with oligoclonal dominance.

Functional and structural characterization of patient-derived anti-PcrV mAbs

To functionally characterize the specificity and potency of anti-PcrV antibodies, 79 recombinant human mAbs were generated, of which 43 exhibited high-affinity binding to PcrV in ELISA (median

EC_{50}: 23.66 ng/mL). Hemolysis inhibition assays at 5 µg/mL identified 20 mAbs with strong neutralizing properties (>50% inhibition), several outperforming the murine benchmark 1F3 and the antibiotic gentamicin. Subsequent IC_{50} assessments revealed that 14 of these mAbs exhibited greater potency than 1F3. Importantly, binding affinity did not predict functional efficacy, suggesting epitope-specific differences in neutralization mechanisms. Competition ELISAs further stratified these antibodies into distinct epitope-binding clusters, with clusters IVa and IVb containing the most potent neutralizers. To map functional epitopes, structural studies using cryogenic electron microscopy (cryo-EM) were performed on two mAb-Fab/PcrV complexes: the potent neutralizer 30-B8 and the non-neutralizer 11-E5. Complexes were resolved to ~5 Å, with discernible binding at the C-terminal region of PcrV. For 30-B8, binding localized to the external surface of the pentameric PcrV structure, whereas 11-E5 engaged an inward-facing epitope, possibly occluded in the native conformation. This structural distinction reinforces the importance of surface accessibility and spatial configuration in mediating neutralization.

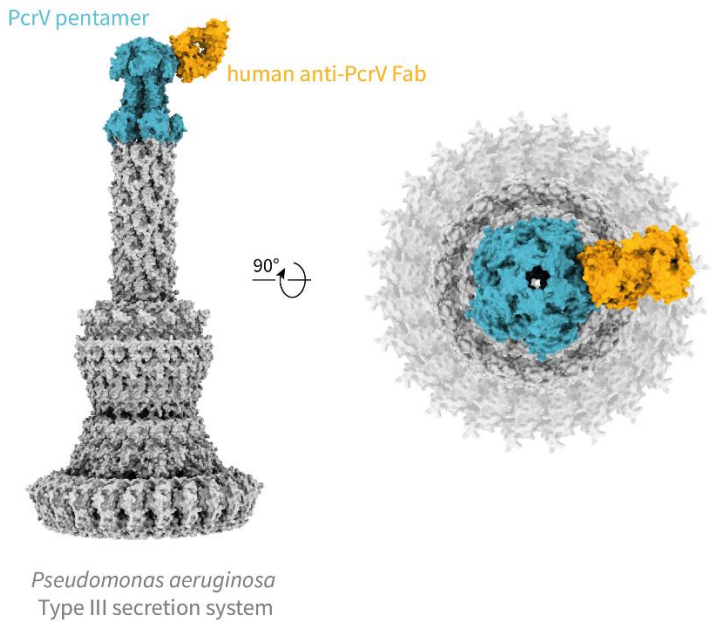

Figure 4: Cryo-EM structure determination of binding epitope of 30-B8 to the PcrV protein

Binding of the Fab fragment of 30-B8 (yellow) to the PcrV pentamer (cyan) of the T3SS complex (grey).

To further test potency of patient-derived anti-PcrV mAbs A549 lung epithelial cells were used to evaluate T3SS-dependent cytotoxicity and antibody-mediated protection (**Figure 4A and 4B**). Of 20 tested mAbs, seven conferred >80% cell viability, with three achieving >90%, matching or exceeding the protection offered by gentamicin (**Figure 4C**). Mouse-derived antibodies and IVIG lacked comparable efficacy. Dose-response studies confirmed superior IC_{50} values for select patient-derived mAbs, with 30-D9 exhibiting a 144-fold improved potency over MEDI3902 (79.5 ng/mL vs. 11.46 µg/mL) (**Figure 4D**).

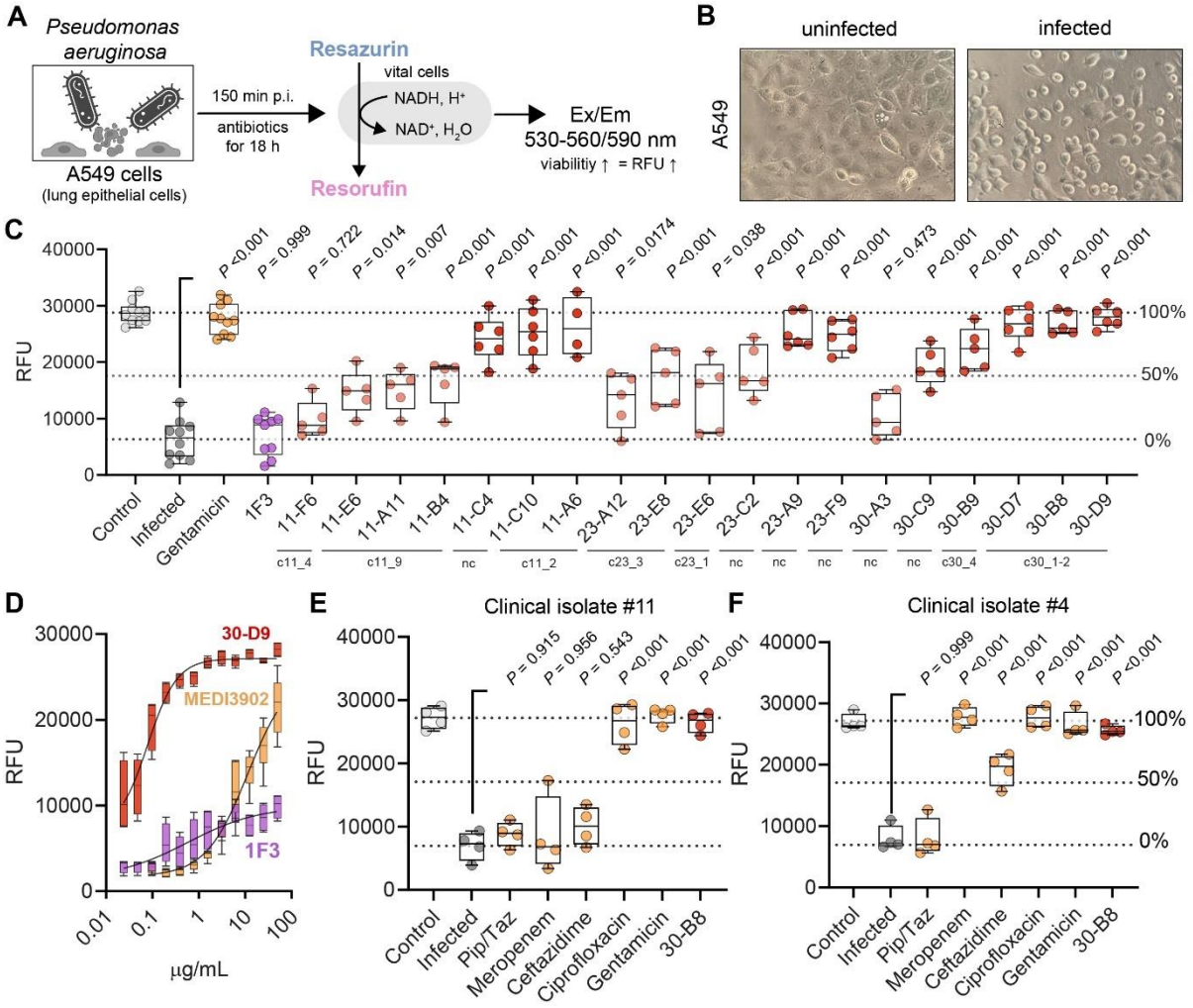

Figure 4: Identification of T3SS-neutralizing antibodies in chronically infected individuals with cystic fibrosis

(**A**) Schematic of the experimental setup. (**B**) A549 cells were infected with the PA wild-type strain PAO1 (MOI = 0.5) for 150 min. Bacteria-induced cytotoxicity was assessed by changes in cell morphology using bright-field microscopy. (**C**) A549 cells were infected with PAO1 (MOI = 0.5, 150 min) in the presence of patient-derived anti-PcrV mAbs (50 µg/mL; n = 20, red). Controls included uninfected cells (grey), infected cells with mock treatment (dark grey), cells treated with a humanized mouse anti-PcrV antibody (1F3, 50 µg/mL; purple), or gentamicin (20 µg/mL; orange). Cell viability was measured as relative fluorescence units (RFU) after resazurin addition. Clonal groups identified by single B cell sequencing are indicated (nc = non-clonal). Statistical significance was determined relative to infected mock-treated cells using one-way ANOVA with Tukey's multiple comparisons test. (**D**) A549 cells were infected as above in the presence of anti-PcrV mAb 30-D9, MEDI3902, and 1F3 across a concentration range (50 µg/mL to 24 ng/mL). (E, F) A549 cells were infected as in (C) with multidrug-resistant PA clinical isolates #11 (**E**) and #4 (**F**) from bloodstream infections. Treatments included piperacillin/tazobactam (16 µg/mL), meropenem (8 µg/mL), ceftazidime (8 µg/mL), ciprofloxacin (1 µg/mL), gentamicin (4 µg/mL) (all in orange), or selected patient-derived anti-PcrV mAbs (50 µg/mL; red). Significance was assessed relative to infected mock-treated cells (dark grey) using one-way ANOVA with Tukey's test. Box plots show medians, interquartile ranges, and minimum/maximum values. Data points represent the technical mean of independent experiments.

To address translational relevance, neutralizing capacity was tested against multiple clinical PA isolates, including drug-resistant strains. Antibody efficacy remained consistent, unaffected by observed *pcrV* mutations, which were predominantly silent or conservative. Notably, the potent

mAb 30-B8 retained full activity against all tested variants including drug-resistant isolates (**Figure 4E and 4F**).

Finally, three experimental mouse models were employed to evaluate the *in vivo* performance of anti-PcrV mAbs. Pharmacokinetic analysis showed rapid systemic distribution post-administration, with prolonged serum half-lives and peak concentrations exceeding *in vitro* IC_{50} values. In a pneumonia model induced via aerosolized PA, both 30-B8 and 30-D9 significantly reduced bacterial lung burden and systemic cytokine levels, mirroring or surpassing levofloxacin efficacy (**Figure 5A – C**). Histological analysis revealed reduced pulmonary hemorrhaging in treated animals (**Figure 5D**). A direct comparison with MEDI3902 in a neutropenic lung infection model revealed that 30-B8 and 30-D9 were more effective at reducing bacterial counts at both high and low doses. In a prophylactic thigh infection model, pre-treatment with these mAbs achieved bacterial reductions comparable to triple-dose levofloxacin.

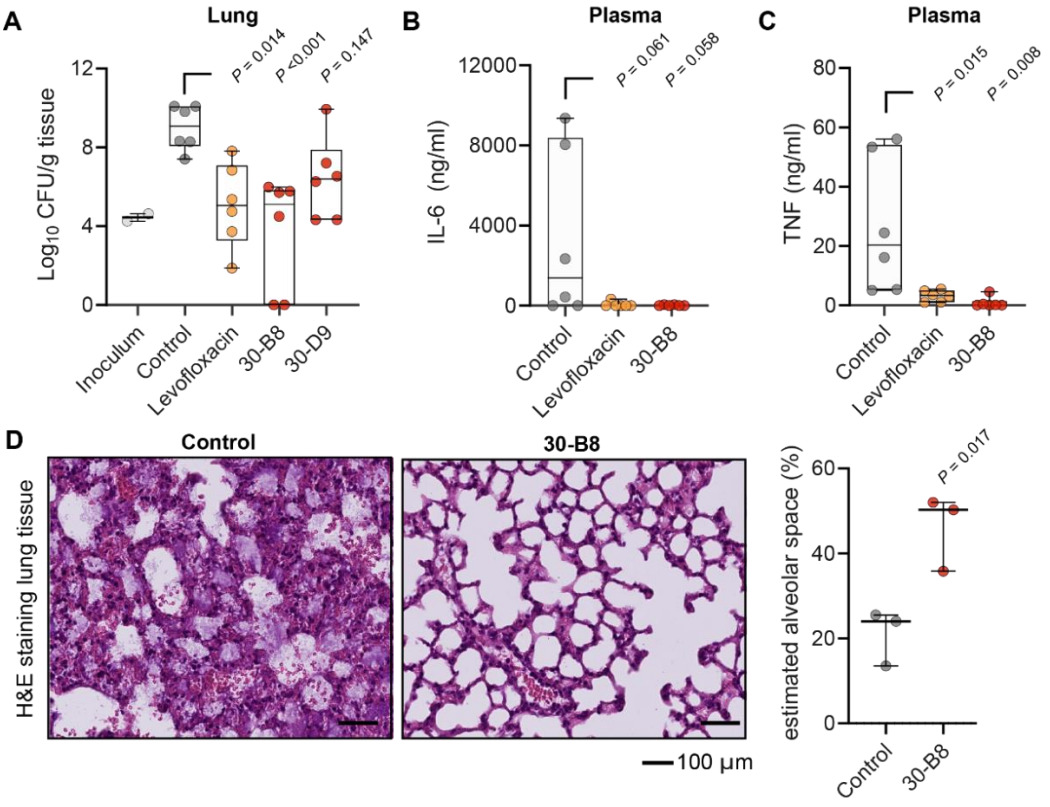

Figure 5: *In vivo* antibacterial activity of human anti-PcrV mAbs

(**A–C**) CD-1 mice were rendered neutropenic by intraperitoneal cyclophosphamide treatment on days –4 and –1. Pulmonary infection was induced via nebulization with PA (Boston 41501 strain). To confirm bacterial delivery, an inoculum control group was included (grey, n = 2). Treatment groups received vehicle (PBS, dark grey, n = 6), levofloxacin (100 mg/kg, orange, n = 6), or mAbs (5 mg/kg, red, n = 6) intraperitoneally 2 h post-infection. After 24 h, mice were sacrificed, lungs homogenized, and bacterial burden (CFUs) quantified. Plasma samples were analyzed for IL-6 (B) and TNF (C). Statistical significance was determined relative to untreated animals using one-way ANOVA with Tukey's multiple comparisons test. (**D**) Lungs from mice treated with control (n = 3) or mAb 30-B8 (n = 3) were fixed, paraffin-

embedded, and stained with H&E. Alveolar space was quantified relative to total lung area, using four representative sections per animal. Statistical significance was calculated by Student's t-test.

Concluding Remarks

This work demonstrates that the humoral immune response against the T3SS tip-protein PcrV in chronically infected pwCF generates a broad and potent spectrum of mAbs with therapeutic potential. Through a comprehensive strategy encompassing functional screening assays, single B cell sequencing, structural epitope mapping, and *in vitro* and *in vivo* validation, we identified fully human mAbs that display superior neutralizing efficacy compared to existing murine-derived candidates such as MEDI3902 and 1F3. Importantly, our structural studies provide mechanistic insights into the neutralizing activity of these antibodies, revealing that specific epitopes within the peripheral C-terminal region of the PcrV pentamer represent highly vulnerable sites of antibody recognition. The distinct binding geometry of patient-derived mAbs compared to MEDI3902 offers a plausible explanation for their improved potency and cytoprotective capacity.

Our findings support the concept that chronic infection, characterized by prolonged and repetitive antigen exposure, can shape the human B cell repertoire to yield antibodies with high affinity and broad neutralization potential. This mirrors successful strategies in viral immunology, where elite neutralizers have been studied to isolate broadly neutralizing antibodies against HIV.[111] Extending this approach to bacterial pathogens provides a powerful framework for identifying therapeutic antibodies, particularly when directed against virulence factors rather than essential metabolic pathways.

In our study, potent anti-PcrV mAbs not only protected host cells from T3SS-mediated cytotoxicity *in vitro* but also demonstrated striking *in vivo* efficacy in murine models of acute infection. Their protective effects were comparable to those of the bactericidal antibiotic levofloxacin, with reductions in bacterial burden and systemic inflammation. These results imply that mAbs may exert antibiotic-mimicking activity *in vivo* by targeting virulence pathways critical for host colonization and infection progression. Nevertheless, translating these findings into clinical practice requires a nuanced understanding of patient populations and pathogen adaptation. While pwCF provided the optimal source for isolating potent neutralizers, they are unlikely to represent the main therapeutic target group, since long-term adaptation of PA in the host frequently involves reduced T3SS expression.[73,115]

This phenomenon may explain the lack of efficacy observed in prior clinical trials of murine-derived anti-PcrV antibodies in pwCF or ventilated patients already colonized with PA.[96,99] By contrast, acute infections, including bloodstream infections, are typically caused by T3SS-positive strains, making these patient groups highly relevant candidates for future clinical

applications.[39] High-risk populations such as individuals undergoing allogeneic stem cell transplantation, who are particularly vulnerable to fulminant bacterial infections, may also benefit from passive immunization strategies employing long-lived IgG mAbs.

In addition to their direct antibacterial effects, human anti-PcrV mAbs underscore a broader idea that the adaptive immune responses of infected individuals provide a natural reservoir for the discovery of highly effective antibacterial antibodies. This strategy is particularly relevant in the context of the growing global crisis of antimicrobial resistance, which risks undermining decades of advances in infectious disease treatment. Compared with traditional therapies, mAbs provide several advantages, such as extended serum persistence, favorable safety profiles, and the ability to harness host immune effector functions.[117,118]

Taken together, our findings demonstrate that human-derived anti-PcrV mAbs possess strong neutralizing activity, defined structural specificity, and broad in vivo efficacy against drug-resistant PA. These results identify PcrV as a particularly susceptible target for antibacterial immunotherapy and show that antibody discovery strategies traditionally used in virology can be successfully applied to bacterial pathogens. Importantly, the data also support future clinical translation by underscoring the importance of careful patient selection, with particular emphasis on individuals at risk of acute infection caused by T3SS-positive strains.

6.3. Protocol for developing *Pseudomonas aeruginosa* type III secretion system-neutralizing monoclonal antibodies from human B cells

This chapter outlines a comprehensive and optimized protocol for the isolation and characterization of human mAbs specifically targeting the PcrV protein of PA. Given the pivotal role of the T3SS in PA pathogenesis and the pronounced immunogenicity of PcrV, this strategy aims to isolate and generate functionally neutralizing antibodies from human donors. To this end, single-cell antibody isolation methods were adapted and expanded, with specific modifications to enable targeted analysis of the PcrV-specific B cell repertoire. The resulting approach integrates immunological, molecular, and cellular techniques in a coordinated pipeline, enabling the discovery and generation of recombinant human mAbs with strong neutralizing activity against the T3SS.

1. Donor Recruitment and Sample Processing

Participants with a documented history of chronic or recurrent PA infection were recruited. Peripheral blood samples were collected for both serum analysis and isolation of peripheral blood mononuclear cells (PBMCs). Serum samples were processed to inactivate complement activity and stored in aliquots at -80 °C to prevent degradation. PBMCs were isolated using Ficoll density gradient centrifugation, subjected to red blood cell lysis, and cryopreserved in DMSO-enriched fetal calf serum using controlled-rate freezing.

2. Recombinant PcrV Antigen Production

To ensure consistent antigen availability for downstream applications, the pcrV gene was cloned into an inducible bacterial expression system (pQE80 vector). The recombinant protein was expressed in *E. coli* BL21 cells, purified via Ni-NTA affinity chromatography under native conditions, and buffer-exchanged into PBS. Protein integrity and purity were confirmed by SDS-PAGE followed by InstantBlue staining.

3. Screening for Anti-PcrV Immune Responses

To identify individuals with robust anti-PcrV responses, sera were screened using a PcrV-specific ELISA. Functional neutralization capacity was evaluated using a hemolysis assay, leveraging PA T3SS-mediated red blood cell lysis as a readout. Samples demonstrating significant inhibition (>50% reduction at 1:800 dilution) were considered for further B cell analysis.

4. Isolation of Antigen-Specific B Cells

PBMCs from selected donors were thawed, enriched for $CD19^+$ B cells using magnetic bead separation, and stained with dual-labeled PcrV antigen conjugated to distinct fluorophores (e.g., Alexa Fluor 488 and 647). Following blocking and incubation with fluorescent antibodies, flow

cytometric analysis was used to identify and single-cell sort PcrV-specific IgG⁺ B cells into individual wells containing a protective lysis buffer (**Figure 6 A – E**).

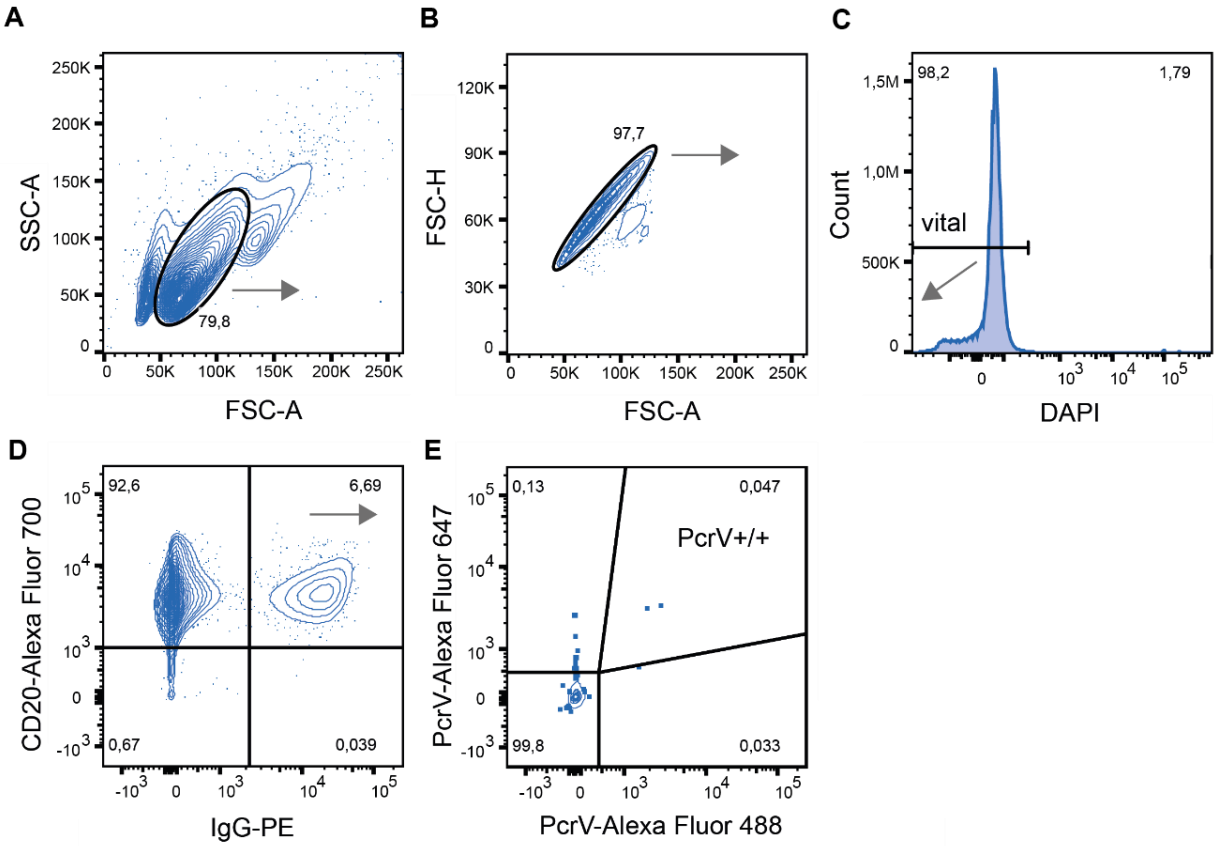

Figure 6: Gating strategy for the isolation of PcrV-specific B cells.

(**A**) Lymphocytes were identified and gated. (**B**) The lymphocyte gate was refined to exclude doublets. (**C**) Cells from panel B were further analyzed for DAPI staining, and only DAPI-negative cells were retained. (**D**) The DAPI-negative population was subsequently evaluated for IgG (x-axis) and CD20 (y-axis) expression, with double-positive ($CD20^+IgG^+$) cells localized in the upper-right quadrant. (**E**) Within this subset, cells exhibiting dual positivity for CD20/IgG and PcrV binding (upper-right quadrant) were selected for single-cell sorting.

7. Reverse Transcription and Immunoglobulin Gene Amplification

Total RNA from single sorted B cells was reverse transcribed using random hexamer primers. A two-step PCR was performed to amplify the heavy (VH) and light (VL) chain variable regions using a comprehensive set of degenerate primers targeting human immunoglobulin gene families. Amplicons were visualized via agarose gel electrophoresis and subjected to Sanger sequencing for verification (**Figure 7**). Functional sequences were cloned into mammalian expression vectors using sequence- and ligation-independent cloning (SLIC).

8. Expression and Purification of Recombinant mAbs

Plasmids encoding validated VH and VL sequences were co-transfected into HEK293-6E cells using polyethylenimine as a transfection reagent. After 7 days, culture supernatants were harvested, and recombinant mAbs were purified via Protein G affinity chromatography. The eluted

antibodies were buffer-exchanged into PBS, sterile-filtered, and quantified using UV/Vis spectroscopy.

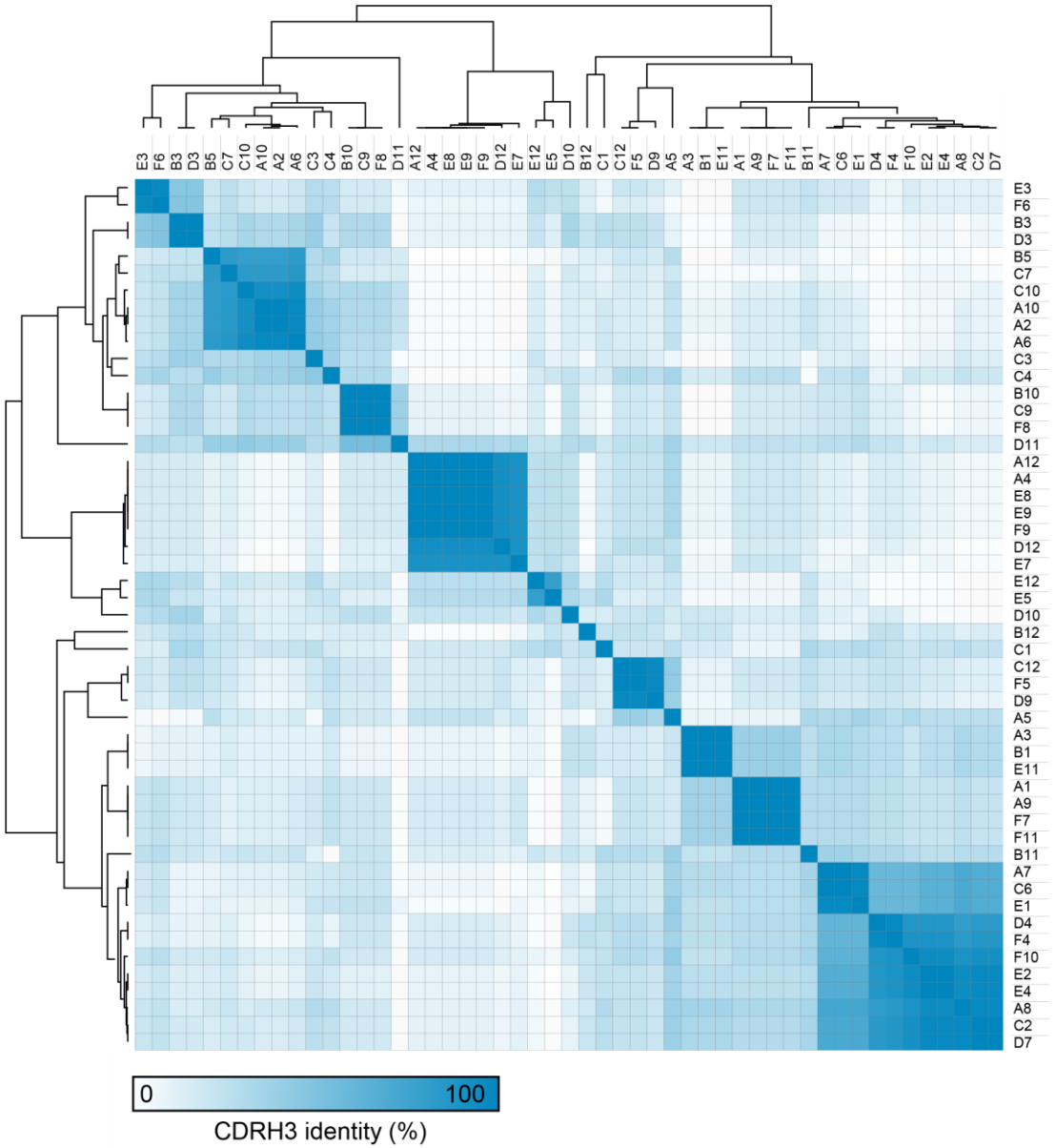

Figure 7: CDRH3 identity of single PcrV-specific B cells.

The CDRH3 sequences of single PcrV-specific B cells (n = 51) isolated from one donor were analyzed. Hierarchical clustering was performed using Clustal Omega (ClustalO), and a similarity matrix was constructed based on Pearson correlation.

9. Functional Characterization of mAbs

Recombinant anti-PcrV mAbs were evaluated for antigen binding via ELISA and assessed for functional neutralization using two independent assays: hemolysis of human red blood cells and cytotoxicity toward A549 lung epithelial cells infected with PA. Neutralization efficacy was determined by measuring residual cell viability using resazurin-based metabolic assays. IC_{50} values were calculated for each mAb clone.

10. Expected Outcomes

A significant proportion of chronically infected individuals (~30%) demonstrated strong anti-PcrV activity. The isolation protocol yielded diverse VH/VJ clonotypes, with some converging into clonally expanded populations. The antibody production pipeline consistently generated yields of 15–25 μg/mL. Functionally, several mAbs achieved neutralizing IC_{50}s below 100 ng/mL, validating the utility of the approach for therapeutic antibody discovery.

11. Limitations and Troubleshooting

While highly effective, the protocol is limited by the inherently low abundance of PcrV-specific B cells (<0.1% of IgG^+ cells), necessitating large starting volumes of PBMCs or the use of leukapheresis. Variability in recombinant protein labeling, low antibody expression yields, and contamination risks during single-cell PCR remain technical challenges. Troubleshooting strategies included optimizing blocking steps in ELISA, confirming protein integrity, and improving transfection conditions.

Concluding Remarks

This methodological framework establishes a robust pipeline for the generation of fully human, functionally validated mAbs targeting the PcrV component of the PA T3SS. The protocol integrates serological screening, single-cell immunology, molecular cloning, recombinant protein expression, and *in vitro* functional validation. The successful application of this workflow highlights its promise as a platform for developing therapeutic mAbs targeting extracellular virulence factors of pathogenic bacteria. Moreover, the platform is broadly adaptable for targeting other components of the T3SS or analogous systems in different bacterial species.

7. References

1. WHO (2020). 10 global health issues to track in 2021. https://www.who.int/news-room/spotlight/10-global-health-issues-to-track-in-2021.
2. Collaborators, G.B.D.A.R. (2024). Global burden of bacterial antimicrobial resistance 1990-2021: a systematic analysis with forecasts to 2050. Lancet *404*, 1199-1226. 10.1016/S0140-6736(24)01867-1.
3. European Antimicrobial Resistance, C. (2022). The burden of bacterial antimicrobial resistance in the WHO European region in 2019: a cross-country systematic analysis. Lancet Public Health *7*, e897-e913. 10.1016/S2468-2667(22)00225-0.
4. Antimicrobial Resistance, C. (2022). Global burden of bacterial antimicrobial resistance in 2019: a systematic analysis. Lancet *399*, 629-655. 10.1016/S0140-6736(21)02724-0.
5. Darby, E.M., Trampari, E., Siasat, P., Gaya, M.S., Alav, I., Webber, M.A., and Blair, J.M.A. (2023). Molecular mechanisms of antibiotic resistance revisited. Nat Rev Microbiol *21*, 280-295. 10.1038/s41579-022-00820-y.
6. WHO (2017). Prioritization of pathogens to guide discovery, research and development of new antibiotics for drug-resistant bacterial infections, including tuberculosis. .
7. CDC (2019). Antibiotic Resistance Threats in the United States, 2019.
8. Prevention., C.f.D.C.a. (2023). HAI Pathogens and Antimicrobial Resistance Report, 2018 – 2021. https://www.cdc.gov/nhsn/hai-report/index.html.
9. Bou, R., Lorente, L., Aguilar, A., Perpinan, J., Ramos, P., Peris, M., and Gonzalez, D. (2009). Hospital economic impact of an outbreak of Pseudomonas aeruginosa infections. J Hosp Infect *71*, 138-142. 10.1016/j.jhin.2008.07.018.
10. Morales, E., Cots, F., Sala, M., Comas, M., Belvis, F., Riu, M., Salvado, M., Grau, S., Horcajada, J.P., Montero, M.M., and Castells, X. (2012). Hospital costs of nosocomial multi-drug resistant Pseudomonas aeruginosa acquisition. BMC Health Serv Res *12*, 122. 10.1186/1472-6963-12-122.
11. Kang, C.I., Kim, S.H., Kim, H.B., Park, S.W., Choe, Y.J., Oh, M.D., Kim, E.C., and Choe, K.W. (2003). Pseudomonas aeruginosa bacteremia: risk factors for mortality and influence of delayed receipt of effective antimicrobial therapy on clinical outcome. Clin Infect Dis *37*, 745-751. 10.1086/377200.
12. Rossi, E., La Rosa, R., Bartell, J.A., Marvig, R.L., Haagensen, J.A.J., Sommer, L.M., Molin, S., and Johansen, H.K. (2021). Pseudomonas aeruginosa adaptation and evolution in patients with cystic fibrosis. Nat Rev Microbiol *19*, 331-342. 10.1038/s41579-020-00477-5.
13. Wilson, R., Aksamit, T., Aliberti, S., De Soyza, A., Elborn, J.S., Goeminne, P., Hill, A.T., Menendez, R., and Polverino, E. (2016). Challenges in managing Pseudomonas aeruginosa in non-cystic fibrosis bronchiectasis. Respir Med *117*, 179-189. 10.1016/j.rmed.2016.06.007.
14. Grasemann, H., and Ratjen, F. (2023). Cystic Fibrosis. N Engl J Med *389*, 1693-1707. 10.1056/NEJMra2216474.
15. Barker, A.F., and Karamooz, E. (2025). Non-Cystic Fibrosis Bronchiectasis in Adults: A Review. JAMA *334*, 253-264. 10.1001/jama.2025.2680.
16. Kerem, E., Viviani, L., Zolin, A., MacNeill, S., Hatziagorou, E., Ellemunter, H., Drevinek, P., Gulmans, V., Krivec, U., Olesen, H., and Group, E.P.R.S. (2014). Factors associated with FEV1 decline in cystic fibrosis: analysis of the ECFS patient registry. Eur Respir J *43*, 125-133. 10.1183/09031936.00166412.
17. Murray, T.S., Egan, M., and Kazmierczak, B.I. (2007). Pseudomonas aeruginosa chronic colonization in cystic fibrosis patients. Curr Opin Pediatr *19*, 83-88. 10.1097/MOP.0b013e3280123a5d.
18. Orenti, A., Mei-Zahav, M., Boracchi, P., Lindblad, A., Shteinberg, M., and Committee, E.S. (2023). Prevalence, trends and outcomes of long-term inhaled antibiotic treatment in

people with cystic fibrosis without chronic Pseudomonas aeruginosa infection - A European cystic fibrosis patient registry data analysis. J Cyst Fibros *22*, 103-111. 10.1016/j.jcf.2022.08.010.

19. Ramsey, B.W., Pepe, M.S., Quan, J.M., Otto, K.L., Montgomery, A.B., Williams-Warren, J., Vasiljev, K.M., Borowitz, D., Bowman, C.M., Marshall, B.C., et al. (1999). Intermittent administration of inhaled tobramycin in patients with cystic fibrosis. Cystic Fibrosis Inhaled Tobramycin Study Group. N Engl J Med *340*, 23-30. 10.1056/NEJM199901073400104.
20. Qin, S., Xiao, W., Zhou, C., Pu, Q., Deng, X., Lan, L., Liang, H., Song, X., and Wu, M. (2022). Pseudomonas aeruginosa: pathogenesis, virulence factors, antibiotic resistance, interaction with host, technology advances and emerging therapeutics. Signal Transduct Target Ther *7*, 199. 10.1038/s41392-022-01056-1.
21. Liao, C., Huang, X., Wang, Q., Yao, D., and Lu, W. (2022). Virulence Factors of Pseudomonas Aeruginosa and Antivirulence Strategies to Combat Its Drug Resistance. Front Cell Infect Microbiol *12*, 926758. 10.3389/fcimb.2022.926758.
22. Arora, S.K., Ritchings, B.W., Almira, E.C., Lory, S., and Ramphal, R. (1998). The Pseudomonas aeruginosa flagellar cap protein, FliD, is responsible for mucin adhesion. Infect Immun *66*, 1000-1007. 10.1128/IAI.66.3.1000-1007.1998.
23. Bucior, I., Pielage, J.F., and Engel, J.N. (2012). Pseudomonas aeruginosa pili and flagella mediate distinct binding and signaling events at the apical and basolateral surface of airway epithelium. PLoS Pathog *8*, e1002616. 10.1371/journal.ppat.1002616.
24. Arhin, A., and Boucher, C. (2010). The outer membrane protein OprQ and adherence of Pseudomonas aeruginosa to human fibronectin. Microbiology (Reading) *156*, 1415-1423. 10.1099/mic.0.033472-0.
25. Mann, E.E., and Wozniak, D.J. (2012). Pseudomonas biofilm matrix composition and niche biology. FEMS Microbiol Rev *36*, 893-916. 10.1111/j.1574-6976.2011.00322.x.
26. Goltermann, L., and Tolker-Nielsen, T. (2017). Importance of the Exopolysaccharide Matrix in Antimicrobial Tolerance of Pseudomonas aeruginosa Aggregates. Antimicrob Agents Chemother *61*. 10.1128/AAC.02696-16.
27. Leid, J.G., Willson, C.J., Shirtliff, M.E., Hassett, D.J., Parsek, M.R., and Jeffers, A.K. (2005). The exopolysaccharide alginate protects Pseudomonas aeruginosa biofilm bacteria from IFN-gamma-mediated macrophage killing. J Immunol *175*, 7512-7518. 10.4049/jimmunol.175.11.7512.
28. Minandri, F., Imperi, F., Frangipani, E., Bonchi, C., Visaggio, D., Facchini, M., Pasquali, P., Bragonzi, A., and Visca, P. (2016). Role of Iron Uptake Systems in Pseudomonas aeruginosa Virulence and Airway Infection. Infect Immun *84*, 2324-2335. 10.1128/IAI.00098-16.
29. Parmely, M., Gale, A., Clabaugh, M., Horvat, R., and Zhou, W.W. (1990). Proteolytic inactivation of cytokines by Pseudomonas aeruginosa. Infect Immun *58*, 3009-3014. 10.1128/iai.58.9.3009-3014.1990.
30. Schultz, D.R., and Miller, K.D. (1974). Elastase of Pseudomonas aeruginosa: inactivation of complement components and complement-derived chemotactic and phagocytic factors. Infect Immun *10*, 128-135. 10.1128/iai.10.1.128-135.1974.
31. Huszczynski, S.M., Lam, J.S., and Khursigara, C.M. (2019). The Role of Pseudomonas aeruginosa Lipopolysaccharide in Bacterial Pathogenesis and Physiology. Pathogens *9*. 10.3390/pathogens9010006.
32. Iglewski, B.H., Liu, P.V., and Kabat, D. (1977). Mechanism of action of Pseudomonas aeruginosa exotoxin Aiadenosine diphosphate-ribosylation of mammalian elongation factor 2 in vitro and in vivo. Infect Immun *15*, 138-144. 10.1128/iai.15.1.138-144.1977.
33. Jorgensen, R., Merrill, A.R., Yates, S.P., Marquez, V.E., Schwan, A.L., Boesen, T., and Andersen, G.R. (2005). Exotoxin A-eEF2 complex structure indicates ADP ribosylation by ribosome mimicry. Nature *436*, 979-984. 10.1038/nature03871.

34. Jenkins, C.E., Swiatoniowski, A., Issekutz, A.C., and Lin, T.J. (2004). Pseudomonas aeruginosa exotoxin A induces human mast cell apoptosis by a caspase-8 and -3-dependent mechanism. J Biol Chem *279*, 37201-37207. 10.1074/jbc.M405594200.
35. O'Malley, Y.Q., Abdalla, M.Y., McCormick, M.L., Reszka, K.J., Denning, G.M., and Britigan, B.E. (2003). Subcellular localization of Pseudomonas pyocyanin cytotoxicity in human lung epithelial cells. Am J Physiol Lung Cell Mol Physiol *284*, L420-430. 10.1152/ajplung.00316.2002.
36. Miller, R.A., Rasmussen, G.T., Cox, C.D., and Britigan, B.E. (1996). Protease cleavage of iron-transferrin augments pyocyanin-mediated endothelial cell injury via promotion of hydroxyl radical formation. Infect Immun *64*, 182-188. 10.1128/iai.64.1.182-188.1996.
37. Ulmer, A.J., Pryjma, J., Tarnok, Z., Ernst, M., and Flad, H.D. (1990). Inhibitory and stimulatory effects of Pseudomonas aeruginosa pyocyanine on human T and B lymphocytes and human monocytes. Infect Immun *58*, 808-815. 10.1128/iai.58.3.808-815.1990.
38. Engel, J., and Balachandran, P. (2009). Role of Pseudomonas aeruginosa type III effectors in disease. Curr Opin Microbiol *12*, 61-66. 10.1016/j.mib.2008.12.007.
39. Hauser, A.R. (2009). The type III secretion system of Pseudomonas aeruginosa: infection by injection. Nat Rev Microbiol *7*, 654-665. 10.1038/nrmicro2199.
40. Pederson, K.J., and Barbieri, J.T. (1998). Intracellular expression of the ADP-ribosyltransferase domain of Pseudomonas exoenzyme S is cytotoxic to eukaryotic cells. Mol Microbiol *30*, 751-759. 10.1046/j.1365-2958.1998.01106.x.
41. Barbieri, A.M., Sha, Q., Bette-Bobillo, P., Stahl, P.D., and Vidal, M. (2001). ADP-ribosylation of Rab5 by ExoS of Pseudomonas aeruginosa affects endocytosis. Infect Immun *69*, 5329-5334. 10.1128/IAI.69.9.5329-5334.2001.
42. Garrity-Ryan, L., Kazmierczak, B., Kowal, R., Comolli, J., Hauser, A., and Engel, J.N. (2000). The arginine finger domain of ExoT contributes to actin cytoskeleton disruption and inhibition of internalization of Pseudomonas aeruginosa by epithelial cells and macrophages. Infect Immun *68*, 7100-7113. 10.1128/IAI.68.12.7100-7113.2000.
43. Dacheux, D., Goure, J., Chabert, J., Usson, Y., and Attree, I. (2001). Pore-forming activity of type III system-secreted proteins leads to oncosis of Pseudomonas aeruginosa-infected macrophages. Mol Microbiol *40*, 76-85. 10.1046/j.1365-2958.2001.02368.x.
44. Galle, M., Schotte, P., Haegman, M., Wullaert, A., Yang, H.J., Jin, S., and Beyaert, R. (2008). The Pseudomonas aeruginosa Type III secretion system plays a dual role in the regulation of caspase-1 mediated IL-1beta maturation. J Cell Mol Med *12*, 1767-1776. 10.1111/j.1582-4934.2007.00190.x.
45. Kaufman, M.R., Jia, J., Zeng, L., Ha, U., Chow, M., and Jin, S. (2000). Pseudomonas aeruginosa mediated apoptosis requires the ADP-ribosylating activity of exoS. Microbiology (Reading) *146 (Pt 10)*, 2531-2541. 10.1099/00221287-146-10-2531.
46. Hauser, A.R., Cobb, E., Bodi, M., Mariscal, D., Valles, J., Engel, J.N., and Rello, J. (2002). Type III protein secretion is associated with poor clinical outcomes in patients with ventilator-associated pneumonia caused by Pseudomonas aeruginosa. Crit Care Med *30*, 521-528. 10.1097/00003246-200203000-00005.
47. Yahr, T.L., and Wolfgang, M.C. (2006). Transcriptional regulation of the Pseudomonas aeruginosa type III secretion system. Mol Microbiol *62*, 631-640. 10.1111/j.1365-2958.2006.05412.x.
48. Hovey, A.K., and Frank, D.W. (1995). Analyses of the DNA-binding and transcriptional activation properties of ExsA, the transcriptional activator of the Pseudomonas aeruginosa exoenzyme S regulon. J Bacteriol *177*, 4427-4436. 10.1128/jb.177.15.4427-4436.1995.
49. Brutinel, E.D., Vakulskas, C.A., Brady, K.M., and Yahr, T.L. (2008). Characterization of ExsA and of ExsA-dependent promoters required for expression of the Pseudomonas aeruginosa type III secretion system. Mol Microbiol *68*, 657-671. 10.1111/j.1365-2958.2008.06179.x.

50. McCaw, M.L., Lykken, G.L., Singh, P.K., and Yahr, T.L. (2002). ExsD is a negative regulator of the Pseudomonas aeruginosa type III secretion regulon. Mol Microbiol *46*, 1123-1133. 10.1046/j.1365-2958.2002.03228.x.
51. Pastor, A., Chabert, J., Louwagie, M., Garin, J., and Attree, I. (2005). PscF is a major component of the Pseudomonas aeruginosa type III secretion needle. FEMS Microbiol Lett *253*, 95-101. 10.1016/j.femsle.2005.09.028.
52. Blaylock, B., Riordan, K.E., Missiakas, D.M., and Schneewind, O. (2006). Characterization of the Yersinia enterocolitica type III secretion ATPase YscN and its regulator, YscL. J Bacteriol *188*, 3525-3534. 10.1128/JB.188.10.3525-3534.2006.
53. Burghout, P., Beckers, F., de Wit, E., van Boxtel, R., Cornelis, G.R., Tommassen, J., and Koster, M. (2004). Role of the pilot protein YscW in the biogenesis of the YscC secretin in Yersinia enterocolitica. J Bacteriol *186*, 5366-5375. 10.1128/JB.186.16.5366-5375.2004.
54. Koster, M., Bitter, W., de Cock, H., Allaoui, A., Cornelis, G.R., and Tommassen, J. (1997). The outer membrane component, YscC, of the Yop secretion machinery of Yersinia enterocolitica forms a ring-shaped multimeric complex. Mol Microbiol *26*, 789-797. 10.1046/j.1365-2958.1997.6141981.x.
55. Goure, J., Pastor, A., Faudry, E., Chabert, J., Dessen, A., and Attree, I. (2004). The V antigen of Pseudomonas aeruginosa is required for assembly of the functional PopB/PopD translocation pore in host cell membranes. Infect Immun *72*, 4741-4750. 10.1128/IAI.72.8.4741-4750.2004.
56. Schoehn, G., Di Guilmi, A.M., Lemaire, D., Attree, I., Weissenhorn, W., and Dessen, A. (2003). Oligomerization of type III secretion proteins PopB and PopD precedes pore formation in Pseudomonas. EMBO J *22*, 4957-4967. 10.1093/emboj/cdg499.
57. Knight, D.A., Finck-Barbancon, V., Kulich, S.M., and Barbieri, J.T. (1995). Functional domains of Pseudomonas aeruginosa exoenzyme S. Infect Immun *63*, 3182-3186. 10.1128/iai.63.8.3182-3186.1995.
58. Pederson, K.J., Vallis, A.J., Aktories, K., Frank, D.W., and Barbieri, J.T. (1999). The amino-terminal domain of Pseudomonas aeruginosa ExoS disrupts actin filaments via small-molecular-weight GTP-binding proteins. Mol Microbiol *32*, 393-401. 10.1046/j.1365-2958.1999.01359.x.
59. Goehring, U.M., Schmidt, G., Pederson, K.J., Aktories, K., and Barbieri, J.T. (1999). The N-terminal domain of Pseudomonas aeruginosa exoenzyme S is a GTPase-activating protein for Rho GTPases. J Biol Chem *274*, 36369-36372. 10.1074/jbc.274.51.36369.
60. Frithz-Lindsten, E., Du, Y., Rosqvist, R., and Forsberg, A. (1997). Intracellular targeting of exoenzyme S of Pseudomonas aeruginosa via type III-dependent translocation induces phagocytosis resistance, cytotoxicity and disruption of actin microfilaments. Mol Microbiol *25*, 1125-1139. 10.1046/j.1365-2958.1997.5411905.x.
61. Krall, R., Schmidt, G., Aktories, K., and Barbieri, J.T. (2000). Pseudomonas aeruginosa ExoT is a Rho GTPase-activating protein. Infect Immun *68*, 6066-6068. 10.1128/IAI.68.10.6066-6068.2000.
62. Sun, J., and Barbieri, J.T. (2003). Pseudomonas aeruginosa ExoT ADP-ribosylates CT10 regulator of kinase (Crk) proteins. J Biol Chem *278*, 32794-32800. 10.1074/jbc.M304290200.
63. Sun, Y., Karmakar, M., Taylor, P.R., Rietsch, A., and Pearlman, E. (2012). ExoS and ExoT ADP ribosyltransferase activities mediate Pseudomonas aeruginosa keratitis by promoting neutrophil apoptosis and bacterial survival. J Immunol *188*, 1884-1895. 10.4049/jimmunol.1102148.
64. Sato, H., Frank, D.W., Hillard, C.J., Feix, J.B., Pankhaniya, R.R., Moriyama, K., Finck-Barbancon, V., Buchaklian, A., Lei, M., Long, R.M., et al. (2003). The mechanism of action of the Pseudomonas aeruginosa-encoded type III cytotoxin, ExoU. EMBO J *22*, 2959-2969. 10.1093/emboj/cdg290.
65. Finck-Barbancon, V., Goranson, J., Zhu, L., Sawa, T., Wiener-Kronish, J.P., Fleiszig, S.M., Wu, C., Mende-Mueller, L., and Frank, D.W. (1997). ExoU expression by Pseudomonas

aeruginosa correlates with acute cytotoxicity and epithelial injury. Mol Microbiol *25*, 547-557. 10.1046/j.1365-2958.1997.4891851.x.

66. Yahr, T.L., Vallis, A.J., Hancock, M.K., Barbieri, J.T., and Frank, D.W. (1998). ExoY, an adenylate cyclase secreted by the Pseudomonas aeruginosa type III system. Proc Natl Acad Sci U S A *95*, 13899-13904. 10.1073/pnas.95.23.13899.
67. Sayner, S.L., Frank, D.W., King, J., Chen, H., VandeWaa, J., and Stevens, T. (2004). Paradoxical cAMP-induced lung endothelial hyperpermeability revealed by Pseudomonas aeruginosa ExoY. Circ Res *95*, 196-203. 10.1161/01.RES.0000134922.25721.d9.
68. Roy-Burman, A., Savel, R.H., Racine, S., Swanson, B.L., Revadigar, N.S., Fujimoto, J., Sawa, T., Frank, D.W., and Wiener-Kronish, J.P. (2001). Type III protein secretion is associated with death in lower respiratory and systemic Pseudomonas aeruginosa infections. J Infect Dis *183*, 1767-1774. 10.1086/320737.
69. El Solh, A.A., Akinnusi, M.E., Wiener-Kronish, J.P., Lynch, S.V., Pineda, L.A., and Szarpa, K. (2008). Persistent infection with Pseudomonas aeruginosa in ventilator-associated pneumonia. Am J Respir Crit Care Med *178*, 513-519. 10.1164/rccm.200802-239OC.
70. Zhuo, H., Yang, K., Lynch, S.V., Dotson, R.H., Glidden, D.V., Singh, G., Webb, W.R., Elicker, B.M., Garcia, O., Brown, R., et al. (2008). Increased mortality of ventilated patients with endotracheal Pseudomonas aeruginosa without clinical signs of infection. Crit Care Med *36*, 2495-2503. 10.1097/CCM.0b013e318183f3f8.
71. Vance, R.E., Rietsch, A., and Mekalanos, J.J. (2005). Role of the type III secreted exoenzymes S, T, and Y in systemic spread of Pseudomonas aeruginosa PAO1 in vivo. Infect Immun *73*, 1706-1713. 10.1128/IAI.73.3.1706-1713.2005.
72. Hotinger, J.A., and May, A.E. (2019). Animal Models of Type III Secretion System-Mediated Pathogenesis. Pathogens *8*. 10.3390/pathogens8040257.
73. Jain, M., Ramirez, D., Seshadri, R., Cullina, J.F., Powers, C.A., Schulert, G.S., Bar-Meir, M., Sullivan, C.L., McColley, S.A., and Hauser, A.R. (2004). Type III secretion phenotypes of Pseudomonas aeruginosa strains change during infection of individuals with cystic fibrosis. J Clin Microbiol *42*, 5229-5237. 10.1128/JCM.42.11.5229-5237.2004.
74. Goodman, A.L., Kulasekara, B., Rietsch, A., Boyd, D., Smith, R.S., and Lory, S. (2004). A signaling network reciprocally regulates genes associated with acute infection and chronic persistence in Pseudomonas aeruginosa. Dev Cell *7*, 745-754. 10.1016/j.devcel.2004.08.020.
75. Ventre, I., Goodman, A.L., Vallet-Gely, I., Vasseur, P., Soscia, C., Molin, S., Bleves, S., Lazdunski, A., Lory, S., and Filloux, A. (2006). Multiple sensors control reciprocal expression of Pseudomonas aeruginosa regulatory RNA and virulence genes. Proc Natl Acad Sci U S A *103*, 171-176. 10.1073/pnas.0507407103.
76. Wu, W., Badrane, H., Arora, S., Baker, H.V., and Jin, S. (2004). MucA-mediated coordination of type III secretion and alginate synthesis in Pseudomonas aeruginosa. J Bacteriol *186*, 7575-7585. 10.1128/JB.186.22.7575-7585.2004.
77. Smith, E.E., Buckley, D.G., Wu, Z., Saenphimmachak, C., Hoffman, L.R., D'Argenio, D.A., Miller, S.I., Ramsey, B.W., Speert, D.P., Moskowitz, S.M., et al. (2006). Genetic adaptation by Pseudomonas aeruginosa to the airways of cystic fibrosis patients. Proc Natl Acad Sci U S A *103*, 8487-8492. 10.1073/pnas.0602138103.
78. La Rosa, R., Johansen, H.K., and Molin, S. (2019). Adapting to the Airways: Metabolic Requirements of Pseudomonas aeruginosa during the Infection of Cystic Fibrosis Patients. Metabolites *9*. 10.3390/metabo9100234.
79. Rasko, D.A., and Sperandio, V. (2010). Anti-virulence strategies to combat bacteria-mediated disease. Nat Rev Drug Discov *9*, 117-128. 10.1038/nrd3013.
80. Kaufmann, S.H.E., Dorhoi, A., Hotchkiss, R.S., and Bartenschlager, R. (2018). Host-directed therapies for bacterial and viral infections. Nat Rev Drug Discov *17*, 35-56. 10.1038/nrd.2017.162.

81. Wagner, S., Sommer, R., Hinsberger, S., Lu, C., Hartmann, R.W., Empting, M., and Titz, A. (2016). Novel Strategies for the Treatment of Pseudomonas aeruginosa Infections. J Med Chem *59*, 5929-5969. 10.1021/acs.jmedchem.5b01698.
82. Kunisch, F., Campobasso, C., Wagemans, J., Yildirim, S., Chan, B.K., Schaudinn, C., Lavigne, R., Turner, P.E., Raschke, M.J., Trampuz, A., and Gonzalez Moreno, M. (2024). Targeting Pseudomonas aeruginosa biofilm with an evolutionary trained bacteriophage cocktail exploiting phage resistance trade-offs. Nat Commun *15*, 8572. 10.1038/s41467-024-52595-w.
83. Dickey, S.W., Cheung, G.Y.C., and Otto, M. (2017). Different drugs for bad bugs: antivirulence strategies in the age of antibiotic resistance. Nat Rev Drug Discov *16*, 457-471. 10.1038/nrd.2017.23.
84. Anantharajah, A., Mingeot-Leclercq, M.P., and Van Bambeke, F. (2016). Targeting the Type Three Secretion System in Pseudomonas aeruginosa. Trends Pharmacol Sci *37*, 734-749. 10.1016/j.tips.2016.05.011.
85. Anantharajah, A., Buyck, J.M., Sundin, C., Tulkens, P.M., Mingeot-Leclercq, M.P., and Van Bambeke, F. (2017). Salicylidene Acylhydrazides and Hydroxyquinolines Act as Inhibitors of Type Three Secretion Systems in Pseudomonas aeruginosa by Distinct Mechanisms. Antimicrob Agents Chemother *61*. 10.1128/AAC.02566-16.
86. Marsden, A.E., King, J.M., Spies, M.A., Kim, O.K., and Yahr, T.L. (2016). Inhibition of Pseudomonas aeruginosa ExsA DNA-Binding Activity by N-Hydroxybenzimidazoles. Antimicrob Agents Chemother *60*, 766-776. 10.1128/AAC.02242-15.
87. Yamazaki, A., Li, J., Zeng, Q., Khokhani, D., Hutchins, W.C., Yost, A.C., Biddle, E., Toone, E.J., Chen, X., and Yang, C.H. (2012). Derivatives of plant phenolic compound affect the type III secretion system of Pseudomonas aeruginosa via a GacS-GacA two-component signal transduction system. Antimicrob Agents Chemother *56*, 36-43. 10.1128/AAC.00732-11.
88. Enquist, P.A., Gylfe, A., Hagglund, U., Lindstrom, P., Norberg-Scherman, H., Sundin, C., and Elofsson, M. (2012). Derivatives of 8-hydroxyquinoline--antibacterial agents that target intra- and extracellular Gram-negative pathogens. Bioorg Med Chem Lett *22*, 3550-3553. 10.1016/j.bmcl.2012.03.096.
89. Felise, H.B., Nguyen, H.V., Pfuetzner, R.A., Barry, K.C., Jackson, S.R., Blanc, M.P., Bronstein, P.A., Kline, T., and Miller, S.I. (2008). An inhibitor of gram-negative bacterial virulence protein secretion. Cell Host Microbe *4*, 325-336. 10.1016/j.chom.2008.08.001.
90. Aiello, D., Williams, J.D., Majgier-Baranowska, H., Patel, I., Peet, N.P., Huang, J., Lory, S., Bowlin, T.L., and Moir, D.T. (2010). Discovery and characterization of inhibitors of Pseudomonas aeruginosa type III secretion. Antimicrob Agents Chemother *54*, 1988-1999. 10.1128/AAC.01598-09.
91. Arnoldo, A., Curak, J., Kittanakom, S., Chevelev, I., Lee, V.T., Sahebol-Amri, M., Koscik, B., Ljuma, L., Roy, P.J., Bedalov, A., et al. (2008). Identification of small molecule inhibitors of Pseudomonas aeruginosa exoenzyme S using a yeast phenotypic screen. PLoS Genet *4*, e1000005. 10.1371/journal.pgen.1000005.
92. Lee, V.T., Pukatzki, S., Sato, H., Kikawada, E., Kazimirova, A.A., Huang, J., Li, X., Arm, J.P., Frank, D.W., and Lory, S. (2007). Pseudolipasin A is a specific inhibitor for phospholipase A2 activity of Pseudomonas aeruginosa cytotoxin ExoU. Infect Immun *75*, 1089-1098. 10.1128/IAI.01184-06.
93. Hotinger, J.A., and May, A.E. (2020). Antibodies Inhibiting the Type III Secretion System of Gram-Negative Pathogenic Bacteria. Antibodies (Basel) *9*. 10.3390/antib9030035.
94. Baer, M., Sawa, T., Flynn, P., Luehrsen, K., Martinez, D., Wiener-Kronish, J.P., Yarranton, G., and Bebbington, C. (2009). An engineered human antibody fab fragment specific for Pseudomonas aeruginosa PcrV antigen has potent antibacterial activity. Infect Immun *77*, 1083-1090. 10.1128/IAI.00815-08.
95. Francois, B., Luyt, C.E., Dugard, A., Wolff, M., Diehl, J.L., Jaber, S., Forel, J.M., Garot, D., Kipnis, E., Mebazaa, A., et al. (2012). Safety and pharmacokinetics of an anti-PcrV

PEGylated monoclonal antibody fragment in mechanically ventilated patients colonized with Pseudomonas aeruginosa: a randomized,double-blind, placebo-controlled trial. Crit Care Med *40*, 2320-2326. 10.1097/CCM.0b013e31825334f6.

96. Jain, R., Beckett, V.V., Konstan, M.W., Accurso, F.J., Burns, J.L., Mayer-Hamblett, N., Milla, C., VanDevanter, D.R., Chmiel, J.F., and Group, K.A.S. (2018). KB001-A, a novel anti-inflammatory, found to be safe and well-tolerated in cystic fibrosis patients infected with Pseudomonas aeruginosa. J Cyst Fibros *17*, 484-491. 10.1016/j.jcf.2017.12.006.
97. Jain, M., Bar-Meir, M., McColley, S., Cullina, J., Potter, E., Powers, C., Prickett, M., Seshadri, R., Jovanovic, B., Petrocheilou, A., et al. (2008). Evolution of Pseudomonas aeruginosa type III secretion in cystic fibrosis: a paradigm of chronic infection. Transl Res *152*, 257-264. 10.1016/j.trsl.2008.10.003.
98. DiGiandomenico, A., Keller, A.E., Gao, C., Rainey, G.J., Warrener, P., Camara, M.M., Bonnell, J., Fleming, R., Bezabeh, B., Dimasi, N., et al. (2014). A multifunctional bispecific antibody protects against Pseudomonas aeruginosa. Sci Transl Med *6*, 262ra155. 10.1126/scitranslmed.3009655.
99. Chastre, J., Francois, B., Bourgeois, M., Komnos, A., Ferrer, R., Rahav, G., De Schryver, N., Lepape, A., Koksal, I., Luyt, C.E., et al. (2022). Safety, efficacy, and pharmacokinetics of gremubamab (MEDI3902), an anti-Pseudomonas aeruginosa bispecific human monoclonal antibody, in P. aeruginosa-colonised, mechanically ventilated intensive care unit patients: a randomised controlled trial. Crit Care *26*, 355. 10.1186/s13054-022-04204-9.
100. Chi, E., Mehl, T., Nunn, D., and Lory, S. (1991). Interaction of Pseudomonas aeruginosa with A549 pneumocyte cells. Infect Immun *59*, 822-828. 10.1128/iai.59.3.822-828.1991.
101. SPECS. World Diversity Set 3. https://www.specs.net/pdf/SPECS-factsheet-world%20diversity%20set.pdf.
102. Lee, J., Attila, C., Cirillo, S.L., Cirillo, J.D., and Wood, T.K. (2009). Indole and 7-hydroxyindole diminish Pseudomonas aeruginosa virulence. Microb Biotechnol *2*, 75-90. 10.1111/j.1751-7915.2008.00061.x.
103. O'NEILL, J. (2016). TACKLING DRUG-RESISTANT INFECTIONS GLOBALLY: FINAL REPORT AND RECOMMENDATIONS.
104. Tacconelli, E., Carrara, E., Savoldi, A., Harbarth, S., Mendelson, M., Monnet, D.L., Pulcini, C., Kahlmeter, G., Kluytmans, J., Carmeli, Y., et al. (2018). Discovery, research, and development of new antibiotics: the WHO priority list of antibiotic-resistant bacteria and tuberculosis. Lancet Infect Dis *18*, 318-327. 10.1016/S1473-3099(17)30753-3.
105. Lewis, K. (2013). Platforms for antibiotic discovery. Nat Rev Drug Discov *12*, 371-387. 10.1038/nrd3975.
106. Yuan, W., Yu, Z., Song, W., Li, Y., Fang, Z., Zhu, B., Li, X., Wang, H., Hong, W., and Sun, N. (2019). Indole-core-based novel antibacterial agent targeting FtsZ. Infect Drug Resist *12*, 2283-2296. 10.2147/IDR.S208757.
107. Kohli, N., Crisp, Z., Riordan, R., Li, M., Alaniz, R.C., and Jayaraman, A. (2018). The microbiota metabolite indole inhibits Salmonella virulence: Involvement of the PhoPQ two-component system. PLoS One *13*, e0190613. 10.1371/journal.pone.0190613.
108. Domiciano, T.P., Wakita, D., Jones, H.D., Crother, T.R., Verri, W.A., Jr., Arditi, M., and Shimada, K. (2017). Quercetin Inhibits Inflammasome Activation by Interfering with ASC Oligomerization and Prevents Interleukin-1 Mediated Mouse Vasculitis. Sci Rep *7*, 41539. 10.1038/srep41539.
109. Lamkanfi, M., Mueller, J.L., Vitari, A.C., Misaghi, S., Fedorova, A., Deshayes, K., Lee, W.P., Hoffman, H.M., and Dixit, V.M. (2009). Glyburide inhibits the Cryopyrin/Nalp3 inflammasome. J Cell Biol *187*, 61-70. 10.1083/jcb.200903124.
110. Broz, P., Newton, K., Lamkanfi, M., Mariathasan, S., Dixit, V.M., and Monack, D.M. (2010). Redundant roles for inflammasome receptors NLRP3 and NLRC4 in host defense against Salmonella. J Exp Med *207*, 1745-1755. 10.1084/jem.20100257.

111. Walker, L.M., and Burton, D.R. (2018). Passive immunotherapy of viral infections: 'super-antibodies' enter the fray. Nat Rev Immunol *18*, 297-308. 10.1038/nri.2017.148.
112. Mulangu, S., Dodd, L.E., Davey, R.T., Jr., Tshiani Mbaya, O., Proschan, M., Mukadi, D., Lusakibanza Manzo, M., Nzolo, D., Tshomba Oloma, A., Ibanda, A., et al. (2019). A Randomized, Controlled Trial of Ebola Virus Disease Therapeutics. N Engl J Med *381*, 2293-2303. 10.1056/NEJMoa1910993.
113. Caskey, M., Schoofs, T., Gruell, H., Settler, A., Karagounis, T., Kreider, E.F., Murrell, B., Pfeifer, N., Nogueira, L., Oliveira, T.Y., et al. (2017). Antibody 10-1074 suppresses viremia in HIV-1-infected individuals. Nat Med *23*, 185-191. 10.1038/nm.4268.
114. Gupta, A., Gonzalez-Rojas, Y., Juarez, E., Crespo Casal, M., Moya, J., Falci, D.R., Sarkis, E., Solis, J., Zheng, H., Scott, N., et al. (2021). Early Treatment for Covid-19 with SARS-CoV-2 Neutralizing Antibody Sotrovimab. N Engl J Med *385*, 1941-1950. 10.1056/NEJMoa2107934.
115. Milagres, L.G., Castro, T.L., Garcia, D., Cruz, A.C., Higa, L., Folescu, T., and Marques, E.A. (2009). Antibody response to Pseudomonas aeruginosa in children with cystic fibrosis. Pediatr Pulmonol *44*, 392-401. 10.1002/ppul.21022.
116. Mauch, R.M., and Levy, C.E. (2014). Serum antibodies to Pseudomonas aeruginosa in cystic fibrosis as a diagnostic tool: a systematic review. J Cyst Fibros *13*, 499-507. 10.1016/j.jcf.2014.01.005.
117. Mankarious, S., Lee, M., Fischer, S., Pyun, K.H., Ochs, H.D., Oxelius, V.A., and Wedgwood, R.J. (1988). The half-lives of IgG subclasses and specific antibodies in patients with primary immunodeficiency who are receiving intravenously administered immunoglobulin. J Lab Clin Med *112*, 634-640.
118. Hansel, T.T., Kropshofer, H., Singer, T., Mitchell, J.A., and George, A.J. (2010). The safety and side effects of monoclonal antibodies. Nat Rev Drug Discov *9*, 325-338. 10.1038/nrd3003.

8. Acknowledgment

I sincerely thank Prof. Dr. Dr. Jan Rybniker for his excellent supervision, helpful guidance, and steady support during this PhD project and in fostering my clinical and scientific career. I am also grateful to Sandra Winter and Edeltraud van Gumpel for their reliable technical assistance, which was an important contribution to this work.

9. Appendix: Publications I – III

I. Comprehensive Host Cell-Based Screening Assays for Identification of Anti-Virulence Drugs Targeting *Pseudomonas aeruginosa* and *Salmonella* Typhimurium. Microorganisms: 14 pages; (p. 40 – 53)

II. Discovery of highly neutralizing human antibodies targeting *Pseudomonas aeruginosa*. Cell: 36 pages; (p. 54 – 89)

III. Protocol for developing *Pseudomonas aeruginosa* type III secretion system-neutralizing monoclonal antibodies from human B cells. STAR Protocols: 24 pages (p. 90 – 113)

microorganisms

MDPI

Article

Comprehensive Host Cell-Based Screening Assays for Identification of Anti-Virulence Drugs Targeting *Pseudomonas aeruginosa* and *Salmonella* Typhimurium

Julia von Ambüren [1,2,†], Fynn Schreiber [1,2,†], Julia Fischer [1,2], Sandra Winter [2], Edeltraud van Gumpel [2], Alexander Simonis [1,2,*,‡] and Jan Rybniker [1,2,3,*,‡]

1 Department I of Internal Medicine, University of Cologne, 50937 Cologne, Germany; j.vonambueren@gmx.de (J.v.A.); f.schreiber@smail.uni-koeln.de (F.S.); julia.fischer@uk-koeln.de (J.F.)
2 Center for Molecular Medicine Cologne (CMMC), University of Cologne, 50931 Cologne, Germany; sandra.winter@uk-koeln.de (S.W.); edeltraud.van-gumpel@uk.koeln.de (E.v.G.)
3 German Center for Infection Research (DZIF), Partner Site Bonn-Cologne, 50937 Cologne, Germany
* Correspondence: alexander.simonis@uk-koeln.de (A.S.); jan.rybniker@uk-koeln.de (J.R.)
† Both authors contributed equally and should be considered as first authors.
‡ Both authors contributed equally and should be considered as senior authors.

Received: 7 July 2020; Accepted: 20 July 2020; Published: 22 July 2020

Abstract: The prevalence of bacterial pathogens being resistant to antibiotic treatment is increasing worldwide, leading to a severe global health challenge. Simultaneously, the development and approval of new antibiotics stagnated in the past decades, leading to an urgent need for novel approaches to avoid the spread of untreatable bacterial infections in the future. We developed a highly comprehensive screening platform based on quantification of pathogen driven host-cell death to detect new anti-virulence drugs targeting *Pseudomonas aeruginosa* (*Pa*) and *Salmonella enterica* serovar Typhimurium (*S*T), both known for their emerging antibiotic resistance. By screening over 10,000 small molecules we could identify several substances showing promising effects on *Pa* and *S*T pathogenicity in our in vitro infection model. Importantly, we could detect compounds potently inhibiting bacteria induced killing of host cells and one novel comipound with impact on the function of the type 3 secretion system (T3SS) of *S*T. Thus, we provide proof of concept data of rapid and feasible medium- to high-throughput drug screening assays targeting virulence mechanisms of two major Gram-negative pathogens.

Keywords: multidrug-resistant pathogens; host-directed therapies; antibiotic drug screening; *Salmonella* Typhimurium; *Pseudomonas aeruginosa*; type 3 secretion system; antibiotic resistance

1. Introduction

Multidrug resistant microorganisms pose a major public health concern and are responsible for around 30,000 annual deaths and a loss of almost 1,000,000 disability-adjusted life-years in Europe alone [1]. Infections by drug-resistant Gram-negative pathogens are eminently challenging and related with an increased mortality and costs [2,3]. Development of novel antibiotic drugs targeting Gram-negative bacteria is complicated by intrinsic and acquired protective mechanisms including multidrug efflux pumps, a high mutation rate, structural properties of the cell wall and antibiotic resistance genes (e.g., antibiotic-degrading or antibiotic-inactivating enzymes like carbapenemases) determined chromosomally or acquired by horizontal gene transfer [4].

Two remarkable representatives of Gram-negative bacteria are *Pseudomonas aeruginosa* (*Pa*), a facultative pathogen that is a major cause of nosocomial infections such as pneumonia, urinary

tract or bloodstream infections and *Salmonella enterica* serovar Typhimurium(*S*T), a common cause of foodborne illness which is also able to cause life threatening infections in immune compromised hosts [5,6]. Both pathogens are known for their high resistance rates [7–10]. To overcome the existing lack of new bactericidal or bacteriostatic substances, the screening for new compounds targeting virulence factors of bacteria or abrogating detrimental effects of these factors in the host seems feasible and promising.

Pathogenicity of *Pa* and *S*T is mediated by several virulence factors including lipopolysaccharide, type 4 pili and the type three secretion system (T3SS). The T3SS has already been in the focus of the development of new drugs with anti-virulence activity but no inhibitor could be implemented in a clinical usage so far [11]. For various chemical derivates, including synthetic small molecules, an inhibitory effect of the T3SS could be described. For instance, salicylidene acylhydrazide interferes with the secretion mechanisms of effector proteins by suppressing corresponding genetic signals on transcriptional levels. Also, several imidazole derivates were described to target transcription factors leading to a downregulation of virulence associated genes without impact on bacterial growth [12]. A different mode of action could be shown for 2-Imino-5-arylidenethiazolidinones derivates, which are capable of manipulating the formation of the T3SS needle complex in *S*T and thus prevent the primary infiltration of virulence factors into the host cell cytosol [13].

However, also the inhibition of other bacterial virulence factors are promising targets to fight bacterial infections: clofoctol specifically inhibits the expression of quorum sensing (QS)-controlled virulence, a bacterial cell–cell communication process, which is involved in pyocyanin production, motility and biofilm formation [14]. Furthermore, in *S*Tseveral quinazoline compounds showed a sufficient downregulation of PhoP/PhoQ-activated genes, which are crucial for environmental adaption including survival within macrophages [15–17]. Notably, not only bacterial factors can be targeted to abrogate pathogenesis. Manipulation of the host cell can also be used for this purpose. For example reduced intracellular bacterial growth of *S*T and *Mycobacterium tuberculosis* could be achieved by modulation of host cell kinases [18]. In *Pa* the function of the acid sphingomyelinase (ASM), an enzyme catalyzing the breakdown of sphingomyelin to ceramide and phosphorylcholine is crucial for cellular response and defense against the pathogen [19,20]. Interestingly, function of the ASM can be modulated by a large group of pharmacological compounds (also called FIASMA = functional inhibitors of acid sphingomyelinase) including several tricyclic antidepressants, calcium channel blockers and H1 antagonists [21].

Here, we established two host cell based medium-throughput screening platforms, which exploit virulence factor dependent killing of *Pa* and *S*T infected of host cells. This method provides a robust, rapid and comprehensive screening platform that theoretically allows for identification of molecules with antibiotic activity, anti-virulence and host-directed drugs, as well as antibiotic prodrugs [22]. Due to the simple batchwise setup of the assay without any required washing-steps, this method is particularly suitable for medium- and high-throughput screenings. Utilizing these platforms, we performed a proof of concept screening with 10,000 diverse chemical compounds [23]. Of note, we could identify several series of novel chemical entities that were able to protect host cells from bacteria-induced cell death without affecting the viability of the eukaryotic cells or bacterial growth, indicating an anti-virulence effect of these compounds.

2. Materials and Methods

2.1. Chemical Compounds

Gentamicin was purchased from Sigma-Aldrich (St. Louis, MO, USA) and moxifloxacin from Cayman Chemical Company (Ann Arbor, MI, USA). For the medium-throughput screening, "The world diversity set III" from Specs (Zoetermeer, Netherlands) was used.

2.2. Cell Culture

A549 human lung adenocarcinoma cells (American Type Culture Collection, Manassas, VA, USA) were cultured in Roswell Park Memorial Institute (RPMI)-1640 medium (ThermoFisher Scientific, Waltham, MA, USA) supplemented with 10% heat-inactivated fetal bovine serum (FBS, PAN-Biotech, Aidenbach, Germany) at 37 °C with 5% CO_2. J774.2 mouse macrophages (Sigma-Aldrich, St. Louis, MO, USA) were grown in Dulbecco's modified Eagle's medium (DMEM) (ThermoFisher, Scientific, Waltham, MA, USA) supplemented with 10% FBS at 37 °C with 5% CO_2.

2.3. Culture Conditions of Bacteria

Pseudomonas aeruginosa O1F wildtype (WT) and PAO1FΔ*pscD* strains were grown in 2 x YT medium (Sigma-Aldrich, St. Louis, MO, USA). For growth inhibition assays PAO1F was grown in Mueller-Hinton broth (Sigma-Aldrich, St. Louis, MO, USA). *Salmonella* Typhimurium strains (SL1344 WT and *invA* mutant strain) were grown in brain heart infusion (BHI) medium (FisherScientific, Hampton, NH, USA).

2.4. Host-Cell Survival Assays

Compounds of "The world diversity set 3" from Specs (dissolved in DMSO) were pre-plated into 96-well plates at a concentration of 200 µM or 500 µM using a volume of 10 µL dH_2O (final concentration 20 or 50 µM). As positive control, gentamicin 200 µg/mL (for *Pa*) or moxifloxacin 100 µg/mL (for *S*T) dissolved in 10 µL dH_2O were pre-plated. As negative control DMSO (Sigma-Aldrich, St. Louis, MO, USA) in dH_2O was added to match the DMSO concentration of the compounds (final volume 10 µL). For drug screening with *Pa* A549 cells were seeded at a density of 2×10^4 cells per well in 70 µL RPMI. After pre-incubation for 3 h at 37 °C with 5% CO_2 to ensure cell adherence, cells were infected with PAO1F with a MOI (multiplicity of infection) of 0.5 in 20 µL RPMI. After 4 h p.i. (post infection) gentamicin and moxifloxacin dissolved in 10 µL dH_2O per well were added at a final concentration of 20 µg/mL and 10 µg/mL respectively to prevent bacterial overgrowth. After overnight incubation the fluorescent dye resazurin (Sigma-Aldrich, St. Louis, MO, USA) was added at a final concentration of 8% (v/v, 10 µL/well). Subsequently the assay plates were incubated at 37 °C with 5% CO_2 for another 4 h. Fluorescence was measured at a wavelength of 560/590 nm (EX-max./EM-max.) using a Tecan Safire II fluorescence reader (Tecan, Maennedorf, Switzerland).

For drug screening with *S*T Specs compounds were dissolved in DSMO and then pre-plated at 10 µL each into 96-well-plates using a final drug concentration as described above (50 µM). J774.2 Mφ cells were seeded at a density of 2×10^4 cells per well in 80 µL DMEM and incubated for 3 h at 37 °C with 5% CO_2. Cells were infected with *S*T SL1344 with a MOI of 0.5 in 20 µL BHI for 3 h. To stop the infection and prevent bacterial overgrowth gentamicin (50 µg/mL) was added and the plates were incubated for another 48 h. To quantify cell viability 10 µL resazurin was added and fluorescence was measured as described above.

2.5. Growth Inhibition Assays

Compounds were pre-plated into 96-well plates at a concentration of 200 µM or 500 µM dissolved in 10 µL dH_2O (final drug concentration per well: 20 or 50 µM). As controls 10 µL gentamicin (20 µg/mL), 10 µL moxifloxacin (10 µg/mL) or 10 µL DMSO were plated. Then bacteria were added at the same concentrations that were used for the host cell-based drug screening described above. Subsequently the plates were incubated overnight for *Pa* and 48 h for *S*T at 37 °C with 5% CO_2. Finally, OD600 of each well were measured by using a Hidex Sense multimodal microplate reader (Hidex, Turku, Finland).

2.6. RNA-Seq in Pseudomonas Aeruginosa

For gene expression analysis *Pa* WT was grown to log-phase with G5 193 (Specs), 7-fluoroindole (7-FI) (Sigma-Aldrich, St. Louis, MO, USA) or DMSO (Sigma-Aldrich, St. Louis, MO, USA) using a final concentration of 100 µM. After RNA purification with an RNAeasy Minikit (Qiagen, Venlo, Netherlands) according to the manufacturer's instructions, library preparation and sequencing were performed by the Cologne Center for Genomics (CCG): briefly, library preparation was performed with the TrueSeq Stranded Total RNA kit (Illumina, San Diego, CA, USA) with 1 µg total RNA input. First steps of the library preparation involved the removal of ribosomal RNA using biotinylated target-specific oligos from the RiboMinus Bacteria Kit (ThermoFisher, Scientific, Waltham, MA, USA). Following purification, the RNA was fragmented and cleaved. RNA fragments were copied into first strand cDNA using reverse transcriptase and random primers, followed by second strand cDNA synthesis using DNA Polymerase I and RNase H. These cDNA fragments then had the addition of a single "A" base and subsequent ligation of the adapter. The products were purified and enriched with PCR to create the final cDNA library. After library validation and quantification (Agilent tape station), equimolar amounts of library were pooled. The pool was quantified by using the KAPA Library Quantification Kit (VWR, Radnor, PA, USA) and the 7900HT Sequence Detection System (Applied Biosystems, Waltham, MA, USA) and sequenced on an NovaSeq6000 sequencing instrument (Illumina) and a PE100 protocol. Analysis of gene expression data were done by Rockhopper (Wellesley College, MA, USA) and Microsoft Excel (Microsoft, Redmond, WA, USA) software.

2.7. T3SS-Secretion Assay

Bacteria were grown overnight under T3SS inducing conditions in LB media containing 5 mM ethylene glycol-bis(2-aminoethylether) (EGTA) (Sigma-Aldrich, St. Louis, MO, USA). The next day the suspension was diluted, and compounds were added to a final concentration of 50 µM in a 50 mL tube. After another 4 h of co-incubation the supernatant was separated via centrifugation and filtered through a 0.45 µm-pore-size low protein-binding filter (ThermoFisher, Scientific, Waltham, MA, USA). Subsequently proteins were precipitated by tricholoroacetic acid (Sigma Aldrich, St. Louis, MO, USA), washed and analyzed by SDS-PAGE using Instant Blue Coomassie dye (Expedeon, Heidelberg, Germany).

2.8. Statistical Analysis

To prove assay-quality the non-dimensional statistical parameter Z'-factor was used to define the data deviation of the respective controls in relation to the corresponding mean values and the dynamic range of the assay [24]. The calculated Z' factor ($Z' = 1 - [(3 * \sigma_{pos} + 3 * \sigma_{neg}) / (\mu_{pos} - \mu_{neg})]$) can range from 0 to 1 and is determined by the assay group's standard deviations σ and means µ of the positive and negative control. Z' factor values of >0.5 indicating a reliable assay quality, which are suitable to perform high throughput screenings [24]. Statistical analysis was performed with GraphPad Prism 8.0.2 software (GraphPad, San Diego, CA, USA). The quantitative data is reported as mean value. Two-tailed Student's t-test with confidence intervals of 95% was used for the statistical analyses of significance. *p*-values less than or equal to 0.05 were considered statistically significant.

3. Results

3.1. Assay Development and Validation for Pseudomonas Aeruginosa

To establish a medium to high throughput assay based on *Pa* (PA01F) dependent killing of host cells, we infected A549 cells in a batch assay that does not require washing steps (Figure 1A). Due to the frequent pulmonary infections caused of *Pa* we selected A549 cells which are commonly used as pulmonary epithelium and *Pa* infection model [25]. First, A549 cells were seeded in 96 well plates in the presence of putative anti-virulence compounds. Following infection with *Pa* for a sufficient amount of time to allow for significant host-cell damage, bacterial growth was stopped by addition

of a combination of gentamicin and moxifloxacin. Both antibiotics were necessary to avoid bacterial overgrowth in all test wells. Continuous incubation overnight led to further reduction of A549 cell counts in *Pa* affected cells. To optimize assay quality, we tested several conditions including alteration of the host-cell number, incubation time, temperature or MOI. For optimal results A549 cells were seeded at a density of 2×10^4 well (96 wells). After preincubation for 3 h cells were infected with a MOI of 0.5 for 4 h and antibiotics were added subsequently. After overnight incubation, resazurin was added for 4 h before cell viability was quantified by fluorescence activity at 560/590 nm (Figure 1A). We evaluated the statistical liability of our screening assays for *Pa* by calculating the Z'factor. As representatively shown in Figure 1B, using a MOI of 0.5 resulted in a Z' value of 0.84, while a decrease of the MOI to 0.3 led to a standard deviation and a narrow separation band of the two control groups (untreated vs gentamicin-treated cells) resulting in a decreased Z' value of 0.38 (Figure A1A). After having determined optimal conditions, we confirmed the capability of the assay to detect disruption of *Pa* virulence by testing a T3SS-deficient strain of *Pa*. Infection of A549 cells with the mutant strain PAO1FΔ*pscD*, which lacks the ability to produce pscD, an essential inner membrane T3SS component [26], led to a 5-fold increase of viability compared to cells infected with the PAO1F wildtype strain (Figure 1C). These data confirmed suitability of the assay for detection of anti-virulence drugs.

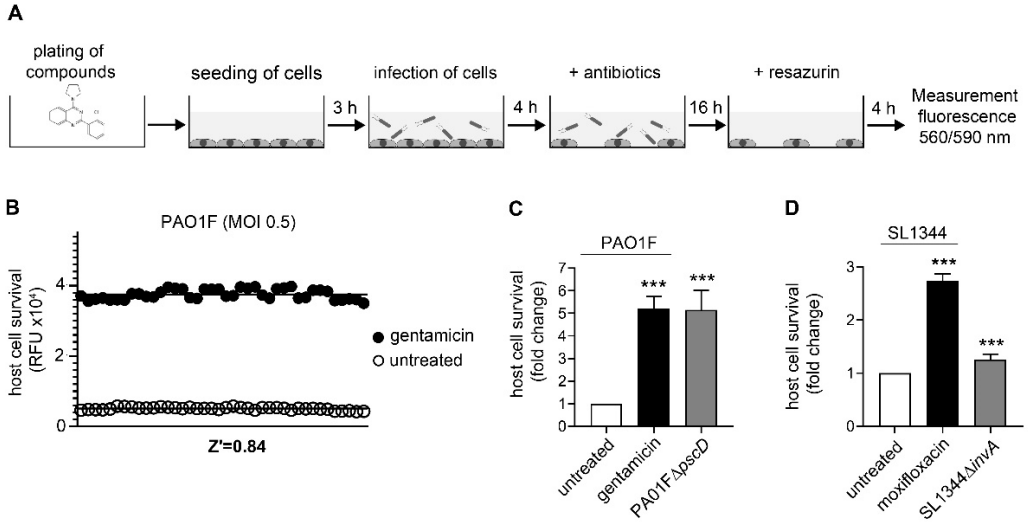

Figure 1. Screening assay validation for high throughput screenings and sensitivity to T3SS mediated toxicity. (**A**) Experimental setup: 96-well plates were pre-plated with compounds before A549 cells were seeded. After preincubation for 3 h to ensure cell adherence, cells were infected with *Pa* strain PAO1F at a MOI of 0.5. After 4 h p.i. antibiotics were added and the fluorescent dye resazurin was added the next day. Subsequently assay plates were incubated for another 4 h and fluorescence was measured at a wavelength of 560/590 nm. (**B**) To test for assay robustness, Z' factor values was calculated under various assay conditions by determining the standard deviations and means of the positive and negative controls as explained in the methods section. 2×10^4 A549 cells/well were seeded into a 96 well plate and subsequently infected with the WT strain PA01F at a MOI of 0.5 in the presence of gentamicin (black dots) or left untreated (white dots). Host cell survival was determined by the fluorescent dye resazurin (RFU = relative fluorescence units). (**C**) Using an optimized assay protocol, A549 cells were co-incubated with the WT strain PA01F (white bar) and the T3SS-deficient mutant strain PA01FΔ*pscD* (gray bar). As positive control gentamicin (20 µg/mL) (black bar) was added to the cells prior to infection. (**D**) For *S*T J774.2 Mφ cells were infected with a MOI of 0.5 with *S*T WT strain SL1344 (white bar) or mutant strain SL1344Δ*invA* (gray bar). Moxifloxacin (10 µg/mL) were added as positive control (black bar). 4 h p.i. bacterial growth was stopped by addition of gentamicin and cells were incubated for 48 h. Subsequently resazurin was added and cell viability were measured by fluorescence reading (560/590 nm). Graphs show mean ± standard error of the mean. *** $p < 0.001$.

3.2. Assay Development and Validation for Salmonella Typhimurium

After establishment of the screening assay for *Pa* we tried to adapt the same assay for *S*T. *S*T was chosen due to comparable structural similarities and virulence factors particularly regarding the type three secretion system. Despite their supposed similarities, initial experiments failed with the same experimental conditions as used before. Importantly, no sufficient *S*T-mediated host-cell killing could be achieved in A549 cells (Figure A1B). The addition of gentamicin at an early stage prevented a sufficient cell invasion by *S*T followed by a measurable host cell cytotoxicity, whereas a prolonged incubation time led to a bacterial overgrowth of the cells, which hinder the fluorometric determination of host cell survival. To overcome this problem, we changed the in vitro model by using a macrophage cell line (J774.2 Mφ) [27]. Due to the presumable enhanced host cell invasion by *S*T, we could achieve a sufficient and timely quantifiable cell death in co-culture conditions without an imminent bacterial overgrowth.

As performed with *Pa*, we tested a large series of different conditions to achieve Z-values >0.5 (Figure A1C): In particular, we observed the necessity for a prolonged co-culture time of *S*T J774.2 Mφ to detect sufficient host-cell killing. Finally, higher gentamicin concentrations were needed to prevent bacterial overgrowth after 4 h. To determine sensitivity to anti-virulence compounds we tested a T3SS-deficient *S*T strain (SL1344Δ*invA*) in our J774.2 Mφ cell-based assay. InvA is part of the inner membrane protein of the *S*T T3SS, which is genetically encoded and regulated via the *Salmonella* pathogenicity island (SPI), a key factor for *S*T virulence [28]. Thus, lack of the *invA* gene leads to an impaired function of the T3SS and a reduction of cytotoxicity in *S*T (Figure 1D). Cell viability was significantly increased using the invA deficient *S*T strain compared to the wildtype strain, indicating sufficient sensitivity of the assay for detection of potential T3SS-inhibiting or other anti-virulence compounds.

3.3. Identification of Novel Compounds with Anti-Virulence Activity against Pseudomonas Aeruginosa

Next we performed a pilot screening with 10,000 diverse chemical small molecules using the Specs "World diversity set 3", a library of diverse screening compounds including molecules with a molecular weight (<500 Da), bond rotation (≤10) and topological polar surface area (tPSA) (≤140Å2) [23]. Exemplary results of a screening assay in a 96-well plate format are shown in Figure 2A. A549 cells were infected with WT strain PAO1F with a MOI of 0.5 for 4 h in the presence of 80 different library compounds tested at a concentration of 20 µM. DMSO (solvent of the compounds) was used as control. Of note, for one compound (G5 193; gray dot) a remarkable increase of the RFU (relative fluorescence units) could be detected indicating increased host cell survival. Altogether, for six out of 10,000 compounds an increase of host cell survival >150% compared to the negative control could be detected. To verify our positive results, single molecules were purchased and validated by re-testing using two different concentrations (20 and of 50 µM) in the host cell survival assay which confirmed dose dependent protection of A549 cells (Figure 2B–D; Figure A1D–F) Interestingly, bacterial growth was not affected by these molecules indicating an anti-virulence effect (Figure 2E). Analysis of the chemical structures of the six substances revealed a common indoline-2-one core structure (Table 1). For compounds sharing this core structure, anti-virulence activity has been described previously: Lee et al. could show that indoline-derivates lead to a downregulation of several quorum sensing related virulence factors, which is associated with an increased host-cell survival upon infection [29].

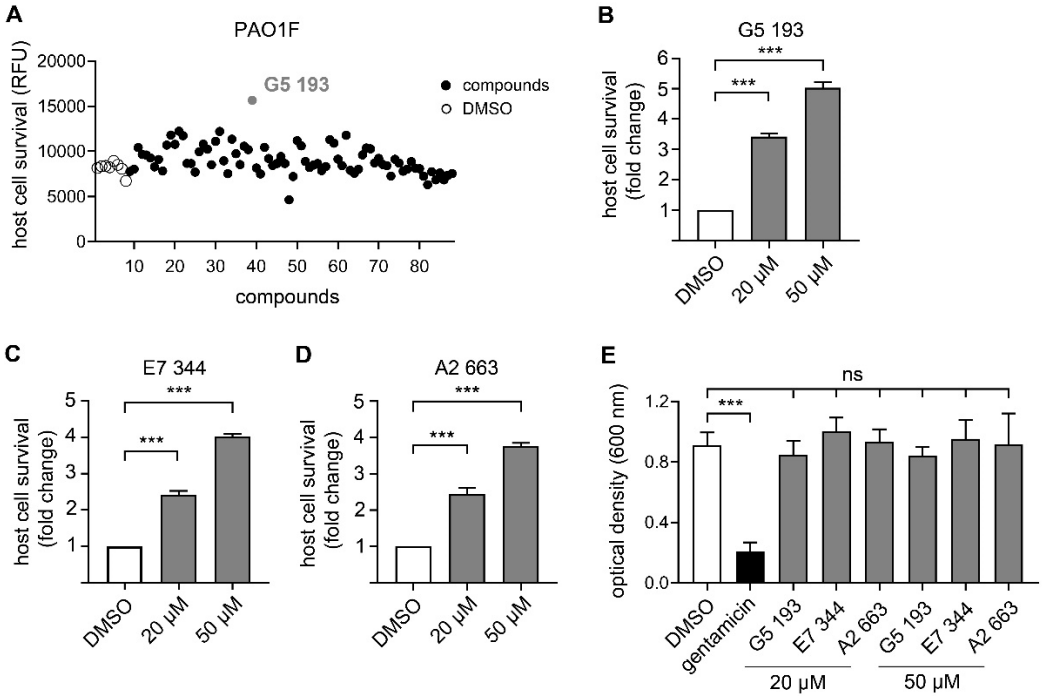

Figure 2. Identification of compounds with antipseudomonal activity. (**A**) A549 cells were infected with *Pa* WT strain PA01F with a MOI of 0.5 in presence of compounds of the Specs library (black dots) (20 µM). Infection was abrogated after 4 h p.i. and cell viability was measured by addition of the fluorescent dye resazurin. Graph represents one 96 well screening plate. One compound (G5 193, gray dot) shows a significant increase of cell viability compared to the negative control (DMSO; white dots). (**B**–**D**) For validation of compounds with effect on cell viability (1.5 fold increase of cell viability compared to DMSO treated cells) experiments were repeated in two different doses of 20 or 50 µM (gray bars). Host cell survival is shown as fold change compared to cells incubated with DMSO (white bars). (**E**) PA01F was grown in Miller Hinton Broth overnight in the presence of DMSO, gentamicin or compounds at a concentration of 20 or 50 µM. Subsequently the OD600 were measured by using a microplate reader. Graphs show mean ± standard error of the mean. None of the tested hit compounds had a growth inhibitory effect on *Pa* in broth. ns = non-significant; *** $p < 0.001$.

To confirm a similar mode of action of our most potent hit (G5 193) we performed an RNA-seq experiment to analyze differential gene regulation in treated versus non-treated *Pa*. In total we were able to identify over 900 genes that were either up- or downregulated by G5 193 with at least a two-fold change. As shown for other indoline-2-one compounds we could observe a downregulation of phzA1, phzB1, phzS, pchD, pvdM and pvdS which play a relevant role in biosynthesis of the virulence factors phenazine, pyochelin and pyoverdine (Table S1). Repressing the production of these proteins at a transcriptional level can explain the host cell protective activity of the identified hit molecule. These findings are in line with the previously described effects of indoline-2-ones by Lee et al., who also could show an inhibition of quorum sensing related proteins and other virulence factors by indole and 7-hydroxyindole [29].

Table 1. Chemical structures of the six substances with antipseudomonal activity.

Internal Number	Specs-ID	Chemical Structure
G5 193	AJ-292/43278258	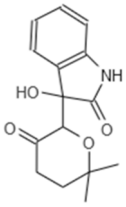
E7 344	AK-968/11036034	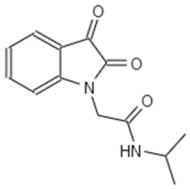
A2 663	AQ-911/40696225	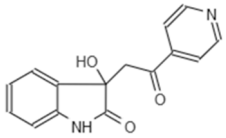
B2 442	AK-918/42028178	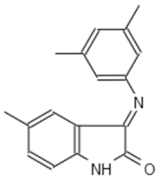
B2 621	AQ-900/41921933	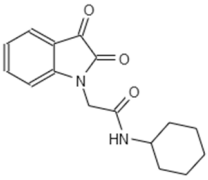
D5 682	AG-219/3696225	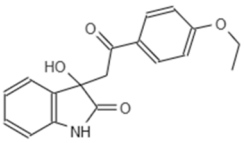

3.4. Chemical Structures of Novel Indole Compounds with Anti-Virulence Activity against Salmonella Typhimurium

Similar to the screening with *Pa*, we expanded our study targeting *S*T by measuring the protective effects of 10,000 synthetic small molecules (Specs "World diversity set 3") on infected J774.2 Mφ. By screening two different species we tried to find compounds with a broad effectiveness but also to reveal specific differences between the species. After pre-plating of library compounds in 96 well plates, cells were seeded and infected with *S*T WT strain SL1344 at a MOI of 0.5 for 3 h. We could identify 69 out of 10,000 substances leading to an increase of host cell survival (Figure 3A shows a summary of the 69 substances from all screening plates). Notably, only one compound impaired bacterial growth in broth, indicating that most of the remaining hit compounds display an anti-virulence or host-cell directed effect (Figure A1G).

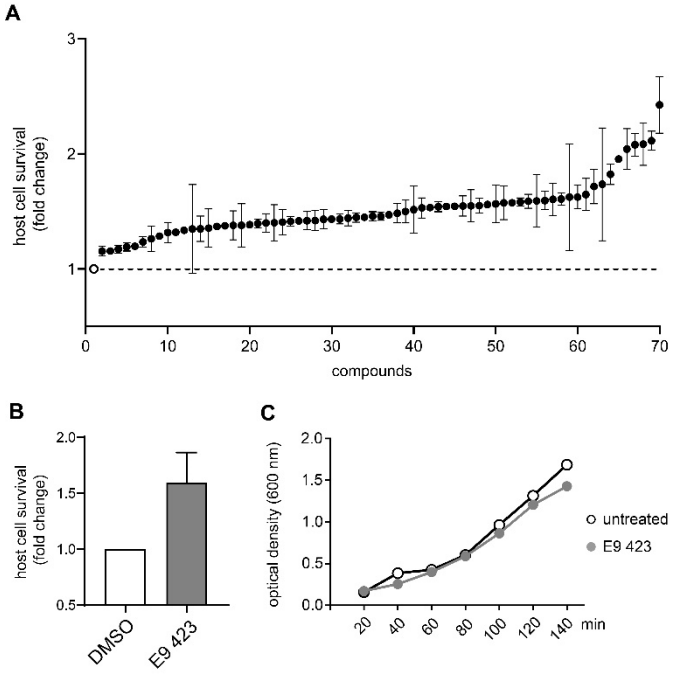

Figure 3. Identification of compounds with cytoprotective effect in a J774.2 Mφ cell-based screening assay targeting *S*T. (**A**) Summary of all compounds (n = 69) which led to an increase host cell survival in the J774.2 Mφ cell-based screening assay. Graph indicates fold change of host cell survival of infected Mφ cells treated with different compounds (black dots) compared to DMSO (white dot; dashed line) (**B**) Graph shows host cell survival of J774.2 Mφ incubated with E9 423 (gray bar) compared to cells treated with DMSO (white bar). Graphs show mean ± standard error of the mean. (**C**) Growth curve of *S*T strain SL 1344 in the presence of DMSO (white dots) or E9 423 (gray dots). Optical density measurements at 600 nm were performed at 20 min intervals.

To get a better understanding of the mechanisms of action of the compounds, we performed an in depth structural analysis. In line with the results of the *Pa* screening, we also could identify compounds with an indoline-2-one core structure, which are known to have a anti-virulence capability in several bacterial species [29]. The unique chemical structure of E9 423 (Table 2) awakened our interest. This compound showed a cytoprotective effect with an increase of host cell survival to 159% compared to cells treated with DMSO (Figure 3B). Furthermore, bacterial growth was not affected by E9 423 (Figure 3C). Thus, we hypothesized a possible T3SS-inhibitory effect of E9 423. To test this, we incubated bacteria overnight in T3SS inducing conditions by adding EGTA into LB broth. Afterwards bacteria were incubated with compounds for 4 h. After protein precipitation, the proteins of the supernatant were washed and analyzed by SDS-PAGE. Remarkably, bacteria treated with E9 423 showed decreased secretion of T3SS proteins in the supernatant (Figure 4). These data indicate that E9 423 protects infected Mφ by a T3SS-inhibitory effect.

Table 2. Chemical structure of E9 423.

Internal Number	Specs-ID	Chemical Structure
E9 423	AN-584/43416482	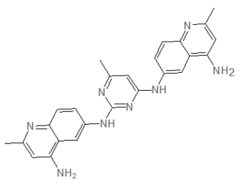

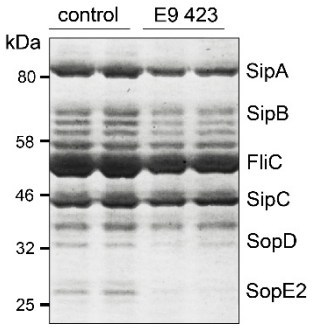

Figure 4. Analyzing of the T3SS-dependent secretion in presence of E9 423. Bacteria were grown overnight under T3SS-inducing conditions in LB media containing 5 mM EGTA. Subsequently bacteria were incubated with E9 423 or a control compound at a concentration of 50 µM for 4 h. After protein precipitation, proteins were washed and analyzed by SDS-Page using a Coomassie staining. Representative example of two individual experiments performed in duplicates.

4. Discussion

In this study, we describe the development of a highly comprehensive screening platform for detection of new anti-virulence drugs targeting *Pseudomonas aeruginosa* and *Salmonella* Typhimurium. Due to its simple batchwise setup without any required washing-steps this platform is in particular suitable for medium- and high-throughput screenings.

Functionality was first confirmed with T3SS-deficient bacterial strains, which indicated the ability to detect substances with anti-virulence activity. By testing 10,000 compounds of the Specs "World diversity set 3" we were able to identify several novel compounds with cytoprotective effects. Importantly, one novel inhibitor of the *S*T T3SS could be identified. Several other hit substances with chemical structures of unknown function provide the possibility for further research and the potential foundation of development of new drugs.

Since their implementation decades ago, usage of antibiotics has been accompanied by appearance of drug-resistant strains. While in the past development of new bactericidal and bacteriostatic substance was in the focus of interest, nowadays substances targeting virulence factors of bacteria and host-directed therapeutics attract more attention, not least due to the lack of new conventional antibiotics [11,30,31]. The difficulty in identification of truly novel antibiotics due to intrinsic resistance is also reflected in our screening results of 10,000 highly diverse compounds: Only one hit compound showed a reduction in bacterial viability in broth which was comparable to the conventional antibiotic moxifloxacin (Figure A1G). Nonetheless, exploiting this chemical library, several compounds with cytoprotective effects could be identified.

In both infection models, the treatment with various indoline-2-one derivates was associated with an increased host cell survival. As previously described we could not detect any growth-inhibitory effect of indoline-2-ones on *Pa* or *S*T. [32]. However, indole and indoline derivates such as 7-fluoroindole are known to inhibit a series of virulence factors of *Pa* such as quorum sensing, swarming and synthesis of pyocyanin, pyochelin and pyoverdine [29]. In *S*T an inhibition of motility as well as a reduced expression of SPI-1 encoded virulence genes in response to indoline exposure were described previously [33]. Indole was also shown to reduce flagellar motility and in vitro invasion of *S*T [34]. Furthermore Lee et al. described various impacts of indole and 7-hydroxyindole on the regulation of *Pa* virulence factors by microarray experiments [29]. By exploiting RNA-seq, we used a similar approach and were able to show indoline-2-one mediated downregulation of phzA1, phzB1, phzS, pchD, pvdM and pvdS, genes which are crucial for the biosynthesis of phenazine, pyochelin and pyoverdine [33,34]. The substance also led to a substantial downregulation of the T3SS export protein pscI. Inhibition of these factors may explain the host cell protective activity of our identified hit molecules.

Interestingly, differences in the efficacies of structurally distinct indoline-2-one derivates in *Pa* and *S*T could be observed: Only one compound (E7 344) was associated with an increased host cell survival

of > 150% for both pathogens. This observation indicates that besides the species-overarching effects of indoline-2-one derivates, also some derivates are species-specific most likely due to differences in transcriptional regulation of virulence factors.

In our study we also identified one novel compound (E9 423), which was able to reduce T3SS-mediated exotoxin secretion in *S*T. This compound is not an indoline-2-one derivate and, to our knowledge, similar chemical structures have not been described in the context of anti-bacterial or anti-T3SS activity. Further analyses are needed clarify the exact mechanism of E9 423 in *S*T.

Interestingly, we identified several cytoprotective compounds which failed to inhibit the T3SS of *S*T. An in-depth structural analysis revealed striking similarities in some of these compounds with known inhibitors of NLPR3 (NOD-, LRR- and pyrin domain-containing protein 3), a key regulator of pyroptotic cell death (Table A1) [35,36]. This indicates that these substances rather target host cell functions and that the observed cytoprotective effect may be mediated by preventing regulated necrotic cell death such as pyroptosis. Pyroptosis occurs upon activation of the innate immune response and the associated release of pro-inflammatory cytokines resulting in cell death in response to *S*T [37] These findings indicate that the here described host cell-based drug screening assays can identify inhibitors targeting both bacterial virulence factors as well as their effector mechanisms on the host side.

In summary, this study provides a robust and cost effective screening platform suitable for medium- and high-throughput screens that enables to identify not only molecules with antibiotic activity, but also anti-virulence and host-directed drugs, such as antibiotic prodrugs. By screening of 10,000 chemical compounds we could detect several substances with anti-virulence properties. In particular, one novel *S*T T3SS inhibitor and several novel indole-like inhibitors for one of which we identified dysregulation of *Pa* virulence associated genes by RNAseq. Finally, three potential inhibitors of necrotic host cell death could be identified in our *S*T screening. Further studies are now required to clarify the exact mechanism of action of these compounds. In addition, larger screening campaigns with more compounds should now be performed for the identification of novel inhibitors targeting these important Gram-negative pathogens.

Supplementary Materials: The following are available online at http://www.mdpi.com/2076-2607/8/8/1096/s1, Table S1: RNAseq *Pa*.

Author Contributions: Conceptualization and experimental design: J.R.; performed experiments and modelling: J.v.A., F.S., S.W., E.v.G.; analysis of data and model refinement: J.v.A., F.S., A.S.; supervision: J.R., A.S.; discussed the data: J.F.; discussed the data and wrote the manuscript: J.R., A.S., J.v.A., F.S. All authors have read and agreed to the published version of the manuscript.

Funding: This study was supported by a DZIF (German center for infection research) grant to F.S. and J.v.A. A.S. is supported by a fellowship of the Cologne Clinician Scientist Program (CCSP), funded by the German Research Council (FI 773/15-1). J.F. received funding from the German Center for Infection Research (DZIF) (TI 07.005_Fischer_00), the Cologne Fortune Program and the medical faculty of the University of Cologne, Germany (Gusyk funding).

Acknowledgments: PAO1F wildtype (WT), PAO1FΔ*pscD* mutant strain were kindly provided by A. Rietsch, Case Western Reserve University, Cleveland, Ohio, USA. We gratefully thank J. Altmueller, Cologne Center for Genomics (CCG) for assistance with the RNAseq experiments.

Conflicts of Interest: The authors declare no conflict of interest.

Appendix A

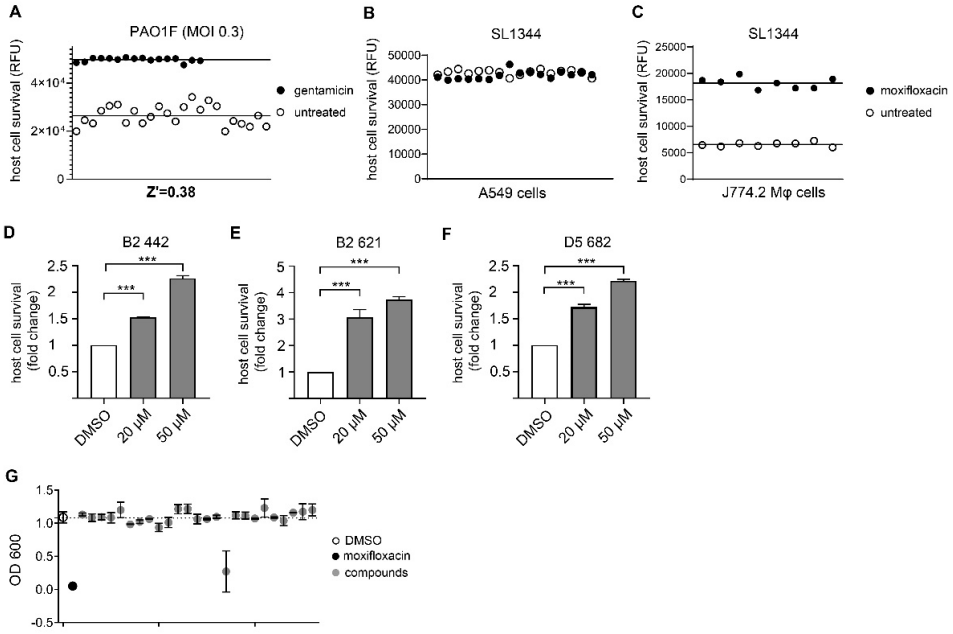

Figure A1. (**A**) A549 cells/well were seeded into a 96 well plate and subsequently infected with the WT strain PA01F with a MOI of 0.3 in the presence of gentamicin (black dots) or left untreated (white dots). Host cell survival was determined by addition of the fluorescent dye resazurin (RFU = relative fluorescence units). (**B**) A549 cells/well or J774.2 Mφ cells (**C**) were seeded into a 96 well plate and subsequently infected with the *S*T strain SL1344. DMSO (white dot), moxifloxacin (10 µM) (black dot). (**D**–**F**) A549 cells were infected with WT strain PA01F with a MOI of 0.5 in presence of 20 or 50 µM of different compounds (gray bars) which could be identified in the screening assay. Infection was abrogated after 4 h p.i. and cell viability was measured by fluorescence. Graphs show mean ± standard error of the mean compared to the negative control (DMSO). *** $p < 0.001$. (**G**) SL 1344 was grown for 24 h in BHI medium in presence of DMSO (white dot), moxifloxacin (10 µM) (black dot) or compounds of the Specs library (50 µM) (gray dots). Subsequently OD600 were measured using a microplate reader. Graph shows mean ± standard error of the mean.

Table A1. Selection of compounds with similarity to known NLRP3 inhibitors and cytoprotective effects in our *Salmonella*-infection model.

Internal Number	Specs-ID	Chemical Structure
D1 666	AQ-750/42209760	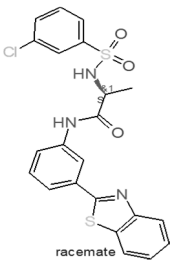 racemate
A2 668	AF-399/42309870	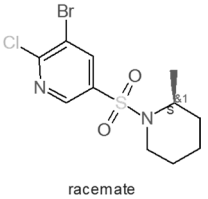 racemate

Table A1. *Cont.*

Internal Number	Specs-ID	Chemical Structure
G6 120	AO-079/15259251	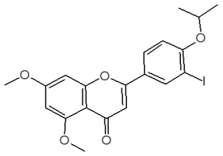

References

1. Cassini, A.; Hogberg, L.D.; Plachouras, D.; Quattrocchi, A.; Hoxha, A.; Simonsen, G.S.; Colomb-Cotinat, M.; Kretzschmar, M.E.; Devleesschauwer, B.; Cecchini, M.; et al. Attributable deaths and disability-adjusted life-years caused by infections with antibiotic-resistant bacteria in the EU and the European Economic Area in 2015: A population-level modelling analysis. *Lancet Infect. Dis.* **2019**, *19*, 56–66. [CrossRef]
2. Bassetti, M.; Peghin, M.; Vena, A.; Giacobbe, D.R. Treatment of Infections Due to MDR Gram-Negative Bacteria. *Front. Med. (Lausanne)* **2019**, *6*, 74. [CrossRef] [PubMed]
3. Eichenberger, E.M.; Thaden, J.T. Epidemiology and Mechanisms of Resistance of Extensively Drug Resistant Gram-Negative Bacteria. *Antibiotics* **2019**, *8*, 37. [CrossRef] [PubMed]
4. Exner, M.; Bhattacharya, S.; Christiansen, B.; Gebel, J.; Goroncy-Bermes, P.; Hartemann, P.; Heeg, P.; Ilschner, C.; Kramer, A.; Larson, E.; et al. Antibiotic resistance: What is so special about multidrug-resistant Gram-negative bacteria? *GMS Hyg. Infect. Control.* **2017**, *12*, Doc05. [CrossRef] [PubMed]
5. Pragasam, A.K.; Veeraraghavan, B.; Nalini, E.; Anandan, S.; Kaye, K.S. An update on antimicrobial resistance and the role of newer antimicrobial agents for Pseudomonas aeruginosa. *Indian J. Med. Microbiol* **2018**, *36*, 303–316. [CrossRef]
6. Uche, I.V.; MacLennan, C.A.; Saul, A. A Systematic Review of the Incidence, Risk Factors and Case Fatality Rates of Invasive Nontyphoidal Salmonella (iNTS) Disease in Africa (1966 to 2014). *PLoS Negl. Trop. Dis.* **2017**, *11*, 0005118. [CrossRef]
7. Dodds, D.R. Antibiotic resistance: A current epilogue. *Biochem. Pharm.* **2017**, *134*, 139–146. [CrossRef]
8. Pang, Z.; Raudonis, R.; Glick, B.R.; Lin, T.J.; Cheng, Z. Antibiotic resistance in Pseudomonas aeruginosa: Mechanisms and alternative therapeutic strategies. *Biotechnol. Adv.* **2019**, *37*, 177–192. [CrossRef]
9. Peng, M.; Salaheen, S.; Buchanan, R.L.; Biswas, D. Alterations of Salmonella enterica Serovar Typhimurium Antibiotic Resistance under Environmental Pressure. *Appl. Environ. Microbiol.* **2018**, *84*. [CrossRef]
10. Tacconelli, E.; Magrini, N.; Kahlmeter, G.; Singh, N. *Global Priority List of Antibiotic-Resistant Bacteria to Guide Research, Discovery, and Development of New Antibiotics*; World Health Organization: Geneva, Switzerland, 2017.
11. Anantharajah, A.; Mingeot-Leclercq, M.P.; Van Bambeke, F. Targeting the Type Three Secretion System in Pseudomonas aeruginosa. *Trends Pharmacol. Sci.* **2016**, *37*, 734–749. [CrossRef]
12. Gu, L.; Zhou, S.; Zhu, L.; Liang, C.; Chen, X. Small-Molecule Inhibitors of the Type III Secretion System. *Molecules* **2015**, *20*, 17659–17674. [CrossRef] [PubMed]
13. Felise, H.B.; Nguyen, H.V.; Pfuetzner, R.A.; Barry, K.C.; Jackson, S.R.; Blanc, M.P.; Bronstein, P.A.; Kline, T.; Miller, S.I. An inhibitor of gram-negative bacterial virulence protein secretion. *Cell Host Microbe* **2008**, *4*, 325–336. [CrossRef]
14. D'Angelo, F.; Baldelli, V.; Halliday, N.; Pantalone, P.; Polticelli, F.; Fiscarelli, E.; Williams, P.; Visca, P.; Leoni, L.; Rampioni, G. Identification of FDA-Approved Drugs as Antivirulence Agents Targeting the pqs Quorum-Sensing System of Pseudomonas aeruginosa. *Antimicrob. Agents Chemother.* **2018**, *62*, 11. [CrossRef] [PubMed]
15. Carabajal, M.A.; Asquith, C.R.M.; Laitinen, T.; Tizzard, G.J.; Yim, L.; Rial, A.; Chabalgoity, J.A.; Zuercher, W.J.; Garcia Vescovi, E. Quinazoline-Based Antivirulence Compounds Selectively Target Salmonella PhoP/PhoQ Signal Transduction System. *Antimicrob. Agents Chemother.* **2019**, *64*, e01744-19. [CrossRef] [PubMed]
16. Groisman, E.A. The pleiotropic two-component regulatory system PhoP-PhoQ. *J. Bacteriol.* **2001**, *183*, 1835–1842. [CrossRef] [PubMed]
17. Miller, S.I. PhoP/PhoQ: Macrophage-specific modulators of Salmonella virulence? *Mol. Microbiol.* **1991**, *5*, 2073–2078. [CrossRef]
18. Kuijl, C.; Savage, N.D.; Marsman, M.; Tuin, A.W.; Janssen, L.; Egan, D.A.; Ketema, M.; van den Nieuwendijk, R.; van den Eeden, S.J.; Geluk, A.; et al. Intracellular bacterial growth is controlled by a kinase network around PKB/AKT1. *Nature* **2007**, *450*, 725–730. [CrossRef]

19. Becker, K.A.; Riethmuller, J.; Seitz, A.P.; Gardner, A.; Boudreau, R.; Kamler, M.; Kleuser, B.; Schuchman, E.; Caldwell, C.C.; Edwards, M.J.; et al. Sphingolipids as targets for inhalation treatment of cystic fibrosis. *Adv. Drug Deliv. Rev.* **2018**, *133*, 66–75. [CrossRef]
20. Grassme, H.; Jendrossek, V.; Riehle, A.; von Kurthy, G.; Berger, J.; Schwarz, H.; Weller, M.; Kolesnick, R.; Gulbins, E. Host defense against Pseudomonas aeruginosa requires ceramide-rich membrane rafts. *Nat. Med.* **2003**, *9*, 322–330. [CrossRef]
21. Kornhuber, J.; Tripal, P.; Reichel, M.; Muhle, C.; Rhein, C.; Muehlbacher, M.; Groemer, T.W.; Gulbins, E. Functional Inhibitors of Acid Sphingomyelinase (FIASMAs): A novel pharmacological group of drugs with broad clinical applications. *Cell Physiol. Biochem.* **2010**, *26*, 9–20. [CrossRef]
22. Rybniker, J.; Vocat, A.; Sala, C.; Busso, P.; Pojer, F.; Benjak, A.; Cole, S.T. Lansoprazole is an antituberculous prodrug targeting cytochrome bc1. *Nat. Commun.* **2015**, *6*, 7659. [CrossRef]
23. SPECS Company. Available online: https://specs.net/pdf/SPECS-factsheet-world%20diversity%20set.pdf (accessed on 4 June 2020).
24. Zhang, J.H.; Chung, T.D.; Oldenburg, K.R. A Simple Statistical Parameter for Use in Evaluation and Validation of High Throughput Screening Assays. *J. Biomol. Screen.* **1999**, *4*, 67–73. [CrossRef] [PubMed]
25. Chi, E.; Mehl, T.; Nunn, D.; Lory, S. Interaction of Pseudomonas aeruginosa with A549 pneumocyte cells. *Infect. Immun.* **1991**, *59*, 822–828. [CrossRef] [PubMed]
26. Sun, Y.; Karmakar, M.; Taylor, P.R.; Rietsch, A.; Pearlman, E. ExoS and ExoT ADP ribosyltransferase activities mediate Pseudomonas aeruginosa keratitis by promoting neutrophil apoptosis and bacterial survival. *J. Immunol.* **2012**, *188*, 1884–1895. [CrossRef] [PubMed]
27. Foster, N.; Hulme, S.D.; Barrow, P.A. Vasoactive intestinal peptide (VIP) prevents killing of virulent and phoP mutant Salmonella typhimurium by inhibiting IFN-gamma stimulated NADPH oxidative pathways in murine macrophages. *Cytokine* **2006**, *36*, 134–140. [CrossRef] [PubMed]
28. Wemyss, M.A.; Pearson, J.S. Host Cell Death Responses to Non-typhoidal Salmonella Infection. *Front. Immunol.* **2019**, *10*, 1758. [CrossRef]
29. Lee, J.; Attila, C.; Cirillo, S.L.; Cirillo, J.D.; Wood, T.K. Indole and 7-hydroxyindole diminish Pseudomonas aeruginosa virulence. *Microb. Biotechnol.* **2009**, *2*, 75–90. [CrossRef]
30. Lewis, K. Platforms for antibiotic discovery. *Nat. Rev. Drug Discov.* **2013**, *12*, 371–387. [CrossRef]
31. Tacconelli, E.; Carrara, E.; Savoldi, A.; Harbarth, S.; Mendelson, M.; Monnet, D.L.; Pulcini, C.; Kahlmeter, G.; Kluytmans, J.; Carmeli, Y.; et al. Discovery, research, and development of new antibiotics: The WHO priority list of antibiotic-resistant bacteria and tuberculosis. *Lancet Infect. Dis.* **2018**, *18*, 318–327. [CrossRef]
32. Yuan, W.; Yu, Z.; Song, W.; Li, Y.; Fang, Z.; Zhu, B.; Li, X.; Wang, H.; Hong, W.; Sun, N. Indole-core-based novel antibacterial agent targeting FtsZ. *Infect. Drug Resist.* **2019**, *12*, 2283–2296. [CrossRef]
33. Kohli, N.; Crisp, Z.; Riordan, R.; Li, M.; Alaniz, R.C.; Jayaraman, A. The microbiota metabolite indole inhibits Salmonella virulence: Involvement of the PhoPQ two-component system. *PLoS ONE* **2018**, *13*, 190613. [CrossRef] [PubMed]
34. Nikaido, E.; Giraud, E.; Baucheron, S.; Yamasaki, S.; Wiedemann, A.; Okamoto, K.; Takagi, T.; Yamaguchi, A.; Cloeckaert, A.; Nishino, K. Effects of indole on drug resistance and virulence of Salmonella enterica serovar Typhimurium revealed by genome-wide analyses. *Gut Pathog.* **2012**, *4*, 5. [CrossRef] [PubMed]
35. Domiciano, T.P.; Wakita, D.; Jones, H.D.; Crother, T.R.; Verri, W.A., Jr.; Arditi, M.; Shimada, K. Quercetin Inhibits Inflammasome Activation by Interfering with ASC Oligomerization and Prevents Interleukin-1 Mediated Mouse Vasculitis. *Sci. Rep.* **2017**, *7*, 41539. [CrossRef] [PubMed]
36. Lamkanfi, M.; Mueller, J.L.; Vitari, A.C.; Misaghi, S.; Fedorova, A.; Deshayes, K.; Lee, W.P.; Hoffman, H.M.; Dixit, V.M. Glyburide inhibits the Cryopyrin/Nalp3 inflammasome. *J. Cell Biol.* **2009**, *187*, 61–70. [CrossRef]
37. Broz, P.; Newton, K.; Lamkanfi, M.; Mariathasan, S.; Dixit, V.M.; Monack, D.M. Redundant roles for inflammasome receptors NLRP3 and NLRC4 in host defense against Salmonella. *J. Exp. Med.* **2010**, *207*, 1745–1755. [CrossRef]

Cell

Discovery of highly neutralizing human antibodies targeting *Pseudomonas aeruginosa*

Graphical abstract

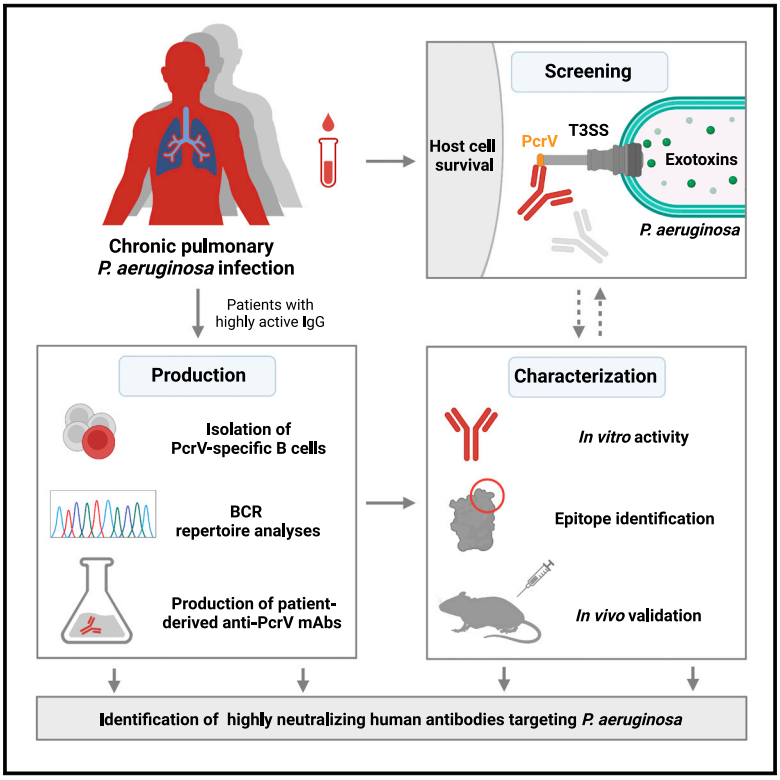

Highlights:

- Chronic *P. aeruginosa* infection leads to the development of anti-PcrV antibodies
- Diverse B cell response to PcrV with the formation of T3SS-neutralizing mAbs
- Highly vulnerable C-terminal PcrV epitopes are targeted by neutralizing antibodies
- Anti-PcrV antibodies may be a therapeutic option for acute infections

Authors

Alexander Simonis, Christoph Kreer, Alexandra Albus, ..., Silke van Koningsbruggen-Rietschel, Florian Klein, Jan Rybniker

Correspondence

alexander.simonis@uk-koeln.de (A.S.), jan.rybniker@uk-koeln.de (J.R.)

In brief

Drug-resistant *Pseudomonas aeruginosa* poses an emerging threat to human health with an urgent need for alternative therapeutic approaches. Elucidation of the human immune response to the *P. aeruginosa* type 3 secretion system reveals highly potent T3SS-neutralizing antibodies with antibiotic-like activity *in vivo*.

Simonis et al., 2023, Cell *186*, 1–16
November 9, 2023
https://doi.org/10.1016/j.cell.2023.10.002

CellPress

Please cite this article in press as: Simonis et al., Discovery of highly neutralizing human antibodies targeting *Pseudomonas aeruginosa*, Cell (2023), https://doi.org/10.1016/j.cell.2023.10.002

Cell

CellPress

Article

Discovery of highly neutralizing human antibodies targeting *Pseudomonas aeruginosa*

Alexander Simonis,[1,2,3,17,*] Christoph Kreer,[4,17] Alexandra Albus,[1,2] Katharina Rox,[5,6] Biao Yuan,[7,8,9] Dmitriy Holzmann,[1,2] Joana A. Wilms,[1,2] Sylvia Zuber,[1,2] Lisa Kottege,[4] Sandra Winter,[1,2] Meike Meyer,[10,11] Kristin Schmitt,[1,2] Henning Gruell,[2,4] Sebastian J. Theobald,[1,2] Anna-Maria Hellmann,[2,12] Christina Meyer,[1,2] Meryem Seda Ercanoglu,[4] Nina Cramer,[13] Antje Munder,[13,14] Michael Hallek,[1,2] Gerd Fätkenheuer,[1,3] Manuel Koch,[15] Harald Seifert,[3,16] Ernst Rietschel,[10,11] Thomas C. Marlovits,[7,8,9] Silke van Koningsbruggen-Rietschel,[10,11] Florian Klein,[2,3,4,17] and Jan Rybniker[1,2,3,17,18,*]

[1]Department I of Internal Medicine, Faculty of Medicine and University Hospital Cologne, University of Cologne, 50937 Cologne, Germany
[2]Center for Molecular Medicine Cologne (CMMC), Faculty of Medicine and University Hospital Cologne, University of Cologne, 50931 Cologne, Germany
[3]German Center for Infection Research (DZIF), partner site Bonn-Cologne, 50937 Cologne, Germany
[4]Laboratory of Experimental Immunology, Institute of Virology, Faculty of Medicine and University Hospital Cologne, University of Cologne, 50931 Cologne, Germany
[5]Department of Chemical Biology, Helmholtz Centre for Infection Research (HZI), 38124 Braunschweig, Germany
[6]German Center for Infection Research (DZIF), partner site Hannover-Braunschweig, 38124 Braunschweig, Germany
[7]Institute of Structural and Systems Biology, University Medical Center Hamburg-Eppendorf (UKE), 22607 Hamburg, Germany
[8]Centre for Structural Systems Biology (CSSB), 22607 Hamburg, Germany
[9]Deutsches Elektronen-Synchrotron Zentrum (DESY), 22607 Hamburg, Germany
[10]CF Centre, Pediatric Pulmonology and Allergology, University Children's Hospital Cologne, Faculty of Medicine and University Hospital Cologne, University of Cologne, 50937 Cologne, Germany
[11]Centre for Rare Diseases, Faculty of Medicine and University Hospital Cologne, University of Cologne, 50937 Cologne, Germany
[12]Department of Experimental Pediatric Oncology, University Children's Hospital Cologne, Faculty of Medicine and University Hospital Cologne, University of Cologne, 50937 Cologne, Germany
[13]Department of Pediatric Pneumology, Allergology and Neonatology, Hannover Medical School, 30625 Hannover, Germany
[14]Biomedical Research in Endstage and Obstructive Lung Disease (BREATH), German Center for Lung Research, 30625 Hannover, Germany
[15]Institute for Dental Research and Oral Musculoskeletal Biology, Center for Biochemistry, Faculty of Medicine and University Hospital Cologne, University of Cologne, 50931 Cologne, Germany
[16]Institute for Medical Microbiology, Immunology and Hygiene, Faculty of Medicine and University Hospital of Cologne, University of Cologne, 50935 Cologne, Germany
[17]These authors contributed equally
[18]Lead contact
*Correspondence: alexander.simonis@uk-koeln.de (A.S.), jan.rybniker@uk-koeln.de (J.R.)
https://doi.org/10.1016/j.cell.2023.10.002

SUMMARY

Drug-resistant *Pseudomonas aeruginosa* (PA) poses an emerging threat to human health with urgent need for alternative therapeutic approaches. Here, we deciphered the B cell and antibody response to the virulence-associated type III secretion system (T3SS) in a cohort of patients chronically infected with PA. Single-cell analytics revealed a diverse B cell receptor repertoire directed against the T3SS needle-tip protein PcrV, enabling the production of monoclonal antibodies (mAbs) abrogating T3SS-mediated cytotoxicity. Mechanistic studies involving cryoelectron microscopy identified a surface-exposed C-terminal PcrV epitope as the target of highly neutralizing mAbs with broad activity against drug-resistant PA isolates. These anti-PcrV mAbs were as effective as treatment with conventional antibiotics *in vivo*. Our study reveals that chronically infected patients represent a source of neutralizing antibodies, which can be exploited as therapeutics against PA.

INTRODUCTION

Antimicrobial resistance (AMR) is an emerging global threat with increasing morbidity and mortality worldwide.[1] This critical situation is aggravated by an innovation and discovery gap leading to a tremendous lack of substances with antibacterial activity.[2] Alternative approaches such as antibody- or bacteriophage-based therapies as well as anti-virulence or host-directed drugs seem to be required to meet the global needs of therapeutics active against drug-resistant bacteria.[3–7]

In the last two decades, several studies demonstrated the therapeutic potential of neutralizing antibodies against viral infections.[8–13] Here, broadly neutralizing antibodies (bNAbs) were mainly identified by performing a comprehensive

Please cite this article in press as: Simonis et al., Discovery of highly neutralizing human antibodies targeting *Pseudomonas aeruginosa*, Cell (2023), https://doi.org/10.1016/j.cell.2023.10.002

assessment of antigen-reactive B cells often derived from infected, convalescent, or vaccinated individuals.[14] While numerous antibodies have been developed to target viral pathogens, there is only a limited number of studies describing potent antibody-mediated treatment approaches against bacterial pathogens.[15–17]

In our work, we focused on the development of therapeutic antibodies targeting *Pseudomonas aeruginosa* (PA), a gram-negative pathogen that frequently causes severe nosocomial infections including pneumonia and sepsis.[18] PA has been classified as a serious threat to the public health by the Centers for Disease Control and Prevention (CDC) and the World Health Organization (WHO) because of extensive intrinsic and extrinsic resistance mechanisms.[19,20] Besides acute infections, PA is also capable of causing chronic infections, for instance, in patients with structural lung diseases such as cystic fibrosis (CF), a monogenetic disease determined by CF transmembrane conductance regulator (CFTR) mutations.[21] Decreased mucociliary clearance of the bronchial system and production of a nutrient-rich, hyper-viscous airway mucus in this disease provide ideal growth conditions for opportunistic pathogens such as PA.[22]

A key virulence factor of PA is the type III secretion system (T3SS), a syringe-like, multiprotein structure that injects effector toxins into the cytosol of host cells leading to cell lysis and tissue damage.[23,24] The T3SS has been linked to bacterial persistence, higher relapse rates, and increased mortality in infected patients.[25,26] PcrV, a pentameric structural protein, forms the T3SS needle-tip complex that is required for appropriate assembly of the PopB/D translocon complex and its insertion into the host cell membrane.[27,28] As immunogenicity of PcrV has been known for decades, several studies have been focusing on antibody-mediated abrogation of PcrV function to inhibit virulence of PA.[29–38] These works relied on immunization of mice to generate PcrV-specific antibody sequences. As PA can reside over years in the airways of people with CF (pwCF), we hypothesized that the repetitive antigen exposure in these patients fosters a highly affinity-matured adaptive immune response, which results in the development of antibodies potently inhibiting virulence of PA.[39,40]

Here, we show that PA-infected pwCF mount a diverse B cell response to PcrV, including the formation of T3SS-neutralizing antibodies in a subgroup of patients. These antibodies can be used as highly effective antipseudomonal agents.

RESULTS

Chronic infection with PA induces the development of T3SS-neutralizing IgG in pwCF

To decipher if chronic infection with PA leads to the development of highly neutralizing PcrV antibodies, we conducted a study in adult pwCF (n = 51) showing persistent detection of PA in sputum. Healthy individuals (n = 51) without any history of PA infection were used as the control group (Table S1). In a first step, serum samples were collected to detect T3SS-neutralizing activity in a phenotypic screening assay (Figure 1A). For this, we established a sensitive cytotoxicity assay relying on T3SS-induced lysis of human erythrocytes (red blood cells [RBCs]), which was determined by measuring the optical density (OD) of cell supernatants as an indicator of hemoglobin release (Figure S1A).[41] Incubation of RBCs with the wild-type PA strain PA14 led to a strong and significant increase of the $OD_{540\ nm}$ (median [IQR (interquartile range)]: 0.047 [0.045–0.052] vs. 0.237 [0.191–0.277]; $p < 0.001$), which could be abrogated by adding the antibiotic gentamicin (median [IQR]: 0.074 [0.062–0.081]; $p < 0.001$) (Figure 1B). Next, we tested heat-inactivated serum from healthy donors and pwCF at different concentrations (1:200 to 1:800). At all concentrations, we observed a stronger inhibition of PA-induced hemolysis (calculated to infected and untreated RBCs relatively) for the pwCF group compared with healthy individuals (median [IQR]: 1:200 serum dilution: 36.95% [22.87%–54.72%] vs. 83.28% [75.10%–98.06%]; $p < 0.001$; 1:800 serum dilution: 64.76% [45.77%–76.45%] vs. 99.64% [85.68%–105.4%]; $p < 0.001$) (Figures 1C and S1B; Table S1). Across all groups, we identified a higher interindividual variety in the CF (cystic fibrosis) group and, importantly, individuals whose sera efficiently blocked hemolysis even at low concentrations (inhibition > 50% at a 1:800 serum dilution: CF 15/51 individuals [range 11.29%–102.6%]; healthy 0/51 [range 72.87%–113.6%]) (Table S1). Notably, immunoglobulin G (IgG)-mediated off-target effects were excluded by using pooled polyclonal IgG from healthy donors (intravenous immunoglobulin [IVIG]) as well as non-IgG-mediated effects (e.g., through patients' medication) by using purified IgG from both groups (Figures S1C–S1E). Incubation of PA with purified IgG had no impact on bacterial growth in broth, indicating that patient-derived IgG does not alter processes essential for bacterial replication (Figure S1F). We next correlated serum-mediated inhibition of hemolysis to anti-PcrV serum IgG titer by performing PcrV-binding ELISA (enzyme-linked immunosorbent assay) with affinity-purified monomeric PcrV (Figure S1G). As expected, we detected increased PcrV titers in serum samples of the CF group compared with healthy individuals with a median half-maximal effective concentration (EC_{50}) at a dilution of 1:330 (healthy; n = 51) vs. 1:892 (CF; n = 51) ($p = 0.0002$) (Figures 1D and S1H; Table S1). In line with our previous results, we detected a higher interindividual variability in serum activity of the CF group with titers ranging from 1:84 – 1:47,725 versus 1:42 – 1:5,634 in the healthy cohort. Increased PcrV titers observed in some healthy controls may derive from asymptomatic colonization or previous infection with PA. Finally, we correlated the PcrV titer with results from the hemolysis assay, revealing a moderate correlation with a Spearman's Rho of −0.602 for the CF group (Figure 1E). However, all individuals whose sera had a strong inhibitory effect (>50%) showed increased PcrV titers (>1:720), indicating that anti-PcrV antibodies play a key role in the antibody-mediated inhibition of hemolysis (Figure 1E; Table S1). Interestingly, we observed a nearly significant correlation between the duration of colonization in individual patients and the corresponding anti-hemolytic activity of their serum, while we found no evidence of a correlation of anti-PcrV antibody levels or anti-hemolytic activity with hospitalization frequency or lung function (Figure S2A).

Chronically infected individuals develop a polyclonal B cell response against the PcrV protein

To link B cell-derived PcrV antibodies to IgG-mediated inhibition of T3SS dependent hemolysis, we aimed to isolate PcrV-reactive

Please cite this article in press as: Simonis et al., Discovery of highly neutralizing human antibodies targeting *Pseudomonas aeruginosa*, Cell (2023), https://doi.org/10.1016/j.cell.2023.10.002

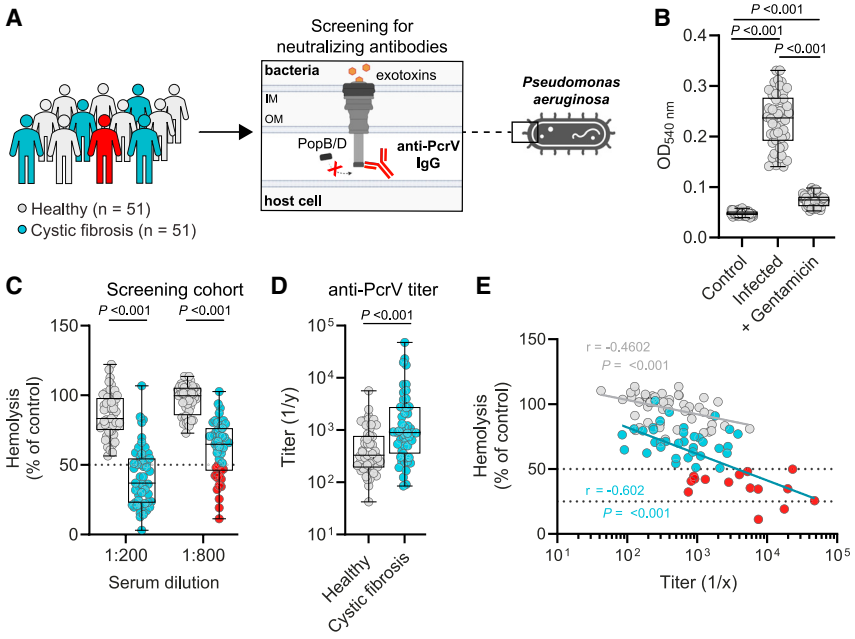

Figure 1. Functional screening of serum indicates presence of T3SS-neutralizing IgG in cystic fibrosis patients

(A) Study design of the project: a cohort of 51 people with cystic fibrosis (pwCF) with persistent detection of PA in sputum and 51 healthy individuals were screened for type III secretion system (T3SS)-neutralizing antibodies.

(B) Human red blood cells (RBCs) were infected with PA wild-type strain PA14: MOI (multiplicity of infection) of 1 ± gentamicin (20 μg/mL) or left uninfected (control). $OD_{540\ nm}$ was quantified as marker of bacteria-induced cell lysis (hemolysis). Significance was calculated using a one-way ANOVA with Tukey's multiple comparisons test.

(C) Heat-inactivated sera of the CF group (n = 51) (cyan) and healthy control group (n = 51) (gray) were added at different concentrations (1:200 and 1:800) during infection of human red blood cells with PA14, as in (B). Percentage of hemolysis for each individual was calculated to infected and untreated red blood cells. Individuals with highly neutralizing serum activity are highlighted in red (hemolysis < 50% at 1:800 dilution). Significance was calculated using a two-way ANOVA with a Sidak's multiple comparisons test comparing each group within one dilution.

(D) PcrV-binding ELISA were performed with diluted serum samples from healthy (n = 51) and individuals with cystic fibrosis (n = 51). Median effective concentrations (EC_{50}) of the calculated binding curves were determined as PcrV titer. Significance was calculated using a Mann-Whitney U test.

(E) Anti-PcrV titer in serum of pwCF (cyan) and healthy individuals (gray) (D) were plotted against the results of the hemolysis assay at a 1:800 serum dilution, as in (C). Significances were tested using Spearman's rank correlations. Individuals with highly neutralizing serum activity are highlighted in red (hemolysis < 50% at 1:800 dilution).

Boxplots indicate the median, the upper and lower quartile, and the minimum and maximum values. Shown data points represent the technical mean of an independent experiment/biological replicate.

See also Figure S1 and Table S1.

B cells by flow cytometry using fluorescently labeled monomeric PcrV. To test our approach, we cloned a PcrV-specific antibody sequence (1F3), which had been generated in PcrV-immunized mice, into a cell-surface expression vector as a surrogate for PcrV-specific B cells.[42] Transfected HEK293T cells bound fluorescent recombinant PcrV ($PcrV^{AF488}$ and $PcrV^{AF647}$), as shown by flow cytometry (Figure 2A). Subsequently, patient-derived peripheral blood mononuclear cells (PBMCs) were isolated, enriched for B cells, co-incubated with $PcrV^{AF488}$/$PcrV^{AF647}$, and analyzed by flow cytometry (Figure 2B). B cells of three individuals with evidence for highly neutralizing antibody titer were selected for in-depth single-B cell and IgG sequence analysis. Fluorescence-activated cell sorting (FACS) revealed a frequency of 0.024%–0.047% for PcrV-specific B cells in the $CD20^+$ IgG^+ population (Figure 2C; Table S2). By analyzing 186 single-cell IgG sequences from all 3 individuals, 151 productive heavy and 138 productive light chains were identified. Despite the relatively low number of cells per individual (CF #11: n = 56; CF #23: n = 55; CF #30: n = 40), we found identical and related sequences within each of the three donors, indicative of a pathogen-specific response with individual dominant clones for each donor (Figure 2D; Table S2). Sequence annotation revealed a broad spectrum of heavy-chain complementarity-determining region 3 (CDRH3) length and V gene distributions that are comparable to whole IgG reference repertoires, without signs of dominant public clonotypes (Figures 2E and 2F; Table S3).[43] Interestingly, while the majority of antibodies belong to the IgG1 isotype, IgG2-class antibodies were enriched in donors CF #11 and CF #30, an observation typically linked to bacterial polysaccharide-binding antibodies and low effector functions (Figure 2G).[44] Taken together, we conclude that chronic infection with PA can induce an oligo- to polyclonal B cell response with development of donor-specific prevalent clones.

Patient-derived anti-PcrV antibodies with high affinity and potent neutralizing activity

To investigate the functionality of anti-PcrV antibodies, we recombinantly produced 79 PcrV-specific monoclonal IgG antibodies, of which 43 (CF #11: n = 20; CF #23: n = 13; CF #30: n = 10) were confirmed to bind PcrV by ELISA with EC_{50} values in the range of 7.22–121.42 ng/mL (median [IQR]: 23.66 ng/mL [15.72–35.09 ng/mL]) (Figures 3A and S2G; Table S4). To determine neutralizing activity, all 43 binding antibodies were initially screened at 5 μg/mL in the hemolysis assay (Figure 1B), revealing a broad range from undetectable to highly potent inhibition of hemolysis (hemolysis compared with a control: range 14.14%–100.02%, median [IQR]: 57.16% [28.25%–75.43%]) (Figure 3B; Table S4). We were able to isolate antibodies from all three individuals that exhibited potent inhibition of hemolysis at 5 μg/mL. The mouse-derived antibody 1F3 as well as

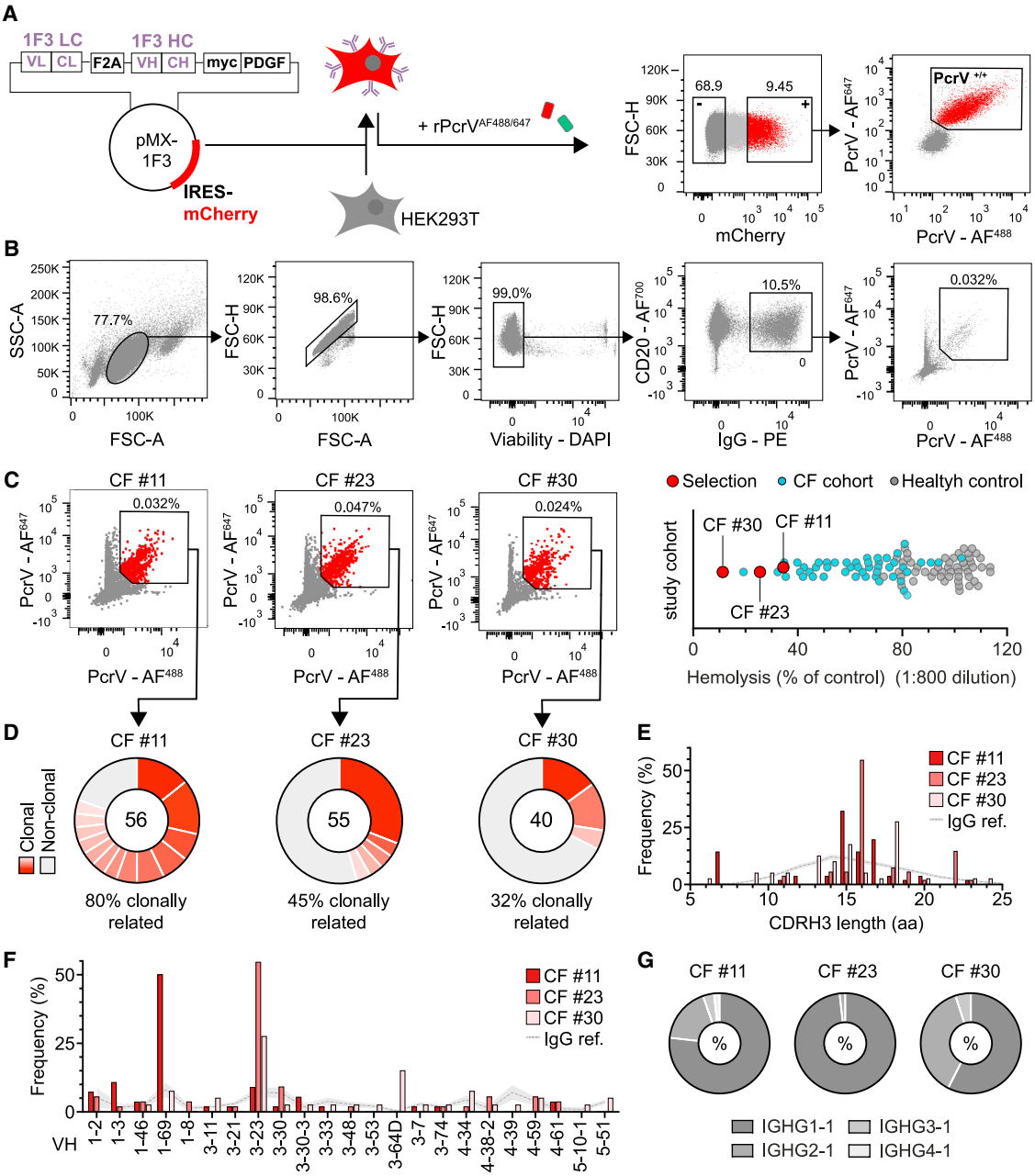

Figure 2. Isolation of PcrV-specific B cells from chronically PA-infected individuals

(A) Variable and constant regions of immunoglobulin (Ig) light (VL, CL) and heavy chains (VH, CH) of a mouse-derived anti-PcrV antibody (1F3) were cloned into a vector with a F2A self-cleaving signal sequence between the VL and VH, followed by a c-*myc* and a platelet-derived growth factor (PDGF) transmembrane domain. Transfected HEK293T mCherry-positive cells were co-incubated with recombinant PcrV labeled with Alexa Fluor 647 and Alexa Fluor 488 and quantified.

(B) Gating strategy for the isolation of PcrV-specific B cells from CD19-enriched PBMCs.

(C) PcrV-specific B cell population, isolated by fluorescence-activated cell sorting (FACS), is shown for every donor. PBMCs from individuals with evidence of highly neutralizing antibodies (red: CF #11, CF #23, CF #30) were used (right plot: CF group is indicated in cyan; healthy individuals in gray; donors in red).

(D) PcrV-specific IgG^{+} B cell clones (identical VH/VJ gene and CDRH3 identity $\geq$ 75%) for each individual are shown in shades of red. B cells without corresponding clones are shown in gray. Clonal size is proportional to the number of clonal members (the total number of analyzed cells is shown in the center of the pie charts).

(E) Heavy-chain CDR3 amino acid length is shown for each donor indicated by individual shades of red. Frequency (%) is calculated to the total number of analyzed cells of each donor. The gray dashed line indicates the mean CDRH3 length distribution of whole peripheral IgG repertoires from a reference dataset of healthy blood donors (n = 57).[43]

(legend continued on next page)

Please cite this article in press as: Simonis et al., Discovery of highly neutralizing human antibodies targeting *Pseudomonas aeruginosa*, Cell (2023), https://doi.org/10.1016/j.cell.2023.10.002

gentamicin (20 μg/mL) were used as controls (Figure 3B). Antibodies with enhanced neutralizing qualities (>50% inhibition of cell lysis, n = 20) were titrated to determine the half-maximal inhibitory concentration (IC_{50}), demonstrating that 14 antibodies showed lower IC_{50} values than 1F3 (Figure 3C; Table S4). Interestingly, PcrV-binding affinity was not correlated with neutralization, pointing toward different binding epitopes as a cause of the observed heterogenicity among the human monoclonal antibodies (mAbs) (Figure S2H). To strengthen this hypothesis, we performed extensive competition ELISA experiments delineating a diverse set of antibodies competing for distinct binding regions (Figure 3D). Importantly, clusters of antibodies with high neutralizing qualities (cluster IVa and IVb) were identified, while non-neutralizing antibodies clustered mainly in other groups.

In order to determine vulnerable PcrV epitopes of antibodies belonging to cluster IVa and IVb (16 antibodies in total), we performed cryoelectron microscopy (cryo-EM) experiments of the potently neutralizing antibody 30-B8 (cluster IVb; Figure 3D) and the non-neutralizing antibody (11-E5; cluster V; Figure 3D) as a control. To this end, we first expressed a PcrV-fusion protein linked to an N-terminal maltose binding protein (MBP) which increased the molecular weight of the target protein from 32 to 74 kDa. Subsequently, MBP-PcrV in complex with antigen-binding fragments (Fab) derived from 30-B8 and 11-E5 were prepared and isolated by size-exclusion chromatography (Figures S3A and S3B). Both complexes (30-B8/MBP-PcrV and 11-E5/MBP-PcrV) were resolved to ~5 Å (Figures 4A, 4B, S3C, and S3D), and models were generated (Figures S3E and S3F; Table S5). While the interaction sites between the C-terminal PcrV region and the antibodies could be clearly identified, no map densities were visible, neither for MBP nor for the N-terminal region of PcrV, suggesting that these domains are highly flexible (Figures 4C–4E). Consistent with the epitope mapping (Figure 3D), our structural data revealed that 30-B8 and 11-E5 bind to different regions of PcrV: while the neutralizing 30-B8 antibody showed an interaction with the periphery of the C-terminal region of the PcrV pentamer (Figures 4D–4H), the non-neutralizing antibody 11-E5 bound to the inner face of the conduit formed by two long helices of PcrV. This suggests that the neutralizing ability is restricted to surface-exposed epitopes of the pentameric form of PcrV (Figures 4F–4H), which provides a vulnerable immunodominant site that can be targeted by numerous cluster IVa and IVb antibodies.

Human anti-PcrV antibodies show a potent anti-virulence effect *in vitro*

To select the most potent mAbs, we adapted a previously described infection assay, which quantifies T3SS-mediated lytic cell death of A549 lung epithelial cells.[45] Here, metabolic activity as indicator for A549 cell viability was determined with resazurin, a cell-permeable, redox-sensitive fluorescent dye (Figures 5A and 5B). T3SS-dependent lysis of A549 cells was confirmed by incubating cells with the T3SS-deficient PAO1FΔ*pscD* strain, which had no impact on cell viability (Figure S4A). We first tested the neutralizing effects of a total of 20 mAbs at a concentration of 50 μg/mL. Of note, all of these antibodies had shown >50% inhibitory activity in the hemolysis-based assay (Figure 5C; Table S4). While most antibodies showed a neutralizing effect, only a few were identified as highly neutralizing antibodies. In total, 7 out of 20 antibodies inhibited bacteria-induced cell death with a cell viability of >80%, which was calculated in comparison with uninfected controls (Table S4). The mouse-derived antibody 1F3 as well as polyclonal human antibodies (IVIG) did not protect cells from PA-mediated cell death in this stringent assay (Figures 5C and S4B; Table S4). Three patient-derived antibodies (30-B8, 30-D7, and 30-D9) protected cells nearly completely (>90%), similar to treatment with the antibiotic gentamicin (30-B8: 90.45%, 30-D7: 91.83%, and 30-D9: 96.42% vs. gentamicin: 95.41% viability) (Figure 5C; Table S4).

We next performed serial dilution experiments to determine IC_{50} values of human anti-PcrV mAbs, 1F3, and MEDI3902 (gremubamab), a bispecific PcrV-Psl antibody, which showed good activity in pre-clinical experiments but did not prevent PA-associated pneumonia in early clinical trials.[36,38,46] MEDI3902 protected A549 cells from PA-induced cytotoxicity with an IC_{50} of 11.46 μg/mL, whereas the most potent patient-derived antibody 30-D9 had a 144-fold improved IC_{50} of 79.5 ng/mL (Figures 5D and S4C–S4G; Table S4). For 1F3, we were not able to determine the IC_{50} in the tested range of antibody concentrations (Figure 5D). Putative binding regions were also tested for MEDI3902 and 1F3, using competition ELISA experiments, which revealed that MEDI3902 exploits other binding sites than the most potent human anti-PcrV mAbs (Figure S4H). All tested human anti-PcrV antibodies showed no sign of autoreactivity in a HepG2 cell-based autoreactivity assay. Moderate cytoplasmatic autoreactivity was observed for the mouse-derived anti-PcrV mAb 1F3 (Figure S4I).

Highly neutralizing antibodies are active against drug-resistant clinical isolates

To further address clinical relevance of our findings, we assessed neutralizing activity of anti-PcrV mAbs against clinical strain isolates from patients with bloodstream infections. Compared with the reference strain PAO1, the human mAbs showed similar activity against clinical isolates, including those with high levels of resistance against commonly used antibiotics (Figures 5E, 5F, S5A, and S5B). To exclude any natural resistance mechanisms by mutations and to estimate the effective spectrum of highly neutralizing patient-derived anti-PcrV mAbs in a clinical setting, the *pcrV* genes of 30 clinical isolates were sequenced and compared with the *pcrV* gene sequence of the reference strain PAO1. In most of the isolates, silent mutations

(F) Differences in frequencies of heavy-chain VH gene segments of different donors (displayed are only segments that have been found at least once in one donor). Gray line shows reference distribution from the same healthy blood donor dataset as in (E).
(G) IgG isotype of analyzed PcrV-specific IgG^+ B cells for each donor. Shades of gray indicate different IgG isotypes as indicated. Size of the pies is proportional and calculated relatively to the total number of analyzed B cells for each donor (CF #11: n = 56; CF #23: n = 55; CF #30: n = 40).
Shown data points represent the technical mean of a biological replicate.
See also Tables S2 and S3.

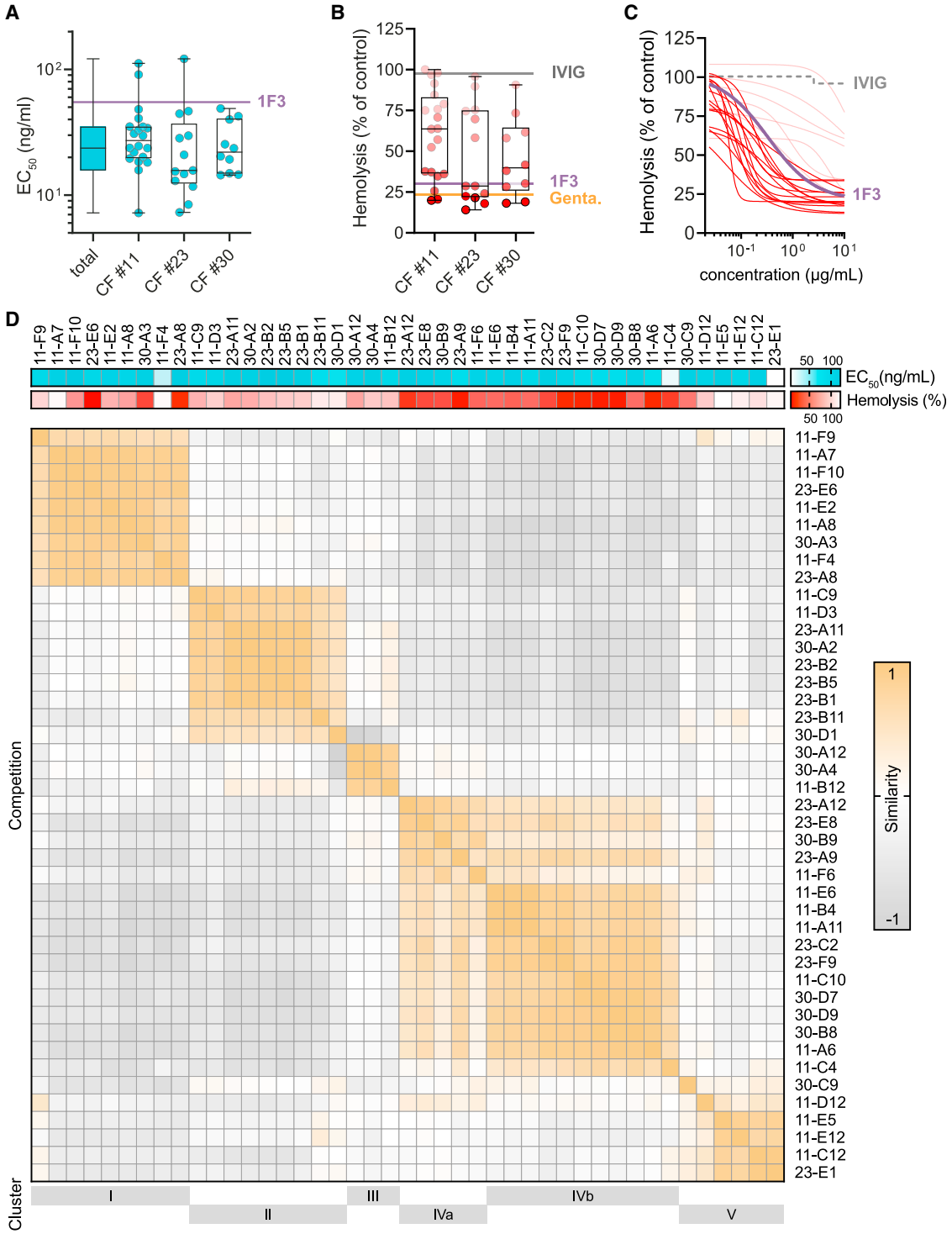

Figure 3. Heterogeneity of human anti-PcrV mAbs

(A) Binding of patient-derived mAbs (n = 43) to the PcrV protein was confirmed by ELISA. Antibodies were serial diluted (4-fold) starting at a concentration of 5 µg/mL. Median effective concentrations (EC_{50}) were calculated for each antibody and are shown for each donor (total n = 43; CF #11: n = 20; CF #23: n = 13; CF #30: n = 10). The EC_{50} of the humanized mouse-derived anti-PcrV antibody (1F3) was determined as a control (purple line).

(B) Corresponding to (A), neutralizing efficacy of the antibodies was determined by measuring bacteria-induced cell lysis of human red blood cells in presence of the respective mAb (5 µg/mL). Degree of hemolysis was measured and calculated for each antibody, compared with the control (infected, untreated cells). As further controls, cells were infected in presence of polyclonal IgG (IVIG) (gray line), 1F3 (5 µg/mL) (purple line), or gentamicin (20 µg/mL) (orange line).

(legend continued on next page)

Please cite this article in press as: Simonis et al., Discovery of highly neutralizing human antibodies targeting *Pseudomonas aeruginosa*, Cell (2023), https://doi.org/10.1016/j.cell.2023.10.002

were detected. In total, five different mutations were detected leading to amino acid changes in PcrV (Table S6). However, none of the observed mutations led to a loss of function of the tested human anti-PcrV mAb 30-B8. Collectively, these data underline the feasibility of this therapeutic approach, particularly against drug-resistant PA isolates (Figures S5A and S5B).

Determination of the *in vivo* potency of patient-derived anti-PcrV mAbs

To assess the *in vivo* function and efficacy of human B cell-derived mAbs, we conducted three different experiments: First, we performed pharmacokinetic studies to determine mAb plasma levels of different human anti-PcrV mAbs (Figure S5C). Application of human anti-PcrV mAbs (n = 3) was tolerated without any adverse effects, and human IgG levels were detectable from the first time point after 15 min and reached a calculated half-maximum concentration between 13.6 min (11-C10) and 84.5 min (30-B8) (Figure S5D). Over a time course of 72 h, we did not observe a relevant decline of human IgG concentrations in plasma of exposed animals. Calculated maximum plasma concentrations ranged between 9.72 μg/mL (11-C10) and 10.05 μg/mL (23-F9) after injection of 5 mg/kg, which was well above the calculated *in vitro* IC_{50} of the respective antibodies. Next, we tested the therapeutic efficacy of two highly neutralizing anti-PcrV mAbs in a pneumonia mouse model.[47] Pneumonia was induced by aerosolized delivery of PA (Boston 41501 strain). Anti-PcrV mAbs (5 mg/kg), a vehicle control, or the conventional antimicrobial levofloxacin (100 mg/kg) was administered 2 h later intraperitoneally (Figure S5E). After 24 h, mice were sacrificed and the bacterial load was determined by counting colony-forming units (CFUs) in lung tissue homogenates. The treatment of animals with patient-derived anti-PcrV mAbs led to a pronounced reduction of the bacterial burden in mouse lungs (Figure 6A). For the mAb 30-B8, growth inhibitory effects were comparable to treatment with levofloxacin (mean CFUs: control 1.00×10^9 vs. levofloxacin 1.15×10^5, 30-B8 4.59×10^3, and 30-D9 2.70×10^6). Moreover, mAb treatment strongly reduced the systemic inflammatory response in infected animals, as shown by a significant decline of cytokine plasma levels (mean interleukin [IL]-6/tumor necrosis factor [TNF] plasma concentration: control 3,362.54/27 pg/mL vs. levofloxacin 54.88/3.15 pg/mL and 30-B8 15.92/0.84 pg/mL) (Figures 6B and 6C). In line with these findings, we observed a nearly complete prevention of hemorrhagic infiltrate formation in lung sections of infected and mAb-treated animals (Figures 6D, 6E, and S6). To confirm that the higher *in vitro* activity of human anti-PcrV mAbs correlates with increased *in vivo* activity, we conducted a direct comparison of the human antibodies 30-B8 and 30-D9 with the mouse-derived antibody MEDI3902 in the acute neutropenic lung infection model. At 5 mg/kg, treatment with MEDI3902 resulted in a nearly significant reduction of CFUs, compared with the untreated control group. At a lower dose of 1.5 mg/kg, MEDI3902 had no significant impact on CFU counts in the lungs (mean CFUs: MEDI3902 5.93×10^5 vs. 30-B8 1.21×10^4 and 30-D9 2.08×10^4) (Figure 6F). Treatment with the antibodies 30-B8 and 30-D9 demonstrated a significant reduction in CFUs at both the 5 mg/kg and 1.5 mg/kg doses (Figure 6F). Finally, human anti-PcrV mAbs were assessed for prophylactic activity in a neutropenic thigh infection model.[48] Antibodies were applied intraperitoneally 2 h prior to intramuscular injection of PA into the left and right lateral thigh, followed by terminal analysis 24 h later. Treatment of mice with human anti-PcrV mAbs led to a significant reduction of the bacterial burden in tissue, compared with a control antibody (MCA1; anti-MERS-CoV S glycoprotein antibody) (Figure 6G).[49] Efficacy of anti-PcrV mAbs 30-B8 and 30-D9 was comparable to levofloxacin treatment (administered three times after infection vs. single dose mAbs with 5 mg/kg before infection) (Figure 6G). In comparison to the lung infection model, the systemic inflammatory response observed in this experiment was lower. Nevertheless, anti-PcrV mAb treatment and levofloxacin treatment reduced plasma IL-6 levels to the same extent (Figure 6H). Taken together, these experiments illustrate the therapeutic and prophylactic potential of patient-derived mAbs targeting the T3SS of PA.

DISCUSSION

Here, we show that the humoral immune response toward the bacterial antigen PcrV supports the formation of a broad spectrum of mAbs that can potentially be exploited as therapeutic and prophylactic agents against PA (Figure 6I). Although antibody-mediated immunity directed against PcrV in humans is well known, detailed functional analyses are scarce.[31–36,50,51] By conducting an in-depth evaluation of the PcrV-specific B cell response, we were able to produce a series of diverse and fully human mAbs.

Until now, only a few mAb-based antibacterial approaches have been successfully implemented in clinical care. This includes antibodies neutralizing secreted toxins of *Clostridioides difficile* and mAbs for the prophylaxis and treatment of inhaled anthrax.[52–56] To date, one of the most promising candidates against PA is MEDI3902 (gremubamab), a bispecific antibody targeting PcrV as well as Psl, a PA-derived exopolysaccharide required for biofilm formation.[36] MEDI3902 passed a phase I study without safety concerns but failed to prevent pneumonia in mechanically ventilated

(C) mAbs with evidence of neutralizing qualities were serial diluted and tested in the described hemolysis assay starting at 50 μg/mL. IC_{50} values were calculated using titration curves. The mAb 1F3 (purple) and IVIG (gray) were used as controls. mAbs with IC_{50} values below the IC_{50} calculated for 1F3 are highlighted in dark red.

(D) Competition ELISA of human mAbs binding to recombinant PcrV. Values were calculated relative to a positive control with hierarchical clustering. A similarity matrix was applied (Pearson correlation). In total six different clusters were identified. EC_{50} and *in vitro* efficacy (hemolysis) of each mAb is indicated above. Boxplots indicate the median, the upper and lower quartile, and the minimum and maximum values. Shown data points represent the technical mean of an independent experiment.

See also Figure S2 and Table S4.

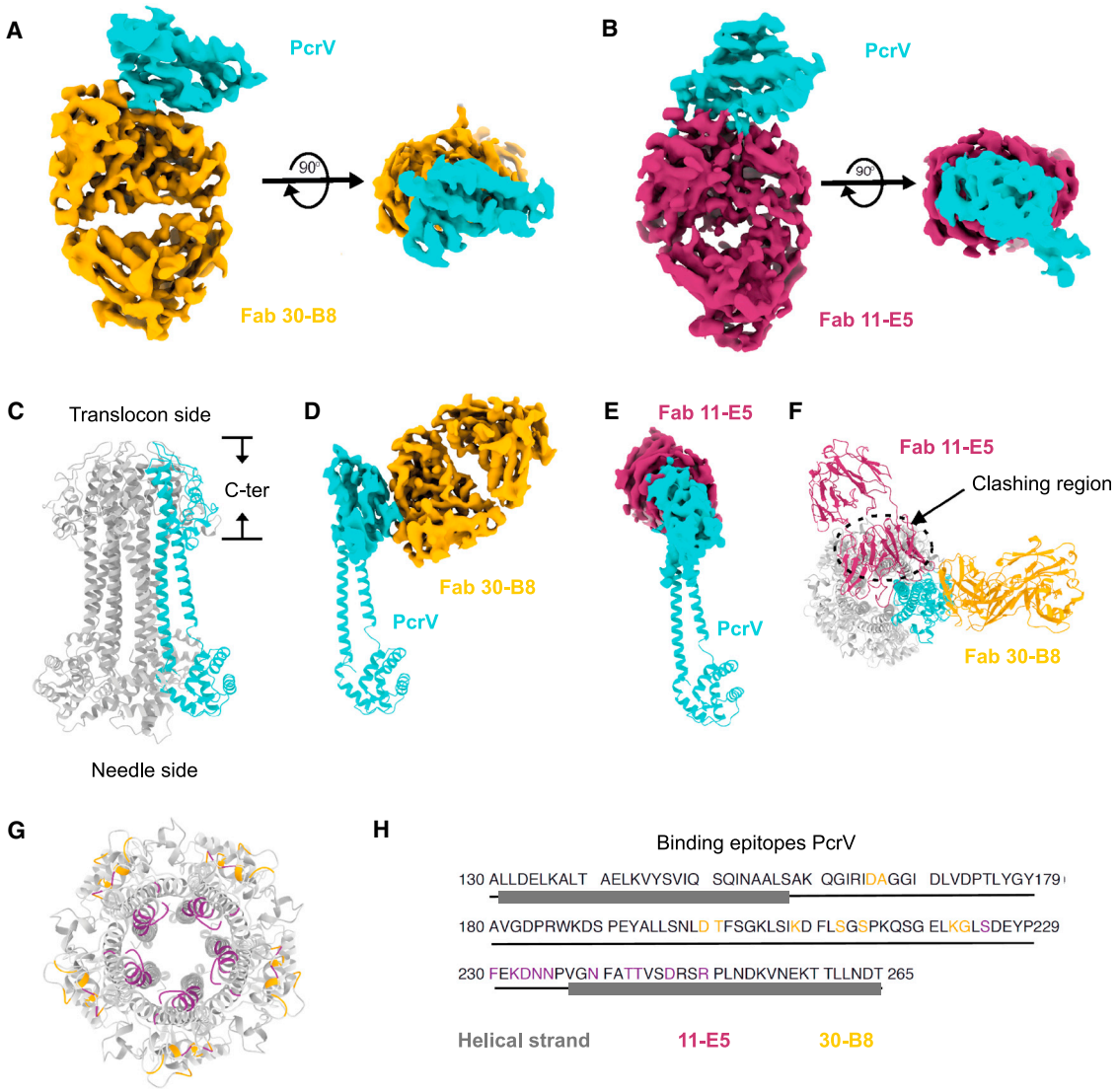

Figure 4. Cryo-EM structure determination of human anti-PcrV antibody-binding epitopes

(A and B) Cryo-EM density maps of Fab fragments obtained from human anti-PcrV antibodies in complex with MBP-PcrV. The map density corresponding to the PcrV structure is colored in cyan. Fab fragments obtained from the highly neutralizing human anti-PcrV antibody 30-B8 (orange) and the non-neutralizing anti-PcrV-antibody 11-E5 (purple) are colored as indicated.

(C) AlphaFold structure prediction of the PcrV pentamer. The PcrV pentamer is shown in side view. The T3SS needle filament and translocon connection sites are indicated. PcrV protomer is colored in cyan. C-ter, C-terminal.

(D and E) Fab fragments bind to one PcrV protomer. The position of the PcrV was fixed as the colored protomer in (C). The PcrV protomer was fitted in the cryo-EM maps of 30-B8/PcrV and 11-E5/PcrV as indicated.

(F) Fab fragments bind theoretically to the PcrV pentamer. 30-B8 (orange) binds to the periphery of the PcrV pentamer. 11-E5 (purple) binds to the oligomeric interface of the PcrV pentamer and clashes with the adjacent protomer.

(G and H) Visualization of neutralizing epitopes on PcrV. The binding sites of 30-B8 (orange) and 11-E5 (purple) were mapped on the PcrV pentamer (G). Neutralizing epitopes of 30-B8 and 11-E5 are shown in the amino acid sequence of the cryo-EM-resolved PcrV fragment (H).

See also Figure S3 and Table S5.

intensive care unit patients colonized with PA in a phase II trial.[36,38,46]

Of note, all of these antibacterial antibodies were developed using immunized animal models, while many of the highly effective and broadly neutralizing mAbs targeting viruses were isolated and produced from infected, vaccinated, or convalescent individuals.[14] Often, those studies relied on functional screening assays to identify so-called "elite neutralizers," followed by in-depth analyses of antigen-specific B cells for identification and recombinant expression of antiviral bNAbs.[10,57]

In order to extend the application of this approach from viral to bacterial infections, we focused on pwCF. Here,

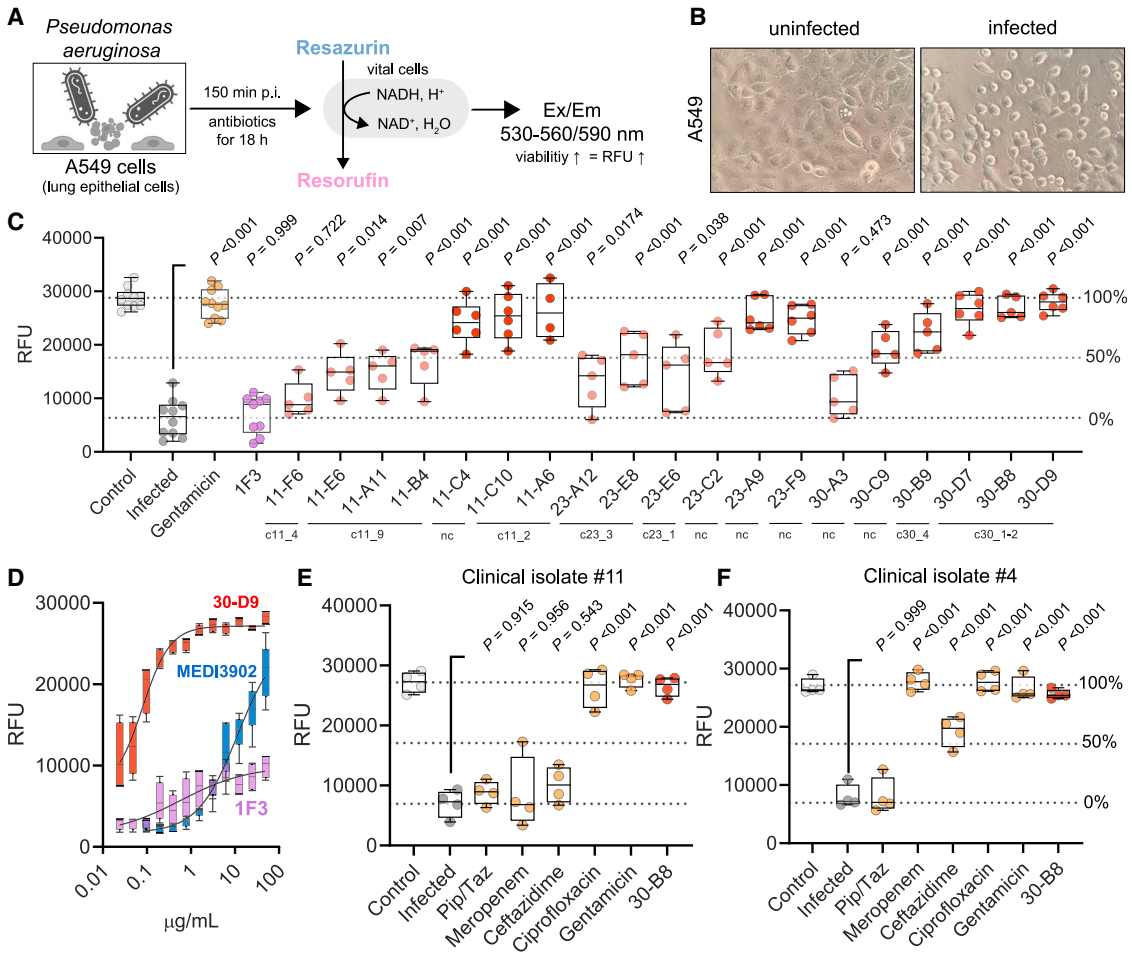

Figure 5. Human anti-PcrV mAbs reveal highly neutralizing effects *in vitro*

(A) Illustration of the experimental setup.

(B) A549 cells were infected with *PA* wild-type strain PAO1 for 150 min with a MOI of 0.5. Changes of cell morphology, indicating bacteria-induced cell death, were documented by bright-field microscopy.

(C) A549 cells were infected with PAO1 for 150 min with a MOI of 0.5 in presence of patient-derived monoclonal anti-PcrV antibodies (50 µg/mL) (n = 20) (red). As control, cells were left uninfected (gray) or were infected in presence of a mock control (dark gray), a humanized mouse anti-PcrV antibody (1F3) (50 µg/mL) (purple), or gentamicin (20 µg/mL) (orange). Relative fluorescence units (RFUs) were measured after adding resazurin. Clonal groups determined by single-B cell sequencing are indicated below the graph (nc, non-clonal). Significance was calculated to infected cells treated with a mock control using a one-way ANOVA with Tukey's multiple comparisons test.

(D) A549 cells were infected as described before in presence of the human anti-PcrV mAb 30-D9, MEDI3902, and 1F3 at a concentration ranging from 50 to 24 ng/ml.

(E and F) A549 cells were infected as described in (C) using drug-resistant PA strains #11 (E) and #4 (F), both isolated from patients with bloodstream infections. Cells were treated with piperacillin/tazobactam (16 µg/mL), meropenem (8 µg/mL), ceftazidime (8 µg/mL), ciprofloxacin (1 µg/mL), gentamicin (4 µg/mL) (all orange), as well as selected patient-derived monoclonal anti-PcrV antibodies (50 µg/mL) (red). Significance was calculated in comparison with infected cells treated with a mock control (dark gray) using a one-way ANOVA with Tukey's multiple comparisons test.

Boxplots indicate the median, the upper and lower quartile, and the minimum and maximum values. Shown data points represent the technical mean of an independent experiment.

See also Figures S4 and S5 and Table S5.

previous studies revealed an upregulation of bacterial genes encoding components of the T3SS in chronically infected patients, including PcrV.[58,59] While high PcrV and T3SS-specific antibody titers can be frequently found in sera of pwCF, a sufficient humoral immune response toward PcrV could not be detected in patients with acute bloodstream infections, despite expression of PcrV in most of the isolated PA strains.[29,30,60] Thus, chronically infected patients and a carefully selected study cohort seem to be important for the detection of mAbs targeting PA-associated virulence factors. This is also illustrated by our clinical data linking the duration of colonization to T3SS neutralizing activity in serum. These findings align with our hypothesis that prolonged or repetitive exposure to bacterial antigens in chronically infected patients

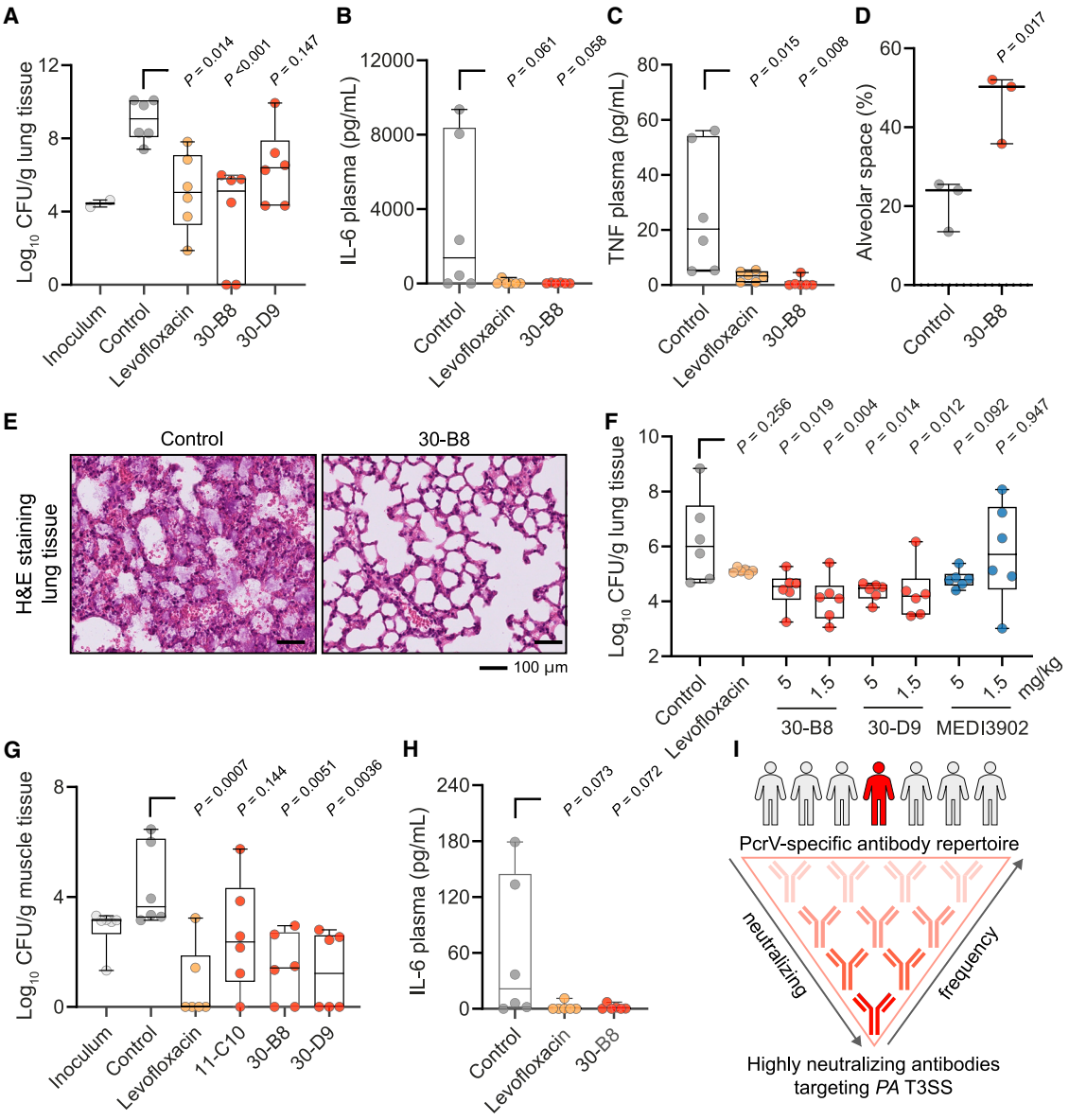

Figure 6. Human anti-PcrV mAbs show antibacterial effects *in vivo*

(A–C) CD-1 mice were treated with cyclophosphamide intraperitoneally at day −4 and day −1 to induce neutropenia. Subsequently, pulmonary infection was induced by nebulization of PA (Boston 41501 strain). To confirm successful application of bacteria, an inoculum group (gray) (n = 2) was used. A vehicle control (PBS) (dark gray) (n = 6), levofloxacin (100 mg/kg) (orange) (n = 6), or mAbs (5 mg/kg) (red) (each n = 6) were administered 2 h later intraperitoneally. After 24 h, experiments were terminated and lungs were homogenized, followed by quantifications of CFUs. Plasma was used to quantify IL-6 (B) and TNF (C) levels. Significance was calculated to untreated animals using a one-way ANOVA with Tukey's multiple comparisons test.

(D) Lungs of animals treated with a control (n = 3) or 30-B8 (n = 3) were fixed, embedded in paraffin, and stained with H&E. Alveolar space for each animal was calculated relatively to the total surface area. For each animal four representative image sections were selected. Significance was calculated using a Student's t test.

(E) Two representative images of an animal treated with the control (right) or the human anti-PcrV mAb 30-B8 (left) are shown.

(F) Similar to (A), CD-1 mice were treated with cyclophosphamide prior to pulmonary infection with PA (Boston 41501 strain). A vehicle control (PBS) (gray) (n = 6), levofloxacin (100 mg/kg) (orange) (n = 6), human anti-PcrV mAbs (5 or 1.5 mg/kg) (red), or MEDI3902 (5 or 1.5 mg/kg) (each n = 6) was administered 2 h later intraperitoneally. After 24 h, experiments were terminated and lungs were homogenized, followed by quantifications of CFUs. Significance was calculated to untreated animals (control) using a one-way ANOVA with Tukey's multiple comparisons test.

(G) 2 h prior to infection, a control mAb (MCA1) (n = 6) or mAbs 30-B8 or 30-D9 (5 mg/kg) (red) (each n = 6) were administered intraperitoneally. Infection was initiated by intramuscular injection of 1.2×10^5 CFU/mL PA (Boston 41501) into each lateral thigh. As a control, levofloxacin (100 mg/kg) (orange) (n = 6) was given 2, 6, and 10 h post infection. To confirm bacterial infection after injection, six animals were used as inoculum control group (gray). After 24 h animals were euthanized, muscles were homogenized, and CFUs were determined. Significance was calculated to animals treated with the control antibody using a one-way ANOVA with Tukey's multiple comparisons test.

(legend continued on next page)

Please cite this article in press as: Simonis et al., Discovery of highly neutralizing human antibodies targeting *Pseudomonas aeruginosa*, Cell (2023), https://doi.org/10.1016/j.cell.2023.10.002

leads to the production of highly effective neutralizing antibodies.

By identifying potent neutralizers using several screening assays with increasing stringency, we were able to produce a diverse set of human mAbs targeting defined PcrV epitopes. For some patient-derived mAbs, the levels of cytoprotection were improved by more than a 100-fold when compared with the mouse-derived mAbs. Location and geometry of the antibody-binding epitope play an important role in the neutralizing potency as well as the magnitude of fragment crystallizable region (Fc) receptor-mediated antimicrobial effector functions of therapeutic mAbs.[61,62] Thus, epitope selectivity and specificity may be one reason for the strong *in vitro* cytoprotective effects we observed. Our structural data support these findings by providing mechanistic insight on non-neutralizing and neutralizing activity of anti-PcrV mAbs. Using cryo-EM, we were able to map the exact binding interface of the macromolecular complex for a potently neutralizing patient-derived mAb, revealing that the periphery of the C-terminal region of the PcrV pentamer is a highly vulnerable target. The binding site of the MEDI3902 mAb differs from this epitope, which can explain the different neutralizing efficacy of human anti-PcrV mAbs.[63]

Small molecules or antibodies targeting bacterial virulence factors do not necessarily attenuate bacterial growth or viability of bacteria, which represents a possible disadvantage when compared with conventional antibiotics. Interestingly, when applied in two different infection models *in vivo*, our most potent human anti-PcrV mAbs exhibited similar efficacy as the bactericidal antibiotic levofloxacin, resulting in a significant reduction of the bacterial burden in tissue and strongly reduced inflammatory parameters. A possible explanation for this antibiotic-like activity *in vivo* could be mAb-mediated abrogation of local tissue damage and bacterial dissemination as well as Fc-mediated activation of the innate immune response including activation of the complement system followed by bacteriolysis, which has been demonstrated for other antimicrobial antibodies.[64,65]

In contrast to most antimicrobial agents, mAbs show an extraordinarily long half-life in plasma, which we also confirmed for mAbs identified in this study. Therapeutic plasma levels persisting several weeks after application enable passive immunization strategies in vulnerable patients.[14,66,67] Moreover, side effect profiles of most human therapeutic IgG mAbs are favorable with low incidences of severe adverse events.[68] Therefore, human mAbs targeting virulence factors of PA represent a promising approach for the treatment and prevention of infections. However, with regard to mAbs inhibiting the T3SS, future clinical studies may require careful selection of specific target populations. Previously performed phase II clinical trials with mouse-derived anti-PcrV antibodies failed to improve respiratory parameters in pwCF or to prevent the development of pneumonia in mechanically ventilated patients already colonized with PA.[37,38,69] The reason for this may be found in the characteristic evolutionary adaptation of PA populations during pulmonary colonization, which is characterized by a loss of T3SS functionality and biofilm formation.[58] Accordingly, it was found that the majority of PA strains isolated from chronically infected pwCF failed to secrete T3SS effector proteins.[70] These adaptive processes offer a potential explanation for the lack of efficacy observed in anti-PcrV-directed therapies.[71] Thus, while it is important to acknowledge that chronically infected patients played an important role in identifying potent human anti-PcrV antibodies, these patients represent an unlikely target group for future clinical applications of mAbs identified in this study. In contrast, a substantial body of data underscore the significance of the T3SS as a prominent virulence factor in acute infections.[24,72] In line, the majority of PA strains isolated from patients with sepsis and bloodstream infections express a fully functional T3SS, emphasizing the importance of including this patient population as, thus far, an overlooked target population in future clinical trials.[60] This may also include passive immunization strategies in individuals with an elevated risk for acute bloodstream infections and sepsis, such as patients undergoing allogeneic stem cell transplantation.

In conclusion, we show that PA infections with repetitive and prolonged antigen exposure induce the formation of highly neutralizing antibacterial antibodies. These mAbs were broadly active against drug-resistant clinical strains and reduced bacterial burden as well as systemic inflammation *in vivo*, thus paving the way for clinical application of these antibacterial agents. Our approach can be adapted to other secreted and surface-exposed bacterial targets, providing a tool for the treatment and prevention of bacterial infections.

Limitations of the study

Application of human mAbs in bacterial infections might be limited by the accessibility of IgG to the source of infection, especially in abscess-forming infections or infections affecting certain compartments, which are not typically crossed by IgG (e.g., skin, biofilms, or blood-brain barrier). Animal experiments with additional PA infection models are required to assess the therapeutic potential of anti-PcrV mAbs in these clinical settings. Moreover, neutralization of secreted or surface-exposed bacterial targets may not always translate into inhibition of bacterial growth or viability of bacteria *in vivo*. Modification of human mAbs, for example, as altered glycosylation, Fc point mutations, Fab fragments, antibody-drug conjugates, or bispecific antibodies might overcome these limitations to some extent.[73–76] Finally, it is important to note that not all bacterial pathogens are capable of inducing chronic infections and colonization. Thus, more research is required to identify suitable pathogens and infected target populations for isolation of antibody-producing B cells. This may include patients with difficult-to-treat infections such

(H) IL-6 levels were quantified in plasma. Significance was calculated to animals treated with the control antibody using a one-way ANOVA with Tukey's multiple comparisons test.

(I) Summary of the findings of this study.

Boxplots indicate the median, the upper and lower quartile, and the minimum and maximum values. Shown data points represent the technical mean of an independent experiment.

See also Figures S5 and S6.

as endocarditis or bone or soft tissue infections in which the immune system is exposed to bacterial antigens for several weeks to months. This requires the establishment of suitable clinical cohorts and comprehensive testing strategies revealing the production of antibacterial antibodies targeting clinically relevant pathogens.

STAR★METHODS

Detailed methods are provided in the online version of this paper and include the following:

- KEY RESOURCES TABLE
- RESOURCE AVAILABILITY
  - Lead contact
  - Materials availability
  - Data and code availability
- EXPERIMENTAL MODEL AND STUDY PARTICIPANT DETAILS
- METHOD DETAILS
  - Isolation of serum and PBMCs from whole blood
  - Bacterial strains, culture, and growth kinetics of *Pseudomonas aeruginosa*
  - Hemolysis assay
  - Recombinant expression and isolation of PcrV
  - IgG isolation from patient serum
  - Determination of anti-PcrV titers in serum
  - Cell surface expression of a PcrV-specific antibody to validate identification of PcrV-specific B cell populations
  - Isolation of PcrV-specific B cells
  - Ig heavy-/light-chain amplification and sequence analysis
  - Cloning and production of PcrV-specific mAbs
  - ELISA analysis to determine antibody binding activity to PcrV
  - A549 cytotoxicity assay
  - Sequencing of *pcrV* in clinical isolates
  - Competition ELISA
  - Cryo-EM sample preparation and data collection
  - Cryo-EM data processing, model building, and refinement
  - Pharmacokinetic profiles of human anti-PcrV mAbs
  - *In vivo* infection experiments
  - Microscopic analysis
  - Statistical analysis

SUPPLEMENTAL INFORMATION

Supplemental information can be found online at https://doi.org/10.1016/j.cell.2023.10.002.

ACKNOWLEDGMENTS

We thank all participants of this study. Graphical illustrations were created with BioRender.com. PAO1 wild-type and PAO1FΔ*pscD* mutant strain were kindly provided by A. Rietsch, Case Western Reserve University, Cleveland, Ohio, USA. PMX-vector was kindly provided by Matthias Zehner, Laboratory of Experimental Immunology, University of Cologne, Germany. We thank Edeltraud van Gumpel, Andrea Ahlers, Kimberley Vivien Sander, Janine Schreiber, Jennifer Wolf, and Nadine Hemstedt for technical support. This work was funded by the German Federal Ministry of Education and Research (BMBF) (01KI2108, Junior Research Groups Infectious Diseases to A.S.); the Cologne Clinician Scientist Program (CCSP, to A.S.); the German Research Council (DFG, FI 773/15-1 [CCSP] to A.S., CRC 1310 to F.K. and C.K., FOR 2722 to M.K., and CRC 1403 to J.R.); the Koeln Fortune Program (to A.S.) and the CMMC Career Advancement Program (to A.S. and J.R.), Faculty of Medicine and University Hospital of Cologne, University of Cologne; and the German Center for Infection Research (DZIF, to F.K., TTU 09.719 and participation in DZIF TTU 09.718 to K.R., and DZIF TTU 02.806 to J.R.). A.M.-H. is supported by the Else Kröner Forschungskolleg Cologne.

Cryo-EM data collections were performed at the cryo-EM Facility at CSSB Hamburg (supported by the University of Hamburg, the University Medical Center Hamburg-Eppendorf, and DFG grants INST152/772-1, 152/774-1, 152/775-1, 152/776-1, and 152/777-1 FUGG.). High-performance computing was possible with the HPC at DESY/Hamburg (Germany). This project was supported in part through funds available to T.C.M. through the Behörde für Wissenschaft, Forschung und Gleichstellung of the city of Hamburg at the Institute of Structural and Systems Biology at the University Medical Center Hamburg-Eppendorf (UKE), Deutsches Elektronen Synchrotron (DESY).

AUTHOR CONTRIBUTIONS

Conceptualization, A.S. and J.R.; methodology, A.S., C.K., K.R., B.Y., F.K., and J.R.; software, C.K., B.Y., and T.C.M.; validation, A.S., C.K., K.R., B.Y., F.K., and J.R.; formal analysis, A.S., C.K., A.A., K.R., and B.Y.; investigation, A.S., C.K., A.A., B.Y., D.H., J.A.W., L.K., S.W., K.R., S.Z., M.S.E., K.S., H.G., S.J.T., A.-M.H., C.M., N.C., and A.M.; resources, A.S., C.K., K.R., H.S., M.H., G.F., E.R., T.C.M., S.v.K.-R., F.K., and J.R.; data curation, A.S. and C.K.; writing – original draft, A.S. and J.R.; writing – review & editing, C.K., A.A., K.R., B.Y., J.A.W., H.G., S.J.T., A.-M.H., A.M., G.F., H.S., T.C.M, S.v.K.-R., F.K., and J.R.; visualization, A.S., C.K., and B.Y.; supervision and project administration, A.S., C.K., T.C.M., F.K., and J.R.; funding acquisition, A.S., C.K., K.R., T.C.M., F.K., and J.R.

DECLARATION OF INTERESTS

A patent application encompassing aspects of this work has been filed by the University of Cologne, listing A.S., C.K., F.K., and J.R. as inventors.

INCLUSION AND DIVERSITY

We support inclusive, diverse, and equitable conduct of research.

Received: March 22, 2023
Revised: July 17, 2023
Accepted: October 2, 2023
Published: November 1, 2023

REFERENCES

1. Antimicrobial Resistance Collaborators (2022). Global burden of bacterial antimicrobial resistance in 2019: a systematic analysis. Lancet *399*, 629–655. https://doi.org/10.1016/S0140-6736(21)02724-0.
2. World Health Organization (2022). 2021 Antibacterial agents in clinical and preclinical development: an overview and analysis. A technical document from the World Health Organization, May 27, 2022. Licence: CC BY-NC-SA 3.0 IGO. https://www.who.int/publications/i/item/9789240047655.
3. Rasko, D.A., and Sperandio, V. (2010). Anti-virulence strategies to combat bacteria-mediated disease. Nat. Rev. Drug Discov. *9*, 117–128. https://doi.org/10.1038/nrd3013.
4. Kaufmann, S.H.E., Dorhoi, A., Hotchkiss, R.S., and Bartenschlager, R. (2018). Host-directed therapies for bacterial and viral infections. Nat. Rev. Drug Discov. *17*, 35–56. https://doi.org/10.1038/nrd.2017.162.
5. Van Nieuwenhuyse, B., Van der Linden, D., Chatzis, O., Lood, C., Wagemans, J., Lavigne, R., Schroven, K., Paeshuyse, J., de Magnée, C., Sokal,

E., et al. (2022). Bacteriophage-antibiotic combination therapy against extensively drug-resistant Pseudomonas aeruginosa infection to allow liver transplantation in a toddler. Nat. Commun. *13*, 5725. https://doi.org/10.1038/s41467-022-33294-w.

6. Morrison, C. (2015). Antibacterial antibodies gain traction. Nat. Rev. Drug Discov. *14*, 737–738. https://doi.org/10.1038/nrd4770.
7. Wagner, S., Sommer, R., Hinsberger, S., Lu, C., Hartmann, R.W., Empting, M., and Titz, A. (2016). Novel strategies for the treatment of Pseudomonas aeruginosa infections. J. Med. Chem. *59*, 5929–5969. https://doi.org/10.1021/acs.jmedchem.5b01698.
8. Fenwick, C., Turelli, P., Ni, D., Perez, L., Lau, K., Herate, C., Marlin, R., Lana, E., Pellaton, C., Raclot, C., et al. (2022). Patient-derived monoclonal antibody neutralizes SARS-CoV-2 Omicron variants and confers full protection in monkeys. Nat. Microbiol. *7*, 1376–1389. https://doi.org/10.1038/s41564-022-01198-6.
9. Corti, D., Misasi, J., Mulangu, S., Stanley, D.A., Kanekiyo, M., Wollen, S., Ploquin, A., Doria-Rose, N.A., Staupe, R.P., Bailey, M., et al. (2016). Protective monotherapy against lethal Ebola virus infection by a potently neutralizing antibody. Science *351*, 1339–1342. https://doi.org/10.1126/science.aad5224.
10. Schommers, P., Gruell, H., Abernathy, M.E., Tran, M.K., Dingens, A.S., Gristick, H.B., Barnes, C.O., Schoofs, T., Schlotz, M., Vanshylla, K., et al. (2020). Restriction of HIV-1 escape by a highly broad and potent neutralizing antibody. Cell *180*, 471–489.e22. https://doi.org/10.1016/j.cell.2020.01.010.
11. Gupta, A., Gonzalez-Rojas, Y., Juarez, E., Crespo Casal, M., Moya, J., Falci, D.R., Sarkis, E., Solis, J., Zheng, H., Scott, N., et al. (2021). Early treatment for Covid-19 with SARS-CoV-2 neutralizing antibody sotrovimab. N. Engl. J. Med. *385*, 1941–1950. https://doi.org/10.1056/NEJMoa2107934.
12. Mulangu, S., Dodd, L.E., Davey, R.T., Jr., Tshiani Mbaya, O., Proschan, M., Mukadi, D., Lusakibanza Manzo, M., Nzolo, D., Tshomba Oloma, A., Ibanda, A., et al. (2019). A randomized, controlled trial of Ebola virus disease therapeutics. N. Engl. J. Med. *381*, 2293–2303. https://doi.org/10.1056/NEJMoa1910993.
13. Caskey, M., Schoofs, T., Gruell, H., Settler, A., Karagounis, T., Kreider, E.F., Murrell, B., Pfeifer, N., Nogueira, L., Oliveira, T.Y., et al. (2017). Antibody 10–1074 suppresses viremia in HIV-1-infected individuals. Nat. Med. *23*, 185–191. https://doi.org/10.1038/nm.4268.
14. Walker, L.M., and Burton, D.R. (2018). Passive immunotherapy of viral infections: 'super-antibodies' enter the fray. Nat. Rev. Immunol. *18*, 297–308. https://doi.org/10.1038/nri.2017.148.
15. Watson, A., Li, H., Ma, B., Weiss, R., Bendayan, D., Abramovitz, L., Ben-Shalom, N., Mor, M., Pinko, E., Bar Oz, M., et al. (2021). Human antibodies targeting a Mycobacterium transporter protein mediate protection against tuberculosis. Nat. Commun. *12*, 602. https://doi.org/10.1038/s41467-021-20930-0.
16. Rollenske, T., Szijarto, V., Lukasiewicz, J., Guachalla, L.M., Stojkovic, K., Hartl, K., Stulik, L., Kocher, S., Lasitschka, F., Al-Saeedi, M., et al. (2018). Cross-specificity of protective human antibodies against Klebsiella pneumoniae LPS O-antigen. Nat. Immunol. *19*, 617–624. https://doi.org/10.1038/s41590-018-0106-2.
17. Pennini, M.E., De Marco, A., Pelletier, M., Bonnell, J., Cvitkovic, R., Beltramello, M., Cameroni, E., Bianchi, S., Zatta, F., Zhao, W., et al. (2017). Immune stealth-driven O2 serotype prevalence and potential for therapeutic antibodies against multidrug resistant Klebsiella pneumoniae. Nat. Commun. *8*, 1991. https://doi.org/10.1038/s41467-017-02223-7.
18. Sadikot, R.T., Blackwell, T.S., Christman, J.W., and Prince, A.S. (2005). Pathogen-host interactions in Pseudomonas aeruginosa pneumonia. Am. J. Respir. Crit. Care Med. *171*, 1209–1223. https://doi.org/10.1164/rccm.200408-1044SO.
19. Centers for Disease Control and Prevention (2019). Antibiotic resistance threats in the United States. Report of the Centers for Disease Control and Prevention, 2019. https://www.hhs.gov/sites/default/files/michael-craig-cdc-talk-thursday-am-508.pdf.
20. World Health Organization (2017). Prioritization of pathogens to guide discovery, research and development of new antibiotics for drug-resistant bacterial infections, including tuberculosis. A technical document from the World Health Organization, September 4, 2017. https://www.who.int/publications/i/item/WHO-EMP-IAU-2017.12.
21. Ratjen, F., and Döring, G. (2003). Cystic fibrosis. Lancet *361*, 681–689. https://doi.org/10.1016/S0140-6736(03)12567-6.
22. La Rosa, R., Johansen, H.K., and Molin, S. (2019). Adapting to the airways: metabolic requirements of Pseudomonas aeruginosa during the infection of cystic fibrosis patients. Metabolites *9*, 234. https://doi.org/10.3390/metabo9100234.
23. Liao, C., Huang, X., Wang, Q., Yao, D., and Lu, W. (2022). Virulence factors of Pseudomonas aeruginosa and antivirulence strategies to combat its drug resistance. Front. Cell. Infect. Microbiol. *12*, 926758. https://doi.org/10.3389/fcimb.2022.926758.
24. Hauser, A.R. (2009). The type III secretion system of Pseudomonas aeruginosa: infection by injection. Nat. Rev. Microbiol. *7*, 654–665. https://doi.org/10.1038/nrmicro2199.
25. Hauser, A.R., Cobb, E., Bodi, M., Mariscal, D., Vallés, J., Engel, J.N., and Rello, J. (2002). Type III protein secretion is associated with poor clinical outcomes in patients with ventilator-associated pneumonia caused by Pseudomonas aeruginosa. Crit. Care Med. *30*, 521–528. https://doi.org/10.1097/00003246-200203000-00005.
26. El Solh, A.A., Akinnusi, M.E., Wiener-Kronish, J.P., Lynch, S.V., Pineda, L.A., and Szarpa, K. (2008). Persistent infection with Pseudomonas aeruginosa in ventilator-associated pneumonia. Am. J. Respir. Crit. Care Med. *178*, 513–519. https://doi.org/10.1164/rccm.200802-239OC.
27. Mueller, C.A., Broz, P., Müller, S.A., Ringler, P., Erne-Brand, F., Sorg, I., Kuhn, M., Engel, A., and Cornelis, G.R. (2005). The V-antigen of Yersinia forms a distinct structure at the tip of injectisome needles. Science *310*, 674–676. https://doi.org/10.1126/science.1118476.
28. Goure, J., Pastor, A., Faudry, E., Chabert, J., Dessen, A., and Attree, I. (2004). The V antigen of Pseudomonas aeruginosa is required for assembly of the functional PopB/PopD translocation pore in host cell membranes. Infect. Immun. *72*, 4741–4750. https://doi.org/10.1128/IAI.72.8.4741-4750.2004.
29. Moss, J., Ehrmantraut, M.E., Banwart, B.D., Frank, D.W., and Barbieri, J.T. (2001). Sera from adult patients with cystic fibrosis contain antibodies to Pseudomonas aeruginosa type III apparatus. Infect. Immun. *69*, 1185–1188. https://doi.org/10.1128/IAI.69.2.1185-1188.2001.
30. Milagres, L.G., Castro, T.L., Garcia, D., Cruz, A.C., Higa, L., Folescu, T., and Marques, E.A. (2009). Antibody response to Pseudomonas aeruginosa in children with cystic fibrosis. Pediatr. Pulmonol. *44*, 392–401. https://doi.org/10.1002/ppul.21022.
31. Sawa, T., Yahr, T.L., Ohara, M., Kurahashi, K., Gropper, M.A., Wiener-Kronish, J.P., and Frank, D.W. (1999). Active and passive immunization with the Pseudomonas V antigen protects against type III intoxication and lung injury. Nat. Med. *5*, 392–398.
32. Frank, D.W., Vallis, A., Wiener-Kronish, J.P., Roy-Burman, A., Spack, E.G., Mullaney, B.P., Megdoud, M., Marks, J.D., Fritz, R., and Sawa, T. (2002). Generation and characterization of a protective monoclonal antibody to Pseudomonas aeruginosa PcrV. J. Infect. Dis. *186*, 64–73. https://doi.org/10.1086/341069.
33. Shime, N., Sawa, T., Fujimoto, J., Faure, K., Allmond, L.R., Karaca, T., Swanson, B.L., Spack, E.G., and Wiener-Kronish, J.P. (2001). Therapeutic administration of anti-PcrV F(ab')(2) in sepsis associated with Pseudomonas aeruginosa. J. Immunol. *167*, 5880–5886. https://doi.org/10.4049/jimmunol.167.10.5880.
34. Imamura, Y., Yanagihara, K., Fukuda, Y., Kaneko, Y., Seki, M., Izumikawa, K., Miyazaki, Y., Hirakata, Y., Sawa, T., Wiener-Kronish, J.P., and Kohno, S. (2007). Effect of anti-PcrV antibody in a murine chronic airway

Pseudomonas aeruginosa infection model. Eur. Respir. J. *29*, 965–968. https://doi.org/10.1183/09031936.00147406.

35. Warrener, P., Varkey, R., Bonnell, J.C., DiGiandomenico, A., Camara, M., Cook, K., Peng, L., Zha, J., Chowdury, P., Sellman, B., and Stover, C.K. (2014). A novel anti-PcrV antibody providing enhanced protection against Pseudomonas aeruginosa in multiple animal infection models. Antimicrob. Agents Chemother. *58*, 4384–4391. https://doi.org/10.1128/AAC.02643-14.

36. DiGiandomenico, A., Keller, A.E., Gao, C., Rainey, G.J., Warrener, P., Camara, M.M., Bonnell, J., Fleming, R., Bezabeh, B., Dimasi, N., et al. (2014). A multifunctional bispecific antibody protects against Pseudomonas aeruginosa. Sci. Transl. Med. *6*, 262ra155. https://doi.org/10.1126/scitranslmed.3009655.

37. Jain, R., Beckett, V.V., Konstan, M.W., Accurso, F.J., Burns, J.L., Mayer-Hamblett, N., Milla, C., VanDevanter, D.R., and Chmiel, J.F.; KB001-A Study Group (2018). KB001-A, a novel anti-inflammatory, found to be safe and well-tolerated in cystic fibrosis patients infected with Pseudomonas aeruginosa. J. Cyst. Fibros. *17*, 484–491. https://doi.org/10.1016/j.jcf.2017.12.006.

38. Chastre, J., François, B., Bourgeois, M., Komnos, A., Ferrer, R., Rahav, G., De Schryver, N., Lepape, A., Koksal, I., Luyt, C.-E., et al. (2022). Safety, efficacy, and pharmacokinetics of gremubamab (MEDI3902), an anti-Pseudomonas aeruginosa bispecific human monoclonal antibody, in P. aeruginosa-colonised, mechanically ventilated intensive care unit patients: a randomised controlled trial. Crit. Care *26*, 355. https://doi.org/10.1186/s13054-022-04204-9.

39. Murray, T.S., Egan, M., and Kazmierczak, B.I. (2007). Pseudomonas aeruginosa chronic colonization in cystic fibrosis patients. Curr. Opin. Pediatr. *19*, 83–88. https://doi.org/10.1097/MOP.0b013e3280123a5d.

40. Klockgether, J., Cramer, N., Fischer, S., Wiehlmann, L., and Tümmler, B. (2018). Long-term microevolution of Pseudomonas aeruginosa differs between mildly and severely affected cystic fibrosis lungs. Am. J. Respir. Cell Mol. Biol. *59*, 246–256. https://doi.org/10.1165/rcmb.2017-0356OC.

41. Dacheux, D., Goure, J., Chabert, J., Usson, Y., and Attree, I. (2001). Pore-forming activity of type III system-secreted proteins leads to oncosis of Pseudomonas aeruginosa-infected macrophages. Mol. Microbiol. *40*, 76–85. https://doi.org/10.1046/j.1365-2958.2001.02368.x.

42. Numata, Y., Yamano, Y., Sato, T., and Tsuji, T. (2013). Antibody against PcrV. filed August 1, 2009, and granted August 6, 2013. US patent US 8501179 B2.

43. Kreer, C., Lupo, C., Ercanoglu, M.S., Spisak, N., Grossbach, J., Schlotz, M., Schommers, P., Gruell, H., Dold, L., Beyer, A., et al. (2022). Probabilities of HIV-1 bNAb development in healthy and chronically infected individuals. Preprint at bioRxiv. https://doi.org/10.1101/2022.07.11.499584.

44. Vidarsson, G., Dekkers, G., and Rispens, T. (2014). IgG subclasses and allotypes: from structure to effector functions. Front. Immunol. *5*, 520. https://doi.org/10.3389/fimmu.2014.00520.

45. von Ambüren, J., Schreiber, F., Fischer, J., Winter, S., van Gumpel, E., Simonis, A., and Rybniker, J. (2020). Comprehensive host cell-based screening assays for identification of anti-virulence drugs targeting Pseudomonas aeruginosa and Salmonella typhimurium. Microorganisms *8*, 1096. https://doi.org/10.3390/microorganisms8081096.

46. Ali, S.O., Yu, X.Q., Robbie, G.J., Wu, Y., Shoemaker, K., Yu, L., DiGiandomenico, A., Keller, A.E., Anude, C., Hernandez-Illas, M., et al. (2019). Phase 1 study of MEDI3902, an investigational anti-Pseudomonas aeruginosa PcrV and Psl bispecific human monoclonal antibody, in healthy adults. Clin. Microbiol. Infect. *25*, 629.e1–629.e6. https://doi.org/10.1016/j.cmi.2018.08.004.

47. Rox, K., Becker, T., Schiefer, A., Grosse, M., Ehrens, A., Jansen, R., Aden, T., Kehraus, S., König, G.M., Krome, A.K., et al. (2022). Pharmacokinetics and pharmacodynamics (PK/PD) of corallopyronin A against methicillin-resistant Staphylococcus aureus. Pharmaceutics *15*, 131. https://doi.org/10.3390/pharmaceutics15010131.

48. Rox, K. (2022). Influence of tramadol on bacterial burden in the standard neutropenic thigh infection model. Sci. Rep. *12*, 19606. https://doi.org/10.1038/s41598-022-24111-x.

49. Chen, Z., Bao, L., Chen, C., Zou, T., Xue, Y., Li, F., Lv, Q., Gu, S., Gao, X., Cui, S., et al. (2017). Human neutralizing monoclonal antibody inhibition of Middle East respiratory syndrome coronavirus replication in the common marmoset. J. Infect. Dis. *215*, 1807–1815. https://doi.org/10.1093/infdis/jix209.

50. Faure, K., Fujimoto, J., Shimabukuro, D.W., Ajayi, T., Shime, N., Moriyama, K., Spack, E.G., Wiener-Kronish, J.P., and Sawa, T. (2003). Effects of monoclonal anti-PcrV antibody on Pseudomonas aeruginosa-induced acute lung injury in a rat model. J. Immune Based Ther. Vaccines *1*, 2. https://doi.org/10.1186/1476-8518-1-2.

51. Baer, M., Sawa, T., Flynn, P., Luehrsen, K., Martinez, D., Wiener-Kronish, J.P., Yarranton, G., and Bebbington, C. (2009). An engineered human antibody fab fragment specific for Pseudomonas aeruginosa PcrV antigen has potent antibacterial activity. Infect. Immun. *77*, 1083–1090. https://doi.org/10.1128/IAI.00815-08.

52. Lowy, I., Molrine, D.C., Leav, B.A., Blair, B.M., Baxter, R., Gerding, D.N., Nichol, G., Thomas, W.D., Jr., Leney, M., Sloan, S., et al. (2010). Treatment with monoclonal antibodies against Clostridium difficile toxins. N. Engl. J. Med. *362*, 197–205. https://doi.org/10.1056/NEJMoa0907635.

53. Tsai, C.W., and Morris, S. (2015). Approval of raxibacumab for the treatment of inhalation anthrax under the US Food and Drug Administration "animal rule". Front. Microbiol. *6*, 1320. https://doi.org/10.3389/fmicb.2015.01320.

54. Migone, T.S., Subramanian, G.M., Zhong, J., Healey, L.M., Corey, A., Devalaraja, M., Lo, L., Ullrich, S., Zimmerman, J., Chen, A., et al. (2009). Raxibacumab for the treatment of inhalational anthrax. N. Engl. J. Med. *361*, 135–144. https://doi.org/10.1056/NEJMoa0810603.

55. Yamamoto, B.J., Shadiack, A.M., Carpenter, S., Sanford, D., Henning, L.N., Gonzales, N., O'Connor, E., Casey, L.S., and Serbina, N.V. (2016). Obiltoxaximab prevents disseminated Bacillus anthracis infection and improves survival during pre- and postexposure prophylaxis in animal models of inhalational anthrax. Antimicrob. Agents Chemother. *60*, 5796–5805. https://doi.org/10.1128/AAC.01102-16.

56. Greig, S.L. (2016). Obiltoxaximab: first global approval. Drugs *76*, 823–830. https://doi.org/10.1007/s40265-016-0577-0.

57. Gieselmann, L., Kreer, C., Ercanoglu, M.S., Lehnen, N., Zehner, M., Schommers, P., Potthoff, J., Gruell, H., and Klein, F. (2021). Effective high-throughput isolation of fully human antibodies targeting infectious pathogens. Nat. Protoc. *16*, 3639–3671. https://doi.org/10.1038/s41596-021-00554-w.

58. Rossi, E., La Rosa, R., Bartell, J.A., Marvig, R.L., Haagensen, J.A.J., Sommer, L.M., Molin, S., and Johansen, H.K. (2021). Pseudomonas aeruginosa adaptation and evolution in patients with cystic fibrosis. Nat. Rev. Microbiol. *19*, 331–342. https://doi.org/10.1038/s41579-020-00477-5.

59. Kordes, A., Preusse, M., Willger, S.D., Braubach, P., Jonigk, D., Haverich, A., Warnecke, G., and Häussler, S. (2019). Genetically diverse Pseudomonas aeruginosa populations display similar transcriptomic profiles in a cystic fibrosis explanted lung. Nat. Commun. *10*, 3397. https://doi.org/10.1038/s41467-019-11414-3.

60. Thaden, J.T., Keller, A.E., Shire, N.J., Camara, M.M., Otterson, L., Huband, M., Guenther, C.M., Zhao, W., Warrener, P., Stover, C.K., et al. (2016). Pseudomonas aeruginosa bacteremic patients exhibit nonprotective antibody titers against therapeutic antibody targets PcrV and psl exopolysaccharide. J. Infect. Dis. *213*, 640–648. https://doi.org/10.1093/infdis/jiv436.

61. He, W., Tan, G.S., Mullarkey, C.E., Lee, A.J., Lam, M.M., Krammer, F., Henry, C., Wilson, P.C., Ashkar, A.A., Palese, P., and Miller, M.S. (2016). Epitope specificity plays a critical role in regulating antibody-dependent cell-mediated cytotoxicity against influenza A virus. Proc.

Natl. Acad. Sci. USA *113*, 11931–11936. https://doi.org/10.1073/pnas.1609316113.

62. Zhang, A., Stacey, H.D., D'Agostino, M.R., Tugg, Y., Marzok, A., and Miller, M.S. (2023). Beyond neutralization: Fc-dependent antibody effector functions in SARS-CoV-2 infection. Nat. Rev. Immunol. *23*, 381–396.
63. Tabor, D.E., Oganesyan, V., Keller, A.E., Yu, L., McLaughlin, R.E., Song, E., Warrener, P., Rosenthal, K., Esser, M., Qi, Y., et al. (2018). Pseudomonas aeruginosa PcrV and psl, the molecular targets of bispecific antibody MEDI3902, are conserved among diverse global clinical isolates. J. Infect. Dis. *218*, 1983–1994. https://doi.org/10.1093/infdis/jiy438.
64. Zhang, Y.K., Li, X., Zhao, H.R., Jiang, F., Wang, Z.H., and Wu, W.X. (2019). Antibodies specific to membrane proteins are effective in complement-mediated killing of Mycoplasma bovis. Infect. Immun. *87*, e00740-19. https://doi.org/10.1128/IAI.00740-19.
65. Lindorfer, M.A., Köhl, J., and Taylor, R.P. (2013). Interactions between the complement system and Fcγ receptors. In Antibody FcLinking Adaptive and Innate Immunity, First edition (Academic Press), pp. 49–74. https://doi.org/10.1016/B978-0-12-394802-1.00003-0.
66. Mankarious, S., Lee, M., Fischer, S., Pyun, K.H., Ochs, H.D., Oxelius, V.A., and Wedgwood, R.J. (1988). The half-lives of IgG subclasses and specific antibodies in patients with primary immunodeficiency who are receiving intravenously administered immunoglobulin. J. Lab. Clin. Med. *112*, 634–640.
67. Pollard, A.J., and Bijker, E.M. (2021). A guide to vaccinology: from basic principles to new developments. Nat. Rev. Immunol. *21*, 83–100. https://doi.org/10.1038/s41577-020-00479-7.
68. Hansel, T.T., Kropshofer, H., Singer, T., Mitchell, J.A., and George, A.J. (2010). The safety and side effects of monoclonal antibodies. Nat. Rev. Drug Discov. *9*, 325–338. https://doi.org/10.1038/nrd3003.
69. François, B., Luyt, C.E., Dugard, A., Wolff, M., Diehl, J.L., Jaber, S., Forel, J.M., Garot, D., Kipnis, E., Mebazaa, A., et al. (2012). Safety and pharmacokinetics of an anti-PcrV pegylated monoclonal antibody fragment in mechanically ventilated patients colonized with Pseudomonas aeruginosa: a randomized,double-blind, placebo-controlled trial. Crit. Care Med. *40*, 2320–2326. https://doi.org/10.1097/CCM.0b013e31825334f6.
70. Jain, M., Ramirez, D., Seshadri, R., Cullina, J.F., Powers, C.A., Schulert, G.S., Bar-Meir, M., Sullivan, C.L., McColley, S.A., and Hauser, A.R. (2004). Type III secretion phenotypes of Pseudomonas aeruginosa strains change during infection of individuals with cystic fibrosis. J. Clin. Microbiol. *42*, 5229–5237. https://doi.org/10.1128/JCM.42.11.5229-5237.2004.
71. Motley, M.P., Banerjee, K., and Fries, B.C. (2019). Monoclonal antibody-based therapies for bacterial infections. Curr. Opin. Infect. Dis. *32*, 210–216. https://doi.org/10.1097/QCO.0000000000000539.
72. Engel, J., and Balachandran, P. (2009). Role of Pseudomonas aeruginosa type III effectors in disease. Curr. Opin. Microbiol. *12*, 61–66. https://doi.org/10.1016/j.mib.2008.12.007.
73. Kelley, R.F., and Meng, Y.G. (2012). Methods to engineer and identify IgG1 variants with improved FcRn binding or effector function. Methods Mol. Biol. *901*, 277–293. https://doi.org/10.1007/978-1-61779-931-0_18.
74. Liu, Z., Gunasekaran, K., Wang, W., Razinkov, V., Sekirov, L., Leng, E., Sweet, H., Foltz, I., Howard, M., Rousseau, A.M., et al. (2014). Asymmetrical Fc engineering greatly enhances antibody-dependent cellular cytotoxicity (ADCC) effector function and stability of the modified antibodies. J. Biol. Chem. *289*, 3571–3590. https://doi.org/10.1074/jbc.M113.513366.
75. Lin, C.W., Tsai, M.H., Li, S.T., Tsai, T.I., Chu, K.C., Liu, Y.C., Lai, M.Y., Wu, C.Y., Tseng, Y.C., Shivatare, S.S., et al. (2015). A common glycan structure on immunoglobulin G for enhancement of effector functions. Proc. Natl. Acad. Sci. USA *112*, 10611–10616. https://doi.org/10.1073/pnas.1513456112.
76. Lu, R.M., Hwang, Y.C., Liu, I.J., Lee, C.C., Tsai, H.Z., Li, H.J., and Wu, H.C. (2020). Development of therapeutic antibodies for the treatment of diseases. J. Biomed. Sci. *27*, 1. https://doi.org/10.1186/s12929-019-0592-z.
77. Bleves, S., Soscia, C., Nogueira-Orlandi, P., Lazdunski, A., and Filloux, A. (2005). Quorum sensing negatively controls type III secretion regulon expression in Pseudomonas aeruginosa PAO1. J. Bacteriol. *187*, 3898–3902. https://doi.org/10.1128/JB.187.11.3898-3902.2005.
78. Sun, Y., Karmakar, M., Taylor, P.R., Rietsch, A., and Pearlman, E. (2012). ExoS and ExoT ADP ribosyltransferase activities mediate Pseudomonas aeruginosa keratitis by promoting neutrophil apoptosis and bacterial survival. J. Immunol. *188*, 1884–1895. https://doi.org/10.4049/jimmunol.1102148.
79. Budzik, J.M., Rosche, W.A., Rietsch, A., and O'Toole, G.A. (2004). Isolation and characterization of a generalized transducing phage for Pseudomonas aeruginosa strains PAO1 and PA14. J. Bacteriol. *186*, 3270–3273. https://doi.org/10.1128/JB.186.10.3270-3273.2004.
80. Kreer, C., Döring, M., Lehnen, N., Ercanoglu, M.S., Gieselmann, L., Luca, D., Jain, K., Schommers, P., Pfeifer, N., and Klein, F. (2020). openPrimeR for multiplex amplification of highly diverse templates. J. Immunol. Methods *480*, 112752. https://doi.org/10.1016/j.jim.2020.112752.
81. Tiller, T., Meffre, E., Yurasov, S., Tsuiji, M., Nussenzweig, M.C., and Wardemann, H. (2008). Efficient generation of monoclonal antibodies from single human B cells by single cell RT-PCR and expression vector cloning. J. Immunol. Methods *329*, 112–124. https://doi.org/10.1016/j.jim.2007.09.017.
82. Ehrhardt, S.A., Zehner, M., Krähling, V., Cohen-Dvashi, H., Kreer, C., Elad, N., Gruell, H., Ercanoglu, M.S., Schommers, P., Gieselmann, L., et al. (2019). Polyclonal and convergent antibody response to Ebola virus vaccine rVSV-ZEBOV. Nat. Med. *25*, 1589–1600. https://doi.org/10.1038/s41591-019-0602-4.
83. Scheres, S.H. (2012). RELION: implementation of a Bayesian approach to cryo-EM structure determination. J. Struct. Biol. *180*, 519–530. https://doi.org/10.1016/j.jsb.2012.09.006.
84. Jumper, J., Evans, R., Pritzel, A., Green, T., Figurnov, M., Ronneberger, O., Tunyasuvunakool, K., Bates, R., Žídek, A., Potapenko, A., et al. (2021). Highly accurate protein structure prediction with AlphaFold. Nature *596*, 583–589. https://doi.org/10.1038/s41586-021-03819-2.
85. Rohou, A., and Grigorieff, N. (2015). CTFFIND4: fast and accurate defocus estimation from electron micrographs. J. Struct. Biol. *192*, 216–221. https://doi.org/10.1016/j.jsb.2015.08.008.
86. Wagner, T., Merino, F., Stabrin, M., Moriya, T., Antoni, C., Apelbaum, A., Hagel, P., Sitsel, O., Raisch, T., Prumbaum, D., et al. (2019). SPHIRE-crYOLO is a fast and accurate fully automated particle picker for cryo-EM. Commun. Biol. *2*, 218. https://doi.org/10.1038/s42003-019-0437-z.
87. Chen, V.B., Arendall, W.B., 3rd, Headd, J.J., Keedy, D.A., Immormino, R.M., Kapral, G.J., Murray, L.W., Richardson, J.S., and Richardson, D.C. (2010). MolProbity: all-atom structure validation for macromolecular crystallography. Acta Crystallogr. D Biol. Crystallogr. *66*, 12–21. https://doi.org/10.1107/S0907444909042073.
88. Liebschner, D., Afonine, P.V., Baker, M.L., Bunkóczi, G., Chen, V.B., Croll, T.I., Hintze, B., Hung, L.W., Jain, S., McCoy, A.J., et al. (2019). Macromolecular structure determination using X-rays, neutrons and electrons: recent developments in Phenix. Acta Crystallogr. D Struct. Biol. *75*, 861–877. https://doi.org/10.1107/S2059798319011471.
89. Ye, J., Ma, N., Madden, T.L., and Ostell, J.M. (2013). IgBLAST: an immunoglobulin variable domain sequence analysis tool. Nucleic Acids Res. *41*, W34–W40. https://doi.org/10.1093/nar/gkt382.

90. Sievers, F., Wilm, A., Dineen, D., Gibson, T.J., Karplus, K., Li, W., Lopez, R., McWilliam, H., Remmert, M., Söding, J., et al. (2011). Fast, scalable generation of high-quality protein multiple sequence alignments using Clustal Omega. Mol. Syst. Biol. *7*, 539. https://doi.org/10.1038/msb.2011.75.

91. Schneider, C.A., Rasband, W.S., and Eliceiri, K.W. (2012). NIH Image to ImageJ: 25 years of image analysis. Nat. Methods *9*, 671–675. https://doi.org/10.1038/nmeth.2089.

92. Pettersen, E.F., Goddard, T.D., Huang, C.C., Meng, E.C., Couch, G.S., Croll, T.I., Morris, J.H., and Ferrin, T.E. (2021). UCSF ChimeraX: structure visualization for researchers, educators, and developers. Protein Sci. *30*, 70–82. https://doi.org/10.1002/pro.3943.

93. Lugmayr, W., Kotov, V., Goessweiner-Mohr, N., Wald, J., DiMaio, F., and Marlovits, T.C. (2023). StarMap: a user-friendly workflow for Rosetta-driven molecular structure refinement. Nat. Protoc. *18*, 239–264. https://doi.org/10.1038/s41596-022-00757-9.

Please cite this article in press as: Simonis et al., Discovery of highly neutralizing human antibodies targeting *Pseudomonas aeruginosa*, Cell (2023), https://doi.org/10.1016/j.cell.2023.10.002

STAR★METHODS

KEY RESOURCES TABLE

REAGENT or RESOURCE	SOURCE	IDENTIFIER
Antibodies		
Anti-Human IgG-PE (Clone G18-145)	BD Biosciences	Cat.# 560951; RRID:AB_10563761
Anti-Human CD20-Alexa Fluor 700 (Clone 2H7)	BD Biosciences	Cat.# 560631; RRID: AB_1727447
anti-human IgG-HRP (Southern Biotech)	Southern Biotech	Cat.# 2040-05; RRID: AB_2795644
Peroxidase-AffiniPure Goat Anti-Human IgG (H+L)	Jackson ImmunoResearch	Cat.#109-035-003; RRID: AB_2337577
Goat Anti-Human IgG	Biotrend	Cat.# 2040-01
Human IgG1 Lambda	Biotrend	Cat.# 151L-01
Gremubamab Recombinant Human Monoclonal Antibody	Thermo Fisher	Cat.# MA5-42275; RRID:AB_2911418
	ProteoGenix	PX-TA1591
1F3	Numata et al.[42]	N/A
MCA1; MERS-CoV S glycoprotein antibody	Chen et al.[49]	RRID:AB_2833219
Human anti-PcrV mAbs	This study	N/A
Immunglobulin G	Sigma-Aldrich	Cat.# 56834-100MG
Bacterial and virus strains		
E. coli DH5α	Thermo Fisher	Cat.#18263012
BL21(DE3) Competent E. coli	NEB	Cat.# C2527H
Pseudomonas aeruginosa PAO1	Bleves et al.[77]	N/A
Pseudomonas aeruginosa PAO1 Δ*PscD*	Sun et al.[78]	N/A
Pseudomonas aeruginosa PA14	Budzik et al.[79]	N/A
Pseudomonas aeruginosa Boston 41591	ATCC	Cat.# 27853
Clinical *Pseudomonas aeruginosa* isolates	This Study	N/A
Biological samples		
PBMCs, Plasma, and IgGs of donors	This study	N/A
Human red blood cells	This study	N/A
Chemicals, peptides, and recombinant proteins		
DMSO	Merck	Cat.# D2650
Ficoll® Paque Plus	Cytiva	Cat.# 17-1440-03
LB-Medium (Luria/Miller)	Carl Roth	Cat.# X968.2
Phusion™ High-Fidelity DNA Polymerase	Thermo Fisher	Cat.# F530L
BamHI-HF	NEB	Cat.# R3136
HindIII-HF	NEB	Cat.# R3104
EcoRI-HF	NEB	Cat.# R3101
BsiWI-HF	NEB	Cat.# R3553
NheI-HF	NEB	Cat.# R3131
SalI-HF	NEB	Cat.# R3138
XhoI	NEB	Cat.# R0146
EDTA	Thermo Fisher	Cat.# AM9260G
DNA loading dye	Thermo Fisher	Cat.# R0611
Ampicillin sodium salt	Sigma-Aldrich	Cat.# A0166
IPTG (Isopropyl-β-D-thiogalactopyranosid)	Sigma-Aldrich	Cat.# I6758
Imidazole	Sigma-Aldrich	Cat.# I202
InstantBlue™ Protein Stain	Expedeon	Cat.# ISB1L
Tween 20	Merck	Cat.# 817072
Ethanol	Carl Roth	Cat.# 9065.4

(*Continued on next page*)

Continued

REAGENT or RESOURCE	SOURCE	IDENTIFIER
Sulfuric acid	Carl Roth	Cat.# X945.1
Glycine	Carl Roth	Cat.# 3187.3
Tris-(hydroxymethyl)-aminomethane	Carl Roth	Cat.# 4855.3
Bovine serum albumin (BSA)	Sigma-Aldrich	Cat.# A9418
Lipofectamine™ 3000	Thermo Fisher	Cat.# L3000001
Opti-MEM™	Thermo Fisher	Cat.# 51985034
DAPI	Thermo Fisher	Cat.# D1306
DTT	Promega	Cat.# P1171
RNasin	Promega	Cat.# N2515
RNaseOUT	Thermo Fisher	Cat.# 10777019
SuperScript™ IV Reverse Transcriptase	Thermo Fisher	Cat.# 18090050
Platinum™ Taq DNA Polymerase	Thermo Fisher	Cat.# 10966034
Platinum™ Taq Green Hot Start	Thermo Fisher	Cat.# 11966034
Q5® Hot Start High Fidelity DNA Polymerase	NEB	Cat.# M0493L
Q5® High-Fidelity DNA Polymerase	NEB	Cat.# M0491S
T4 DNA Polymerase	NEB	Cat.# M0203L
NP-40	Thermo Fisher	Cat.# 85124
dNTP Mix	Thermo Fisher	Cat.# R1122
Polyethylenimine, 25 kDa	Sigma-Aldrich	Cat.# 408727
FreeStyle™ Expression Medium	Thermo Fisher	Cat.# 12338001
Protein G Sepharose™ 4 Fast Flow	GE Life Sciences	Cat.# 17061805
NZY Auto-Induction LB medium	NZYTech	Cat.# MB179
ABTS solution	Thermo Fisher	Cat.# 002024
1-Step™ Ultra TMB-ELISA solution	Thermo Fisher	Cat.# 34029
RPMI 1640	Thermo Fisher	Cat.# 11875093
DMEM	Thermo Fisher	Cat.# 11960-044
DPBS	Thermo Fisher	Cat.# 14190250
10x PBS	Thermo Fisher	Cat.# AM9625
Fetal bovine serum (FBS)	Thermo Fisher	Cat.# 10270-106
Trypsin-EDTA	Thermo Fisher	Cat.# 25300-096
Pen-Strep	Thermo Fisher	Cat.# 15070-063
Sodium Pyruvate	Thermo Fisher	Cat.# 11360-070
L-Glutamin	Thermo Fisher	Cat.# 25030081
Gentamicin-sulfat	Sigma-Aldrich	Cat.# G1914
Moxifloxacin-hydrochlorid	Sigma-Aldrich	Cat.# SML1581
Levofloxacin	Sigma-Aldrich	Cat.# 28266
Resazurin	Sigma-Aldrich	Cat.# R7017
Cyclophosphamid	Sigma-Aldrich	Cat.# C7397
Tramadol	Dechra	N/A
Formalin solution	Sigma-Aldrich	Cat.# HT501128
Critical commercial assays		
DNeasy® Blood & Tissue Kit	Qiagen	Cat.# 69504
In-Fusion® HD EcoDry™ Cloning Kit	Takara Bio	Cat.# 080318
QIAprep® Spin Miniprep Kit	Qiagen	Cat.# 27104
B-PER™ Bacterial Protein Extraction Reagent	Thermo Fisher	Cat.# 90084
HisPur™ Ni-NTA Resin	Thermo Fisher	Cat.# 88221
PureCube 100 Ni-INDIGO Agarose	Cube Biotech	Cat.# 75103
NucleoSpin 96 PCR Clean-up	Macherey-Nagel	Cat.# 740658.4
CD19-Microbeads	Miltenyi Biotec	Cat.# 130-050-301

(*Continued on next page*)

Continued

REAGENT or RESOURCE	SOURCE	IDENTIFIER
Alexa Fluor™ 647 Microscale Protein Labeling Kit	Thermo Fisher	Cat.# A30009
Alexa Fluor™ 488 Microscale Protein Labeling Kit	Thermo Fisher	Cat.# A30006
One-Step Antibody Biotinylation Kit	Miltenyi Biotec	Cat.# 130-093-385
Streptavidin-HRP	Thermo Fisher	Cat.# N100
IgG (Total) Human Uncoated ELISA Kit	Thermo Fisher	Cat.# 88-50550-86
IL-6 Mouse Uncoated ELISA Kit	Thermo Fisher	Cat.# 88-7064-88
TNF alpha Mouse Uncoated ELISA Kit	Thermo Fisher	Cat.# 88-7324-88
Gibson Assembly® Master Mix	NEB	Cat.# E2611S
NOVA® Lite Hep-2 ANA Kit	Inova Diagnostics	Cat.# 066708100
Deposited data		
Cloned and tested human anti-PcrV antibodies	This study	Upon request
Experimental models: Cell lines		
A549	ATCC	Cat.# CCL-185; RRID:CVCL_0023
HEK293-6E	NRC	NRC file 11565
HEK293T/17	ATCC	Cat.# CRL-11268; RRID:CVCL_1926
Experimental models: Organisms/strains		
CD-1 mice	Charles River	RRID: IMSR_CRL:022
Oligonucleotides		
PcrV recombinant expression Primer forward (TCACCATCACGGATCCGAAGTCAGAAACC TTAATG)	This study	N/A
PcrV recombinant expression Primer reverse (TCAGCTAATTAAGCTTCTAGATCGCGCTGA GAATG)	This study	N/A
PcrV Sequencing Primer I forward (GCAGGG CGAGCAGGGTACC)	This study	N/A
PcrV Sequencing Primer II forward (GCCGAT GCGTGGCTTGTTG)	This study	N/A
PcrV Sequencing Primer I reverse (GCCTGT TGCTGGTCGGTGTC)	This study	N/A
PcrV Sequencing Primer II reverse (GCTGGT CGGTGTCGGAAGG)	This study	N/A
MBP fwd GCAGCTAGCAAAACTGAAGAA GGTAAAC	This study	N/A
MBP rev CATTAAGGTTTCTGACTTCATCGA CAGTCTGACGACCG	This study	N/A
MBP-PcrV fwd GAAGTCAGAAACCTTAATG	This study	N/A
MBP-PcrV rev TGTGGATCCCTAGATCGCG CTGAGAATG	This study	N/A
Single-cell PCR Primer	Kreer et al.[80]	N/A
Random Hexamer Primer	Thermo Fisher	Cat.# SO142
Recombinant DNA		
pQE-80L	Qiagen, NovoPro	Cat.# V010777
Human antibody expression vectors (IgG1, Igλ, Igκ)	Tiller et al.[81]	N/A
pMX vector	Ehrhardt et al.[82]	N/A
pET-28a(+)	Novagen	Cat.# 69864
Software and algorithms		
Relion 4.0	Scheres[83]	RRID:SCR_005375
ChimeraX 1.3	USCF, CA, USA	RRID:SCR_015872
AlphaFold	Jumper et al.[84]	N/A

(*Continued on next page*)

Please cite this article in press as: Simonis et al., Discovery of highly neutralizing human antibodies targeting *Pseudomonas aeruginosa*, Cell (2023), https://doi.org/10.1016/j.cell.2023.10.002

Continued

REAGENT or RESOURCE	SOURCE	IDENTIFIER
CTFFIND	Rohou and Grigorieff[85]	RRID:SCR_016732
crYOLO	Wagner et al.[86]	RRID:SCR_018392
MolProbity	Chen et al.[87]	RRID:SCR_014226
Geneious R10 and Geneious Prime	Geneious	RRID: SCR_010519
Phenix	Liebschner et al.[88]	RRID:SCR_014224
Prism	GraphPad	RRID: SCR_002798
Python 3.6.8	Python Software Foundation	RRID: SCR_008394
SciPy	SciPy developers	RRID: SCR_008058
IgBLAST 1.13.0	Ye et al.[89]	RRID: SCR_002873
Clustal Omega 1.2.3	Sievers et al.[90]	RRID: SCR_001591
ImageJ	Schneider et al.[91]	RRID: SCR_003070
OMERO	OME	RRID: SCR_002629
FlowJo 10.5.3	FlowJo, LLC	RRID: SCR_008520
Morpheus	Broad Institute	RRID: SCR_017386
Biorender	BioRender	RRID: SCR_018361
Word 2021	Microsoft	www.microsoft.com
Excel 2021	Microsoft	www.microsoft.com
Adobe Illustrator 2022	Adobe	RRID:SCR_010279

RESOURCE AVAILABILITY

Lead contact

Further information and requests for resources and reagents should be directed to and will be fulfilled by the lead contact Jan Rybniker (jan.rybniker@uk-koeln.de).

Materials availability

Reasonable amounts of antibodies will be made available by the lead contact upon request under a Material Transfer Agreement (MTA) for non-commercial usage.

Data and code availability

All data reported in this paper including antibody sequences will be shared by the lead contact upon request. This paper does not report original code. Any additional information required to reanalyze the data reported in this paper is available from the lead contact upon request.

EXPERIMENTAL MODEL AND STUDY PARTICIPANT DETAILS

The study protocol (20-1287_1) was approved by the Institutional Review Board (IRB) of the University of Cologne, Germany. All participants gave written informed consent before participation in the study and all aspects of study conduct were in accordance with Good Clinical Practice (GCP) guidelines and ethical principles of the Declaration of Helsinki. Individuals with cystic fibrosis were included by the Cystic Fibrosis Center Cologne. Detailed patients' information can be found in Table S1.

METHOD DETAILS

Isolation of serum and PBMCs from whole blood

Serum collection tubes (Sarstedt, Nuembrecht, Germany) were centrifuged at 3800 × g for 10 min at 4°C to separate serum from clotted blood. Serum was heat-inactivated at 56°C for 30 min and stored at -80°C. PBMCs were collected in Compoflex® CPDA-1 blood bags (Fresenius, Bad Homburg, Germany). PBMCs were purified by density gradient centrifugation using Cytiva Ficoll®-Paque (GE Healthcare, Chicago, USA) and Leucosep™ tubes (Greiner, Kremsmuenster, Austria). Subsequently, cells were stored in FBS (Thermo Fisher Scientific, Waltham, MA, USA) containing 10% (v/v) dimethyl sulfoxide (DMSO) (Merck, Darmstadt, Germany) at −150°C.

Please cite this article in press as: Simonis et al., Discovery of highly neutralizing human antibodies targeting *Pseudomonas aeruginosa*, Cell (2023), https://doi.org/10.1016/j.cell.2023.10.002

Bacterial strains, culture, and growth kinetics of *Pseudomonas aeruginosa*

Pseudomonas aeruginosa strains PAO1, PAO1Δ*pscD*, PA14 and clinical strains were used for *in vitro* experiments. All clinical strains were isolated from patients with bloodstream infection. For infection experiments we inoculated bacteria (stored in glycerol stocks at −80°C) in 5 mL LB broth (LB) (Carl Roth, Karlsruhe, Germany) and incubated shaking at 37°C. The next day cultures were transferred into fresh LB and adjusted to an optical density (OD_{600}) of 0.2. Cultures were then incubated at 37°C/200 rpm until an exponential growth was achieved (OD_{600} 0.8 – 1.5). Cultures were washed twice in Dulbecco's phosphate buffered saline (DPBS) (Thermo Fisher Scientific) before infection. Growth kinetics were performed in 96-well plates (Thermo Fisher Scientific) in a Hidex Sense Reader (Hidex, Turku, Finland) using 100 μL of bacterial culture per well, incubated at 37°C with orbital shaking at 300 rpm. Optical density at 600 nm was measured every 60 min.

Hemolysis assay

Human red blood cells from healthy donors were washed four times with DPBS to remove residual serum components and were diluted to a final concentration of 2.5 × 10^8 cells/mL. 100 μL of the suspension were added to a 96-well plate and were infected with bacteria at a multiplicity of infection (MOI) of 1 (2.5 × 10^8 bacteria/mL in DPBS). Subsequently, the plate was centrifuged at 1000 × g for 5 min and incubated for 2h at 37°C. After 2 h cells were resuspended followed by a centrifugation step at 1500 × g for 10 min. 100 μL of the supernatant of each well were transferred to a new plate and the OD at 540 nm was measured using a plate reader.

Recombinant expression and isolation of PcrV

Genomic DNA from strain PAO1 was isolated using a DNeasy® Blood & Tissue Kit (Qiagen, Hilden, Germany) according to the manufacturer's instruction. The *pcrV* gene was amplified using the Phusion high fidelity polymerase (Thermo Fisher Scientific) and the primer pair: *fwd* TCACCATCACGGATCCGAAGTCAGAAACCTTAATG and *rev TCAGCTAATTAAG CTTCTA GATCGCGCTGAGAATG*. After digestion of the expression vector (pQE80, Qiagen) with the restriction enzymes BamHI and HindIII (both NEB, Ipswich, MA, USA), the purified PCR product was cloned into the expression vector using the In-Fusion® HD EcoDry™ Cloning Kit with Stellar cells from Takara Bio (Kusatsu, Japan). Clones were selected on ampicillin supplemented agar plates (Sigma-Aldrich, St. Louis, MO, USA) and accurate insert of the *pcrV* gene into the expression vector was verified by sequencing. Colonies containing vectors were grown in liquid cultures, plasmids were isolated using a QIAprep® Spin Miniprep Kit (Qiagen) and transformed into competent BL21 *E. coli* by heat shock and selected on agar plates with ampicillin. Single clones were picked, incubated overnight in LB-media, and transferred into fresh LB-media. After reaching an OD_{600} of 0.5 300 μM IPTG (isopropyl-β-D-thiogalactopyranosid) (Sigma-Aldrich) was added, and bacteria were incubated for additional 3 h with shaking at 30°C. Subsequently, bacteria were centrifuged at 4000 × g for 5 min and lysed using the B-PER™ Bacterial Protein Extraction Reagent (Thermo Fisher Scientific) according to the manufacturer's instruction. Recombinant PcrV was isolated using HisPur™ Ni-NTA Resin (Thermo Fisher Scientific) by gravity-flow column (Carl Roth). Briefly, the bacterial lysate was equilibrated with 15 mM imidazole (Sigma-Aldrich) and added on the Ni-NTA resin containing gravity columns. After washing multiple times with phosphate buffered saline (PBS) containing 25 mM imidazole, His-labeled PcrV was released using 250 mM imidazole and buffer was exchanged to PBS using 10 kDa centrifugal filters (Sigma-Aldrich). Purity of the recombinant PcrV was determined by SDS-PAGE using 4-12% Bis-Tris protein gels (Thermo Fisher Scientific) and InstantBlue™ Protein Stain (Expedeon, Heidelberg, Germany).

The MBP - *pcrV* fusion DNA was amplified by overlap PCR using the Q5® High-Fidelity DNA polymerase (New England Biolabs, Ipswich, MA, USA) and the primer pair: *fwd GCAGCTAGCAAAACTGAAGAAGGTAAAC* and *rev CATTAAGGTTTCTGACTTCATCGA CAGTCTGACGACCG* (EFI22037; aa: 27-384; I28T, D108A, K109A, E198A, N199A, A241H, K245H, H279Q, A338V, I343V) and the primer pair: *GAAGTCAGAAACCTTAATG* and *TGTGGATCCCTAGATCGCGCTGAGAATG* (WP_003109502; aa: 2-294). Subsequently the PCR product was cloned into an expression vector (pET-28a(+) containing a 5' 8-histidine) using NheI and BamHI restriction sites. For the protein production the plasmid was transformed into competent BL21(DE3) *E. coli* (New England Biolabs) by heat shock and selected on agar plates with kanamycin. A Single clone was picked, incubated overnight in LB-media, and transferred into fresh NZY Auto-Induction LB medium (NZYTech, Lisboa, Portugal). The bacteria were incubated at 30°C overnight. Subsequently, bacteria were centrifuged at 4000 × g for 5 min and lysed in Tris-buffered saline (TBS) pH 8.0 by sonification. After an additional centrifugation step at 30.000 x g the supernatant was applied to INDIGO-Ni Resin (Cube Biotech, Monheim am Rhein) by gravity-flow. After an initial washing step, the bound fusion protein was eluted step wise with 5, 10, 20, 40, 80, 100, 250, and 500 mM imidazole (Sigma-Aldrich). The purity of the recombinant MBP-PcrV was determined by SDS-PAGE. Eluted protein fraction was dialyzed against TBS pH 7.4.

IgG isolation from patient serum

Serum samples were diluted in PBS and incubated overnight with Protein G Sepharose® 4 Fast Flow (GE Healthcare, Chicago, IL, USA) rotating at 4°C. The next day the tubes were centrifuged at 300 × g without brake and the beads were resuspended in 2 mL PBS after removing the supernatant containing the diluted serum sample. Before adding the resolved Protein G beads, Polyprep® Chromatography Columns with 2 mL bed volume (Bio-Rad Laboratories, Hercules, CA, USA) were washed with 70% (v/v) ethanol and equilibrated with PBS. After three washing steps with PBS, IgG were eluted with 10-fold bed volume of 0.1 M glycine (pH 3.0) and

collected in 1/10th of 1 M Tris-HCl (pH 8.0) (both Sigma-Aldrich). Subsequently, flow-through was transferred to 50 kDa cut-off centrifugal filter (Sigma-Aldrich) and washed several times to exchange the buffer to PBS.

Determination of anti-PcrV titers in serum

High-binding 96-well ELISA plates (Corning Inc., Corning, NY, USA) were coated with recombinant PcrV protein (2 μg/mL) in ELISA coating buffer (Biolegend, San Diego, CA, USA) at 4°C overnight, washed four times with PBS/0.05% Tween (Merck) (PBST) and blocked with PBS, containing 5% BSA (Sigma-Aldrich) for 120 min at RT. Thereafter, serum was added in serial dilutions in PBS/5% BSA for 60 min at RT. After washing with PBST, plates were incubated with horseradish peroxidase-conjugated goat anti-human IgG antibody (Jackson ImmunoResearch West Grove, PA, USA; 1:2500 in PBS/5% BSA) for 60 min at RT. ELISAs were developed using 3,3',5,5'-tetramethylbenzidine (TMB) (Thermo Fisher Scientific). After 15 min sulfuric acid (Carl Roth) was added and absorbance was measured at 450 nm using a multiplate reader (Hidex, Turku, Finland).

Cell surface expression of a PcrV-specific antibody to validate identification of PcrV-specific B cell populations

Variable regions of the mouse derived mAb 1F3 were cloned into the pMX vector with heavy and light chain constant regions, a self-splicing signal F2A, PDGF-R transmembrane domain and mCherry reporter protein using Gibson Assembly Master Mix (NEB).[42,82] HEK293T cells were transfected with Lipofectamine 3000 diluted in Opti-MEM™ medium (both Thermo Fisher Scientific). For transfection HEK293T cells were incubated in starving medium (DMEM with 2% FBS, 1% Pen-Strep, 1% sodium pyruvate, 1% L-glutamine). Cells were harvested three days post transfection, suspended in FACS buffer (PBS with 2% FBS, 1% BSA and 2 mM ethylenediaminetetraacetic acid [EDTA]) and incubated for 20 min at 4°C with Alexa Fluor™ 488 (PcrV^{AF488}) and Alexa Fluor™ 647 (PcrV^{AF647}) labeled PcrV, respectively (Microscale Protein Labeling Kit; both Thermo Fisher). After washing, binding of PcrV to PcrV-specific cells was assessed by flow cytometry with FACSCanto™ II (BD Biosciences, East Rutherford, NJ, USA).

Isolation of PcrV-specific B cells

PBMCs were enriched for CD19^{+} cells using CD19 micro beads (Miltenyi Biotec, Bergisch-Gladbach, Germany) according to the manufacturer's instruction. After a washing step with FACS buffer, cells were spun down and blocked for 30 min in 10% FCS. Subsequently, cells were resuspended in buffer with 4′,6-diamidino-2-phenylindole (DAPI) (Thermo Fisher Scientific) (1:100), anti-human IgG-PE (clone: G18-145) (BD Biosciences) and anti-human CD20-Alexa Fluor 700 (clone: 2H7) (Biolegend), PcrV^{AF488} and PcrV^{AF647} (each 10 μg/mL) and incubated for 20 min at 4°C. Finally, cells were washed with 15 mL FACS buffer, spun down and resuspended in 500 μL FACS buffer. Cell suspensions were used for further sorting in a single cell manner into 96-well plates using a BD FACSAria™ Fusion (BD Biosciences). All wells contained 4 μL lysis buffer, consisting of PBS, 0.5 U/μL RNAsin (Promega), 0.5 U/μL RNaseOUT™ (Thermo Fisher Scientific), and 10 mM DTT (Thermo Fisher Scientific). After sorting, plates were immediately stored at −80°C until further processing.

Ig heavy-/light-chain amplification and sequence analysis

Single-cell amplification of antibody heavy and light chains was performed as previously described.[57] Briefly, cDNA was generated by reverse transcription using Random Hexamer Primer and Superscript IV reverse transcriptase (both Thermo Fisher Scientific) in presence of RNaseOUT™ (Thermo Fisher Scientific) and RNasin® (Promega). Sequential semi-nested PCR using a Platinum™ Taq Hot Start polymerase (Thermo Fisher Scientific) and optimized V gene-specific primer mixes were used to amplify target sequences and sequenced subsequently.[80] Sequences were annotated with IgBLAST and trimmed to extract only the variable region from FWR1 to the end of the J gene.[89] To identify clonally related sequences within a single subject, heavy chain sequences of that particular subject were grouped by identical VH and VJ genes and pairwise Levenshtein distances between CDRH3s within a VH/VJ group were determined. Sequences were assigned to the same clone if they shared the same VH/VJ gene combination and had a minimal CDRH3 amino acid identity of 75% (with respect to the shortest CDRH3). All clones were cross validated by the investigators taking shared mutations, IGHG isotype, and light chain information into account, where available.

Cloning and production of PcrV-specific mAbs

Antibody cloning from 1st PCR products was performed as previously described.[57] Amplicons for cloning were produced from the 1st PCR using a Q5® Hot Start High Fidelity DNA Polymerase (New England Biolabs) and specific primer for overhangs for sequence and ligation independent cloning (SLIC). After purification (NucleoSpin® 96 PCR Clean-up, Macherey-Nagel, Dueren, Germany), target sequences were cloned into expression vectors by SLIC using T4 DNA polymerase (New England Biolabs) and chemical competent *E. coli* DH5α.[81] After verification of positive colonies by colony PCR and Sanger sequencing, plasmids were amplified and purified from midi cultures (Macherey-Nagel). HEK293-6E cells were co-transfected with human heavy chain (IgG1 isotype) and light chain antibody expression plasmids using polyethylenimine (PEI) (Sigma-Aldrich) and maintained in FreeStyle 293 Expression Medium (Thermo Fisher Scientific) with 0.2% penicillin/streptomycin (Thermo Fisher Scientific) at 37°C and 6% CO2 and kept under constant shaking at 90-120 rpm. To isolate monoclonal antibodies, supernatants were centrifuged seven days post transfection, filtrated using PES filters and incubated with Protein G-coupled Sepharose® beads (GE Life Sciences). Beads were centrifuged, washed with PBS and antibodies were eluted from the Protein G-coupled beads in chromatography columns using 0.1 M glycine (pH = 3) and buffered using 1 M Tris (pH = 8). Buffer exchange to PBS was performed using

Amicon® 30 kDa filter tubes (Millipore). Antibody concentrations were determined using UV spectrophotometry (Nanodrop, Thermo Fisher Scientific) and antibodies were stored at 4°C.

ELISA analysis to determine antibody binding activity to PcrV

ELISA plates (Thermo Fisher Scientific) were coated with 2.5 μg/mL recombinant PcrV in PBS at 4°C overnight. ELISA plates were blocked with 2.5% BSA and 2.5% dry milk powder in PBS/0.05% Tween-20 (PBST) for 60 min at RT, incubated with primary antibody in 2.5% BSA and 2.5% dry milk powder in PBST for 120 min, followed by goat anti-human IgG-HRP (Southern Biotech) diluted 1:2000 in PBS for 60 min at RT. Between each step plates were washed three times with PBST. ELISA plates were developed with ABTS solution (Thermo Fisher Scientific) and absorbance was measured at 415 nm and 695 nm. Positive binding was defined by a minimal top OD $\geq$ 0.2 and an $EC_{50} \leq 30$ μg/mL.

A549 cytotoxicity assay

Human lung epithelial cells (A549) (ATCC, Manassas, VA, USA) were seeded in 100 μL RPMI-medium (Thermo Fisher Scientific) with 10% FBS at a density of 2×10^5 cells/mL in a 96-well plate (TPP, Trasadingen, Switzerland) and incubated at 37°C with 5% CO_2. After 24 h, the supernatant was removed and cells were infected with bacteria resuspended in RPMI/10% FBS (100 μL/well). After 150 min, cells were washed with RPMI and 100 μL RPMI/10% FCS supplemented with 20 μg/mL gentamicin and 10 μg/mL moxifloxacin were added. After additional 18 h, 10 μL resazurin (Sigma-Aldrich) was added and the cells were incubated for 140 min. Fluorescence was measured at a wavelength of $Ex_{560\ nm}/Em_{590\ nm}$.

Sequencing of *pcrV* in clinical isolates

Bacterial genomic DNA was extracted with a DNeasy® Kit (Qiagen) according to the manufacturer's instruction. The *pcrV* gene region was amplified using a primer set fwd 5'-GCA GGG CGA GCA GGG TAC C-3' / 5'-GCC GAT GCG TGG CTT GTT G-3' and rev 5'GCC TGT TGC TGG TCG GTG TC-3' / 5'-GCT GGT CGG TGT CGG AAG G-3' and sequenced (Microsynth Seqlab, Balgach, Switzerland).

Competition ELISA

ELISA plates (Thermo Fisher Scientific) were coated with 50 ng/mL recombinant PcrV in PBS at 4°C overnight. After three washing steps with PBST plates were blocked with 5% BSA in PBS for 120 min at RT. Subsequently, unlabeled mAbs (200 μg/mL) and corresponding biotinylated mAbs (2 μg/mL) were premixed and added. For biotinylation the One-Step Antibody Biotinylation Kit (Miltenyi Biotec) was used. After 2 h of incubation at RT, plates were washed and Streptavidin-HRP was added (1:10.000) (Thermo Fisher Scientific). ELISAs were developed with TMB solution (Thermo Fisher Scientific). Optical density at 450 nm was measured after adding sulfuric acid. Data were analyzed and hierarchical clustered using Morpheus Software.

Cryo-EM sample preparation and data collection

Fab fragments were prepared using the Pierce™ Fab preparation kit (Thermo Fisher Scientific). The recombinantly expressed MBP-PcrV was incubated with the individual Fab fragment at a molar ratio of 1:1 on ice for 1 h. Then, the sample was further concentrated with a final volume of 500 μl, and separated by gel filtration on a Superdex® 200 Increase 10/300 GL. Main peak fractions were analyzed by SDS-PAGE and cryo-EM.

For MBP-PcrV/30-B8, 1.3 mg/mL protein complex was vitrified on Quantifoil® 300 gold mesh 2.0/1.0 grids in liquid ethane/propane mix using the Vitrobot™ Mark IV. The vitrified sample was imaged on a Titan Krios G3i (Thermo Fisher Scientific) operating at 300 eV and equipped with an energy filter (15 eV slit width). Images were acquired in counting mode on a Gatan K3 direct electron detector using EPU software at a nominal magnification of 105,000 x (pixel size 0.85 Å/pix) with a defocus range set between 1.0 and 2.5 μm. For individual frames, an electron dose per frame of 1.5 e/A^2 was used, corresponding to a cumulative electron dose of 60 e/A^2 over 40 frames. The MBP-PcrV/11-E5, 0.4 mg/mL protein complex was vitrified on Quantifoil® 200 copper mesh 2.0/1.0 grids in liquid ethane/propane mix using the Vitrobot™ Mark IV. The vitrified sample was imaged on the same microscope and images were recorded with an electron dose of 1.24 e/A^2 per frame, corresponding to a cumulative electron dose of 62 e/A^2 over 50 frames.

Cryo-EM data processing, model building, and refinement

Single particle analysis was performed using Relion 4.0.[83] Briefly, movies were motion-corrected using MotionCorr. Particle picking and CTF estimation was performed on motion-corrected images using crYOLO and CTFFIND, respectively.[85,86] The picked particles were extracted into 168 x 168 boxes, and binned by four. Two-dimensional classifications were performed on split datasets and particles were rejoined from selected class averages. Additional 2D classification, and subsequent selections generated a new data set, which was subjected to a few rounds of 3D classifications, selection, auto-refinement, CTF-refinement, particle polishing and a final round of auto-refinement. The resolution was determined using the gold-standard procedure and a Fourier shell correlation cutoff of FSC = 0.143. Local resolution was calculated in Relion/4.0.

The Fab fragments and PcrV models were first generated using AlphaFold.[84] They were used as initial models and fitted in the density maps with help of the ISOLDE plugin in Chimerax1.3.[92] The resulting coordinate files were further refined with real-space

refinement in Phenix and Rosetta refinement in Starmap.[88,93] Model validation was carried out using the MolProbity server.[87] The statistics for data collection, processing, and model building are listed in Table S5.

Pharmacokinetic profiles of human anti-PcrV mAbs

For pharmacokinetic and pharmacodynamic experiments, outbred 5 - 6 weeks old CD-1 mice (Charles River, Netherlands) were used. The animal studies were conducted in accordance with the recommendations of the European Community (Directive EEC2010/63/EU, 1st January 2013). All animal procedures were performed in strict accordance with the German regulations of the Society for Laboratory Animal Science (GV- SOLAS) and the European Health Law of the Federation of Laboratory Animal Science Associations (FELASA). The experiments were approved by the ethical board of the Niedersächsisches Landesamt für Verbraucherschutz und Lebensmittelsicherheit, Oldenburg, Germany.

For single dosing PK studies, mouse antibodies were administered intraperitoneally (i.p.) at 5 mg/kg. About 20 μl of whole blood was collected serially from the lateral tail vein at time points 0.25, 0.5, 1, 2, 4 and 6, 24 and 48 h. After 72 h mice were sacrificed, blood was collected from the heart and lungs were removed, weighed, and homogenized in 3 mL 0.9% NaCl. Whole blood was collected into tubes coated with 0.5 M EDTA and immediately spun down at 13,000 rpm for 10 min at 4°C. The plasma was transferred into a new tube and then stored at -80°C until analysis. Human IgG concentrations of the samples were determined using a commercial total human IgG ELISA Kit (Thermo Fisher Scientific) and ELISA plates coated with goat anti-human IgG (Biotrend, Cologne, Germany) using Human IgG1 Lambda (Biotrend) as standard and a horseradish peroxidase-conjugated goat anti-human IgG antibody (Jackson ImmunoResearch) as secondary antibody.

In vivo infection experiments

For the therapeutic pneumonia model, female CD-1 mice were rendered neutropenic by administration of 150 mg/kg and 100 mg/kg cyclophosphamide intraperitoneally (i.p.) on day -4 and -1, respectively. At day 0, mice were infected by nebulization of 20 μl $1.7x10^9$ CFU/ml *PA* (Boston 41501). After 2 h, mice were treated with 5 mg/kg mAbs, 100 mg/kg levofloxacin or a vehicle control. To control bacterial burden after nebulization, two animals were used as inoculum control group. After 24 h p.i., mice were sacrificed for terminal analysis. After isolation of blood, lung and kidney were removed, weighed and homogenized in 3 mL 0.9% NaCl. For determination of CFUs, suspensions of homogenized organs were serially diluted, plated on agar plates and incubated overnight at 37°C. CFUs were determined by manual counting. TNF and IL-6 were determined in plasma using commercial ELISA Kits (all Thermo Fisher Scientific) according to the manufacturer's instruction. Human IgG concentrations were determined as described above.

A prophylactic approach was tested with a neutropenic thigh infection model. Male CD-1 mice were rendered neutropenic by administration of 150 mg/kg and 100 mg/kg cyclophosphamide i.p. on day -4 and -1, respectively. 2 h prior infection antibodies were administered (5 mg/kg) intraperitoneally. Infection was initiated by intramuscular injection of $1.2x10^5$ CFU/ml *PA* (Boston 41501) (in 30 μl) into each lateral thigh. As control, levofloxacin (100 mg/kg) was given 2, 6 and 10 h after infection. To control the bacterial burden after injection, six animals were used as inoculum control group. For analgesia, all animals were treated with tramadol 20 mg/kg subcutaneously. After 24 h experiments were terminated and whole blood was collected into tubes coated with 0.5 m EDTA and immediately spun down at 13,000 rpm for 10 min at 4°C. The plasma was transferred into a new tube and analyzed as described above. Infected muscles were removed, homogenized and CFUs were determined.

Microscopic analysis

To determine autoreactivity, HepG2 cells (NOVA Lite HEp-2 ANA Kit) (Inova Diagnostics, San Diego, CA, USA) were stained with 100 μg/mL mAbs for 30 min at room temperature followed by washing with PBS and labeling with a second FITC-conjugated anti-human IgG antibody for 30 min. Stained slides were mounted and analyzed by microscopy. Each mAb was tested at least in duplicate.

For histological analyses mouse lungs were fixed for 24 h in formalin and stored in 70% ethanol. Fixed lungs were embedded in paraffin, cut by a microtome and stained with H&E. Slides were scanned using a S360 slide scanner (Hamamatsu Photonics, Hamamatsu, Japan) and images were generated using OMERO software (OME University of Dundee & Open Microscopy Environment). ImageJ software was used to quantify alveolar space by using a threshold of 205 and 246 respectively. Alveolar space was quantified relative to the total surface area.

Statistical analysis

Statistical analysis was performed with GraphPad Prism 8.0.2 software (GraphPad). Statistical parameters (number of samples tested, statistical tests etc.) are provided in the figure legends. *P*-values less than or equal to 0.05 were considered statistically significant. Comparison of multiple groups was done by one- or two-way ANOVA depending on the dataset (for all groups homogeneity variance was tested). T-test with Welsh's corrections were used for comparison of two groups. Box plots indicate the median, the upper and lower quartile and the minimum and maximum values. Shown data points represent the technical mean of an independent experiment / biological replicate.

Supplemental figures

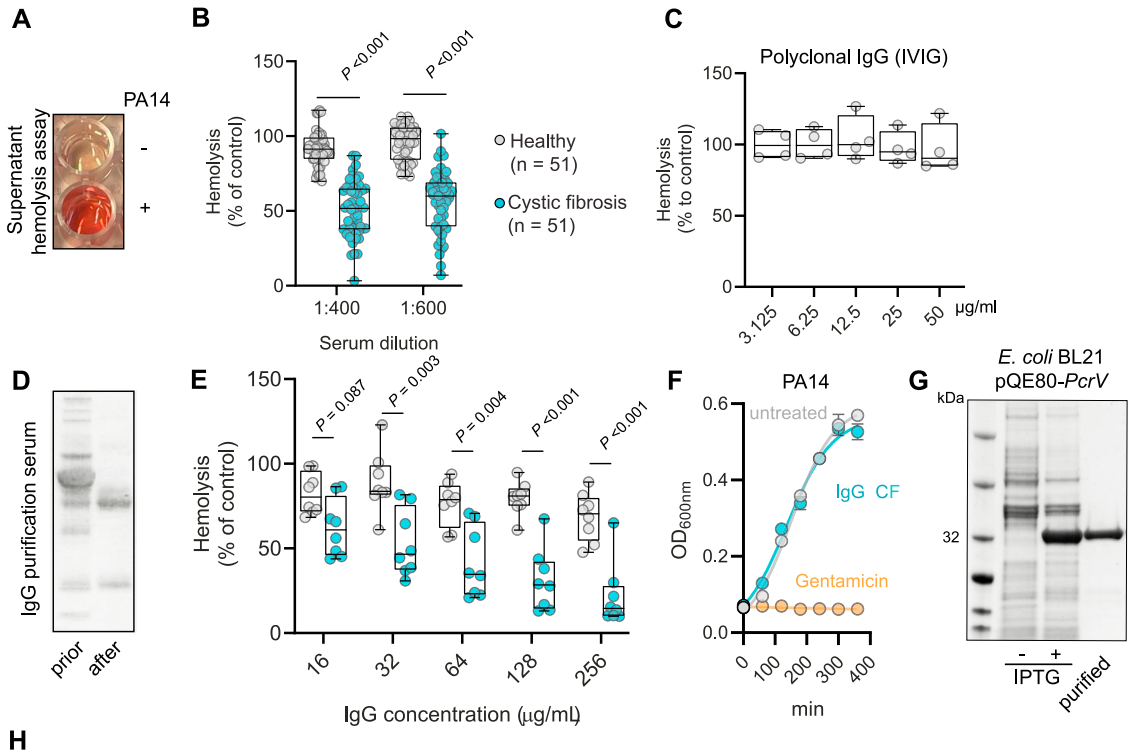

H

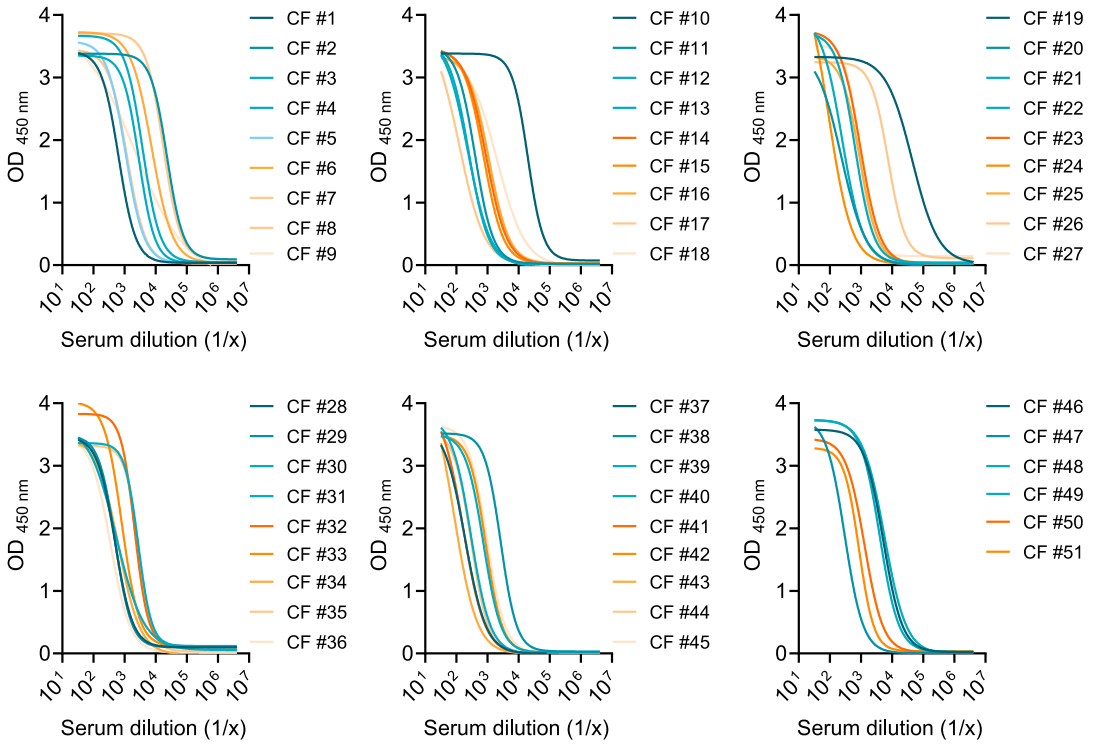

(legend on next page)

Figure S1. Neutralizing and PcrV-binding activity of patient-derived serum or IgG, related to Figure 1

(A) Human red blood cells (RBCs) were infected with PA wild-type strain PA14 for 2 h with a MOI of 1. After 2 h, RBCs were centrifuged, and supernatants were transferred to a new microtiter plate. Image shows visible release of hemoglobin due to bacteria-induced hemolysis (+), compared with non-infected RBCs (−).

(B) Heat-inactivated serum of pwCF (n = 51) and healthy individuals (n = 51) was tested for inhibition of hemolysis at different concentrations (1:400 and 1:600). Human red blood cells were infected with PA14. Percentage of hemolysis for each sample was calculated to infected red blood cells without treatment. Significance was calculated using a two-way ANOVA with a Sidak's multiple comparisons test comparing each group within one dilution.

(C) Human polyclonal IgGs (IVIG) were tested in serial dilution in the above-described hemolysis assay.

(D) IgG was purified from serum using protein G beads. SDS-PAGE loaded with serum prior to protein G treatment (left) and purified IgG after isolation (right).

(E) RBCs were infected with PA wild-type strain PA14 in presence of purified IgG from pwCF (cyan) and healthy individuals (gray) at different concentrations. After 2 h, OD values at 540 nm were quantified as an indicator of bacteria-induced cell lysis (hemolysis). Significance was calculated using a two-way ANOVA with a Sidak's multiple comparisons test, comparing the CF group with healthy individuals for every dilution.

(F) Growth curve of PA in the presence of human IgG isolated from a pwCF, compared with untreated bacteria and bacteria treated with gentamicin (20 μg/mL). Bacteria were grown in LB media at 37°C shaking with 200 rpm. The OD was determined at 600 nm every 60 min for a total of 6 h.

(G) The PA *pcrV* gene was PCR amplified and cloned into a pQE80 expression vector. Plasmids were transformed into *E. coli* BL21. Coomassie-stained SDS-PAGE of bacterial lysates. Bacteria were grown with (+) or without (−) 300 μM IPTG (isopropyl-β-D-thiogalactopyranosid) to induce protein expression. The last lane shows the recombinant Ni-NTA affinity purified His-tagged PcrV protein.

(H) PcrV-binding ELISAs were performed with diluted serum samples of CF patients (n = 51). Median effective concentrations (EC_{50}) were determined based on binding curves.

Boxplots indicate the median, the upper and lower quartile, and the minimum and maximum values. Shown data points represent the technical mean of an independent experiment/biological replicate.

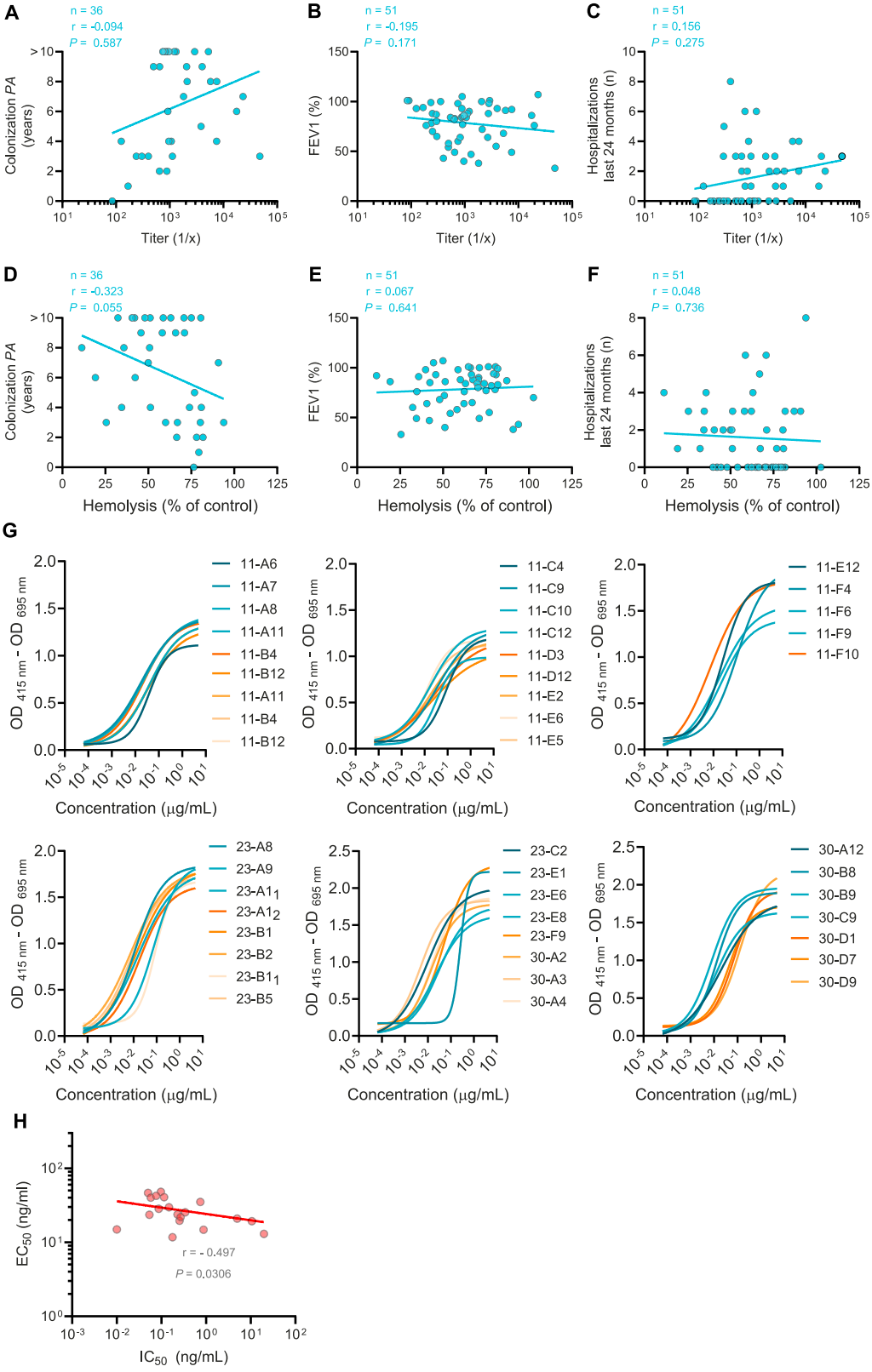

(legend on next page)

Figure S2. Correlation of clinical characteristics and representative binding curves of human anti-PcrV mAbs and correlation analysis, related to Figures 1 and 2

(A–C) Colonization, defined as period between the first and last positive sputum culture of PA relative FEV1 (forced expiratory volume in the first second of forced expiration relatively to normal values), and frequency of hospitalization in the last 24 months of each pwCF (cyan) were plotted against the respective anti-PcrV titer. Significances were tested using Spearman's correlation.

(D–F) Corresponding to (A)–(C), clinical characteristics were plotted against the results of the hemolysis screening at a 1:800 serum dilution. Significances were tested using Spearman's correlation.

(G) Patient-derived mAbs were tested in PcrV-binding ELISA with 4-fold serial dilutions. EC_{50} values were calculated on the basis of binding curves.

(H) Correlation analysis of selected antibodies with high neutralizing activity. Binding capacity (EC_{50}) was correlated with the mean inhibitory concentration (IC_{50}). Significance was tested using a Spearman's correlation.

Shown data points represent the technical mean of an independent experiment/biological replicate.

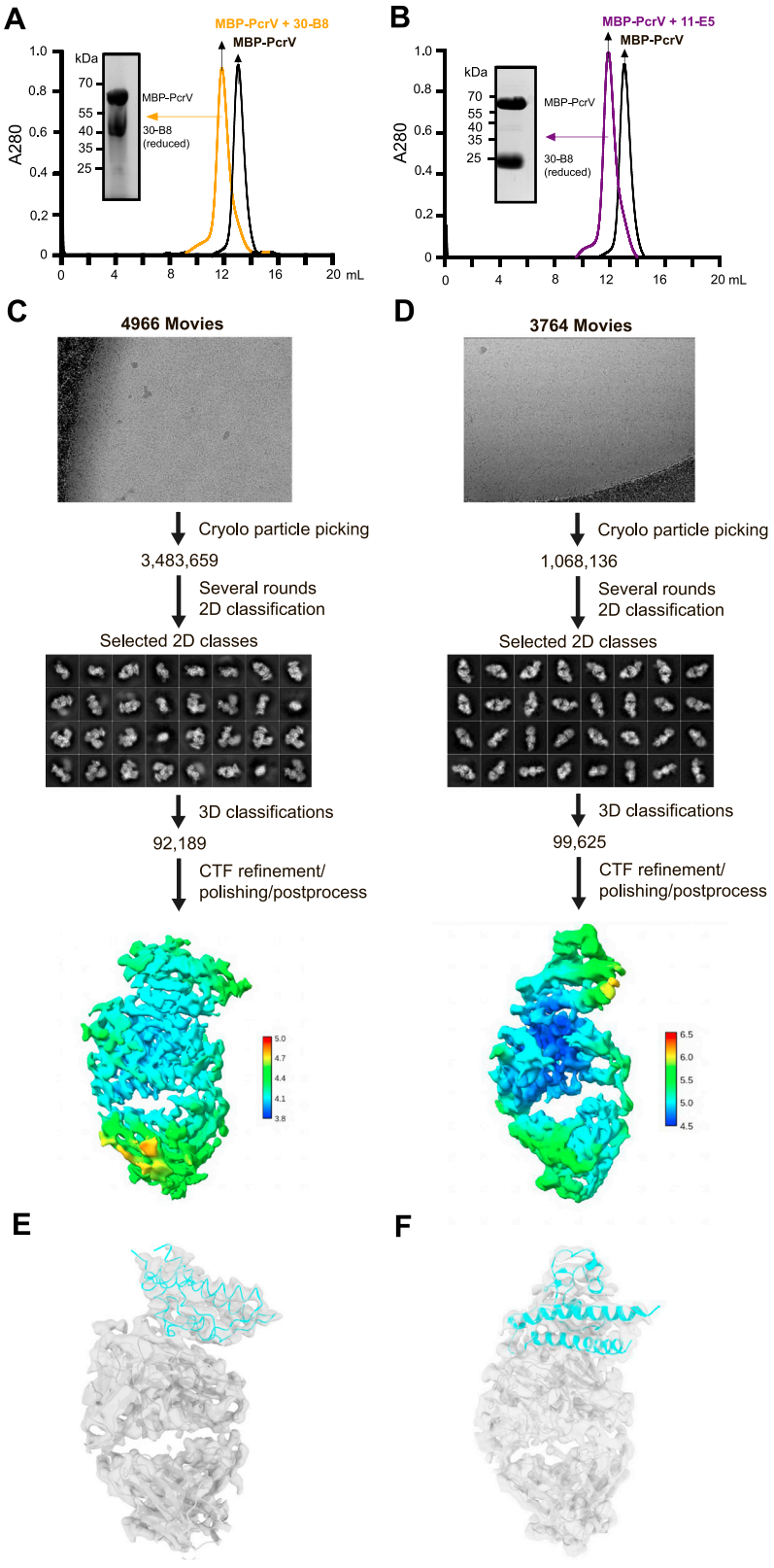

(legend on next page)

Figure S3. Cryo-EM structure determination of mAbs 30-B8 and 11-E5 bound to the T3SS needle-tip protein PcrV, related to Figure 4

(A and B) Purification of MBP-PcrV/Fab fragments used for cryo-EM structure determination. Size-exclusion chromatography profiles of the reconstituted MBP-PcrV/Fab and the MBP-PcrV alone. The MBP-PcrV/Fab was reconstituted with roughly 1:1 molar ratio and further purified using Superdex200 10/300 GL column. The peak fraction of MBP-PcrV/Fab was analyzed by SDS-PAGE.

(C and D) Workflow of data-processing required for the final cryo-EM maps with a resolution below 5Å.

(E and F) The generated structures were fitted in the reconstructed cryo-EM maps (E: 30-B8/PcrV; F: 11-E5/PcrV).

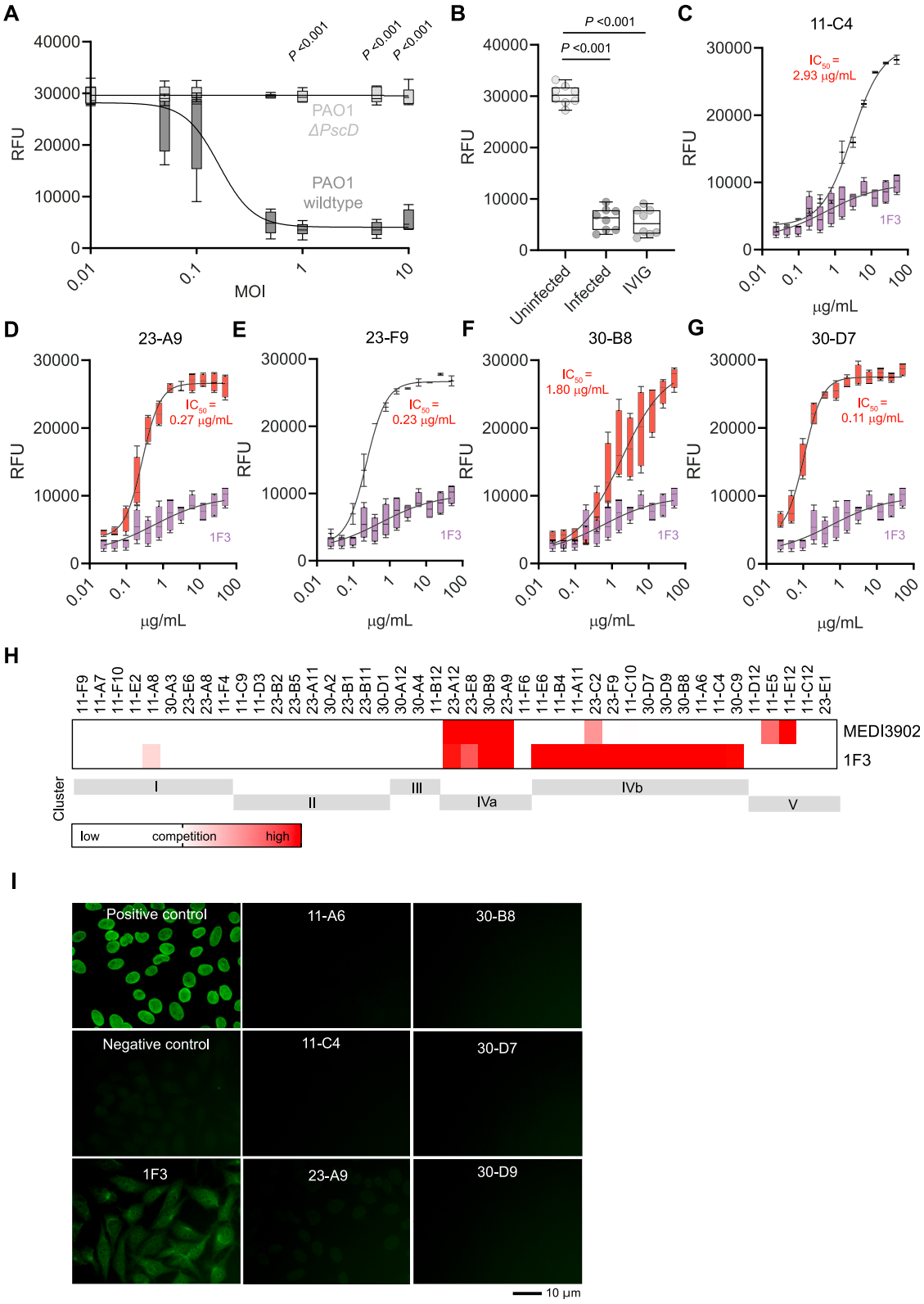

(legend on next page)

Figure S4. Human anti-PcrV mAb mediates inhibition of bacteria-induced cytotoxicity in A549 cells, related to Figure 5

(A) Wild-type strain PAO1 (dark gray) and type III secretion system-deficient mutant strain PAO1 Δ*PscD* (light gray) were used in the A549 survival assay with various MOI ranging from 0.01 to 10. Significance was calculated using a two-way ANOVA with a Sidak's multiple comparisons.

(B) A549 cells were infected with PAO1 for 150 min with a MOI of 0.5 in presence of polyclonal human IgG (intravenous IgG = IVIG; 50 μg/mL). Uninfected and infected cells were used as a control. Relative fluorescence units (RFUs) were measured after adding resazurin. Significance was calculated to uninfected cells treated with a mock control using a one-way ANOVA with Tukey's multiple comparisons test.

(C–G) A549 cells were infected as described before in presence of human anti-PcrV mAbs from donor CF #11 (C), CF#23 (D and E), and CF #30 (F and G) at a concentration ranging from 50 to 24 ng/mL. For mAbs 11-C4 and 23-F9, the results of one exemplary experiment are shown. The calculated half-maximal inhibitory concentration (IC_{50}) for the antibodies is specified in each in graph. 1F3 was used as a control (purple).

(H) Competition ELISA showing binding sites of 1F3 and MEDI3902 in comparison with human anti-PcrV mAbs.

(I) HepG2 cells were stained with anti-PcrV mAbs and subsequently incubated with a second FITC-conjugated anti-human IgG antibody. A positive control was used according to the instructions of the kit we used. As negative control, PBS was used instead of a primary antibody. Stained slides were mounted and analyzed by microscopy with a 40-fold magnification.

Boxplots indicate the median, the upper and lower quartile, and the minimum and maximum values. Shown data points represent the technical mean of an independent experiment.

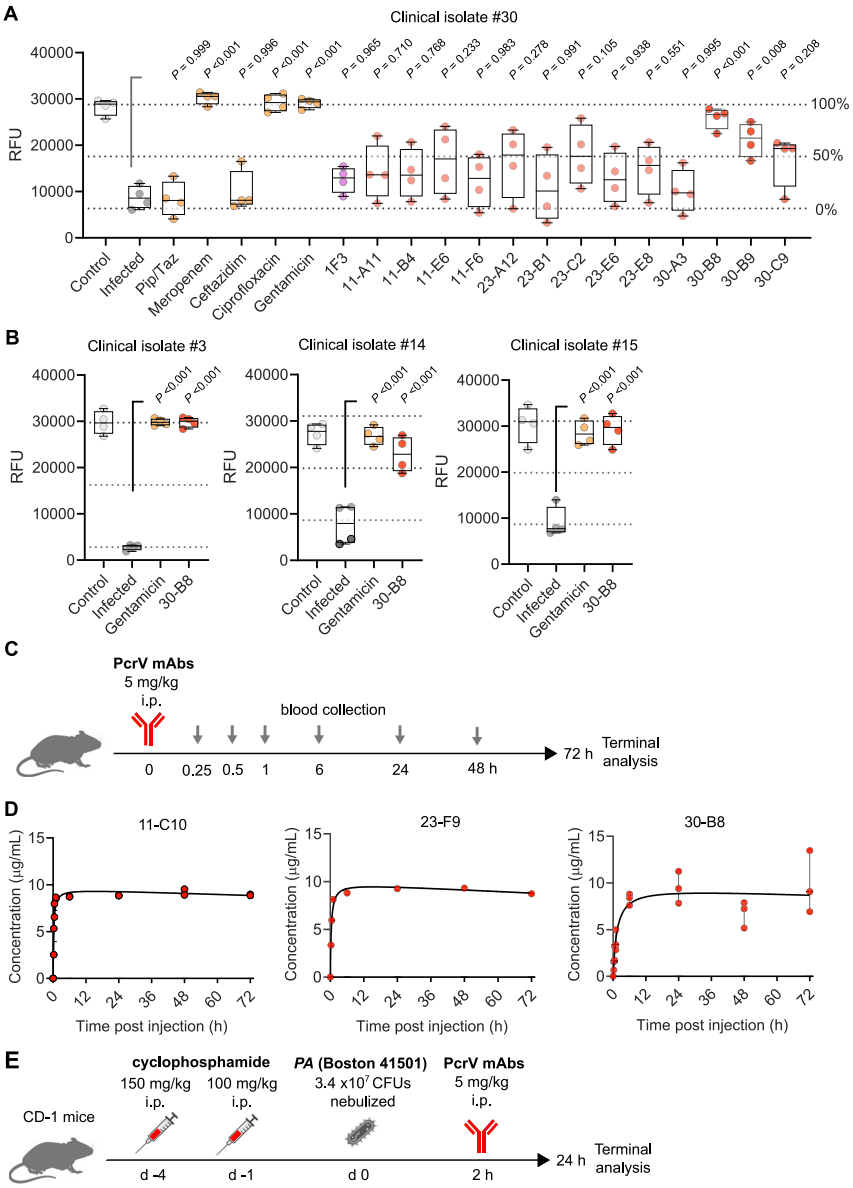

Figure S5. Human anti-PcrV mAbs are broadly active in clinical PA isolates and are detectable in mouse plasma levels after intraperitoneal administration, related to Figures 5 and 6

(A) A549 cells were infected with a clinical isolate (#30) for 150 min (MOI of 0.5) in presence of patient-derived monoclonal anti-PcrV antibodies (50 µg/mL) (red). Control cells were left uninfected (gray) or were infected in presence of a mock control (dark gray), the humanized mouse anti-PcrV antibody 1F3 (50 µg/mL) (purple), or were treated with piperacillin/tazobactam (16 µg/mL), meropenem (8 µg/mL), ceftazidime (8 µg/mL), ciprofloxacin (1 µg/mL), or gentamicin (4 µg/mL) (all orange). Relative fluorescence units (RFUs) were measured after adding resazurin. Significance was calculated to infected cells treated with a mock control using a one-way ANOVA with Tukey's multiple comparisons test.

(B) A549 cells were infected with different clinical isolates (#3, 14, 15) for 150 min (MOI of 0.5) in presence of the anti-PcrV mAb 30-B8 (50 µg/mL) (red). Control cells were left uninfected (gray) or were infected in presence of a mock control (dark gray) or antibiotics (orange). Significance was calculated to infected cells treated with a mock control using a one-way ANOVA with Tukey's multiple comparisons test.

(C) Anti-PcrV mAbs were administered intraperitoneally (i.p.) at 5 mg/kg. About 20 µL of whole blood was collected at time points 0.25, 0.5, 1, 2, 4, and 6, 24, and 48 h. After 72 h, mice were sacrificed, and blood was collected by heart puncture.

(D) Human IgG levels for each antibody were quantified by ELISA.

(E) Experimental scheme of the pneumonia infection model. CD-1 mice were treated with cyclophosphamide intraperitoneally at day −4 and day −1 to induce neutropenia. Subsequently, pulmonary infection was induced by nebulization of PA (Boston 41501 strain). A vehicle control (PBS), levofloxacin, or mAbs (5 mg/kg) were administered 2 h later intraperitoneally. After 24 h, experiments were terminated and lungs were homogenized, followed by quantifications of CFUs. Plasma was used to quantify IL-6 and TNF levels.

Boxplots indicate the median, the upper and lower quartile, and the minimum and maximum values. Shown data points represent the technical mean of an independent experiment.

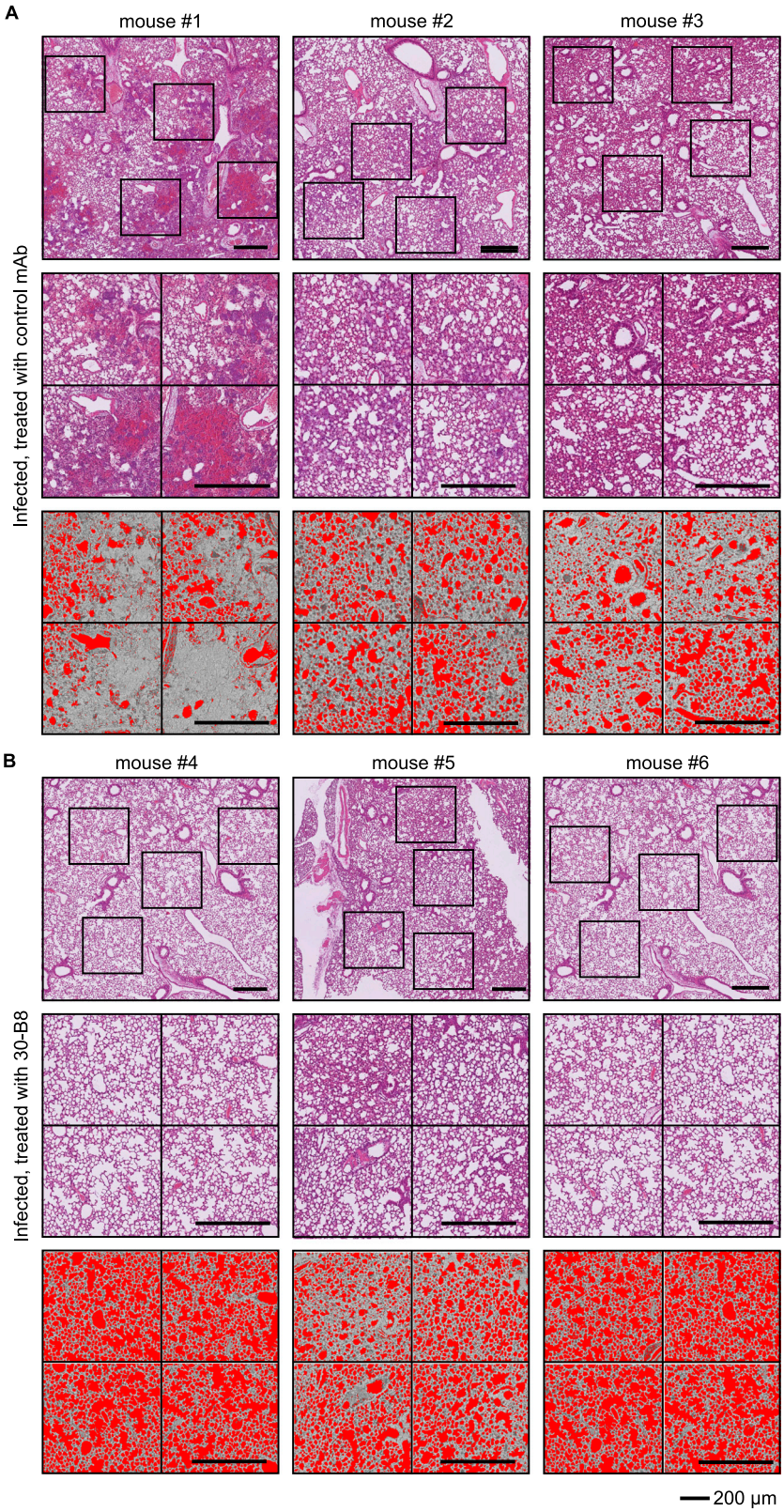

(legend on next page)

Figure S6. Lung tissue analysis of PA-infected mice treated with mAbs, related to Figure 6

(A and B) CD-1 mice were treated with cyclophosphamide at d −4 and d −1 to induce neutropenia. Pulmonary infection was induced by nebulization of PA (Boston 41501 strain). A control antibody (MCA1) (n = 3) (A) or the mAb 30-B8 (5 mg/kg) (n = 3) (B) were administered 2 h later intraperitoneally. Experiments were terminated after 24 h and lungs were fixed, embedded in paraffin, and stained with H&E. For each animal, four representative image sections were selected (upper and middle row) and the approximate alveolar space was marked (red) (lower panel).

STAR Protocols

CellPress
OPEN ACCESS

Protocol

Protocol for developing *Pseudomonas aeruginosa* type III secretion system-neutralizing monoclonal antibodies from human B cells

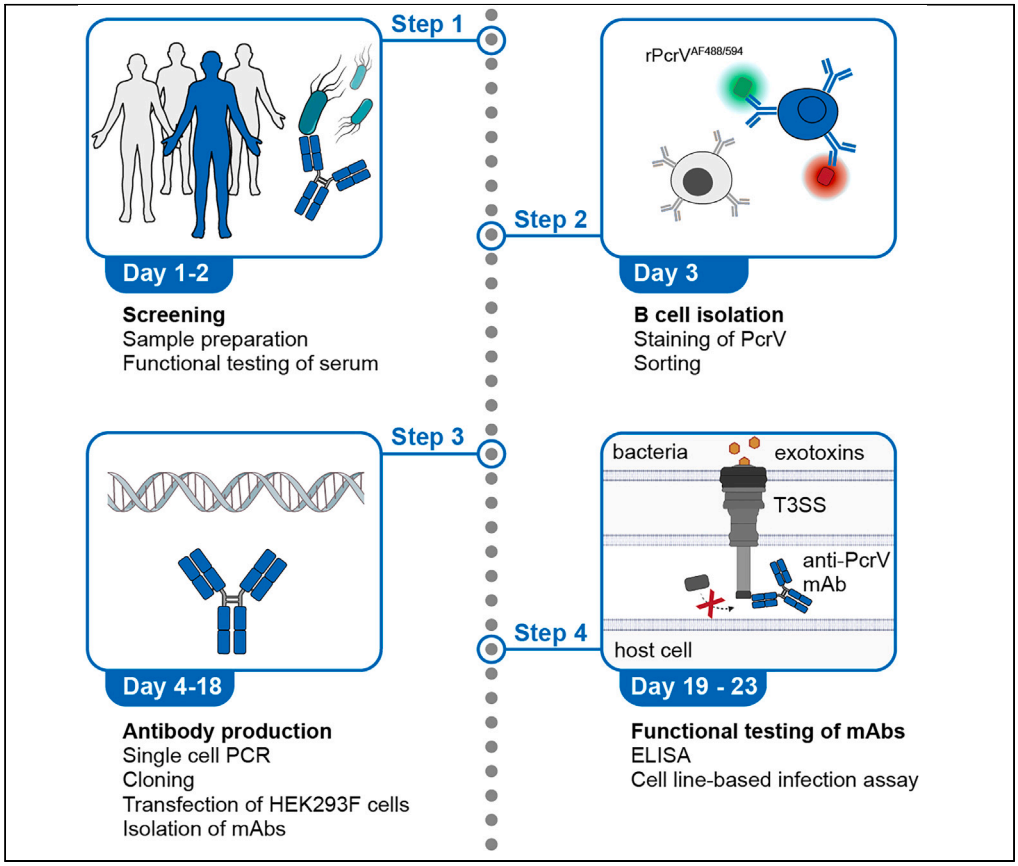

Monoclonal antibodies (mAbs) targeting bacterial virulence factors may represent promising therapeutics in the fight against severe bacterial infections. Here, we present an approach for developing human-derived antibodies targeting the type III secretion system (T3SS) of *Pseudomonas aeruginosa* (PA) by neutralizing the function of the T3SS-tip protein PcrV. The protocol involves identifying individuals with protective antibodies, isolating PcrV-specific B cells from these individuals, and producing and testing anti-PcrV mAbs derived from single B cells.

Publisher's note: Undertaking any experimental protocol requires adherence to local institutional guidelines for laboratory safety and ethics.

Alexandra Albus, Christoph Kreer, Florian Klein, Jan Rybniker, Alexander Simonis

alexander.simonis@uk-koeln.de

Highlights

Functional screening for type III secretion system-neutralizing antibodies in humans

Production of patient-derived anti-PcrV antibodies from single B cells

In vitro characterization of anti-PcrV antibodies

Albus et al., STAR Protocols 5, 103440
December 20, 2024
https://doi.org/10.1016/j.xpro.2024.103440

STAR Protocols

CellPress
OPEN ACCESS

Protocol

Protocol for developing *Pseudomonas aeruginosa* type III secretion system-neutralizing monoclonal antibodies from human B cells

Alexandra Albus,[1,2] Christoph Kreer,[3] Florian Klein,[3,4] Jan Rybniker,[1,4] and Alexander Simonis[1,2,4,5,6,*]

[1]Department I of Internal Medicine, Faculty of Medicine and University Hospital Cologne, University of Cologne, 50937 Cologne, Germany

[2]Center for Molecular Medicine Cologne (CMMC), Faculty of Medicine and University Hospital Cologne, University of Cologne, 50931 Cologne, Germany

[3]Laboratory of Experimental Immunology, Institute of Virology, Faculty of Medicine and University Hospital Cologne, University of Cologne, 50931 Cologne, Germany

[4]German Center for Infection Research (DZIF), Partner Site Bonn-Cologne, 50937 Cologne, Germany

[5]Technical contact

[6]Lead contact

*Correspondence: alexander.simonis@uk-koeln.de
https://doi.org/10.1016/j.xpro.2024.103440

SUMMARY

Monoclonal antibodies (mAbs) targeting bacterial virulence factors may represent promising therapeutics in the fight against severe bacterial infections. Here, we present an approach for developing human-derived antibodies targeting the type III secretion system (T3SS) of *Pseudomonas aeruginosa* (PA) by neutralizing the function of the T3SS-tip protein PcrV. The protocol involves identifying individuals with protective antibodies, isolating PcrV-specific B cells from these individuals, and producing and testing anti-PcrV mAbs derived from single B cells.

For complete details on the use and execution of this protocol, please refer to Simonis et al.[1]

BEFORE YOU BEGIN

This protocol details the methodology for developing human-derived mAbs that neutralize the type III T3SS function of PA. The T3SS is a critical virulence factor correlated with increased disease severity, functioning as a syringe-like structure that injects effector toxins into host cells, leading to cell lysis and tissue damage.[2] The PcrV protein is essential for this mechanism, forming the T3SS-needle tip complex required for the assembly and insertion of the PopB/D translocon into host cell membranes.[3]

Given the pivotal role of virulence factors in the pathogenesis of bacterial infections, investigating the human antibody repertoire against these factors and identifying neutralizing patient-derived antibodies presents a promising therapeutic strategy.[4] This protocol facilitates the identification of highly T3SS-neutralizing antibodies from humans, offering potential new treatments for PA infections.

The presented workflow is based on the antibody isolation protocol from Gieselmann et al.[5] but modified for the production of anti-PcrV mAbs and complemented with critical PA-specific assays, which can also be adapted for other T3SS proteins. Before initiating the study, it is necessary to recruit a cohort with individuals with prolonged or chronic PA infections and collect serum samples, peripheral blood mononuclear cells (PBMCs), and to produce purified PcrV protein.

Table 1. PcrV PCR master mix

Reagent	Amount per tube (µL)
Nuclease-free H_2O	16.38
5× Phusion GC Buffer	6.0
DMSO	0.9
dNTP mix (25 mM)	0.6
PcrV fwd primer (10 µM)	3.0
PcrV rev primer (forward) (10 µM)	3.0
Phusion High-Fidelity DNA Polymerase	0.12
Total	30

Institutional permissions

The use of human samples for laboratory experiments requires approved institutional review board (IRB) approval. Your institution may require additional and/or region-specific permissions, as well as restrictions with some materials/reagents. Therefore, do not start working before the necessary approvals have been obtained. Data shown in this protocol were obtained under the approval of the Institutional Review Board (IRB) of the University of Cologne, Germany (20-1287_1).

Pseudomonas aeruginosa is classified as biosafety level 2. Please note that you must fulfill all biosafety regulations before starting.

Preparation of serum samples and PBMCs

Timing: 120 min

⚠ CRITICAL: Antigen exposure is essential for the induction of a B cell response. Therefore, the study cohort should include individuals who have previously been infected or colonized with PA.

1. Serum preparation.
   a. Collect 4 – 9 mL peripheral blood in a 9 mL serum blood collection tube.
   b. After blood clotting, centrifuge the tube for 10 min at 3,000 × *g* at room temperature (RT = 18 – 24°C).
   c. Transfer the supernatant (serum) into 1.5 mL microcentrifuge tubes.
   d. Incubate the serum at 56°C for 30 min (e.g., in a dry block heater) to inactivate the complement.
   e. Centrifuge the tube for 1 min at 15,000 × *g* at RT and transfer supernatant into a new tube.
   f. Store the heat-inactivated serum at −80°C until further use.

   Note: Preparation of small volume aliquots is recommended to avoid repeated freeze-thaw cycles of serum samples.

2. Preparation of PBMCs samples.
   PBMCs samples are required for the isolation of PcrV-specific B cells.

   Note: We recommend PBMCs sampling after identification of individuals in the screening assay (see section 'identification of individuals for single B cell sorting').

   a. Collect 150 – 400 mL of peripheral blood in 9 mL ethylenediaminetetraacetic acid (EDTA) collection tubes or a blood bag with citrate phosphate dextrose adenine solution (CPDA-1).

   Note: The maximal volume of blood donation should be adapted to the body weight and health status of the donor. PBMC yield ranges between 0.5 – 3 × 10^6 cells per mL blood.

Table 2. PcrV PCR program

Steps	Temperature	Time	Cycles
Initial Denaturation	95°C	2.5 min	1
Denaturation	95°C	30 s	35 cycles
Annealing	68°C	30 s	
Extension	72°C	60 s	
Final extension	72°C	10 min	1
Hold	4°C	forever	

For isolation of PcrV-specific B cells a minimum of 1×10^8 PBMCs should be used. Higher yields can be achieved by using leukapheresis.

b. Dilute peripheral blood with phosphate buffered saline (PBS) containing 2 mM EDTA in a 1:1 ratio and transfer 30 mL per LeucoSEP tube. Prepare each LeucoSEP tube with 15 mL Ficoll beforehand. One LeucoSEP tube will be required for every 15 mL of peripheral blood.

Note: Instead of using LeucoSEP tubes, samples can be loaded directly on 15 mL Ficoll for gradient centrifugation.

c. Centrifuge LeucoSEP tubes for 15 min at 800 × *g* at 4°C. Perform this step with acceleration set to 9 and deceleration set to 0.

Note: After centrifugation, four distinct layers can be observed from top to bottom: plasma, PBMCs, Ficoll, and erythrocytes. The PBMC layer will appear as a thin whitish line just below the yellowish plasma layer at the top.

d. Carefully transfer the PBMC layers of all LeucoSEP tubes to a new 50 mL tube and add ice-cold PBS containing 2 mM EDTA to a final volume of 45 mL. Use several new 50 mL tubes if needed.

Note: An additional incubation step with 0.83% ammonium chloride in PBS containing 2 mM EDTA for 5 min on ice can reduce contamination with RBCs and increase PBMC purity.

e. Centrifuge the tube for 10 min at 400 × *g* at 4°C. Perform this step with acceleration set to 9 and deceleration set to 9 (all subsequent centrifugation steps are performed with these settings).
f. Discard the supernatant and repeat the washing step twice with ice-cold PBS containing 2 mM EDTA for 10 min at 200 × g at 4°C.

Note: Centrifugation steps with 200 × *g* are necessary to discard thrombocytes.

g. Resuspend the cell pellet in 45 mL PBS containing 2 mM EDTA and determine the cell count.
h. Centrifuge the tube for 10 min at 300 × *g* at 4°C.
i. Resuspend pellet in ice-cold freezing medium (Fetal calf serum (FCS) with 10% (v/v) dimethyl sulfoxide (DMSO); filtered with a 0.2 μm filter) and transfer into a cryovial.

Note: We recommend $5 \times 10^7 - 1 \times 10^8$ cells/mL freezing medium.

j. Store samples at −150°C until further use.

Note: For cryopreservation use a controlled rate cryo-freezer or a cryo-freezing container. We recommend labeling the cryovials prior to aliquoting the cells, as it is not advisable to keep the cells in cryopreservation medium for extended periods. Place the cryovials in a

freezing container and store them immediately at −80°C for 24 h. For long-term storage, transfer the vials to liquid nitrogen or at least −150°C.

Recombinant expression of PcrV

Timing: 5 days

3. Cloning of the *pcrV* gene into an pQE80 vector.
   a. Isolate genomic DNA from a PA strain of interest using the DNeasy Blood & Tissue Kit according to the manufacturer's instructions (Manual).
   b. Amplify the *pcrV* gene using Phusion High Fidelity Polymerase with the following primer pair:
      Forward: TCACCATCACGGATCCGAAGTCAGAAACCTTAATG.
      Reverse: TCAGCTAATTAAGCTTCTAGATCGCGCTGAGAATG.
      A detailed PCR protocol is provided in Tables 1 and 2.
   c. Digest 1 μg of the expression vector (pQE80) with BamHI and HindIII (1 μL each = 20 units) for 15 min at 37°C.
   d. Load complete sample on a 1.5% agarose gel and run at 120 V.
   e. Cut the linearized vector band (approximately 4600 bp) from the gel and purify it using a gel extraction kit (e.g., QIAquick Gel Extraction Kit).
   f. Purify the PCR product by using a PCR purification kit (e.g., QIAquick PCR Purification Kit) and clone it into the linearized expression vector with a 1:1 ratio with 200 ng using the In-Fusion HD EcoDry Cloning Kit according to the manufacturer's instructions (Manual).
   g. Select clones on ampicillin-supplemented agar plates (ampicillin concentration 100 μg/mL).

Note: Selection of antibiotic is dependent on the expression vector.

4. Transformation and protein expression.
   a. Grow colonies containing the recombinant vectors in 5 mL LB (lysogeny broth) liquid cultures supplemented with 100 μg/mL ampicillin.
   b. Isolate plasmids using the QIAprep Spin Miniprep Kit.

Note: Verify the accurate insertion of the *pcrV* gene by sequencing. For sequencing, use a pQE80 forward- (GCTTTGTGAGCGGATAACAATT) or reverse primer (ACTCCATCTGGA TTTGTTCA).

   c. Transform a plasmid with correct insert into competent BL21 *E. coli* cells by heat shock. Add 1 μg of the plasmid to a vial containing 50 μL BL21 *E. coli* cell suspension and incubate on ice for 30 min.
   d. Perform a heat shock by placing the vial in a 42°C water bath for 30 s, followed by a 2-min incubation on ice.
   e. Add 950 μL SOC (Super optimal broth with 20 mM glucose)-medium and incubate for shaking with 120 rpm for 1 h at 37°C.
   f. Plate 100 μL of the suspension onto an agar plate containing ampicillin (100 μg/mL) and incubate at 37°C overnight. Pick a single colony on the next day, transfer it into 10 mL LB media supplemented with 100 μg/mL ampicillin and incubate overnight.
   g. Transfer the overnight culture into 240 mL fresh LB media.
   h. Grow the culture to an optical density (OD) at 600 nm of 0.5, then induce protein expression by adding isopropyl β- d-1-thiogalactopyranoside (IPTG) to a final concentration of 300 μM.
   i. Incubate the culture for an additional 3 h with shaking at 30°C with 120 rpm.
   j. Centrifuge bacterial suspension at 4000 × *g* for 15 min.
   k. Lyse the bacterial pellet using B-PER Bacterial Protein Extraction Reagent according to the manufacturer's instructions (Manual).

l. Equilibrate the bacterial lysate with 30 mM imidazole in a 1:1 ration (final concentration 15 mM imidazole).
m. Load the lysate onto a 10 mL chromatography column with 2 mL bed volume loaded with 2 mL HisPur Ni-NTA resin and collect flowthrough. Repeat the step three times.
n. Wash the columns eight times with 10 mL PBS containing 25 mM imidazole.
o. Elute the His tag-labeled PcrV with 2 mL 250 mM imidazole.
p. Exchange the buffer to PBS using Amicon Ultra-4 10 kDa spin filters by repetitive washing steps.
q. Determine the purity of the recombinant PcrV by SDS-PAGE (e.g., by using a NuPAGE 4%–12% Bis-Tris midi gel) and staining of protein bands e.g., with InstantBlue Protein Stain.

KEY RESOURCES TABLE

REAGENT or RESOURCE	SOURCE	IDENTIFIER
Antibodies		
Anti-human CD20-Alexa Fluor 700 (clone 2H7) (1:100)	BD Biosciences	Cat.# 560631; RRID: AB_1727447
Anti-human IgG-PE (clone G18-145) (1:20)	BD Biosciences	Cat.# 560951; RRID:AB_10563761
Goat anti-human IgG	Biotrend	Cat.# 2040-01
Goat anti-human IgG-HRP (1:5,000)	SouthernBiotech	Cat.# 2040-05; RRID: AB_2795644
Immunoglobulin G	Sigma-Aldrich	Cat.# 56834-100MG
Bacterial and virus strains		
E. coli DH5α	Thermo Fisher Scientific	Cat.#18263012
E. coli BL21 (DE3)	NEB	Cat.#C2527H
Pseudomonas aeruginosa PAO1	Bleves et al.[6]	N/A
Pseudomonas aeruginosa PA14	Budzik et al.[7]	N/A
Biological samples		
Human red blood cells	This study	N/A
PBMCs, serum, and IgGs of donors	This study	N/A
Chemicals, peptides, and recombinant proteins		
10× PBS	Thermo Fisher Scientific	Cat.# AM9625
ABTS solution	Thermo Fisher Scientific	Cat.# 002024
Ampicillin sodium salt	Sigma-Aldrich	Cat.# A0166
BamHI-HF	NEB	Cat.#R3136
Bovine serum albumin (BSA)	Sigma-Aldrich	Cat.# A9418
BsiWI-HF	NEB	Cat.#R3553
Calf intestinal phosphatase	NEB	Cat.#M0525S
CutSmart buffer	NEB	Cat.#B6004S
DAPI	Thermo Fisher Scientific	Cat.#D1306
DMSO	Merck	Cat.#D2650
DNA loading dye	Thermo Fisher Scientific	Cat.#R0611
dNTP mix	Thermo Fisher Scientific	Cat.#R1122
DPBS	Thermo Fisher Scientific	Cat.# 14190250
DTT	Promega	Cat.#P1171
EcoRI-HF	NEB	Cat.#R3101
EDTA	Thermo Fisher Scientific	Cat.# AM9260G
ELISA coating buffer	BioLegend	Cat.# 421701
Ethanol	Carl Roth	Cat.# 9065.4
Fetal calf serum (FCS)	Thermo Fisher Scientific	Cat.# 10270-106
Ficoll-Paque Plus	Cytiva	Cat.# 17-1440-03
FreeStyle expression medium	Thermo Fisher Scientific	Cat.# 12338001
Gentamicin sulfate	Sigma-Aldrich	Cat.#G1914
Glycerol	Merck	Cat.#G5516
Glycine	Carl Roth	Cat.# 3187.3

(*Continued on next page*)

Continued

REAGENT or RESOURCE	SOURCE	IDENTIFIER
HindIII-HF	NEB	Cat.#R3104
Imidazole	Sigma-Aldrich	Cat.#I202
InstantBlue protein stain	Expedeon	Cat.# ISB1L
IPTG (isopropyl β-d-1-thiogalactopyranoside)	Sigma-Aldrich	Cat.#I6758
KB extender (part of the Platinum Taq DNA polymerase)	Thermo Fisher Scientific	Cat.# 10966034
LB medium (Luria/Miller)	Carl Roth	Cat.#X968.2
$MgCl_2$ 50 mM (part of the Platinum Taq DNA polymerase)	Thermo Fisher Scientific	Cat.# 10966034
Moxifloxacin-hydrochloride	Sigma-Aldrich	Cat.# SML1581
NEB 2.1 buffer	NEB	Cat.#B6002S
NP-40	Thermo Fisher Scientific	Cat.# 85124
Nuclease-free water	Thermo Fisher Scientific	Cat.# AM9937
Phusion high-fidelity GC buffer	Thermo Fisher Scientific	Cat.#F519L
Phusion high-fidelity DNA polymerase	Thermo Fisher Scientific	Cat.#F530L
Platinum Taq DNA polymerase	Thermo Fisher Scientific	Cat.# 10966034
Platinum Taq Green PCR Buffer (part of the Platinum Taq Green Hot Start)	Thermo Fisher Scientific	Cat.# 11966034
Platinum Taq Green Hot Start	Thermo Fisher Scientific	Cat.# 11966034
PEI (Polyethylenimine), 25 kDa	Sigma-Aldrich	Cat.# 408727
Protein G Sepharose 4 fast flow	GE Life Sciences	Cat.# 17061805
Q5 high GC enhancer (part of the Q5 high-fidelity DNA polymerase)	NEB	Cat.#M0491S
Q5 high-fidelity DNA polymerase	NEB	Cat.#M0491S
Q5 hot start high-fidelity DNA polymerase	NEB	Cat.#M0493L
Q5 PCR buffer (part of the Q5 high-fidelity DNA polymerase)	NEB	Cat.#M0491S
Random hexamer primer	Thermo Fisher Scientific	Cat.# SO142
Resazurin	Sigma-Aldrich	Cat.#R7017
RNaseOUT	Thermo Fisher Scientific	Cat.# 10777019
RNasin	Promega	Cat.#N2515
RPMI 1640	Thermo Fisher Scientific	Cat.# 11875093
SalI-HF	NEB	Cat.#R3138
Skim milk powder	Merck	Cat.# 70166
SOC medium	Thermo Fisher Scientific	Cat.# 15544034
SuperScript IV reverse transcriptase	Thermo Fisher Scientific	Cat.# 18090050
T4 DNA polymerase	NEB	Cat.#M0203L
Tris-(hydroxymethyl)-aminomethane	Carl Roth	Cat.# 4855.3
Trypsin-EDTA	Thermo Fisher Scientific	Cat.# 25300-096
Tween 20	Merck	Cat.# 817072
XhoI	NEB	Cat.#R0146
Critical commercial assays		
Alexa Fluor 488 microscale protein labeling kit	Thermo Fisher Scientific	Cat.# A30006
Alexa Fluor 647 microscale protein labeling kit	Thermo Fisher Scientific	Cat.# A30009
Amicon Ultra-4 10 kDa spin filters	Millipore	Cat.# UFC901008
Amicon Ultra-4 30 kDa spin filters	Millipore	Cat.# UFC903008
B-PER bacterial protein extraction reagent	Thermo Fisher Scientific	Cat.# 90084
CD19 MicroBeads	Miltenyi Biotec	Cat.# 130-050-301
DNeasy blood & tissue kit	QIAGEN	Cat.# 69504
HisPur Ni-NTA resin	Thermo Fisher Scientific	Cat.# 88221
In-Fusion HD EcoDry cloning kit	Takara Bio	Cat.# 080318
LeucoSEP	Greiner	Cat.# 227290
LS columns	Miltenyi Biotec	Cat.# 130-042-401
NucleoSpin 96 PCR clean-up	MACHEREY-NAGEL	Cat.# 740658.4
Nunc-Immuno 96 MicroWell	Merck	Cat.#M5785-1CS
NuPAGE 4%–12%, Bis-Tris	Thermo Fisher Scientific	Cat.# WG1402BOX
Poly-Prep chromatography columns	Bio-Rad	Cat.# 7311550

(*Continued on next page*)

Continued		
REAGENT or RESOURCE	SOURCE	IDENTIFIER
QIAquick gel extraction kit	QIAGEN	Cat.# 28704
QIAprep spin miniprep kit	QIAGEN	Cat.# 27104
QIAquick PCR purification kit	QIAGEN	Cat.# 28104
Experimental models: Cell lines		
A549	ATCC	Cat.# CCL-185; RRID:CVCL_0023
HEK293-6E	NRC	NRC file 11565
Oligonucleotides		
PcrV fwd (TCACCATCACGGATCCGAAGTCAGAAACCTTAATG)	This study	N/A
PcrV rev (TCAGCTAATTAAGCTTCTAGATCGCGCTGAGAATG)	This study	N/A
pQE80 forward primer (GCTTTGTGAGCGGATAACAATT)	This study	N/A
pQE80 reverse primer (ACTCCATCTGGATTTGTTCA)	This study	N/A
Random hexamer primer	Thermo Fisher Scientific	Cat.# SO142
Single-cell PCR primer 1st PCR (oPR-IGHV, IGKV, IGLV and reverse primers)	Gieselmann et al.,[5] Kreer et al.[8]	N/A
Single-cell PCR primer 2nd PCR (oPR-IGHV, IGKV, IGLV and reverse primers)	Gieselmann et al.,[5] Kreer et al.[8]	N/A
SLIC primer (SLIC_oPR_IGHV, SLIC_oPR_IGKV,SLIC_ oPR_IGLV and reverse primers)	Gieselmann et al.[5]	N/A
Recombinant DNA		
Human antibody expression vectors (IgG1, Igλ, Igκ)	Tiller et al.[9]	N/A
pQE-80L	QIAGEN, NovoPro	Cat.#V010777
Software and algorithms		
Clustal Omega 1.2.3 (http://www.clustal.org/omega/)	Sievers et al.,[10] Ye et al.[11]	RRID: SCR_001591
IgBLAST 1.13.0 (https://ftp.ncbi.nih.gov/blast/executables/igblast/release/LATEST/)	Ye et al.[11]	RRID: SCR_002873

MATERIALS AND EQUIPMENT

MACS buffer		
Reagent	Final concentration	Amount
EDTA (0.5 M)	2 mM	2 mL
BSA	1% (w/v)	5 g
PBS	N/A	Up to 500 mL
Store at 4°C for up to 3 months.		

FACS buffer		
Reagent	Final concentration	Amount
FCS	2% (v/v)	10 mL
EDTA (0.5 M)	2 mM	2 mL
BSA	1% (w/v)	5 g
PBS	N/A	Up to 500 mL
Store at 4°C for up to 3 months.		

Blocking buffer (ELISA)		
Reagent	Final concentration	Amount
BSA	2.5% (w/v)	2.5 g
Skim milk	2.5% (w/v)	2.5 g
Tween 20	0.05% [v/v]	50 µL
PBS	N/A	Up to 100 mL
Store at 4°C for up to 1 week.		

Blocking buffer (Cell sorting)		
Reagent	Final concentration	Amount
FCS	10% (v/v)	5 mL
BSA	5% (w/v)	2.5 g
PBS	N/A	Up to 50 mL
Store at 4°C for up to 3 months.		

Staining buffer (Cell sorting)		
Reagent	Final concentration	Amount per 100 μL
Anti-Human CD20-AF700	1:100	1 μL
IgG-PE	1:20	5 μL
DAPI (Live/Dead)	3 μM	105 ng
$PcrV^{AF488}$	10 μg/mL	1 μg
$PcrV^{AF647}$	10 μg/mL	1 μg
FACS Buffer	N/A	Up to 100 μL

Sorting buffer		
Reagent	Final concentration	Amount per 1 mL
Nuclease-free H_2O	N/A	775 μL
RNasin (40 U/μL)	2 U/μL	50 μL
RNaseOut (40 UL)	1 U/L	25 μL
PBS (10×)	0.5 ×	50 μL
DTT (100 mM)	1 mM	100 μL
Use directly or store at −80°C for up to 3 months.		

STEP-BY-STEP METHOD DETAILS

Identification of individuals for single B cell sorting

Timing: 2 days

To identify individuals with highly neutralizing anti-PcrV antibodies, a combination of PcrV-binding ELISA and functional assays should be used. Screening can be conducted using either serum samples or isolated IgG. If serum samples are utilized, it is recommended to measure the IgG concentrations to normalize the results based on the IgG content of each sample. The effects measured in functional assays should be specifically sensitive to T3SS-dependent activities such as T3SS-mediated cytotoxicity. Due to its sensitivity and specificity, we recommend the described hemolysis assay. However, other functional assays that rely on T3SS functionality may also be suitable.

1. PcrV-binding ELISA.
   a. Dilute PcrV protein in ELISA coating buffer (e.g., from BioLegend) to a final concentration of 2 μg/mL.
   b. Add 100 μL of the diluted PcrV solution to each well of a MaxiSorp ELISA 96-well plate.
   c. Seal the plate and incubate overnight at 4°C.
   d. Wash the ELISA plate three times with PBST (PBS + 0.05% [v/v] Tween 20) and discard the washing buffer.
   e. Incubate the plate with blocking buffer (2.5% [w/v] bovine serum albumin [BSA] and 2.5% [w/v] skim milk in PBST) for at least 1 h at room temperature (RT) with constant agitation.
   f. Dilute patient sera (from step 1) in a 1:4 serial dilution on a separate non-binding microplate (96-well) in blocking buffer. We recommend starting with a serum dilution of 1:32, progressing to a final dilution of 1:32,768.

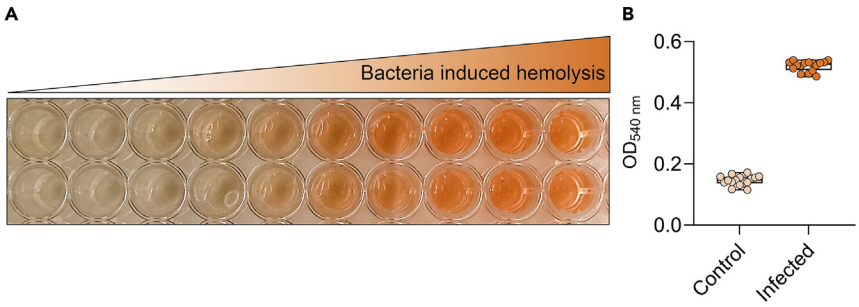

Figure 1. Quantification of PA-induced hemolysis

(A) Supernatant of RBCs with increasing bacteria-induced hemolysis shown in duplicates.

(B) Hemolysis was quantified by measuring the optical density (OD) at 540 nm from uninfected RBCs (control) and RBCs infected at an MOI of 1. Boxplots indicate the median, the upper and lower quartile, and the minimum and maximum values. Shown data points represent the technical mean of an independent experiment.

g. Discard the blocking buffer from the ELISA plate and wash the ELISA plate three times with PBST, discard the washing buffer.
h. Transfer 100 µL of the diluted sera from the titration plate to the ELISA plate.
i. Incubate for 2 h at RT with constant agitation (80 rpm).
j. Wash the ELISA plate three times with PBST and discard the washing buffer.
k. Add 100 µL goat anti-human IgG-HRP secondary antibody in blocking buffer (1:5,000) to each well.
l. Incubate for 1 h at RT at 80 rpm.
m. Wash the ELISA plate four times with PBST and discard the washing buffer.
n. Add 100 µL of ABTS substrate solution to each well and incubate at RT.
o. Measure the absorbance at 415 nm after 15 min using a microplate reader.

2. Functional testing of serum using hemolysis assay.

⚠ CRITICAL: A Class 2 safety cabinet is required for working with PA. All steps involving open handling with PA should be performed under a Class II safety cabinet. Ensure all biosafety level 2 handling requirements are met. For the calculation of T3SS neutralization, including a positive control (infection of RBCs without serum) and a negative control (incubation of RBCs with PBS without bacteria) is necessary.

a. Grow PA strain PA14 overnight at 37°C with shaking at 180 rpm.
b. Adjust the $OD_{600\ nm}$ of the overnight culture to 0.2 in fresh LB media and incubate at 180 rpm at 37°C until the $OD_{600\ nm}$ reaches 1.
c. During growth of bacteria prepare human blood samples:
   i. Collect 9 mL of peripheral blood in a 9 mL EDTA collection tube.
   ii. Transfer the blood into a 50 mL tube an add PBS to a final volume of 45 mL.
   iii. Centrifuge at 200 × *g* at RT for 10 min with deceleration set to 0.
   iv. Discard the supernatant carefully and resuspend the blood in PBS to a total volume of 45 mL. Repeat the washing step two more times.
   v. Adjust the red blood cell (RBC) count to 5×10^8 cells/mL in PBS.

Note: Washed blood can be stored for up to 5 days at 4°C in RPMI containing 10% FCS. Before reuse, the cell culture medium must be removed by washing. Centrifuge the tube at 200 × *g* at RT for 10 min. Discard the supernatant, then fill the tube with PBS up to 45 mL and repeat the centrifugation. Perform the PBS washing step one more time.

d. After reaching an $OD_{600\ nm}$ of 1, centrifuge bacteria suspension at 4,000 *g* at RT for 10 min.
e. Resuspend bacteria pellet in PBS to reach a concentration of 5×10^8 bacteria/mL.

Note: At an $OD_{600\ nm}$ of 1 PA concentration is approximately 1.5×10^8 bacteria/mL. Correlation of $OD_{600\ nm}$ and bacterial count should be determined by plating and count of colony forming units (CFUs) before experiments are performed.

f. Transfer 125 μL bacteria suspension per well into a round-bottom microplate and add serum to reach a final serum dilution between 1:100–1:800. Use PBS at the corresponding dilutions as control.
g. Seal the plate and preincubate for 20 min at RT with constant agitation (80 rpm).
h. After 20 min, add 125 μL of the erythrocyte suspension to each well and reseal the plate.
i. Centrifuge the plate at 1,000 × *g* at RT for 5 min.
j. Remove the sealing tape and incubate the plate in an incubator at 37°C with 5% CO_2 for 2 h.
k. Resuspend each well, reseal, and centrifuge at 1,500 × *g* at RT for 10 min.
l. Carefully transfer 100 μL of the supernatant from each well to a flat-bottom 96-well microplate and measure the OD at 540 nm to quantify bacteria-induced hemolysis (Figure 1).

Note: Avoiding air bubbles and resuspension of RBC is crucial, as these can cause false positive measurements.

Isolation of PcrV-specific B cells

Timing: 1 day

Isolation of PcrV-specific B cells is pivotal for the protocol. As PcrV-specific B cells are expected under 0.1% of all IgG^+ B cells, we recommend using at least 1×10^8 PBMCs for the experiments. The workflow follows the protocol from Gieselmann et al.[5] with some minor modifications and has been adapted to recombinant PcrV-protein as a sorting bait.

⚠ CRITICAL: Stringent selection of the target population, using controls (e.g., PBMCs from a healthy donor), careful adjustments of the cell sorter as well as sterile/RNA and DNA-free preparations of the sorting buffer and PCR plate are crucial to obtain reliable results.

3. Flurophore-labeling of PcrV.
   a. Label two batches of PcrV (each 100 μg) (from step 'recombinant expression of PcrV') with two different fluorophores separately. We recommend using commercially available labeling kits (e.g., Alexa Fluor Microscale Protein Labeling Kit) according to the manufacturer's instructions and the settings of the cell sorter (Manual). To avoid spectral overlaps, we recommend using Alexa Fluor 488 Microscale Protein Labeling Kit for one batch and Alexa Fluor 647 Microscale Protein Labeling Kit from Thermo Fisher Scientific for the other batch.

Note: Labeled PcrV can be stored at 4°C protected from light. Given the uncertain long-term stability of labeled PcrV, it is advisable to use it within a few days after labeling.

4. B cell enrichment and staining.
   a. Thaw PBMCs of a donor with a high PcrV titer and evidence of neutralizing effects in the screening assay (see 'identification of individuals for single B cell sorting'), transfer to a 50 mL tube and fill the tube with ice-cold MACS buffer to 45 mL final volume.
   b. Centrifuge at 300 × *g* at 4°C for 10 min and discard the supernatant.
   c. Repeat the washing step, resuspend the pellet in 10 mL ice-cold MACS buffer and count the cells.
   d. Centrifuge at 300 × *g* at 4°C for 10 min and resuspend the pellet with 80 μL MACS buffer per 1×10^7 cells.
   e. Add 20 μL magnetic CD19-microbeads per 1×10^7 cells and incubate the cells for 15 min at 4°C.

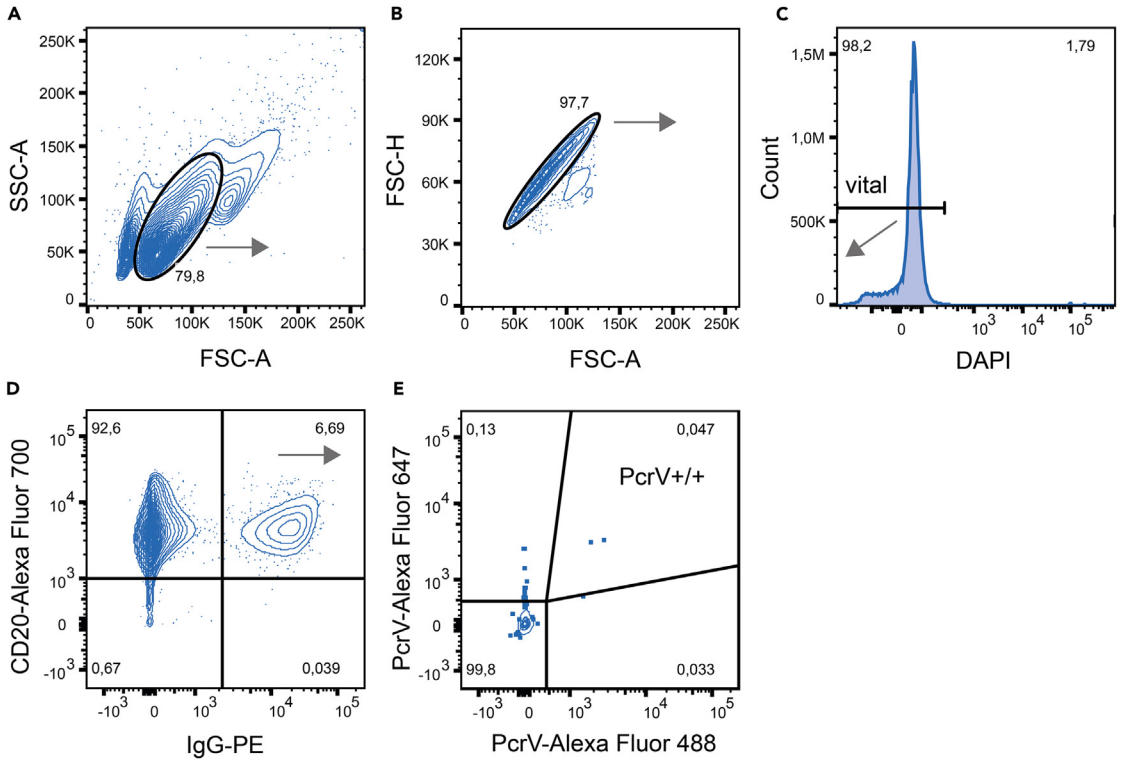

Figure 2. Gating strategy for the isolation of PcrV-specific B cells

(A) The gate represents the lymphocyte population.

(B) The gated population from A is plotted, with settings adjusted to exclude doublets.

(C) The gated population from B is further analyzed for DAPI staining, and only DAPI-negative cells are selected for subsequent gating.

(D) The DAPI-negative cells from C are analyzed for IgG (x-axis) and CD20 (y-axis) expression. Double-positive cells ($CD20^+$ IgG^+) in the upper right quadrant are selected for further analysis.

(E) $CD20^+$ IgG^+ cells which are double-positive for PcrV-binding (upper right quadrant) will be sorted in a single-cell manner.

f. Add 20 mL MACS buffer and centrifuge at 300 × *g* at 4°C for 10 min.

g. Resuspend the pellet in 0.5 mL MACS buffer per 1 × 10^8 cells.

h. Place a cell strainer on LS columns for positive cell selection and place the columns in a corresponding magnetic cell separator. Wash columns with 5 mL MACS buffer.

i. Load the cell suspension onto the prepared column, collect flow through (if needed) and wash the column three times with 5 mL MACS buffer.

j. Discard the cell strainer and fill the column with 5 mL fresh MACS buffer. Detach the column from the magnetic cell separator and use the syringe plunger to elute the $CD19^+$ cells.

Note: Use the plunger carefully to elute the cells from the column. Slow down when foam appears.

k. Centrifuge the flow through at 300 × *g* at 4°C for 10 min in a 50 mL tube. Discard the supernatant.

l. Resuspend $CD19^+$ cells in 5 mL fresh MACS buffer and count the cells.

Note: The expected amount of $CD19^+$ cells are around 10% of the initial PBMC number.

m. Centrifuge the cells at 300 × *g* at 4°C for 10 min. Discard the supernatant.

n. Resuspend $CD19^+$ cells in blocking buffer (PBS containing 10% FCS and 5% BSA) for 30 min at 4°C.

Table 3. 1st RT master mix

Reagent	Amount per well (μL)	Amount per plate (μL)
Nuclease-free H_2O	5.6	616
Random hexamer primers (200 ng/μL)	0.75	82.5
NP40 (10% (vol/vol))	0.5	55
RNaseOut (40 U/μL)	0.15	16.5
Total	7	770

o. Add 20 mL FACS (Fluorescence Activated Cell Sorting) buffer and centrifuge at 300 × *g* at 4°C for 10 min. Discard the supernatant.
p. Add staining buffer to the cells (100 μL/1 × 10^7 cells), resuspend and incubate for 20 min at 4°C protected from light.
q. Wash the cells with 45 mL FACS buffer and resuspend the cells in FACS buffer at a final concentration of 2.5 × 10^6 /mL.
r. Transfer the stained cells through a 40 μm cell strainer into a tube compatible with the respective cell sorter.

5. Single Cell Sorting.
   a. Before sorting, prepare PCR plates with sorting buffer.
      i. Add 4 μL sorting buffer per well into a PCR clean 96-well PCR plate.
      ii. Seal the plate using PCR-suitable foil. Store the sorting plates on ice for immediate use or at −80°C for long-term storage if prepared in advance.
   b. Set sorter specifications for different lasers and perform compensation for each fluorophore.

Note: We recommend using the $CD19^-$ fraction and staining these cells with CD3 antibodies for each fluorophore. Additionally, use B cells from healthy donors without a PcrV titer as a negative control and for defining the gate of the PcrV-positive cells.

   c. Sort PcrV-specific B cells in a single-cell manner (Figure 2).

Note: To minimize the risk of contamination, it is recommended to perform sorting with a cell sorter within a laminar flow hood.

   d. Seal the plate immediately after sorting and store at −80°C until further use.

Single B cell PCR and production of anti-PcrV mAbs

Timing: 14 days

The production of mAbs is a critical component of this project. Given the sensitivity of single B cell PCR, it is imperative to handle this step with extreme care to prevent contamination or sample mix-up. Maintaining an organized working and storage structure is essential. B cell PCR, B cell receptor cloning, and antibody production are performed according to the antibody isolation protocol from Gieselmann et al.[5]

⚠ CRITICAL: To prepare for single B cell work, clean all surfaces and pipettes with 70% ethanol followed by RNase away, and then expose to UV irradiation. Additionally, wear disinfected sleeves and a face mask to further minimize contamination. We strongly recommend to perform all work under a PCR hood.

6. Reverse Transcription.
   a. Prepare the 1st (Table 3) and the 2nd RT master mix (Table 4), excluding addition of SuperScript IV.

Table 4. 2nd RT master mix

Reagent	Amount per well (μL)	Amount per plate (μL)
Nuclease-free H_2O	2.05	205
SuperScript IV RT Buffer (5×)	3	300
dNTP mix (25 mM)	0.5	50
DTT (100 mM)	1	100
RNasin (40 U/μL)	0.1	11
RNaseOut (40 U/μL)	0.1	11
Intermediate sum	6.75	675
SuperScript IV (200 U/μL)	0.25	25
Total	7	700

b. Thaw the sorting plate on ice and centrifuge at 600 × *g* at 4°C for 1 min.
c. Transfer 1st RT master mix into a sterile reservoir, carefully add 7 μL per well into the sorting plate and resuspend several times.

Note: Use of multichannel pipettes is recommended.

⚠ CRITICAL: Use new tips for each well to avoid cross-contamination between wells.

d. Seal the plate with PCR foil and incubate at 65°C for 2.5 min.
e. Place the plate on ice for at least 2 min.
f. Add SuperScript IV to the 2nd RT master mix and transfer 7 μL per well, then seal the plate.
g. Centrifuge at 600 × *g* at 4°C for 1 min.
h. Place the plate in a thermocycler and run the reverse transcription program (Table 5).
i. Add 16 μL of nuclease-free water per well.
j. Store the plate at −80°C until further use or proceed with 1st PCR.

7. Amplification of heavy and light chain genes.
a. Prepare the 1st PCR master mix for amplifying heavy and light chain genes (Tables 6 and 7).
b. Add 19 μL of master mix per well in a 96-well PCR plate.
c. Thaw the RT plate from step 6.
d. Resuspend and transfer 3.8 μL per well from the RT plate to the PCR plate.
e. Seal the plate and centrifuge at 600 × *g* at 4°C for 1 min.
f. Place the plate in a thermocycler and run the 1st PCR protocol (Table 8).
g. Proceed with h.) or store the plate at 4°C for short-term storage or at −80°C for long-term storage.
h. Prepare separate 2nd PCR master mix (Tables 9 and 10).
i. Add 19 μL of 2nd PCR master mix per well in a 96-well PCR plate.
j. Resuspend and transfer 3 μL per well from the 1st to 2nd PCR plates (1× heavy, 1× kappa, 1× lambda).
k. Seal the plate and centrifuge at 600 × *g* at 4°C for 1 min.
l. Place the plate in a thermocycler and run the 2nd PCR protocol (Table 11).
m. Proceed to step 3 or store the plate at 4°C for short-term storage or at −80°C for long-term storage.

Table 5. Reverse transcription program

Steps	Temperature	Time	Cycles
1	42°C	10 min	1
2	25°C	10 min	1
3	50°C	10 min	1
4	94°C	5 min	1
Hold	4°C	forever	

Table 6. 1st PCR master mix

Reagent	Amount per well (μL)
Nuclease-free H_2O	14.68
Platinum Taq PCR buffer (10×)	2.05
KB Extender (6%)	1.23
$MgCl_2$ (50 mM)	0.61
dNTP mix (25 mM)	0.16
oPR_1st_fwd primer mix (50 μM)	0.09
oPR_1st_IgG_rev primer mix (50 μM)	0.09
Platinum Taq DNA Polymerase	0.09
Total	19.0

8. Verification and analysis of heavy and light chain genes.
   a. Load 4 μL/sample on a 2% agarose gel and run at 120 V.

   Note: Expected product lengths for heavy chains will be around 500 bp and 450 bp for light chains.

   b. Evaluate amplicons by sequencing. Use the respective chain-specific reverse primer that was used for the second PCR.
   c. Analyze sequencing results using tools such as NIH IgBlast. Sequences that are in-frame, without stop codons, and contain the full variable region should be considered productive.
9. Amplification of heavy and kappa or lambda chains using SLIC-Primer.
   a. Prepare separate master mixes for the amplification of heavy and kappa or lambda chains (Tables 12 and 13).
   b. Add 46 μL of the SLIC master mix per well in a 96-well PCR plate.
   c. Use the PCR plate of the 1st PCR (from step 7), thaw if necessary.
   d. Resuspend and transfer 1 μL per well per chain from the first PCR plate to the SLIC PCR plate.
   e. Seal the plate and centrifuge at 600 × *g* at 4°C for 1 min.
   f. Run the SLIC PCR protocol in a thermocycler (Table 14).
   g. Load 4 μL/sample on a 2% agarose gel and run at 120 V.

   Note: Expected product lengths for heavy chains will be around 600 bp and 550 bp for light chains.

   h. Proceed to step 5 or store the plate at 4°C for short-term storage or at −80°C for long-term storage.
10. Linearization of expression vector.
   a. Prepare digestion for vector linearization (Table 15).
   b. Heat digest at 37°C for 16 h and inactivate enzymes at 65°C for 20 min after digest.
   c. Add 0.5 μL of calf intestinal phosphatase (CIP) per reaction and incubate at 37°C for 30 min.
   d. Load complete sample on a 2% agarose gel and run at 120 V.
   e. Cut the linearized plasmid using a clean scalpel for each plasmid to avoid cross-contamination.
   f. Purify plasmids using a plasmid preparation kit.

Table 7. Primer 1st PCR

oPR_1st_fwd[5,8]	oPR_1st_IgG_rev[5,8]
oPR-IGHV-1_fw 1–15	Cg RT
oPR-IGKV fw 1–8	3′ Cκ 543
oPR-IGLV 1–15_fw	3′ Cλ

Table 8. 1st PCR program

Steps	Temperature	Time	Cycles
Initial Denaturation	94°C	2 min	1
Denaturation	94°C	30 s	50 cycles
Annealing	57°C	30 s	
Extension	72°C	55 s	
Final extension	72°C	6 min	1
Hold	4°C	forever	

g. Proceed to step 11 or store the plate at 4°C for short-term storage or at −80°C for long-term storage.

11. Sequence and ligation independent cloning (SLIC).
    a. Ligate the SLIC product with 8 ng/μL of linearized vector (Table 16). The molar ratio should be 1:6 to 1:2.
    b. Incubate at 24°C for 15 min using a thermocycler. Place on ice for 10 min afterward.
    c. Thaw competent *E. coli* DH5α on ice.

    Note: Instead, commercially available vials, *E. coli* DH5α can be made competent by using calcium chloride.

    d. Add 4 μL of the SLIC reaction to the competent *E. coli* and incubate for at least 30 min.
    e. Incubate the reaction mix for 45 s at 42°C. Use a water-bath or a thermocycler.
    f. Place the vial on ice after heat-shock immediately.
    g. Add 50 μL SOC medium to each ligation mix.
    h. Incubate at 37°C and 200 rpm for 1 h.
    i. Plate ligation mixes on ampicillin-supplemented agar plates (ampicillin concentration 100 μg/mL) plates and incubate overnight at 37°C.

    Note: Colonies may be visible after 16 h. Proceed to step 7 or store plates with colonies at 4°C for up to two weeks.

12. Colony PCR and sequencing.
    a. Prepare Colony PCR master mixes for each chain type according to the number of colonies and transfer to PCR tubes (Table 17). Additionally, prepare 15 mL tubes with 5 mL LB-medium supplemented with ampicillin (100 μg/mL).
    b. Pick a colony and resuspend it in the LB + ampicillin media. Use the same tip to resuspend in the designated PCR tube.
    c. Run the protocol for the Colony PCR (Table 18).
    d. Load 4 μL/sample on a 2% agarose gel and run at 120 V.

Table 9. 2nd PCR master mix

Reagent	Amount per well (μL)
Nuclease-free H2O	14.68
Platinum Taq Green PCR buffer (10×)	2.05
KB Extender (6%)	1.23
MgCl2 (50 mM)	0.61
dNTP mix (25 mM)	0.16
5′ primer mix (50 μM)	0.09
3′ primer (50 μM)	0.09
Platinum Taq DNA polymerase	0.09
Total	19.0

Table 10. Primer 2nd PCR

IgG1 heavy chain[5,8]	Kappa chain[5,8]	Lambda chain[5,8]
oPR-IGHV-1_fw 1–15	oPR-IGKV-1_fw 1–8	oPR-IGLV-1_fw 1–15
3′ IgG (internal) (rev)	3′ Cκ 494 (rev)	3′ XhoI Cλ (rev)

Note: Expected product lengths for heavy chains will be around 680 bp and 630 bp for light chains.

e. Incubate LB-media of colonies with correct insert size at 37°C and 180 rpm overnight.
f. Centrifuge at 4,000 × *g* at RT for 10 min.
g. Isolate plasmids using a Plasmid Preparation Kit (e.g., QIAprep Spin Miniprep Kit).
h. Verify correct insertion by sequencing using the 5′ Ab-sense primer.[5]
i. Plasmids can be stored at 4°C for short-term or at −20°C for long-term storage.

Note: We recommend preparing glycerol stocks of *E. coli* containing plasmids with the correct insertion for long-term storage and plasmid preparation. Mix glycerol and LB medium in a 1:1 ratio. Then, combine 600 μL of the overnight culture with 600 μL of the LB-glycerol mixture in a labeled tube, and store the stock at −80°C.

13. Recombinant expression of antibodies.
    a. Grow HEK293E cells using Erlenmeyer culture flask in shaking incubator at 37°C at 120 rpm and 8% CO_2.
    b. For transfection adjust a cell concentration of 0.8–1.2 × 10^6 cells/mL.
    c. Prepare transfection mix according to Table 19.

⚠ CRITICAL: First, add the heavy and light chain plasmids to PBS. Immediately after adding PEI (Polyethylenimine), vortex for 15 s.

    d. Incubate for 10 min at RT and gently add the mixture to cells under constant agitation.
    e. Incubate the cells for 7 d at 37°C, 8% CO_2 and 120 rpm.
    f. After 7 d, centrifuge the cells at 3,800 × *g* at RT for 10 min.
    g. Transfer the supernatant into 50 mL tubes.

Note: The supernatant can be stored for up to two weeks at 4°C.

    h. Add Protein G Sepharose to the supernatant.

Note: We recommend at least 4 μL Protein G Sepharose per mL of supernatant. The IgG concentration in the supernatant can be measured using a human IgG Fc ELISA to determine the appropriate amount of Protein G resin. Protein G Sepharose has a binding capacity of 20 mg of human IgG per mL of resin.

    i. Incubate for 2 h at RT or at 4°C overnight under constant agitation.

Table 11. 2nd PCR program

Steps	Temperature	Time	Cycles
Initial Denaturation	94°C	2 min	1
Denaturation	94°C	30 s	50 cycles
Annealing	57°C	30 s	
Extension	72°C	45 s	
Final extension	72°C	6 min	1
Hold	4°C	forever	

Table 12. SLIC PCR master mix

Reagent	Amount per well (µL)
Nuclease-free H_2O	24.1
Q5 PCR buffer (5×)	10
dNTP mix (25 mM)	0.4
5′ primer mix (50 µM)	0.5
3′ primer (50 µM)	0.5
Q5 High GC Enhancer (5×)	10
Q5 high-fidelity DNA polymerase	0.5
Total	46

j. Centrifuge at 600 *g* at 4°C for 5 min (with deceleration set to 0).
k. Discard the supernatant and resuspend the Protein G Sepharose with 5 mL PBS per 1 mL Protein G Sepharose.
l. Prepare Poly-Prep chromatography columns by adding 10 mL with 70% ethanol followed by 10 mL PBS.
m. Add the resuspended Protein G Sepharose to the columns and wash three times with 10 mL PBS.
n. Elute IgG directly into tubes containing 500 µL of 1 M Tris buffer (pH 8) by adding 2.5 mL of 0.1 M Glycine buffer (pH 2.7) on the columns.
o. Prepare Amicon Ultra-4 30 kDa spin filters using 2 mL PBS and centrifuge at 3,800 × *g* at 4°C for 5 min.
p. Discard flowthrough and apply eluate with antibody concentrations greater than 20 µg/mL to spin filters.

Note: Antibody concentration can be measured using UV/Vis spectroscopy, using a 1:10 dilution of Tris in glycine buffer as the blank.

q. Exchange buffer by repeatedly adding up to 4 mL PBS and centrifuging at 3,800 × *g* at 4°C for 10 min.

Note: Dilute Tris/Glycine at least by 1:200.

r. After buffer exchange, filter the mAbs using a 0.2 µm sterile filter to prevent contamination and remove aggregates.

Note: Purified antibodies can be stored at 4°C for up to 6 months.

Functional validation of anti-PcrV mAbs in an A549-based cytotoxicity assay

Timing: 3 days

Before proceeding with functional testing, the affinity of PcrV mAbs should be assessed using a PcrV-binding ELISA (see step 1 'PcrV-binding ELISA'). Additionally, we recommend conducting functional testing with the described hemolysis assay to evaluate neutralizing activity.

Table 13. Primer SLIC PCR

IgG1 heavy chain[5]	Kappa chain[5]	Lambda chain[5]
SLIC_oPR_IGHV 1–15	SLIC_oPR_IGKV 1–8	SLIC_oPR_IGLV 1–15
SLIC_oPR_IgG_HC_rev	SLIC_oPR_IGKV_rev	SLIC_oPR_IGLV_rev

Table 14. SLIC PCR program

Steps	Temperature	Time	Cycles
Initial Denaturation	98°C	30 s	1
Denaturation	98°C	10 s	35 cycles
Annealing	72°C	40 s	
Final extension	72°C	2 min	1
Hold	4°C	forever	

14. A549 cytotoxicity assay.
    a. Culture A549 cells in RPMI medium supplemented with 10% FCS (RF) in a T75 flask, maintaining the flask in a humidified incubator at 37°C with 5% CO_2.
    b. Seed 20,000 cells/well in 100 µL RF medium in a 96-well cell culture plate.
    c. Inoculate PAO1 into 5 mL LB media and incubate at 37°C with 180 rpm shaking overnight.
    d. Prepare a fresh PAO1 culture by transferring 1 mL of the overnight culture into 9 mL of fresh LB and incubating at 37°C with 180 rpm shaking until reaching an $OD_{600\ nm}$ of 1.
    e. Prepare a serial dilution of anti-PcrV mAbs starting at a final concentration of 50 µg/mL to 5 ng/mL on a 96-well non-binding titration plate. Dilute mAbs in RF medium with a final volume of 10 µL.

    Note: Use an unspecific IgG antibody as well as gentamicin (20 µg/mL) as controls.

    f. Use PAO1 culture to prepare a bacterial suspension with 222,000 bacteria/mL in RF medium to reach a final multiplicity of infection (MOI) of 0.5.
    g. Add to each mAb 90 µL of the bacterial suspension.
    h. Seal the plate and preincubate at room temperature for 20 min with shaking at 80 rpm.
    i. Discard the cell culture medium from the A549 cells and replace it with the PAO1/mAb mixture (from step e).
    j. Incubate the cells for 3 h in the humidified incubator at 37°C with 5% CO_2.
    k. Wash the cells by discarding the media and replacing it with fresh RF medium.
    l. Discard the medium and replace it with 100 µL/well RF medium containing 20 µg/mL gentamicin and 10 µg/mL moxifloxacin.
    m. Incubate the plate in the humidified incubator at 37°C with 5% CO_2 for 16 h.
    n. Add 10 µL/well of resazurin (0.25 mg/mL).
    o. Incubate the plate in the humidified incubator at 37°C with 5% CO_2.
    p. Measure fluorescent signal using 530–570 nm excitation wavelength and 585 – 590 nm emission wavelength after 120 min (Figure 3).

EXPECTED OUTCOMES

With the present protocol, we present a workflow for the identification of individuals with highly neutralizing antibodies targeting PcrV of the T3SS of PA. Successful completion of the protocol should enable the generation of human-derived neutralizing PcrV mAbs.

Table 15. Restriction digests

IgG1 heavy chain	Kappa chain	Lambda chain
10 µg vector	10 µg vector	10 µg vector
2.5 µL EcoRI-HF (50 U)	2.5 µL EcoRI-HF (50 U)	2.5 µL EcoRI-HF (50 U)
2.5 µL SalI-HF (50 U)	2.5 µL BsiWI-HF (50 U)	2.5 µL XhoI (50 U)
5 µL CutSmart Buffer	5 µL CutSmart Buffer	5 µL CutSmart Buffer
40 µL nuclease-free H_2O	30 µL nuclease-free H_2O	30 µL nuclease-free H_2O

Table 16. SLIC reaction master mix

Reagent	Amount/well (μL)
Nuclease-free water	to 4
Linearized vector	Final concentration 8 ng/μL
NEB Buffer 2.1 (10×)	1
T4 DNA Polymerase (3.000 u/mL)	0.2
Total	4

Expected percentage of individuals with highly neutralizing antibodies

In a predominantly chronically infected cystic fibrosis cohort, approximately 30% of individuals exhibited serum with neutralizing effects, reducing PA-induced cytotoxicity by more than 50% at a 1:800 dilution.[1] Notably, none of the healthy control group (n = 51) reached this threshold at either a 1:800 or 1:200 serum dilution.[1] This finding underscores the importance of careful cohort selection and should be considered prior to initiating the protocol.

Expected clonality of PcrV-specific B cells

To analyze PcrV-specific B cells, we recommend examining the VH/VJ gene distribution and assessing both germline and CDRH3 identities among the individual B cells. By defining clonal groups based on identical VH/VJ genes and CDRH3 identities of $\geq$75%, we identified several clusters. These clusters can be utilized for the selection of monoclonal antibody (mAb) candidates (Figure 4).

Expected yield of anti-PcrV mAbs

The yield of anti-PcrV monoclonal antibodies varied among different clones. At a cell concentration of 0.8–1.2 × 10^6 cells/mL, the average antibody yield is approximately 20 μg/mL.

Expected neutralizing capacity of anti-PcrV mAbs

Through this workflow, we identified individuals with highly neutralizing serum, followed by the recombinant expression of anti-PcrV mAbs. The neutralizing capabilities varied among different clones and donors, with a minimum IC50 of 56 ng/mL (Figure 5).

LIMITATIONS

The identification of individuals for the described workflow is based on the functional characterization of T3SS activity and the detection of anti-PcrV mAbs in their serum. It is important to consider that T3SS inhibition may also be attributable to antibodies binding to other T3SS proteins, rather than exclusively to PcrV.

TROUBLESHOOTING

Problem 1

PcrV titer measurement in serum shows high background (related to step 1).

Table 17. Colony PCR reaction master mix

Reagent	Amount/well (μL)
Nuclease-free water	17.43
Platinum Tag Green PCR Buffer (10×)	2.20
KB Extender (6%)	1.28
$MgCl_2$ (50 mM)	0.65
dNTP Mix (25 mM)	0.2
5′ Ab-sense (50 μM)	0.08
3′ primer (50 μM)	0.08
Platinum Taq DNA Polymerase	0.08
Total	22.00

Table 18. Colony PCR cycling conditions

Steps	Temperature	Time	Cycles
Initial Denaturation	94°C	5 min	1
Denaturation	94°C	30 s	28 cycles
Annealing	55°C	30 s	
Extension	72°C	1 min	
Final extension	72°C	5 min	1
Hold	4°C	forever	

Potential solution

- Increase blocking time up to 3 h at RT or block overnight at 4°C and add 2 additional washing steps to each (step 1).
- Verify PcrV purity by SDS-PAGE.

Problem 2

Low number of PcrV-specific B cells (related to step 5).

Potential solution

- Low recovery or viability of isolated PBMCs can be mitigated by isolating PBMCs promptly after collection and ensuring meticulous cryopreservation techniques.
- Percentage of PcrV-specific B cells is low (<0.1% of all $CD20^+$ IgG^+), therefore, it is highly recommended to obtain a minimum of 1×10^8 PBMCs. The total number of PBMCs can be significantly increased by utilizing leukapheresis instead of conventional blood drawing.
- Test sufficient fluorophore-labeling of PcrV by spectrophotometry.
- Re-evaluate the individual's PcrV titer. If necessary, select or screen for an individual with a high PcrV titer.

Problem 3

Low antibody yields (related to step 13).

Potential solution

- Production of antibodies decreases with increasing passages of HEK293-6E cells. Obtain a new batch of HEK293-6E cells and repeat the transfection process.

Problem 4

Produced human-derived mAbs do not bind PcrV (related to step 13).

Potential solution

- Ensure proper blocking before staining to avoid excessive PcrV positivity.
- Compensation and accurate gating before sorting are crucial (Figure 2).
- Use a negative control (B cells from a donor without titer) to accurately distinguish specific PcrV binding.

Table 19. Transfection

Reagent	Amount/1 mL culture volume
DPBS	45 μL
Heavy chain plasmid	0.5 μg
Light chain plasmid	0.5 μg
PEI (0.45 mg/mL)	3.4 μL

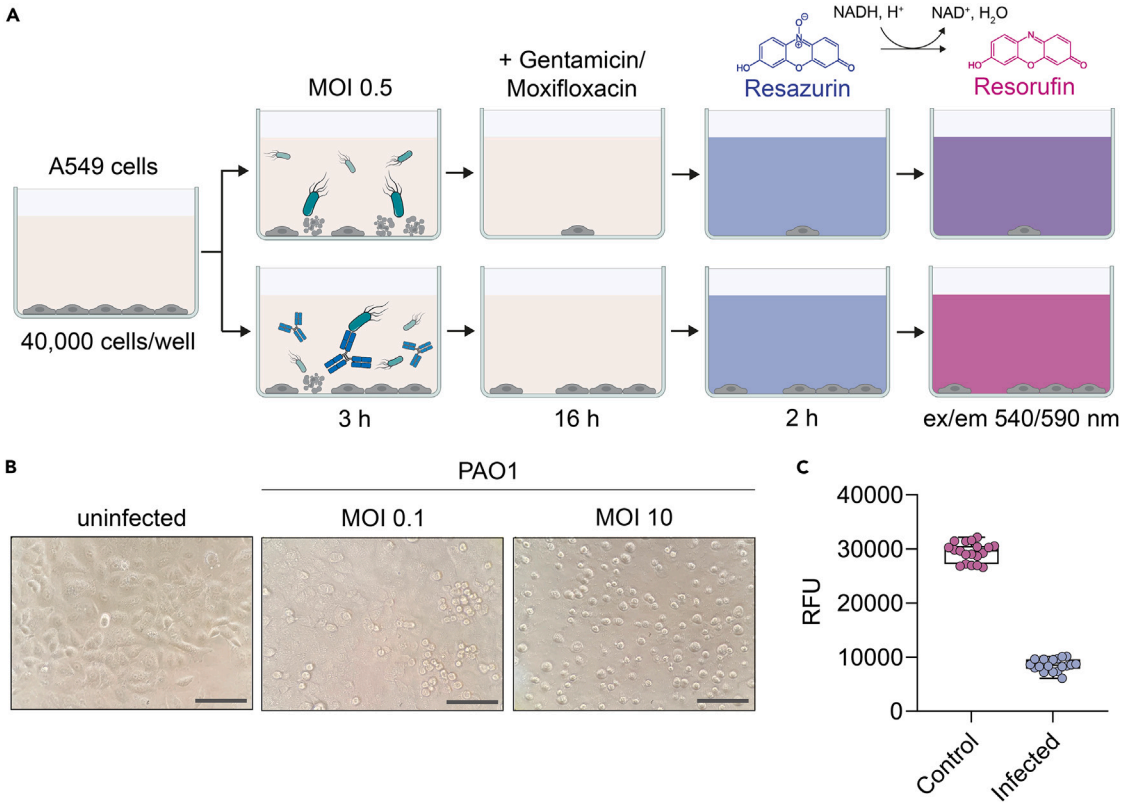

Figure 3. A549-based cytotoxicity assay

(A) Illustration of the experimental setup, which is described in this protocol (step 14).

(B) A549 cells were infected with the PA wild-type strain PAO1 at a MOI of 0.1 and 10 for 3 h. Uninfected cells were used as a control. Changes in cell morphology, indicative of bacteria-induced cell death, were documented using bright-field microscopy. Scale bar indicate 20 μm.

(C) Relative fluorescence units (RFU) were measured after adding resazurin to uninfected cells (control) and cells infected with a MOI of 0.5 for 3 h. Boxplots indicate the median, the upper and lower quartile, and the minimum and maximum values. Shown data points represent the technical mean of an independent experiment.

RESOURCE AVAILABILITY

Lead contact

Further information and requests for resources and reagents should be directed to and will be fulfilled by the lead contact, Alexander Simonis (alexander.simonis@uk-koeln.de).

Technical contact

For detailed technical questions, please reach out to the technical contact, Alexander Simonis (alexander.simonis@uk-koeln.de).

Materials availability

All materials except for generated mAbs and patient material is available as mentioned in the materials section. Primers have been ordered by local provider. Plasmids used in this study have been ordered from Addgene.

Data and code availability

All data reported in this protocol will be shared by the lead contact upon request, and this protocol does not report original code.

ACKNOWLEDGMENTS

This study was supported by the German Federal Ministry of Education and Research (BMBF) (01KI2108, Junior Research Groups Infectious Diseases to A.S.); the Cologne Clinician Scientist Program (CCSP, to A.S.); the German Research Council (DFG) (FI 773/15-1 [CCSP] to A.S., CRC 1310 to F.K. and C.K., and CRC 1403 to J.R.); the Koeln Fortune Program (to A.S.) and the CMMC Career Advancement Program (to A.S. and J.R.), the Faculty of Medicine and University Hospital

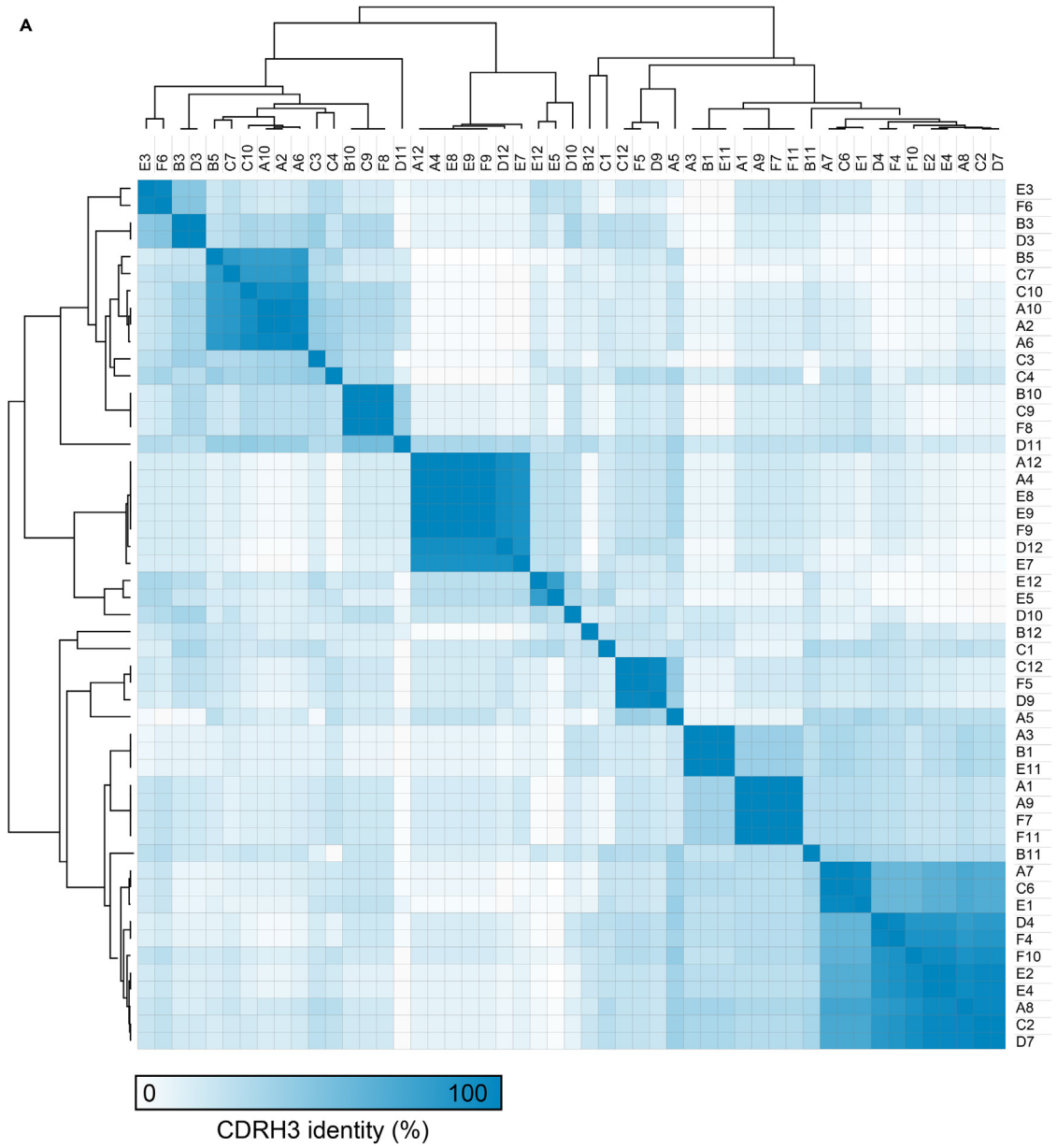

Figure 4. CDRH3 Identity of Single PcrV-Specific B Cells

(A) CDRH3 identity of single PcrV-specific B cells (n = 51) from a single donor was analyzed. Sequences were hierarchically clustered using Clustal Omega (ClustalO), and a similarity matrix was generated based on Pearson correlation.

of Cologne, University of Cologne; and the German Center for Infection Research (DZIF) (to F.K., TTU 09.719 and DZIF TTU 02.806 to J.R.). Graphical illustrations were created with BioRender.com.

AUTHOR CONTRIBUTIONS

Conceptualization, F.K., J.R., and A.S.; methodology, A.A., C.K., and A.S.; investigation, A.A.; formal analysis, A.A. and A.S.; writing – original draft, A.A. and A.S.; writing – review and editing, C.K., F.K., J.R., and A.S.; supervision, A.S.; funding acquisition, F.K., J.R., and A.S.

DECLARATION OF INTERESTS

A patent application for a set of highly neutralizing antibodies developed using the described workflow has been filed by the University of Cologne, with A.S., C.K., F.K., and J.R. listed as inventors.

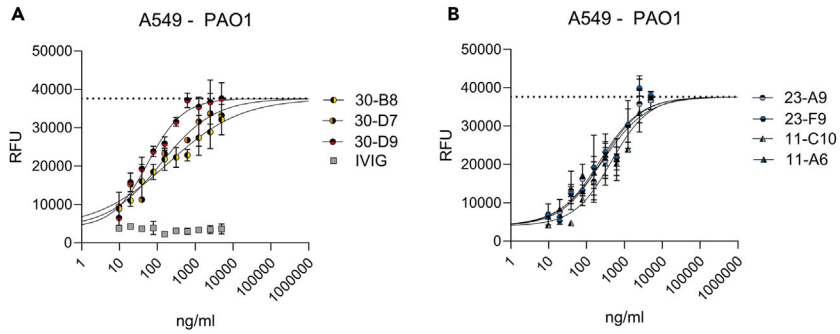

Figure 5. A549-based cytotoxicity assay

(A and B) A549 cells were infected with PAO1 for 150 min with a MOI of 0.5 in presence of patient-derived monoclonal anti-PcrV antibodies (at a concentration ranging from 5 μg/mL to 10 ng/mL) (n = 7). As control, cells were left uninfected (dotted line) or were treated with polyclonal IgG (intravenous IgG = IVIG). Relative fluorescence units (RFU) were measured after adding resazurin. Shown data points represent the technical mean of an independent experiment. Error bars indicate standard deviation of the mean.

REFERENCES

1. Simonis, A., Kreer, C., Albus, A., Rox, K., Yuan, B., Holzmann, D., Wilms, J.A., Zuber, S., Kottege, L., Winter, S., et al. (2023). Discovery of highly neutralizing human antibodies targeting Pseudomonas aeruginosa. Cell *186*, 5098–5113.e19. https://doi.org/10.1016/j.cell.2023.10.002.

2. Hauser, A.R. (2009). The type III secretion system of Pseudomonas aeruginosa: infection by injection. Nat. Rev. Microbiol. *7*, 654–665. https://doi.org/10.1038/nrmicro2199.

3. Goure, J., Pastor, A., Faudry, E., Chabert, J., Dessen, A., and Attree, I. (2004). The V antigen of Pseudomonas aeruginosa is required for assembly of the functional PopB/PopD translocation pore in host cell membranes. Infect. Immun. *72*, 4741–4750. https://doi.org/10.1128/IAI.72.8.4741-4750.2004.

4. Dickey, S.W., Cheung, G.Y.C., and Otto, M. (2017). Different drugs for bad bugs: antivirulence strategies in the age of antibiotic resistance. Nat. Rev. Drug Discov. *16*, 457–471. https://doi.org/10.1038/nrd.2017.23.

5. Gieselmann, L., Kreer, C., Ercanoglu, M.S., Lehnen, N., Zehner, M., Schommers, P., Potthoff, J., Gruell, H., and Klein, F. (2021). Effective high-throughput isolation of fully human antibodies targeting infectious pathogens. Nat. Protoc. *16*, 3639–3671. https://doi.org/10.1038/s41596-021-00554-w.

6. Bleves, S., Soscia, C., Nogueira-Orlandi, P., Lazdunski, A., and Filloux, A. (2005). Quorum sensing negatively controls type III secretion regulon expression in Pseudomonas aeruginosa PAO1. J. Bacteriol. *187*, 3898–3902. https://doi.org/10.1128/JB.187.11.3898-3902.2005.

7. Budzik, J.M., Rosche, W.A., Rietsch, A., and O'Toole, G.A. (2004). Isolation and characterization of a generalized transducing phage for Pseudomonas aeruginosa strains PAO1 and PA14. J. Bacteriol. *186*, 3270–3273. https://doi.org/10.1128/JB.186.10.3270-3273.2004.

8. Kreer, C., Döring, M., Lehnen, N., Ercanoglu, M.S., Gieselmann, L., Luca, D., Jain, K., Schommers, P., Pfeifer, N., and Klein, F. (2020). openPrimeR for multiplex amplification of highly diverse templates. J. Immunol. Methods *480*, 112752. https://doi.org/10.1016/j.jim.2020.112752.

9. Tiller, T., Meffre, E., Yurasov, S., Tsuiji, M., Nussenzweig, M.C., and Wardemann, H. (2008). Efficient generation of monoclonal antibodies from single human B cells by single cell RT-PCR and expression vector cloning. J. Immunol. Methods *329*, 112–124. https://doi.org/10.1016/j.jim.2007.09.017.

10. Sievers, F., Wilm, A., Dineen, D., Gibson, T.J., Karplus, K., Li, W., Lopez, R., McWilliam, H., Remmert, M., Söding, J., et al. (2011). Fast, scalable generation of high-quality protein multiple sequence alignments using Clustal Omega. Mol. Syst. Biol. *7*, 539. https://doi.org/10.1038/msb.2011.75.

11. Ye, J., Ma, N., Madden, T.L., and Ostell, J.M. (2013). IgBLAST: an immunoglobulin variable domain sequence analysis tool. Nucleic Acids Res. *41*, W34–W40. https://doi.org/10.1093/nar/gkt382.

10. Declaration

Ich versichere, dass ich die von mir vorgelegte Dissertation selbständig angefertigt, die benutzten Quellen und Hilfsmittel vollständig angegeben und die Stellen der Arbeit – einschließlich Tabellen, Karten und Abbildungen -, die anderen Werken im Wortlaut oder dem Sinn nach entnommen sind, in jedem Einzelfall als Entlehnung kenntlich gemacht habe; dass diese Dissertation noch keiner anderen Fakultät oder Universität zur Prufung vorgelegen hat; dass sie – abgesehen von unten angegebenen Teilpublikationen – noch nicht veröffentlicht worden ist sowie, dass ich eine solche Veröffentlichung vor Abschluss des Promotionsverfahrens nicht vornehmen werde. Die Bestimmungen dieser Promotionsordnung sind mir bekannt. Die von mir vorgelegte Dissertation ist von Professor Dr. Dr. Jan Rybniker betreut worden.

Übersicht der Publikationen:

von Ambüren J, Schreiber F, Fischer J, Winter S, van Gumpel E, **Simonis A**, Rybniker J. Comprehensive Host Cell-Based Screening Assays for Identification of Anti-Virulence Drugs Targeting *Pseudomonas aeruginosa* and *Salmonella* Typhimurium. Microorganisms. 2020 Jul 22;8(8):1096. doi: 10.3390/microorganisms8081096

Simonis A, Kreer C, Albus A, Rox K, Yuan B, Holzmann D, Wilms JA, Zuber S, Kottege L, Winter S, Meyer M, Schmitt K, Gruell H, Theobald SJ, Hellmann AM, Meyer C, Ercanoglu MS, Cramer N, Munder A, Hallek M, Fätkenheuer G, Koch M, Seifert H, Rietschel E, Marlovits TC, van Koningsbruggen-Rietschel S, Klein F, Rybniker J. Discovery of highly neutralizing human antibodies targeting *Pseudomonas aeruginosa*. Cell. 2023 Nov 9;186(23):5098-5113.e19. doi: 10.1016/j.cell.2023.10.002.

Albus A, Kreer C, Klein F, Rybniker J, **Simonis A**. Protocol for developing *Pseudomonas aeruginosa* type III secretion system-neutralizing monoclonal antibodies from human B cells. STAR Protoc. 2024 Dec 20;5(4):103440. doi: 10.1016/j.xpro.2024.103440.

Ich versichere, dass ich alle Angaben wahrheitsgemäß nach bestem Wissen und Gewissen gemacht habe und verpflichte mich, jedmögliche, die obigen Angaben betreffenden Veränderungen, dem Promotionsausschuss unverzüglich mitzuteilen.

Köln den 06.05.2026